[redacted]

~~CONFIDENTIAL~~

X75 10257

NASA TM X-3203

NASA TECHNICAL MEMORANDUM

NASA TM X-3203

TRANSONIC AERODYNAMIC CHARACTERISTICS OF THE 10-PERCENT-THICK NASA SUPERCRITICAL AIRFOIL 31 (U)

Charles D. Harris

Langley Research Center

Hampton, Va. 23665

NATIONAL AERONAUTICS AND SPACE ADMINISTRATION • WASHINGTON, D. C. • MARCH 1975

~~CONFIDENTIAL~~

C[redacted]

1. Report No.
NASA TM X-3203

2. Government Accession No.

3. Recipient's Catalog No.

4. Title and Subtitle
TRANSONIC AERODYNAMIC CHARACTERISTICS OF THE 10-PERCENT-THICK NASA SUPERCRITICAL AIRFOIL 31 (U)

5. Report Date
March 1975

6. Performing Organization Code

7. Author(s)
Charles D. Harris

8. Performing Organization Report No.
L-9841

10. Work Unit No.
505-06-31-02

9. Performing Organization Name and Address
NASA Langley Research Center
Hampton, Va. 23665

11. Contract or Grant No.

13. Type of Report and Period Covered
Technical Memorandum

12. Sponsoring Agency Name and Address
National Aeronautics and Space Administration
Washington, D.C. 20546

14. Sponsoring Agency Code

15. Supplementary Notes

16. Abstract

This report documents the aerodynamic characteristics of the 10-percent-thick NASA supercritical airfoil 31 and compares them with those of the earlier supercritical airfoil 12 which was designed for the same normal-force coefficient. Integrated section force and moment data and surface-pressure distributions are presented.

17. Key Words (Suggested by Author(s))
Supercritical airfoil
Transonic aerodynamics

18. Distribution Statement
Confidential – Available to U.S. Government Agencies and Their Contractors Only

New Subject Category 02

19. Security Classif. (of this report)	20. Security Classif. (of this page)	21. No. of Pages	22. Price
[redacted]al	Unclassified	136	

"NATIONAL [redacted]ION"
[redacted]re Subject to Criminal Sanctions.

CONFIDENTIAL CLASSIFIED
BY Security Classification Officer, NASA LaRC
SUBJECT TO GENERAL DECLASSIFICATION SCHEDULE OF EXECUTIVE ORDER 11652 AUTOMATICALLY DOWNGRADED AT TWO YEAR INTERVALS AND DECLASSIFIED ON DEC 31 1981

[redacted]L

TRANSONIC AERODYNAMIC CHARACTERISTICS OF THE 10-PERCENT-THICK NASA SUPERCRITICAL AIRFOIL 31 (U)

Charles D. Harris
Langley Research Center

SUMMARY

Refinements in a 10-percent-thick supercritical airfoil (airfoil 31) have produced significant improvements in the drag characteristics compared with those for an earlier supercritical airfoil (airfoil 12) designed for the same normal-force coefficient of 0.7. Drag creep was practically eliminated at normal-force coefficients between about 0.4 and 0.7 and was greatly reduced at other normal-force coefficients. Substantial reductions in the drag levels preceding drag divergence were also achieved at all normal-force coefficients. The Mach numbers at which drag diverges were delayed for airfoil 31 at normal-force coefficients up to about 0.6 (by approximately 0.01 and 0.02 at normal-force coefficients of 0.4 and 0.6, respectively) but drag divergence occurred at slightly lower Mach numbers at higher normal-force coefficients.

INTRODUCTION

An airfoil concept developed by Richard T. Whitcomb (refs. 1 and 2) which operates efficiently over a wide range of lift coefficients in the supercritical or mixed flow conditions of transonic flight has led to significant aerodynamic advances over the past several years. A variety of wind-tunnel and flight investigations (refs. 3 to 6) of several airplane configurations incorporating the supercritical airfoil concept have successfully demonstrated improvements in aerodynamic performance and maneuver capabilities with marked potential for both civilian and military application.

The impact on future aircraft design has been an incentive for expanding supercritical technology by establishing a broad base of systematic experimental data on supercritical airfoils. (See refs. 7 to 12, for example.) Much of the research effort has been focused on 10-percent-thick airfoils designed for section normal-force coefficients of about 0.55 (ref. 13) for application to advanced technology transports expected to cruise near the speed of sound. More recently, a research investigation was undertaken to develop an airfoil with a somewhat higher design section normal-force coefficient (about 0.70) for application to lower sweep, higher aspect ratio wings envisioned to cruise at Mach numbers near those of current transports.

The purpose of this report is to present the aerodynamic characteristics of the resultant airfoil (designated as supercritical airfoil 31) and to show the substantial drag improvements that are observed when these characteristics are compared with those of an earlier supercritical airfoil (supercritical airfoil 12, circa 1970) designed for the same normal-force coefficient. The relative drag characteristics of the two airfoils are discussed and attention is called to selected associated pressure distributions.

SYMBOLS

Values are given in both SI and U.S. Customary Units. Measurements and calculations are made in U.S. Customary Units.

C_p — pressure coefficient, $\frac{p_l - p_\infty}{q_\infty}$

$C_{p,sonic}$ — pressure coefficient corresponding to local Mach number of 1.0

c — chord of airfoil, 63.5 centimeters (25.0 inches)

c_d — section drag coefficient, $\sum_{\text{Wake}} c'_d \frac{\Delta z}{c}$

c'_d — point drag coefficient (ref. 14)

$\Delta c_{d,s}$ — drag increment due to shock wave losses

c_m — section pitching-moment coefficient about the quarter-chord point,

$$\sum_{l} C_p\left(0.25 - \frac{x}{c}\right)\frac{\Delta x}{c} - \sum_{u} C_p\left(0.25 - \frac{x}{c}\right)\frac{\Delta x}{c}$$

c_n — section normal-force coefficient, $\sum_{l} C_p \frac{\Delta x}{c} - \sum_{u} C_p \frac{\Delta x}{c}$

K — surface curvature, reciprocal of local radius of curvature

M — Mach number

m	surface slope, dy/dx
p	static pressure, newtons per meter^2 (pounds per foot^2)
Δp_t	total-pressure loss, newtons per meter^2 (pounds per foot^2)
q	dynamic pressure, newtons per meter^2 (pounds per foot^2)
R	Reynolds number based on airfoil chord
x	ordinate along airfoil reference line measured from airfoil leading edge, centimeters (inches)
y	ordinate normal to airfoil reference line, centimeters (inches)
z	vertical distance in wake profile measured from bottom of rake, centimeters (inches)
α	geometric angle of attack of airfoil reference line, degrees

Subscripts:

l	local point on airfoil
∞	undisturbed stream

Abbreviations:

l	airfoil lower surface
u	airfoil upper surface
T.E.	trailing edge

APPARATUS AND TECHNIQUES

Models

The supercritical airfoil basic concept and detailed design philosophy are discussed in reference 2.

Background.- During initial phases of the two-dimensional supercritical airfoil development program, emphasis was placed upon developing an airfoil with the highest drag divergence Mach number attainable at a normal-force coefficient of 0.7. The normal-force coefficient of 0.7 was chosen as the design goal since, when account was taken of the sweep effect, it was representative of lift coefficients at which the advanced technology near-sonic transports utilizing the supercritical airfoil concept were then expected to cruise. These initial phases resulted in supercritical airfoil 11 which has been reported in reference 9. This airfoil exhibited an undesirable creep or gradual increase in the variation of drag coefficient with Mach number of about 14 counts (c_d increment of 0.0014) between $M = 0.50$ and the drag divergent Mach number at the design normal-force coefficient.

Subsequent design studies of advanced technology transport configurations suggested that the near-sonic cruise lift coefficient requirements would be somewhat lower than originally anticipated. Consequently, the improved supercritical airfoil 26a (ref. 13) was developed with a design normal-force coefficient of about 0.55. The wind-tunnel tests required for this airfoil also provided the opportunity to explore the drag creep problem noted with airfoil 11. Airfoil 26a had no drag creep at normal-force coefficients up to about 0.6 and the drag divergence Mach number varied from approximately 0.82 at a normal-force coefficient of 0.30 to 0.78 at a normal-force coefficient of 0.80. As discussed in reference 13, these improved drag creep characteristics were largely attributed to a more favorable flow recompression over the forward upper surface and the elimination of a region of overexpansion near the three-quarter-chord station.

Recent emphasis on fuel economy has generated considerable interest in a fuel-conserving aircraft envisioned to cruise at Mach numbers near those of current transports. Such an aircraft could utilize supercritical airfoil technology to achieve weight and drag reductions by permitting the use of thicker wings with higher aspect ratios and less sweep. Because the wings with higher aspect ratio would require airfoils with design normal-force coefficients higher than 0.55, a wind-tunnel program was initiated to develop an airfoil with a design normal-force coefficient of about 0.70 without incurring the troublesome drag creep problem of the earlier airfoil 11.

In order to apply the drag creep improvements of airfoil 26a, it was used as the starting point in extending the design normal-force coefficient to 0.70. Initially, the location of maximum thickness above the reference line (upper surface thickness) was moved forward from 0.40c to 0.38c and the rear of the airfoil (both upper and lower surfaces) was displaced downward by an amount which varied from 0.0c at the new position of maximum upper surface thickness to 0.01c at the trailing edge; thereby the aft camber was increased. Moving the position of upper surface maximum thickness forward by 0.02c simply compressed axially the forward upper surface and maintained the same general family resemblence to airfoil 26a.

In addition to the aforementioned changes, several experimental modifications were necessary during the investigation before arriving at the final configuration (airfoil 31). These modifications consisted of small curvature variations near the upper surface leading edge to control better the development of supersonic flow in this region and over the forward lower surface to flatten the forward lower surface pressure distribution.

Wind-tunnel models.- Geometric characteristics of airfoil 31 are shown in figures 1 to 3 and measured section coordinates are presented in table I. Airfoil 12, also defined in figures 1 to 3 and table I, differs very little from airfoil 11 (ref. 13) and has been selected as a basis of comparison because data were available over a wider range of off-design conditions than were available for airfoil 11.

The most significant dissimilarities over the forward region of the two airfoils are the reduced leading-edge radius (fig. 1) and modified curvature distribution (fig. 3) of airfoil 31. Over the rear region, airfoil 31 has increased aft camber (fig. 1), reduced trailing-edge declivity (fig. 2), and reduced surface curvatures over the rearmost 35 percent of the upper surface and generally over the rearmost 50 percent of the lower surface. Irregularities in the upper surface curvature distribution of airfoil 31 around the 10-percent-chord line are believed to account for small irregularities observed in the upper surface pressure distribution in this region for some test conditions. Small surface irregularities are greatly exaggerated when examined from the standpoint of local curvature, however, and these surface irregularities are not discernible in the slope distribution of figure 2. Both airfoils included a trailing-edge cavity (see the insert in fig. 1 and the photographs of fig. 4) which had a favorable effect on the wake as discussed in reference 9.

To simplify comparisons between supercritical airfoils, it has been the custom to present coordinates relative to a common reference line rather than the standard method of defining airfoils relative to a reference line connecting the leading and trailing edges. Presenting airfoil 12 and 31 coordinates in this manner introduces a discrepancy in angle of attack as conventionally defined. If this discrepancy, which amounts to approximately 0.23°, were taken into account, a curve of normal-force coefficient as a function of angle of attack for airfoil 31 would have to be displaced 0.23° in the positive angle-of-attack direction relative to airfoil 12.

The wind-tunnel models, mounted in an inverted position, spanned the width of the tunnel with a span-chord ratio of 3.43. They were constructed with metal leading and trailing edges and with a metal core around which plastic fill was used to form the contours of the airfoils. Angle of attack was changed manually by rotating the model about pivots in the tunnel side walls. A photograph and a drawing of one of the airfoils installed in the tunnel are shown in figures 4 and 5, respectively.

Wind Tunnel

The investigation was conducted in the Langley 8-foot transonic pressure tunnel (ref. 15). This tunnel is a continuous-flow, variable-pressure wind tunnel with controls that permit the independent variation of Mach number, stagnation pressure and temperature, and dewpoint. It has a 2.16-meter-square (85.2-inch-square) test section with filleted corners so that the total cross-sectional area is equivalent to that of a 2.44-meter-diameter (8-foot-diameter) circle. The upper and lower test-section walls are axially slotted to permit testing through the transonic speed range. The total slot width at the position of the model averaged about 5 percent of the width of the upper and lower walls.

The solid side walls and slotted upper and lower walls make this tunnel well suited to the investigation of two-dimensional models since the side walls act as end plates and the slots permit development of the flow field in the vertical direction.

Boundary-Layer Transition

Based on the technique discussed in reference 16, boundary-layer transition was fixed along the 28-percent chord line on the upper and lower surfaces of the models in an attempt to simulate the full-scale Reynolds numbers shown in figure 6 by providing the same relative trailing-edge boundary-layer-displacement thickness at model scale as would exist at full-scale flight conditions. The simulation technique, which requires that laminar flow be maintained ahead of the transition trip, is limited on the upper surface to those test conditions in which shock waves or steep adverse pressure gradients occur behind the point of fixed transition so that the flow is not tripped prematurely. Full-scale simulation on the lower surface would be valid through the Mach number range of the investigation since laminar flow can be maintained ahead of the trip for all conditions. The transition trips consisted of 0.25-cm-wide (0.10-in.) bands of No. 90 carborundum grains.

Measurements

Surface-pressure measurements.- Normal force and pitching moments acting on the airfoils were determined from surface static-pressure measurements. The surface-pressure measurements were obtained from a chordwise row of orifices located approximately 0.32c from the tunnel center line. Orifices were more concentrated near the leading and trailing edges of the airfoil to define the pressure gradients in these regions. In addition, a rearward facing orifice was included in the cavity at the trailing edge (identified at an upper surface x/c location of 1.00). Actual orifice locations are included in table II. The transducers used in the differential pressure scanning valves to measure the static pressure at the airfoil surface had a range of ±68.9 kN/m^2 (10 lb/in^2).

Wake measurements.- Drag forces were determined from vertical variations of the total and static pressures measured across the wake with the profile drag rake shown in figure 5(b). The profiles, schematically illustrated in figure 7, represent the momentum losses as indicated by stagnation-pressure deficits across the wake. The middle section of these profiles reflects viscous and separation losses in the boundary layer, whereas the "wings" of the profile reflect direct losses in stagnation pressure across the shock waves.

The rake was positioned in the vertical center-line plane of the tunnel, approximately 1 chord length rearward of the trailing edge of the airfoil. The total-pressure tubes were flattened horizontally and closely spaced vertically (0.36 percent of the airfoil chord) in the region of the wake associated with skin-friction boundary-layer losses. Outside this region, the tube vertical spacing progressively widened until in the region above the wing where only shock losses were anticipated, the total-pressure tubes were spaced apart about 7.2 percent of the chord. Static-pressure tubes were distributed as shown in figure 5(b). Each static pressure measured was used over a section of the rake to determine local flow conditions in the vicinity of the static-pressure tube rather than using an average of all the static pressures measured. The rake was attached to the conventional center-line sting mount of the tunnel; this arrangement permitted it to be moved vertically to center the close concentration of tubes in the boundary-layer wake. The transducer in the differential-pressure scanning valve connected to total-pressure tubes intended to measure boundary-layer losses had a range of ±17.2 kN/m^2 (2.5 lb/in^2), and the transducers in the valves for measuring shock losses and static pressure had a range of ±6.9 kN/m^2 (1 lb/in^2).

Reduction of Data

Calculation of c_n and c_m.- Section normal-force and pitching-moment coefficients were obtained by numerical integration (based on the trapezoidal method) of the local surface-pressure coefficient measured at each orifice multiplied by an appropriate weighting factor (incremental area).

Calculation of c_d.- To obtain section drag coefficients, point drag coefficients were computed for each total-pressure measurement in the wake by using the procedure of reference 14. These point drag coefficients were then summed by numerical integration across the wake, again based on the trapezoidal method. Drag increments due to shock wave losses ($\Delta c_{d,s}$) were determined from integration of the drag measured across the wings (fig. 7) of the wake profile.

Wind-Tunnel-Wall Effects

Two major types of wind-tunnel-wall interference effects which may be treated separately are solid and wake blockage at zero lift and lift-induced interference. According to reference 17, blockage effects are theoretically small for this particular model-tunnel configuration (Mach number correction would be on the order of 0.003 at $M = 0.80$); consequently, no corrections have been applied to the data to account for blockage effects. Lift interference manifests itself as an effective upward inclination (relative to the tunnel center line) of the stream approaching the inverted model. Reference 17 indicates that this flow angularity is proportional to the amount of lift generated by the model and would result in the aerodynamic angle of attack being less than the measured geometric angle of attack. Experience has indicated, however, that the correction required to account for lift-interference effect is generally much smaller than would be predicted by the theory of reference 17. Because of this uncertainty and since the forces and moments were obtained by surface-pressure and wake measurements which would be unaffected by angular corrections, the uncorrected geometric angles of attack are used in the results presented herein. Data comparisons are made on the basis of equal normal-force coefficient rather than angle of attack.

TEST CONDITIONS

Tests were conducted at Mach numbers from 0.50 to 0.82 for a stagnation pressure of 0.1013 MN/m^2 (1 atm). The stagnation temperature of the tunnel air was automatically controlled at approximately 322 K (120° F) and the air was dried until the dewpoint in the test section was reduced sufficiently to avoid condensation effects. Resultant test Reynolds numbers based on the airfoil chord length are as shown in figure 6. Based on flat-plate skin-friction losses and assuming laminar flow to the point of fixed transition, the variation in Reynolds number indicated in figure 6 would produce an estimated decrease in drag of approximately 2 counts (c_d increment of 0.0002) between $M = 0.50$ and $M = 0.80$. This variation in drag with Mach number has not been taken into account in the data presented herein.

PRESENTATION OF RESULTS

The experimental data reported herein are presented in the following figures:

In addition to the graphical presentation of chordwise pressure distributions, the pressure distributions for airfoil 31 are presented in table II. Surface pressure distributions of airfoil 12 are presented in reference 13.

RESULTS AND DISCUSSION

Normal-Force and Pitching-Moment Characteristics

If the previously discussed angle-of-attack increment due to the choice of reference line for the two airfoils were taken into account, the curve of normal-force coefficient as a function of angle of attack for airfoil 31 in figure 8 would be displaced in the positive angle-of-attack direction by about 0.23° relative to airfoil 12. The remaining difference between the normal-force curves for the two airfoils would be due to the increased camber of airfoil 31. With this in mind, figure 8 does indicate that because of its greater aft camber, airfoil 31 generated more lift (larger normal-force coefficient) than airfoil 12 through the range of test conditions. The differences in pitching moment between the two airfoils varied with both Mach number and normal-force coefficient but was generally less than 0.01.

Drag Characteristics

The drag characteristics of the two airfoils may be divided into three primary areas of interest: first, relative drag levels at the lowest test Mach number (M = 0.50); second, drag-creep characteristics; and third, drag-divergence characteristics. The term drag creep is used herein to denote the gradual increase of drag coefficient as Mach number increases between M = 0.50 and the drag divergence Mach number at a given normal-force coefficient.

Drag characteristics at $M = 0.50$.- Figure 9 indicates substantially reduced drag levels for airfoil 31 at Mach numbers below drag divergence through the range of normal-force coefficients. At $M = 0.50$, the lower drag level of airfoil 31 is related to reduced momentum losses within the boundary layer due to less adverse pressure gradients over the airfoil. As shown in figure 11, several regions of reduced adverse pressure gradient which influence boundary-layer development are identifiable. On the upper surface there was a reduction in the magnitude of the leading-edge pressure peak (less negative pressure coefficient) due to the combined effects of smaller leading-edge radius and less positive geometric angle of attack required to achieve the same normal-force coefficient as with airfoil 12. A similar reduction in the leading-edge negative pressure coefficient occurs on the lower surface (see fig. 11(b)) at low normal-force coefficients. Reduced adverse pressure gradients may also be noted in the upper surface trailing-edge pressure recovery and on the shoulder of the lower surface (around the 65-percent chord line) leading into the lower surface cusp; both are attributable to reduced surface curvatures in these regions. (See fig. 3.) Overall, there was a more gradual pressure recompression on the upper surface of airfoil 31 from the leading-edge peak to the trailing edge, whereas on airfoil 12 there was an expansion or acceleration of the flow around the 80-percent chord line that resulted in a more negative pressure coefficient from which the flow must recover.

Drag creep.- As the Mach number increases beyond 0.50 at $c_n = 0.4$, airfoil 31 maintains an approximately 8- to 12-percent lower drag level than airfoil 12. (See fig. 9.) The drag creep characteristics of the two airfoils appear to be similar except for the delay in drag divergence Mach number of about 0.01 for airfoil 31. The gradual increase in drag coefficient starting at about $M = 0.60$ and continuing until drag divergence was due to increased viscous losses in the boundary layer since there were no discernible shock losses (fig. 10) until about $M = 0.80$. Data are not available on airfoil 12 for comparison with airfoil 31 at normal-force coefficients much below 0.4 but the drag creep of airfoil 31 appears to be greater at $c_n = 0.3$ than at $c_n = 0.4$. The more pronounced drag creep at $c_n = 0.3$ than at 0.4 was due to the sharper peak pressure distribution over the forward lower surface associated with the lower angle of attack. Compare, for example, figure 12(a) with figure 12(c) and figure 13(a) with figure 13(c).

At normal-force coefficients between 0.4 and 0.7, drag creep has been practically eliminated on airfoil 31 because of the improved recompression over the forward upper surface and suppression of the flow expansion near the 80-percent chord line. (See, for example, figs. 14(e) and 15(e).)

At a normal-force coefficient of 0.7, a peak begins to appear in the drag at $M = 0.70$ (fig. 9) and becomes more pronounced as the normal force increases beyond 0.70. This peak is due to the appearance and subsequent strengthening of the shock wave in the forward upper surface recompression (figs. 10 and 13) and to the effect of these shock waves on the boundary layer.

Although drag creep has not been entirely eliminated on airfoil 31 at the higher normal-force coefficients, the magnitude has been reduced substantially below that of airfoil 12. The falloff in drag after $M = 0.70$ for airfoil 31 may be better understood by comparing the pressure distributions for $M = 0.70$ (fig. 13(g)) and $M = 0.76$ (fig. 15(f)). Between $M = 0.70$ and $M = 0.76$, the character of the flow changes from a type with leading-edge peak followed by an abrupt recompression near the leading edge to a type where the leading-edge peak is lower and the shock is moved well to the rear. Even though the strength of the shock does not change significantly, as indicated by figure 10, the reduced pressure jump across the shock combined with the more rearward location apparently produces a less adverse shock—boundary-layer interaction with a corresponding reduction in overall drag.

The overall improvements in viscous losses in the boundary layer for airfoil 31 due to less adverse pressure gradients and shock—boundary-layer interactions are also indicated by the fact that the difference in shock losses between the two airfoils (fig. 10) do not account for the difference in total drag at Mach numbers greater than 0.70.

Drag divergence.- The Mach numbers at which drag diverges were delayed for airfoil 31 at normal-force coefficients up to about 0.6 (by approximately 0.01 at $c_n = 0.4$ and 0.02 at $c_n = 0.6$) but occurred earlier at higher normal-force coefficients. (See fig. 9.)

The pressure distributions for $M = 0.79$ shown in figures 18(b), 18(c), and 18(d) illustrate the reason for the delay in drag divergence for airfoil 31 at the lower normal-force coefficients. At this particular Mach number the curvature distribution over the rear upper surface of airfoil 12 accelerated the flow into a second supersonic pocket at the 80-percent chord line with attendant shock-wave development. (See fig. 10.) The reduced upper surface curvature over the rearmost 35 percent of airfoil 31 (fig. 3) greatly suppresses this zone of supersonic flow and thus delays drag divergence.

At normal-force coefficients greater than about 0.6, the increased upper surface curvature over the midchord region of airfoil 31 (fig. 3(a)) produces a more rapid rearward movement of the shock wave than for airfoil 12 and results in earlier drag divergence. The pressure distributions for $M = 0.78$ and a normal-force coefficient of approximately 0.8 (fig. 17(f)), for example, show higher local induced velocities over the midchord region of airfoil 31 with the shock wave in a more rearward location. As Mach number increases from 0.78 to 0.79 (fig. 18(f)), the shock wave on airfoil 31 moves further rearward and begins to merge with the trailing-edge pressure recovery with rapid increases in drag. Figure 18(f) also shows the flow expanding ahead of the shock on airfoil 31; thus, the flow enters the shock at a higher local Mach number with greater shock losses (fig. 10).

The trade-off between reduced drag levels preceding drag divergence through the range of normal-force coefficients and reduced drag divergence Mach numbers at the higher normal-force coefficients (fig. 9) calls attention to the compromises which are sometimes necessary in the design of airfoils for practical applications over a range of operating conditions.

CONCLUDING REMARKS

Refinements in a 10-percent-thick supercritical airfoil (airfoil 31) have produced significant improvements in the drag characteristics compared with an earlier supercritical airfoil (airfoil 12) designed for the same normal-force coefficient (0.7). Drag creep was practically eliminated at normal-force coefficients between about 0.4 and 0.7 and greatly reduced at other normal-force coefficients. Substantial reductions in the drag levels preceding drag divergence were also achieved at all normal-force coefficients. The Mach numbers at which drag diverges were delayed for airfoil 31 at normal-force coefficients up to about 0.6 (by approximately 0.01 and 0.02 at normal-force coefficients of 0.4 and 0.6, respectively) but occurred slightly lower at higher normal-force coefficients.

Langley Research Center,
National Aeronautics and Space Administration,
Hampton, Va., January 22, 1975.

REFERENCES

1. Whitcomb, Richard T.; and Clark, Larry R.: An Airfoil Shape for Efficient Flight at Supercritical Mach Numbers. NASA TM X-1109, 1965.
2. Whitcomb, Richard T.: Review of NASA Supercritical Airfoils. ICAS Paper No. 74-10, Aug. 1974.
3. Anon.: Supercritical Wing Technology – A Progress Report on Flight Evaluations. NASA SP-301, 1972.
4. Langhans, Richard A.; and Flechner, Stuart G.: Wind-Tunnel Investigation at Mach Numbers From 0.25 to 1.01 of a Transport Configuration Designed To Cruise at Near-Sonic Speeds. NASA TM X-2622, 1972.
5. Bartlett, Dennis W.; and Re, Richard J.: Wind-Tunnel Investigation of Basic Aerodynamic Characteristics of a Supercritical-Wing Research Airplane Configuration. NASA TM X-2470, 1972.
6. Ayers, Theodore G.: A Wind-Tunnel Investigation of the Application of the NASA Supercritical Airfoil to a Variable-Wing-Sweep Fighter Airplane. NASA TM X-2759, 1973.
7. McGhee, Robert J.; and Bingham, Gene J.: Low-Speed Aerodynamic Characteristics of a 17-Percent-Thick Supercritical Airfoil Section, Including a Comparison Between Wind-Tunnel and Flight Data. NASA TM X-2571, 1972.
8. Ferris, James C.: Static Aerodynamic Characteristics of a Model With a 17-Percent-Thick Supercritical Wing. NASA TM X-2551, 1972.
9. Harris, Charles D.: Wind-Tunnel Investigation of Effects of Trailing-Edge Geometry on a NASA Supercritical Airfoil Section. NASA TM X-2336, 1971.
10. Harris, Charles D.; and Blackwell, James A., Jr.: Wind-Tunnel Investigation of Effects of Rear Upper Surface Modification on an NASA Supercritical Airfoil. NASA TM X-2454, 1972.
11. Harris, Charles D.: Aerodynamic Characteristics of Two NASA Supercritical Airfoils With Different Maximum Thicknesses. NASA TM X-2532, 1972.
12. Harris, Charles D.: Aerodynamic Characteristics of Two 10-Percent-Thick NASA Supercritical Airfoils With Different Upper Surface Curvature Distributions. NASA TM X-2977, 1974.
13. Harris, Charles D.: Aerodynamic Characteristics of an Improved 10-Percent-Thick NASA Supercritical Airfoil. NASA TM X-2978, 1974.

14. Baals, Donald D.; and Mourhess, Mary J.: Numerical Evaluation of the Wake-Survey Equations for Subsonic Flow Including the Effect of Energy Addition. NACA WR L-5, 1945. (Formerly NACA ARR L5H27.)

15. Schaefer, William T., Jr.: Characteristics of Major Active Wind Tunnels at the Langley Research Center. NASA TM X-1130, 1965.

16. Blackwell, James A., Jr.: Preliminary Study of Effects of Reynolds Number and Boundary-Layer Transition Location on Shock-Induced Separation. NASA TN D-5003, 1969.

17. Davis, Don D., Jr.; and Moore, Dewey: Analytical Study of Blockage- and Lift-Interference Corrections for Slotted Tunnels Obtained by the Substitution of an Equivalent Homogeneous Boundary for the Discrete Slots. NACA RM L53E07b, 1953.

TABLE I. - SECTION COORDINATES

[c = 63.5 cm (25 in.); airfoil 12 has a leading-edge radius of 0.0212c; airfoil 31 has an upper surface leading-edge radius of 0.0169c and a lower surface leading-edge radius of 0.0176c]

x/c	$(y/c)_u$ Airfoil 12	$(y/c)_l$ Airfoil 12	$(y/c)_u$ Airfoil 31	$(y/c)_l$ Airfoil 31
0.0	0.0	0.0	0.0	0.0
.01	.0181	-.0182	.0159	-.0164
.02	.0232	-.0237	.0209	-.0215
.03	.0267	-.0274	.0244	-.0250
.04	.0294	-.0304	.0271	-.0274
.05	.0316	-.0328	.0294	-.0295
.06	.0335	-.0348	.0313	-.0314
.07	.0351	-.0365	.0329	-.0330
.08	.0366	-.0381	.0344	-.0344
.09	.0378	-.0394	.0357	-.0358
.10	.0390	-.0406	.0369	-.0370
.11	.0401	-.0417	.0380	-.0381
.12	.0410	-.0427	.0391	-.0392
.13	.0419	-.0435	.0401	-.0402
.14	.0427	-.0443	.0410	-.0411
.15	.0434	-.0450	.0418	-.0420
.16	.0440	-.0457	.0426	-.0427
.17	.0447	-.0462	.0433	-.0434
.18	.0452	-.0468	.0440	-.0440
.19	.0457	-.0472	.0446	-.0446
.20	.0462	-.0476	.0452	-.0452
.21	.0466	-.0480	.0457	-.0457
.22	.0470	-.0484	.0462	-.0462
.23	.0474	-.0487	.0467	-.0467
.24	.0477	-.0489	.0471	-.0471
.25	.0480	-.0492	.0475	-.0475
.26	.0483	-.0494	.0478	-.0479
.27	.0486	-.0495	.0481	-.0482
.28	.0488	-.0497	.0484	-.0485
.29	.0490	-.0498	.0487	-.0488
.30	.0492	-.0499	.0489	-.0491

TABLE I. - SECTION COORDINATES – Continued

x/c	$(y/c)_u$	$(y/c)_l$	$(y/c)_u$	$(y/c)_l$
	Airfoil 12		Airfoil 31	
0.31	0.0493	-0.0499	0.0491	-0.0493
.32	.0495	-.0500	.0493	-.0495
.33	.0496	-.0500	.0495	-.0497
.34	.0497	-.0500	.0497	-.0498
.35	.0498	-.0500	.0498	-.0499
.36	.0499	-.0499	.0499	-.0499
.37	.0499	-.0499	.0500	-.0499
.38	.0500	-.0498	.0500	-.0499
.39	.0500	-.0497	.0500	-.0498
.40	.0500	-.0495	.0500	-.0497
.41	.0500	-.0494	.0500	-.0495
.42	.0500	-.0492	.0500	-.0493
.43	.0499	-.0490	.0499	-.0491
.44	.0499	-.0488	.0498	-.0488
.45	.0498	-.0486	.0497	-.0485
.46	.0498	-.0483	.0495	-.0482
.47	.0497	-.0480	.0493	-.0478
.48	.0496	-.0476	.0491	-.0474
.49	.0495	-.0472	.0489	-.0470
.50	.0493	-.0468	.0487	-.0465
.51	.0492	-.0463	.0485	-.0459
.52	.0490	-.0458	.0482	-.0453
.53	.0489	-.0452	.0479	-.0446
.54	.0487	-.0446	.0476	-.0439
.55	.0485	-.0438	.0473	-.0431
.56	.0482	-.0430	.0469	-.0422
.57	.0480	-.0421	.0465	-.0413
.58	.0478	-.0411	.0461	-.0403
.59	.0475	-.0400	.0457	-.0392
.60	.0472	-.0388	.0453	-.0381
.61	.0469	-.0375	.0448	-.0369
.62	.0465	-.0360	.0443	-.0356
.63	.0462	-.0343	.0438	-.0342
.64	.0458	-.0325	.0433	-.0327
.65	.0454	-.0305	.0428	-.0311

TABLE I.- SECTION COORDINATES – Concluded

x/c	$(y/c)_u$	$(y/c)_l$	$(y/c)_u$	$(y/c)_l$
	Airfoil 12		Airfoil 31	
0.66	0.0450	-0.0282	0.0422	-0.0294
.67	.0445	-.0258	.0416	-.0277
.68	.0440	-.0234	.0409	-.0260
.69	.0435	-.0210	.0402	-.0242
.70	.0430	-.0188	.0395	-.0224
.71	.0424	-.0167	.0387	-.0206
.72	.0418	-.0146	.0379	-.0188
.73	.0411	-.0126	.0371	-.0171
.74	.0404	-.0107	.0363	-.0154
.75	.0397	-.0090	.0354	-.0137
.76	.0389	-.0073	.0345	-.0121
.77	.0380	-.0057	.0336	-.0105
.78	.0371	-.0042	.0326	-.0089
.79	.0361	-.0028	.0315	-.0074
.80	.0351	-.0015	.0304	-.0060
.81	.0340	-.0003	.0292	-.0047
.82	.0329	.0007	.0280	-.0035
.83	.0316	.0017	.0267	-.0024
.84	.0303	.0025	.0254	-.0014
.85	.0289	.0031	.0240	-.0006
.86	.0275	.0036	.0225	0.0
.87	.0259	.0040	.0210	.0005
.88	.0242	.0042	.0194	.0007
.89	.0224	.0042	.0176	.0007
.90	.0206	.0040	.0157	.0005
.91	.0186	.0036	.0137	.0001
.92	.0164	.0030	.0116	-.0005
.93	.0142	.0021	.0093	-.0014
.94	.0118	.0010	.0069	-.0026
.95	.0093	-.0005	.0044	-.0041
.96	.0066	-.0022	.0019	-.0059
.97	.0038	-.0043	-.0008	-.0080
.98	.0008	-.0067	-.0037	-.0105
.99	-.0024	-.0095	-.0068	-.0133
1.00	-----	-.0127	-----	-.0164

TABLE II. - SURFACE PRESSURE DISTRIBUTIONS FOR SUPERCRITICAL AIRFOIL 31

(a) α = -1.9°

	CP AT -											
X/C	M=0.50	M=0.60	M=0.70	M=0.74	M=0.76	M=0.77	M=0.78	M=0.79	M=0.80	M=0.81	M=0.82	X/C
UPPER SURFACE												
0.000	1.063	1.084	1.118	1.135	1.143		1.151	1.152	1.162	1.162	1.166	0.000
.002	.513	.593	.691	.747	.750		.755	.781	.785	.791	.797	.002
.011	-.040	.022	.162	.180	.214		.239	.256	.268	.280	.263	.011
.015	-.146	-.091	-.006	.049	.069		.086	.119	.118	.146	.146	.015
.029	-.287	-.260	-.189	-.175	-.148		-.125	-.105	-.089	-.090	-.071	.029
.044	-.293	-.278	-.256	-.236	-.213		-.192	-.168	-.161	-.162	-.145	.044
.069	-.309	-.298	-.276	-.264	-.250		-.239	-.225	-.221	-.201	-.194	.069
.098	-.349	-.349	-.354	-.344	-.336		-.342	-.325	-.329	-.324	-.310	.098
.147	-.320	-.325	-.330	-.330	-.328		-.325	-.320	-.319	-.317	-.315	.147
.199	-.325	-.332	-.343	-.350	-.352		-.349	-.354	-.356	-.350	-.345	.199
.248	-.327	-.337	-.360	-.372	-.374		-.375	-.374	-.379	-.380	-.374	.248
.298	-.320	-.330	-.332	-.350	-.354		-.356	-.362	-.362	-.354	-.349	.298
.348	-.315	-.334	-.355	-.369	-.376		-.390	-.395	-.398	-.397	-.392	.348
.399	-.321	-.335	-.363	-.387	-.397		-.410	-.415	-.427	-.433	-.451	.399
.448	-.329	-.347	-.376	-.397	-.410		-.430	-.440	-.447	-.442	-.467	.448
.497	-.329	-.346	-.376	-.396	-.410		-.431	-.440	-.440	-.492	-.488	.497
.547	-.346	-.365	-.397	-.423	-.441		-.463	-.478	-.491	-.492	-.496	.547
.599	-.345	-.366	-.402	-.434	-.443		-.474	-.489	-.524	-.518	-.527	.599
.648	-.348	-.365	-.402	-.430	-.452		-.478	-.485	-.530	-.551	-.550	.648
.699	-.361	-.381	-.431	-.462	-.479		-.517	-.534	-.529	-.588	-.590	.699
.750	-.369	-.399	-.442	-.476	-.500		-.560	-.588	-.614	-.653	-.661	.750
.799	-.379	-.405	-.444	-.474	-.493		-.531	-.552	-.670	-.716	-.727	.799
.848	-.371	-.389	-.417	-.437	-.441		-.450	-.442	-.431	-.494	-.673	.848
.899	-.325	-.328	-.344	-.343	-.334		-.325	-.314	-.298	-.261	-.228	.899
.950	-.179	-.168	-.145	-.133	-.117		-.105	-.090	-.082	-.068	-.065	.950
.969	-.113	-.095	-.068	-.049	-.042		-.034	-.019	-.017	-.014	-.019	.969
.980	-.068	-.050	-.020	-.010	.002		.010	.019	.020	.013	.003	.980
.989	-.029	-.011	.016	.026	.036		.043	.049	.044	.034	.019	.989
1.000	.007	.022	.041	.047	.058		.055	.061	.054	.045	.024	1.000
LOWER SURFACE												
.007	.005	-.065	-.006	.020	.027		.034	.063	.097	.069	.103	.007
.011	-.278	-.343	-.366	-.367	-.333		-.300	-.281	-.271	-.235	-.220	.011
.020	-.418	-.485	-.583	-.571	-.574		-.555	-.531	-.521	-.495	-.444	.020
.030	-.465	-.545	-.627	-.703	-.734		-.739	-.737	-.706	-.695	-.665	.030
.046	-.413	-.477	-.577	-.606	-.646		-.725	-.746	-.762	-.719	-.713	.046
.068	-.364	-.418	-.486	-.517	-.554		-.611	-.661	-.677	-.664	-.660	.068
.100	-.334	-.394	-.461	-.498	-.529		-.577	-.583	-.601	-.651	-.646	.100
.150	-.304	-.349	-.416	-.448	-.501		-.552	-.602	-.630	-.622	-.646	.150
.200	-.271	-.322	-.367	-.396	-.419		-.463	-.503	-.601	-.646	-.651	.200
.250	-.246	-.304	-.343	-.388	-.401		-.432	-.419	-.371	-.641	-.659	.250
.300	-.256	-.313	-.346	-.386	-.408		-.446	-.463	-.459	-.579	-.664	.300
.349	-.255	-.307	-.348	-.374	-.410		-.455	-.475	-.501	-.431	-.652	.349
.400	-.236	-.268	-.298	-.326	-.356		-.377	-.379	-.388	-.399	-.632	.400
.450	-.226	-.260	-.289	-.321	-.335		-.366	-.354	-.363	-.362	-.291	.450
.501	-.211	-.233	-.269	-.284	-.297		-.314	-.304	-.315	-.320	-.292	.501
.551	-.190	-.213	-.240	-.252	-.261		-.276	-.261	-.275	-.265	-.260	.551
.600	-.140	-.156	-.164	-.159	-.167		-.174	-.160	-.163	-.161	-.157	.600
.650	-.025	-.046	-.032	-.014	-.014		-.016	-.004	-.007	.005	.014	.650
.700	.122	.107	.134	.149	.156		.152	.160	.166	.176	.183	.700
.751	.237	.225	.252	.256	.275		.263	.281	.290	.298	.304	.751
.801	.308	.303	.331	.344	.354		.348	.356	.366	.388	.383	.801
.852	.375	.373	.396	.409	.404		.406	.420	.425	.454	.451	.852
.901	.421	.403	.424	.451	.449		.451	.455	.468	.497	.497	.901
.930	.413	.405	.432	.434	.445		.456	.457	.473	.489	.483	.930
.949	.394	.397	.413	.430	.433		.424	.459	.453	.468	.465	.949
.967	.339	.342	.370	.392	.394		.398	.405	.413	.419	.423	.967
.990	.208	.205	.225	.243	.249		.248	.260	.264	.261	.254	.990
.998	.003	.001	.017	.030	.026		.024	.038	.034	.023	.009	.998

[redacted]

TABLE II. - SURFACE PRESSURE DISTRIBUTIONS FOR SUPERCRITICAL AIRFOIL 31 - Continued

(b) $\alpha = -0.9^{\circ}$

	CP AT -											
X/C	M=0.50	M=0.60	M=0.70	M=0.74	M=0.76	M=0.77	M=0.78	M=0.79	M=0.80	M=0.81	M=0.82	X/C
UPPER SURFACE												
0.000	1.072	1.098	1.137	1.153	1.159		1.170	1.176	1.173	1.179	1.182	0.000
.002	.222	.307	.452	.527	.550		.589	.613	.622	.637	.659	.002
.011	-.326	-.274	-.163	-.080	-.044		.000	.024	.050	.079	.110	.011
.015	-.426	-.404	-.276	-.206	-.169		-.135	-.114	-.097	-.069	-.037	.015
.029	-.536	-.504	-.457	-.391	-.390		-.356	-.325	-.303	-.267	-.246	.029
.044	-.491	-.480	-.461	-.441	-.426		-.405	-.383	-.357	-.341	-.309	.044
.069	-.467	-.467	-.451	-.444	-.427		-.418	-.407	-.398	-.375	-.331	.069
.098	-.475	-.431	-.507	-.530	-.532		-.527	-.521	-.514	-.495	-.464	.098
.147	-.421	-.436	-.458	-.468	-.467		-.484	-.482	-.466	-.459	-.445	.147
.199	-.406	-.432	-.449	-.457	-.478		-.485	-.483	-.481	-.478	-.454	.199
.248	-.383	-.404	-.449	-.469	-.485		-.497	-.506	-.507	-.512	-.503	.248
.298	-.380	-.401	-.420	-.434	-.447		-.448	-.492	-.518	-.516	-.509	.298
.348	-.369	-.400	-.424	-.443	-.465		-.476	-.478	-.448	-.478	-.493	.348
.399	-.369	-.398	-.431	-.455	-.473		-.494	-.535	-.527	-.489	-.506	.399
.448	-.372	-.400	-.430	-.463	-.482		-.513	-.500	-.559	-.535	-.510	.448
.497	-.364	-.395	-.431	-.455	-.477		-.499	-.543	-.591	-.586	-.561	.497
.547	-.375	-.401	-.447	-.476	-.503		-.540	-.528	-.582	-.594	-.585	.547
.599	-.372	-.403	-.449	-.476	-.505		-.546	-.573	-.580	-.621	-.592	.599
.648	-.371	-.401	-.440	-.474	-.504		-.531	-.591	-.582	-.653	-.644	.648
.699	-.384	-.417	-.463	-.499	-.530		-.564	-.576	-.620	-.682	-.675	.699
.750	-.393	-.427	-.470	-.506	-.545		-.602	-.621	-.671	-.724	-.745	.750
.799	-.399	-.429	-.472	-.495	-.521		-.553	-.593	-.689	-.802	-.810	.799
.848	-.376	-.406	-.433	-.446	-.457		-.455	-.443	-.410	-.405	-.472	.848
.899	-.328	-.346	-.352	-.347	-.341		-.325	-.312	-.288	-.241	-.206	.899
.950	-.169	-.177	-.152	-.130	-.119		-.104	-.095	-.084	-.069	-.071	.950
.969	-.108	-.101	-.075	-.053	-.046		-.035	-.027	-.022	-.021	-.036	.969
.980	-.062	-.055	-.028	-.010	-.008		.005	.007	.008	.005	-.023	.980
.989	-.026	-.019	.009	.023	.021		.032	.033	.030	.026	-.009	.989
1.000	.006	.013	.034	.039	.043		.044	.044	.041	.034	.003	1.000
LOWER SURFACE												
.007	.286	.280	.264	.272	.276		.288	.276	.290	.273	.263	.007
.011	.026	.017	-.013	-.038	-.028		-.037	-.046	-.038	-.032	-.046	.011
.020	-.175	-.180	-.214	-.235	-.254		-.254	-.261	-.274	-.278	-.284	.020
.030	-.248	-.254	-.336	-.363	-.383		-.396	-.403	-.414	-.420	-.449	.030
.046	-.224	-.262	-.310	-.362	-.361		-.386	-.400	-.419	-.443	-.450	.046
.068	-.219	-.253	-.295	-.318	-.333		-.353	-.367	-.376	-.389	-.416	.068
.100	-.228	-.237	-.300	-.320	-.345		-.367	-.377	-.388	-.405	-.439	.100
.150	-.230	-.256	-.302	-.315	-.332		-.360	-.387	-.403	-.428	-.493	.150
.200	-.210	-.238	-.284	-.302	-.316		-.332	-.344	-.366	-.390	-.431	.200
.250	-.217	-.232	-.269	-.286	-.303		-.327	-.343	-.360	-.375	-.413	.250
.300	-.206	-.212	-.258	-.281	-.293		-.310	-.314	-.334	-.345	-.370	.300
.349	-.209	-.225	-.263	-.289	-.302		-.329	-.348	-.369	-.391	-.455	.349
.400	-.188	-.193	-.237	-.254	-.265		-.284	-.302	-.313	-.318	-.352	.400
.450	-.194	-.200	-.245	-.248	-.267		-.273	-.292	-.312	-.311	-.338	.450
.501	-.183	-.182	-.219	-.227	-.244		-.251	-.262	-.277	-.280	-.299	.501
.551	-.170	-.176	-.200	-.213	-.213		-.226	-.226	-.231	-.237	-.249	.551
.600	-.126	-.126	-.135	-.132	-.135		-.147	-.137	-.140	-.144	-.150	.600
.650	-.020	-.007	-.002	.004	.006		.009	.009	.008	.019	.004	.650
.700	.126	.146	.158	.172	.177		.174	.180	.182	.182	.183	.700
.751	.232	.258	.284	.290	.295		.297	.305	.307	.313	.301	.751
.801	.326	.353	.369	.378	.380		.383	.388	.392	.399	.389	.801
.852	.398	.417	.440	.453	.456		.453	.454	.462	.463	.456	.852
.901	.430	.455	.468	.490	.487		.497	.502	.508	.507	.497	.901
.930	.415	.437	.457	.481	.481		.494	.485	.489	.495	.487	.930
.949	.391	.417	.440	.461	.462		.463	.478	.473	.475	.471	.949
.967	.337	.377	.393	.406	.413		.418	.420	.421	.424	.414	.967
.990	.193	.215	.234	.251	.248		.256	.261	.260	.262	.239	.990
.998	-.029	-.039	.007	.012	.014		.017	.011	.008	.009	-.036	.998

TABLE II. - SURFACE PRESSURE DISTRIBUTIONS FOR SUPERCRITICAL AIRFOIL 31 - Continued

(c) $\alpha = -0.4^{\circ}$

	CP AT -											
X/C	M=0.50	M=0.60	M=0.70	M=0.74	M=0.76	M=0.77	M=0.78	M=0.79	M=0.80	M=0.81	M=0.82	X/C
					UPPER SURFACE							
0.000	1.053	1.092	1.139	1.149	1.155		1.169	1.175	1.179	1.182	1.187	0.000
.002	.091	.189	.320	.398	.447		.488	.517	.539	.574	.603	.002
.011	-.502	-.411	-.300	-.206	-.164		-.118	-.076	-.056	-.023	.034	.011
.015	-.585	-.506	-.418	-.332	-.299		-.240	-.234	-.168	-.144	-.107	.015
.029	-.636	-.624	-.589	-.569	-.515		-.465	-.441	-.411	-.382	-.326	.029
.044	-.581	-.593	-.571	-.576	-.546		-.509	-.479	-.470	-.438	-.403	.044
.069	-.526	-.537	-.542	-.544	-.538		-.520	-.490	-.483	-.430	-.418	.069
.098	-.532	-.562	-.593	-.604	-.623		-.625	-.605	-.577	-.553	-.522	.098
.147	-.471	-.492	-.517	-.537	-.548		-.551	-.598	-.586	-.556	-.538	.147
.199	-.427	-.453	-.496	-.526	-.534		-.545	-.557	-.563	-.552	-.546	.199
.248	-.414	-.435	-.474	-.517	-.538		-.559	-.572	-.572	-.559	-.544	.248
.298	-.411	-.442	-.481	-.485	-.494		-.564	-.571	-.580	-.580	-.562	.298
.348	-.404	-.423	-.467	-.489	-.508		-.516	-.474	-.540	-.554	-.559	.348
.399	-.399	-.428	-.470	-.494	-.515		-.575	-.560	-.563	-.561	-.569	.399
.448	-.396	-.423	-.462	-.498	-.521		-.554	-.590	-.562	-.594	-.566	.448
.497	-.385	-.409	-.461	-.482	-.509		-.553	-.609	-.608	-.594	-.614	.497
.547	-.390	-.422	-.472	-.502	-.533		-.559	-.611	-.609	-.625	-.607	.547
.599	-.384	-.415	-.466	-.499	-.528		-.580	-.585	-.644	-.646	-.642	.599
.648	-.381	-.418	-.460	-.494	-.521		-.560	-.592	-.676	-.666	-.671	.648
.599	-.393	-.429	-.479	-.512	-.549		-.572	-.600	-.707	-.687	-.707	.699
.750	-.400	-.435	-.484	-.522	-.562		-.626	-.635	-.742	-.769	-.756	.750
.799	-.403	-.434	-.477	-.502	-.524		-.562	-.583	-.710	-.819	-.834	.799
.848	-.385	-.404	-.440	-.451	-.459		-.454	-.441	-.389	-.383	-.409	.848
.899	-.329	-.342	-.349	-.343	-.339		-.325	-.308	-.266	-.223	-.191	.899
.950	-.170	-.163	-.149	-.133	-.120		-.105	-.097	-.075	-.066	-.080	.950
.969	-.105	-.096	-.071	-.055	-.045		-.034	-.031	-.019	-.026	-.051	.969
.980	-.059	-.053	-.025	-.016	-.010		.004	.005	.002	-.000	-.041	.980
.989	-.023	-.011	.309	.018	.023		.027	.028	.023	.019	-.031	.989
1.000	.003	.018	.028	.038	.038		.040	.042	.035	.026	-.022	1.000
					LOWER SURFACE							
.007	.413	.392	.399	.391	.390		.391	.386	.379	.353	.354	.007
.011	.128	.121	.129	.109	.094		.089	.075	.067	.051	.047	.011
.020	-.036	-.085	-.084	-.124	-.125		-.119	-.146	-.144	-.152	-.190	.020
.030	-.127	-.185	-.206	-.246	-.249		-.270	-.261	-.313	-.317	-.337	.030
.046	-.139	-.178	-.214	-.230	-.255		-.275	-.279	-.300	-.309	-.341	.046
.068	-.148	-.176	-.210	-.221	-.237		-.248	-.275	-.276	-.296	-.302	.068
.100	-.171	-.195	-.230	-.251	-.259		-.271	-.293	-.300	-.333	-.338	.100
.150	-.184	-.200	-.242	-.269	-.272		-.288	-.304	-.328	-.338	-.367	.150
.200	-.172	-.199	-.221	-.244	-.262		-.277	-.287	-.303	-.329	-.346	.200
.250	-.177	-.204	-.221	-.247	-.266		-.284	-.284	-.306	-.316	-.350	.250
.300	-.182	-.189	-.210	-.236	-.236		-.251	-.272	-.293	-.306	-.337	.300
.349	-.172	-.198	-.227	-.254	-.266		-.288	-.293	-.322	-.345	-.420	.349
.400	-.157	-.168	-.201	-.222	-.231		-.247	-.261	-.272	-.291	-.321	.400
.450	-.167	-.178	-.202	-.226	-.231		-.247	-.254	-.266	-.295	-.320	.450
.501	-.154	-.165	-.192	-.203	-.218		-.230	-.234	-.245	-.259	-.286	.501
.551	-.151	-.162	-.182	-.189	-.188		-.195	-.210	-.218	-.230	-.242	.551
.600	-.097	-.104	-.110	-.116	-.120		-.118	-.127	-.126	-.141	-.143	.600
.650	-.006	-.002	.013	.012	.020		.025	.026	.024	.014	.015	.650
.700	.129	.149	.167	.177	.187		.190	.182	.194	.188	.182	.700
.751	.245	.256	.282	.295	.301		.313	.313	.312	.308	.302	.751
.801	.332	.350	.380	.388	.396		.401	.398	.400	.397	.394	.801
.852	.402	.422	.455	.451	.464		.475	.466	.470	.463	.463	.852
.901	.440	.448	.483	.489	.501		.512	.506	.507	.498	.500	.901
.930	.417	.440	.474	.478	.488		.501	.501	.497	.495	.488	.930
.949	.410	.413	.453	.454	.466		.478	.477	.479	.473	.470	.949
.967	.347	.365	.409	.410	.417		.426	.429	.428	.421	.413	.967
.990	.195	.213	.234	.242	.256		.262	.262	.260	.247	.233	.990
.998	-.020	-.016	.003	.007	.011		.012	.015	.007	-.815	-.056	.998

TABLE II. - SURFACE PRESSURE DISTRIBUTIONS FOR SUPERCRITICAL AIRFOIL 31 - Continued

(d) α = 0.1°

	CP AT -											
X/C	M=0.50	M=0.60	M=0.70	M=0.74	M=0.76	M=0.77	M=0.78	M=0.79	M=0.80	M=0.81	M=0.82	X/C
UPPER SURFACE												
0.000	1.010	1.063	1.112	1.135	1.151		1.160	1.171	1.171	1.178	1.179	0.000
.002	-.097	.020	.169	.275	.331		.364	.398	.434	.469	.476	.002
.011	-.699	-.633	-.482	-.364	-.327		-.261	-.214	-.197	-.129	-.110	.011
.015	-.767	-.752	-.623	-.498	-.444		-.388	-.330	-.311	-.255	-.225	.015
.029	-.771	-.815	-.778	-.727	-.697		-.604	-.583	-.544	-.481	-.453	.029
.044	-.704	-.722	-.737	-.721	-.708		-.694	-.644	-.606	-.537	-.509	.044
.069	-.607	-.647	-.680	-.693	-.660		-.638	-.606	-.575	-.543	-.483	.069
.098	-.621	-.651	-.701	-.754	-.745		-.735	-.715	-.675	-.635	-.597	.098
.147	-.499	-.527	-.605	-.638	-.687		-.712	-.714	-.655	-.637	-.609	.147
.199	-.484	-.517	-.549	-.593	-.619		-.704	-.687	-.670	-.641	-.616	.199
.248	-.462	-.492	-.531	-.553	-.560		-.684	-.697	-.675	-.656	-.640	.248
.298	-.450	-.485	-.535	-.566	-.582		-.695	-.708	-.687	-.668	-.660	.298
.348	-.435	-.463	-.514	-.550	-.574		-.596	-.699	-.695	-.673	-.664	.348
.399	-.428	-.453	-.506	-.541	-.573		-.514	-.688	-.704	-.698	-.679	.399
.448	-.426	-.448	-.497	-.537	-.563		-.560	-.642	-.698	-.691	-.678	.448
.497	-.410	-.430	-.484	-.518	-.537		-.615	-.582	-.710	-.713	-.700	.497
.547	-.417	-.441	-.495	-.532	-.562		-.637	-.605	-.724	-.737	-.727	.547
.599	-.408	-.432	-.490	-.529	-.556		-.604	-.621	-.683	-.728	-.737	.599
.648	-.404	-.428	-.480	-.518	-.541		-.586	-.617	-.688	-.714	-.733	.648
.699	-.412	-.438	-.496	-.533	-.561		-.588	-.620	-.738	-.755	-.751	.699
.750	-.409	-.440	-.497	-.535	-.563		-.627	-.675	-.780	-.806	-.825	.750
.799	-.413	-.436	-.483	-.508	-.530		-.558	-.643	-.561	-.879	-.880	.799
.848	-.391	-.408	-.444	-.448	-.455		-.448	-.427	-.369	-.348	-.342	.848
.899	-.330	-.339	-.349	-.340	-.330		-.315	-.296	-.254	-.196	-.191	.899
.950	-.170	-.159	-.145	-.123	-.111		-.100	-.087	-.072	-.066	-.092	.950
.969	-.101	-.091	-.068	-.051	-.042		-.031	-.023	-.018	-.031	-.065	.969
.980	-.060	-.050	-.024	-.015	-.007		.002	.004	.011	-.009	-.053	.980
.989	-.026	-.014	.002	.016	.022		.028	.029	.026	.006	-.046	.989
1.000	.005	.015	.025	.032	.032		.040	.039	.037	.011	-.036	1.000
LOWER SURFACE												
.007	.557	.529	.534	.530	.507		.501	.498	.493	.479	.464	.007
.011	.254	.257	.265	.241	.224		.232	.217	.204	.179	.188	.011
.020	.088	.065	.056	.021	.032		.038	.001	.012	-.028	-.031	.020
.030	-.026	-.037	-.066	-.109	-.118		-.109	-.154	-.135	-.179	-.192	.030
.046	-.066	-.063	-.102	-.131	-.132		-.148	-.156	-.164	-.210	-.216	.046
.068	-.071	-.080	-.110	-.139	-.142		-.133	-.161	-.163	-.198	-.211	.068
.100	-.103	-.118	-.144	-.160	-.178		-.175	-.194	-.202	-.226	-.264	.100
.150	-.120	-.143	-.167	-.191	-.206		-.208	-.222	-.231	-.257	-.300	.150
.200	-.127	-.145	-.167	-.194	-.197		-.201	-.217	-.224	-.246	-.280	.200
.250	-.135	-.148	-.167	-.195	-.201		-.205	-.231	-.233	-.258	-.288	.250
.300	-.142	-.148	-.163	-.191	-.196		-.191	-.218	-.220	-.252	-.275	.300
.349	-.145	-.164	-.182	-.204	-.219		-.225	-.252	-.256	-.293	-.319	.349
.400	-.129	-.141	-.160	-.188	-.192		-.204	-.219	-.221	-.245	-.269	.400
.450	-.138	-.158	-.173	-.194	-.202		-.204	-.222	-.224	-.250	-.271	.450
.501	-.132	-.147	-.157	-.182	-.186		-.189	-.201	-.208	-.224	-.254	.501
.551	-.124	-.136	-.150	-.168	-.173		-.171	-.183	-.188	-.205	-.217	.551
.600	-.089	-.084	-.079	-.097	-.104		-.101	-.107	-.100	-.117	-.133	.600
.650	.012	.015	.028	.025	.025		.038	.033	.041	.032	.022	.650
.700	.146	.158	.181	.185	.190		.202	.195	.204	.198	.188	.700
.751	.250	.268	.302	.303	.312		.324	.320	.331	.317	.313	.751
.801	.337	.359	.392	.397	.398		.420	.407	.408	.408	.394	.801
.852	.410	.432	.457	.462	.466		.486	.470	.481	.478	.470	.852
.901	.441	.457	.496	.497	.503		.524	.515	.519	.508	.504	.901
.930	.424	.451	.481	.484	.490		.513	.500	.508	.502	.488	.930
.949	.399	.422	.453	.465	.469		.478	.487	.489	.481	.469	.949
.967	.357	.372	.412	.408	.418		.431	.431	.437	.429	.406	.967
.990	.194	.212	.243	.249	.251		.271	.261	.262	.249	.225	.990
.998	-.018	-.013	.004	-.003	.006		.011	.010	.013	-.022	-.064	.998

TABLE II. - SURFACE PRESSURE DISTRIBUTIONS FOR SUPERCRITICAL AIRFOIL 31 - Continued

(e) $\alpha = 0.6°$

	CP AT -											
X/C	M=0.50	M=0.60	M=0.70	M=0.74	M=0.76	M=0.77	M=0.78	M=0.79	M=0.80	M=0.81	M=0.82	X/C
UPPER SURFACE												
0.000	.948	1.009	1.078	1.114	1.127	1.139	1.138	1.147	1.159	1.166		0.000
.002	-.334	-.218	.040	.124	.204	.239	.267	.299	.346	.379		.002
.011	-.960	-.873	-.634	-.535	-.474	-.419	-.379	-.330	-.273	-.228		.011
.015	-.951	-.925	-.768	-.658	-.578	-.547	-.497	-.441	-.384	-.347		.015
.029	-.942	-.940	-1.005	-.902	-.813	-.779	-.746	-.689	-.648	-.589		.029
.044	-.821	-.866	-.956	-.950	-.896	-.849	-.829	-.782	-.738	-.671		.044
.069	-.727	-.754	-.825	-.848	-.805	-.782	-.771	-.723	-.645	-.610		.069
.098	-.655	-.717	-.824	-.887	-.858	-.838	-.812	-.773	-.737	-.694		.098
.147	-.562	-.592	-.648	-.781	-.864	-.867	-.842	-.810	-.772	-.713		.147
.199	-.533	-.564	-.618	-.607	-.808	-.808	-.794	-.766	-.740	-.693		.199
.248	-.503	-.531	-.595	-.618	-.768	-.781	-.792	-.778	-.752	-.717		.248
.298	-.489	-.514	-.583	-.640	-.716	-.770	-.808	-.781	-.768	-.733		.298
.348	-.468	-.496	-.553	-.603	-.504	-.732	-.781	-.779	-.759	-.731		.348
.399	-.452	-.489	-.542	-.580	-.593	-.486	-.772	-.774	-.763	-.742		.399
.448	-.440	-.476	-.533	-.571	-.594	-.561	-.769	-.776	-.770	-.752		.448
.497	-.427	-.462	-.515	-.551	-.579	-.587	-.792	-.798	-.787	-.771		.497
.547	-.433	-.465	-.519	-.561	-.592	-.597	-.617	-.816	-.818	-.798		.547
.599	-.422	-.456	-.502	-.548	-.590	-.616	-.484	-.831	-.836	-.819		.599
.648	-.416	-.446	-.493	-.537	-.567	-.581	-.543	-.809	-.860	-.848		.648
.699	-.424	-.453	-.502	-.546	-.582	-.586	-.604	-.593	-.864	-.854		.699
.750	-.418	-.455	-.505	-.542	-.579	-.609	-.662	-.465	-.890	-.907		.750
.799	-.415	-.442	-.489	-.512	-.532	-.543	-.567	-.471	-.468	-.669		.799
.848	-.389	-.413	-.443	-.447	-.454	-.455	-.448	-.426	-.319	-.311		.848
.899	-.325	-.345	-.338	-.334	-.326	-.322	-.322	-.295	-.220	-.188		.899
.950	-.168	-.163	-.135	-.123	-.110	-.104	-.107	-.085	-.065	-.089		.950
.969	-.102	-.090	-.063	-.054	-.037	-.035	-.034	-.020	-.020	-.058		.969
.980	-.059	-.050	-.024	-.016	-.006	-.000	.000	.013	-.001	-.041		.980
.989	-.020	-.014	.006	.013	.022	.024	.027	.037	.023	-.039		.989
1.000	.004	.012	.023	.025	.037	.036	.043	.052	.031	-.023		1.000
LOWER SURFACE												
.007	.654	.651	.659	.623	.600	.606	.619	.599	.568	.574		.007
.011	.399	.416	.370	.378	.338	.335	.335	.325	.313	.284		.011
.020	.226	.198	.160	.163	.158	.141	.133	.118	.094	.081		.020
.030	.074	.054	.029	.021	.002	.015	-.005	-.027	-.050	-.069		.030
.046	.043	.008	-.006	-.023	-.044	-.043	-.038	-.061	-.075	-.098		.046
.068	.005	.001	-.012	-.049	-.053	-.061	-.056	-.066	-.072	-.109		.068
.100	-.032	-.051	-.069	-.083	-.101	-.096	-.097	-.106	-.133	-.153		.100
.150	-.073	-.078	-.107	-.119	-.136	-.129	-.139	-.155	-.171	-.194		.150
.200	-.082	-.101	-.120	-.134	-.144	-.136	-.137	-.147	-.169	-.201		.200
.250	-.098	-.113	-.124	-.141	-.159	-.150	-.162	-.170	-.184	-.208		.250
.300	-.109	-.109	-.126	-.138	-.154	-.149	-.159	-.160	-.174	-.205		.300
.349	-.118	-.125	-.147	-.169	-.180	-.188	-.185	-.193	-.202	-.243		.349
.400	-.100	-.117	-.129	-.151	-.166	-.155	-.161	-.173	-.191	-.211		.400
.450	-.118	-.123	-.144	-.159	-.176	-.164	-.173	-.177	-.200	-.223		.450
.501	-.108	-.119	-.134	-.145	-.163	-.154	-.161	-.160	-.185	-.195		.501
.551	-.111	-.115	-.131	-.136	-.145	-.139	-.145	-.156	-.160	-.175		.551
.600	-.063	-.066	-.069	-.073	-.088	-.072	-.077	-.077	-.089	-.098		.600
.650	.025	.035	.038	.048	.043	.049	.055	.054	.053	.040		.650
.700	.163	.174	.192	.200	.198	.208	.214	.214	.209	.208		.700
.751	.263	.283	.309	.314	.320	.323	.330	.336	.335	.320		.751
.801	.354	.369	.398	.406	.405	.415	.417	.425	.420	.415		.801
.852	.414	.436	.468	.474	.472	.486	.489	.489	.491	.483		.852
.901	.444	.468	.500	.504	.504	.522	.522	.519	.520	.505		.901
.930	.434	.455	.489	.492	.499	.510	.512	.510	.513	.505		.930
.949	.413	.435	.462	.472	.476	.480	.491	.496	.494	.478		.949
.967	.353	.382	.407	.420	.420	.440	.440	.446	.435	.422		.967
.990	.199	.218	.244	.252	.248	.263	.267	.272	.258	.238		.990
.998	-.025	-.018	-.001	.002	-.005	.013	.013	.017	-.001	-.053		.998

TABLE II. - SURFACE PRESSURE DISTRIBUTIONS FOR SUPERCRITICAL AIRFOIL 31 - Continued

(f) α = 1.1°

CP AT -											
X/C	M=0.50	M=0.60	M=0.70	M=0.74	M=0.76	M=0.77	M=0.78	M=0.79	M=0.80	M=0.81	M=0.82	X/C
UPPER SURFACE												
0.000	.886	.946	1.043	1.092	1.099	1.114	1.126	1.132	1.147			0.000
.002	-.577	-.433	-.114	.025	.106	.115	.179	.204	.274			.002
.011	-1.157	-1.085	-.809	-.663	-.564	-.513	-.461	-.430	-.370			.011
.015	-1.115	-1.173	-.939	-.767	-.673	-.640	-.597	-.535	-.469			.015
.029	-1.079	-1.167	-1.165	-1.015	-.932	-.881	-.839	-.778	-.713			.029
.044	-.972	-1.026	-1.275	-1.108	-1.010	-.985	-.930	-.896	-.809			.044
.069	-.765	-.864	-1.036	-1.059	-.974	-.931	-.913	-.845	-.774			.069
.098	-.754	-.780	-.878	-1.039	-.962	-.938	-.905	-.848	-.780			.098
.147	-.628	-.668	-.718	-1.014	-.977	-.943	-.912	-.873	-.934			.147
.199	-.593	-.626	-.689	-.904	-.949	-.919	-.898	-.869	-.819			.199
.248	-.549	-.585	-.646	-.526	-.910	-.904	-.894	-.859	-.813			.248
.298	-.531	-.563	-.632	-.615	-.901	-.907	-.886	-.862	-.813			.298
.348	-.502	-.538	-.598	-.616	-.886	-.882	-.873	-.846	-.816			.348
.399	-.483	-.519	-.576	-.613	-.834	-.891	-.883	-.868	-.838			.399
.448	-.467	-.506	-.562	-.605	-.478	-.886	-.890	-.864	-.835			.448
.497	-.450	-.480	-.540	-.574	-.523	-.869	-.904	-.893	-.860			.497
.547	-.451	-.493	-.541	-.587	-.572	-.543	-.908	-.901	-.876			.547
.599	-.440	-.479	-.532	-.569	-.585	-.482	-.907	-.916	-.893			.599
.648	-.428	-.467	-.517	-.556	-.572	-.505	-.873	-.937	-.922			.648
.699	-.437	-.467	-.520	-.564	-.592	-.558	-.441	-.957	-.941			.699
.750	-.433	-.462	-.511	-.560	-.595	-.588	-.449	-.902	-.998			.750
.799	-.427	-.456	-.493	-.524	-.543	-.539	-.450	-.401	-.483			.799
.848	-.396	-.422	-.442	-.456	-.462	-.460	-.393	-.311	-.308			.848
.899	-.332	-.344	-.338	-.335	-.333	-.328	-.294	-.226	-.190			.899
.950	-.169	-.160	-.132	-.120	-.111	-.109	-.095	-.075	-.078			.950
.969	-.099	-.030	-.064	-.054	-.041	-.037	-.025	-.024	-.055			.969
.980	-.057	-.050	-.026	-.013	-.003	.005	.011	.003	-.040			.980
.989	-.024	-.017	.003	.010	.026	.034	.039	.022	-.027			.989
1.000	.002	.009	.016	.020	.039	.047	.050	.030	-.026			1.000
LOWER SURFACE												
.007	.756	.758	.727	.712	.716	.701	.695	.670	.643			.007
.011	.514	.522	.487	.464	.444	.461	.429	.415	.376			.011
.020	.315	.291	.274	.256	.246	.239	.232	.218	.198			.020
.030	.153	.161	.127	.108	.087	.097	.104	.062	.033			.030
.046	.101	.105	.085	.058	.058	.051	.052	.021	-.004			.046
.068	.082	.068	.065	.036	.026	.034	.029	.019	-.021			.068
.100	.024	.009	-.005	-.018	-.026	-.037	-.023	-.051	-.071			.100
.150	-.028	-.048	-.057	-.065	-.073	-.072	-.074	-.095	-.126			.150
.200	-.039	-.054	-.065	-.086	-.075	-.084	-.093	-.105	-.122			.200
.250	-.062	-.068	-.084	-.112	-.102	-.103	-.108	-.128	-.143			.250
.300	-.080	-.079	-.092	-.099	-.101	-.107	-.104	-.126	-.142			.300
.349	-.085	-.100	-.122	-.129	-.132	-.139	-.137	-.160	-.185			.349
.400	-.069	-.088	-.100	-.114	-.117	-.122	-.123	-.138	-.160			.400
.450	-.094	-.110	-.110	-.131	-.128	-.130	-.143	-.145	-.161			.450
.501	-.089	-.104	-.108	-.120	-.119	-.116	-.128	-.144	-.160			.501
.551	-.092	-.097	-.106	-.113	-.123	-.114	-.114	-.130	-.155			.551
.600	-.044	-.055	-.058	-.061	-.056	-.058	-.048	-.068	-.085			.600
.650	.039	.041	.057	.062	.061	.069	.067	.062	.052			.650
.700	.174	.179	.203	.205	.219	.223	.231	.218	.216			.700
.751	.272	.294	.317	.325	.334	.335	.340	.338	.326			.751
.801	.359	.378	.402	.413	.422	.429	.433	.427	.425			.801
.852	.420	.441	.471	.486	.490	.497	.501	.494	.487			.852
.901	.452	.471	.508	.513	.520	.530	.541	.529	.519			.901
.930	.437	.463	.491	.504	.515	.523	.528	.519	.507			.930
.949	.415	.435	.469	.480	.484	.497	.496	.492	.486			.949
.967	.361	.379	.418	.424	.431	.438	.447	.438	.424			.967
.990	.196	.214	.240	.245	.268	.275	.278	.268	.236			.990
.998	-.021	-.020	-.007	-.008	.007	.022	.029	.002	-.049			.998

TABLE II. - SURFACE PRESSURE DISTRIBUTIONS FOR SUPERCRITICAL AIRFOIL 31 - Continued

(g) α = 1.6°

	CP AT -											
X/C	M=0.50	M=0.60	M=0.70	M=0.74	M=0.76	M=0.77	M=0.78	M=0.79	M=0.80	M=0.81	M=0.82	X/C
UPPER SURFACE												
0.000	.786	.679	.999	1.051	1.066	1.085	1.095	1.113	1.119			0.000
.002	-.828	-.645	-.254	-.089	-.009	.046	.070	.128	.177			.002
.011	-1.421	-1.351	-.965	-.765	-.668	-.619	-.563	-.501	-.445			.011
.015	-1.405	-1.417	-1.096	-.905	-.810	-.754	-.689	-.617	-.558			.015
.029	-1.242	-1.384	-1.287	-1.108	-1.011	-.951	-.907	-.849	-.788			.029
.044	-1.102	-1.198	-1.382	-1.208	-1.113	-1.049	-1.000	-.934	-.891			.044
.069	-.842	-.847	-1.289	-1.182	-1.070	-1.013	-.982	-.914	-.862			.069
.098	-.818	-.874	-1.209	-1.174	-1.080	-1.042	-.987	-.941	-.866			.098
.147	-.682	-.729	-.605	-1.145	-1.069	-1.023	-.981	-.934	-.896			.147
.199	-.628	-.670	-.711	-1.111	-1.047	-.999	-.972	-.938	-.898			.199
.248	-.582	-.617	-.676	-1.048	-1.021	-1.002	-.960	-.934	-.884			.248
.296	-.561	-.600	-.665	-1.026	-1.014	-.990	-.974	-.931	-.880			.298
.348	-.530	-.561	-.629	-.544	-.971	-.954	-.953	-.911	-.861			.348
.399	-.508	-.547	-.602	-.507	-.980	-.958	-.954	-.909	-.877			.399
.448	-.493	-.525	-.592	-.563	-.963	-.963	-.950	-.916	-.881			.448
.497	-.476	-.504	-.566	-.558	-.985	-.984	-.964	-.932	-.901			.497
.547	-.474	-.502	-.566	-.586	-.676	-.987	-.977	-.951	-.922			.547
.599	-.462	-.490	-.546	-.573	-.454	-.995	-.990	-.964	-.942			.599
.648	-.445	-.475	-.528	-.556	-.475	-.897	-1.015	-.991	-.970			.648
.699	-.450	-.479	-.533	-.570	-.510	-.420	-1.037	-1.014	-.991			.699
.750	-.443	-.470	-.517	-.555	-.536	-.420	-.544	-1.026	-.911			.750
.799	-.432	-.460	-.493	-.521	-.511	-.429	-.378	-.445	-.422			.799
.848	-.400	-.421	-.437	-.456	-.448	-.396	-.312	-.310	-.307			.848
.899	-.332	-.343	-.329	-.335	-.323	-.291	-.224	-.193	-.208			.899
.950	-.170	-.159	-.132	-.119	-.114	-.095	-.075	-.089	-.125			.950
.969	-.100	-.085	-.062	-.046	-.038	-.029	-.019	-.048	-.121			.969
.980	-.065	-.046	-.028	-.008	.001	.008	.011	-.027	-.115			.980
.989	-.026	-.010	.000	.019	.031	.037	.035	-.018	-.116			.989
1.000	-.001	.002	.012	.032	.051	.056	.047	-.012	-.096			1.000
LOWER SURFACE												
.007	.835	.821	.805	.792	.790	.768	.763	.738	.728			.007
.011	.613	.617	.577	.552	.537	.523	.514	.497	.472			.011
.020	.415	.392	.367	.338	.341	.329	.310	.289	.270			.020
.030	.268	.231	.223	.202	.208	.190	.178	.144	.122			.030
.046	.177	.180	.150	.142	.138	.120	.118	.103	.066			.046
.068	.143	.132	.107	.103	.108	.089	.086	.055	.046			.068
.100	.074	.057	.040	.055	.032	.032	.027	.006	-.017			.100
.150	.015	.007	-.011	-.014	-.012	-.014	-.028	-.037	-.071			.150
.200	-.005	-.012	-.024	-.020	-.031	-.037	-.042	-.065	-.078			.200
.250	-.030	-.039	-.056	-.047	-.058	-.064	-.070	-.082	-.104			.250
.300	-.049	-.059	-.060	-.067	-.064	-.068	-.079	-.096	-.125			.300
.349	-.059	-.069	-.094	-.094	-.088	-.098	-.101	-.123	-.153			.349
.400	-.060	-.071	-.077	-.082	-.086	-.081	-.091	-.113	-.145			.400
.450	-.071	-.084	-.101	-.089	-.096	-.102	-.111	-.128	-.165			.450
.501	-.072	-.079	-.094	-.099	-.094	-.096	-.097	-.120	-.155			.501
.551	-.080	-.078	-.095	-.088	-.068	-.090	-.092	-.105	-.149			.551
.600	-.039	-.041	-.045	-.038	-.032	-.027	-.033	-.053	-.083			.600
.650	.050	.056	.068	.078	.081	.084	.081	.077	.053			.650
.700	.181	.185	.202	.218	.236	.227	.236	.226	.213			.700
.751	.282	.266	.322	.332	.348	.349	.348	.342	.326			.751
.801	.363	.378	.407	.419	.434	.438	.439	.437	.416			.801
.852	.431	.444	.474	.490	.501	.501	.511	.498	.478			.852
.901	.453	.477	.504	.516	.533	.532	.543	.526	.521			.901
.930	.442	.457	.489	.502	.516	.520	.529	.513	.500			.930
.949	.418	.438	.465	.481	.493	.503	.500	.496	.474			.949
.967	.366	.378	.412	.433	.447	.449	.449	.428	.414			.967
.990	.199	.212	.243	.257	.280	.279	.280	.250	.204			.990
.998	-.025	-.017	-.013	.002	.016	.028	.026	-.025	-.121			.998

TABLE II. - SURFACE PRESSURE DISTRIBUTIONS FOR SUPERCRITICAL AIRFOIL 31 - Continued

(h) $\alpha = 2.1°$

	CP AT -											
X/C	M=0.50	M=0.60	M=0.70	M=0.74	M=0.76	M=0.77	M=0.78	M=0.79	M=0.80	M=0.81	M=0.82	X/C
UPPER SURFACE												
0.000	.670	.794	.953	1.001	1.041	1.055	1.070					0.000
.002	-1.153	-.828	-.364	-.186	-.097	-.071	-.011					.002
.011	-1.702	-1.643	-1.129	-.909	-.776	-.714	-.638					.011
.015	-1.694	-1.719	-1.248	-1.016	-.903	-.837	-.748					.015
.029	-1.442	-1.607	-1.414	-1.219	-1.093	-1.046	-.966					.029
.044	-1.282	-1.470	-1.502	-1.297	-1.187	-1.149	-1.058					.044
.069	-.966	-1.001	-1.443	-1.257	-1.170	-1.110	-1.042					.069
.098	-.897	-.981	-1.444	-1.280	-1.187	-1.129	-1.073					.098
.147	-.746	-.789	-1.318	-1.246	-1.155	-1.120	-1.042					.147
.199	-.681	-.723	-.577	-1.203	-1.132	-1.081	-1.032					.199
.248	-.633	-.674	-.580	-1.173	-1.112	-1.066	-1.024					.248
.298	-.594	-.643	-.641	-1.152	-1.088	-1.061	-1.026					.298
.348	-.564	-.601	-.632	-1.129	-1.C85	-1.049	-1.015					.348
.399	-.538	-.575	-.617	-1.117	-1.075	-1.052	-1.021					.399
.448	-.521	-.556	-.602	-.492	-1.069	-1.050	-1.009					.448
.497	-.496	-.530	-.572	-.443	-1.C79	-1.055	-1.026					.497
.547	-.494	-.528	-.57C	-.486	-1.082	-1.063	-1.042					.547
.599	-.474	-.507	-.555	-.512	-1.046	-1.067	-1.052					.599
.648	-.467	-.494	-.536	-.511	-.559	-1.090	-1.063					.648
.699	-.465	-.492	-.535	-.549	-.420	-1.015	-1.086					.699
.750	-.448	-.483	-.524	-.547	-.412	-.487	-.683					.750
.799	-.442	-.467	-.499	-.519	-.421	-.369	-.412					.799
.848	-.407	-.423	-.431	-.453	-.392	-.314	-.304					.848
.899	-.338	-.339	-.328	-.343	-.302	-.244	-.191					.899
.950	-.166	-.158	-.125	-.123	-.105	-.085	-.066					.950
.969	-.100	-.089	-.055	-.047	-.030	-.025	-.035					.969
.980	-.057	-.051	-.022	-.007	.010	.013	-.017					.980
.989	-.026	-.016	.005	.029	.044	.039	-.005					.989
1.000	-.008	.002	.021	.047	.060	.055	-.003					1.000
LOWER SURFACE												
.007	.906	.903	.88C	.859	.851	.822	.806					.007
.011	.715	.692	.659	.628	.621	.610	.582					.011
.020	.503	.486	.453	.444	.422	.399	.373					.020
.030	.368	.329	.313	.293	.283	.257	.221					.030
.046	.259	.238	.228	.229	.208	.205	.177					.046
.068	.201	.195	.179	.175	.169	.166	.128					.068
.100	.134	.127	.106	.101	.103	.089	.070					.100
.150	.065	.058	.057	.C55	.C48	.021	.015					.150
.200	.034	.021	.015	.023	.015	.010	-.018					.200
.250	.005	-.000	-.006	-.001	-.009	-.025	-.040					.250
.300	-.013	-.018	-.024	-.031	-.030	-.040	-.046					.300
.349	-.033	-.045	-.054	-.C52	-.057	-.064	-.083					.349
.400	-.033	-.039	-.046	-.050	-.041	-.057	-.077					.400
.450	-.044	-.058	-.069	-.C64	-.C69	-.078	-.093					.450
.501	-.036	-.062	-.065	-.063	-.060	-.070	-.091					.501
.551	-.056	-.066	-.066	-.C63	-.C59	-.069	-.077					.551
.600	-.023	-.020	-.023	-.C13	-.006	-.023	-.027					.600
.650	.063	.068	.082	.093	.101	.092	.088					.650
.700	.193	.201	.221	.242	.244	.241	.231					.700
.751	.290	.301	.327	.348	.359	.353	.356					.751
.801	.373	.385	.415	.429	.443	.444	.429					.801
.852	.435	.459	.483	.504	.514	.514	.505					.852
.901	.462	.489	.513	.528	.543	.539	.530					.901
.930	.442	.465	.496	.516	.526	.524	.522					.930
.949	.426	.441	.463	.491	.507	.502	.489					.949
.967	.366	.388	.413	.434	.456	.450	.435					.967
.990	.200	.211	.241	.271	.286	.280	.256					.990
.998	-.021	-.028	-.014	.018	.035	.024	-.026					.998

TABLE II. - SURFACE PRESSURE DISTRIBUTIONS FOR SUPERCRITICAL AIRFOIL 31 - Concluded

(i) $\alpha = 3.1°$

	CP AT -										
X/C	M=0.50	M=0.60	M=0.70	M=0.74	M=0.76	M=0.77	M=0.78	M=0.79	M=0.80	M=0.81	M=0.82	X/C
UPPER SURFACE												
0.000	.386	.598	.842	.919	.967	1.001						0.000
.002	-1.696	-1.140	-.564	-.384	-.257	-.189						.002
.011	-2.333	-2.093	-1.366	-1.109	-.982	-.878						.011
.015	-2.163	-2.197	-1.472	-1.224	-1.078	-.996						.015
.029	-1.867	-2.282	-1.633	-1.367	-1.249	-1.158						.029
.044	-1.325	-2.140	-1.700	-1.432	-1.313	-1.245						.044
.069	-1.151	-1.059	-1.641	-1.400	-1.292	-1.221						.069
.098	-1.053	-1.057	-1.638	-1.417	-1.318	-1.250						.098
.147	-.861	-.898	-1.585	-1.415	-1.307	-1.242						.147
.199	-.771	-.812	-1.530	-1.363	-1.258	-1.210						.199
.248	-.707	-.745	-1.482	-1.338	-1.255	-1.190						.248
.298	-.666	-.707	-1.391	-1.317	-1.242	-1.175						.298
.348	-.622	-.658	-.466	-1.288	-1.220	-1.159						.348
.399	-.598	-.620	-.518	-1.288	-1.218	-1.160						.399
.448	-.575	-.596	-.544	-1.270	-1.204	-1.162						.448
.497	-.540	-.566	-.541	-1.271	-1.204	-1.170						.497
.547	-.528	-.554	-.559	-1.271	-1.215	-1.169						.547
.599	-.513	-.540	-.556	-.735	-1.224	-1.187						.599
.648	-.496	-.511	-.536	-.465	-1.240	-1.201						.648
.699	-.486	-.502	-.540	-.401	-.861	-.838						.699
.750	-.477	-.485	-.526	-.394	-.489	-.538						.750
.799	-.452	-.453	-.508	-.406	-.389	-.432						.799
.848	-.416	-.413	-.445	-.379	-.293	-.328						.848
.899	-.333	-.315	-.341	-.297	-.214	-.225						.899
.950	-.161	-.142	-.138	-.108	-.071	-.134						.950
.969	-.091	-.076	-.058	-.037	-.019	-.093						.969
.980	-.055	-.043	-.017	.001	.009	-.088						.980
.989	-.025	-.019	.019	.039	.032	-.062						.989
1.000	-.004	-.008	.033	.064	.037	-.055						1.000
LOWER SURFACE												
.007	1.017	1.003	.965	.955	.938	.923						.007
.011	.844	.821	.774	.774	.740	.721						.011
.020	.652	.650	.607	.572	.559	.521						.020
.030	.478	.479	.446	.435	.405	.378						.030
.046	.385	.379	.371	.347	.332	.301						.046
.068	.306	.306	.298	.285	.263	.257						.068
.100	.229	.219	.217	.207	.186	.180						.100
.150	.147	.137	.140	.131	.121	.110						.150
.200	.108	.100	.106	.107	.092	.079						.200
.250	.071	.064	.072	.071	.054	.045						.250
.300	.042	.037	.045	.049	.038	.023						.300
.349	.022	.019	.017	.008	.002	-.012						.349
.400	.015	.017	.013	.014	.005	-.021						.400
.450	-.004	-.004	-.007	-.005	-.016	-.040						.450
.501	-.013	-.017	-.007	-.001	-.018	-.050						.501
.551	-.025	-.026	-.024	-.007	-.033	-.046						.551
.600	.006	.012	.022	.027	.014	-.008						.600
.650	.085	.091	.111	.130	.123	.105						.650
.700	.201	.218	.244	.261	.257	.245						.700
.751	.302	.317	.346	.374	.365	.359						.751
.801	.378	.404	.439	.452	.452	.444						.801
.852	.448	.464	.498	.519	.515	.507						.852
.901	.470	.489	.535	.547	.549	.536						.901
.930	.452	.473	.514	.529	.523	.516						.930
.949	.421	.450	.488	.506	.506	.484						.949
.967	.367	.387	.432	.446	.450	.424						.967
.990	.197	.213	.262	.289	.279	.228						.990
.998	-.032	-.041	.012	.034	.014	-.085						.998

[redacted]

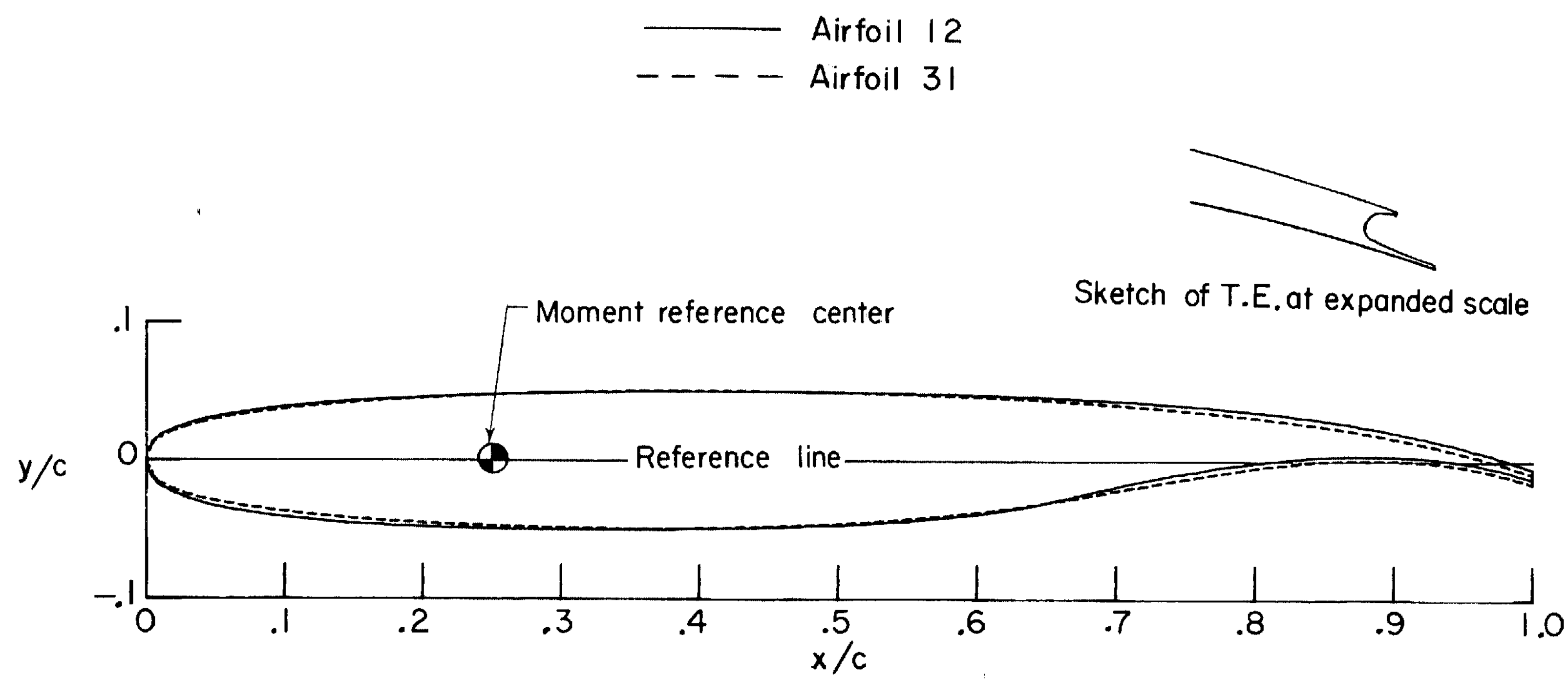

Figure 1.- Sketches of supercritical airfoils 12 and 31.

[redacted]

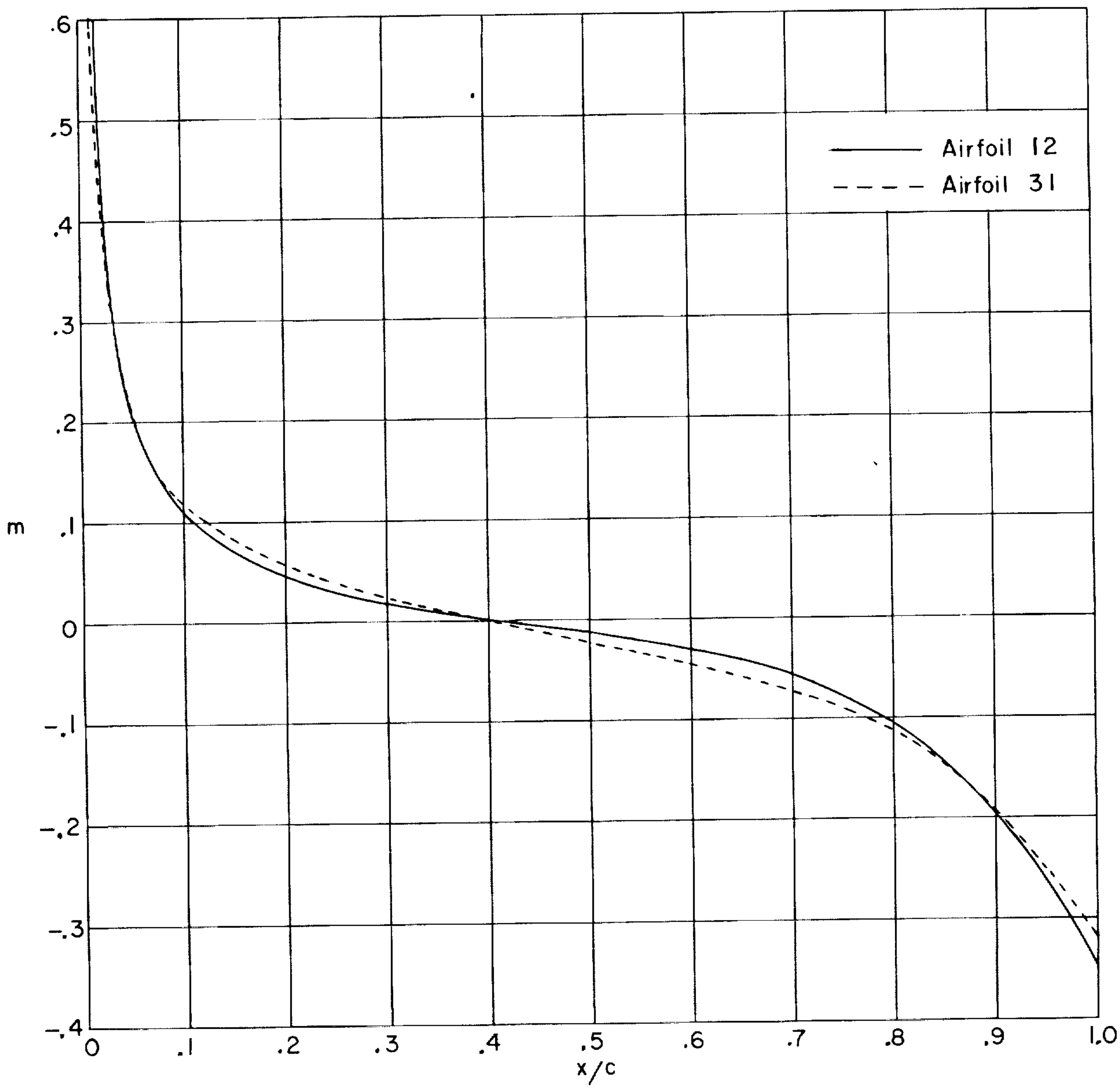

(a) Upper surface.

Figure 2.- Chordwise distribution of airfoil surface slopes.

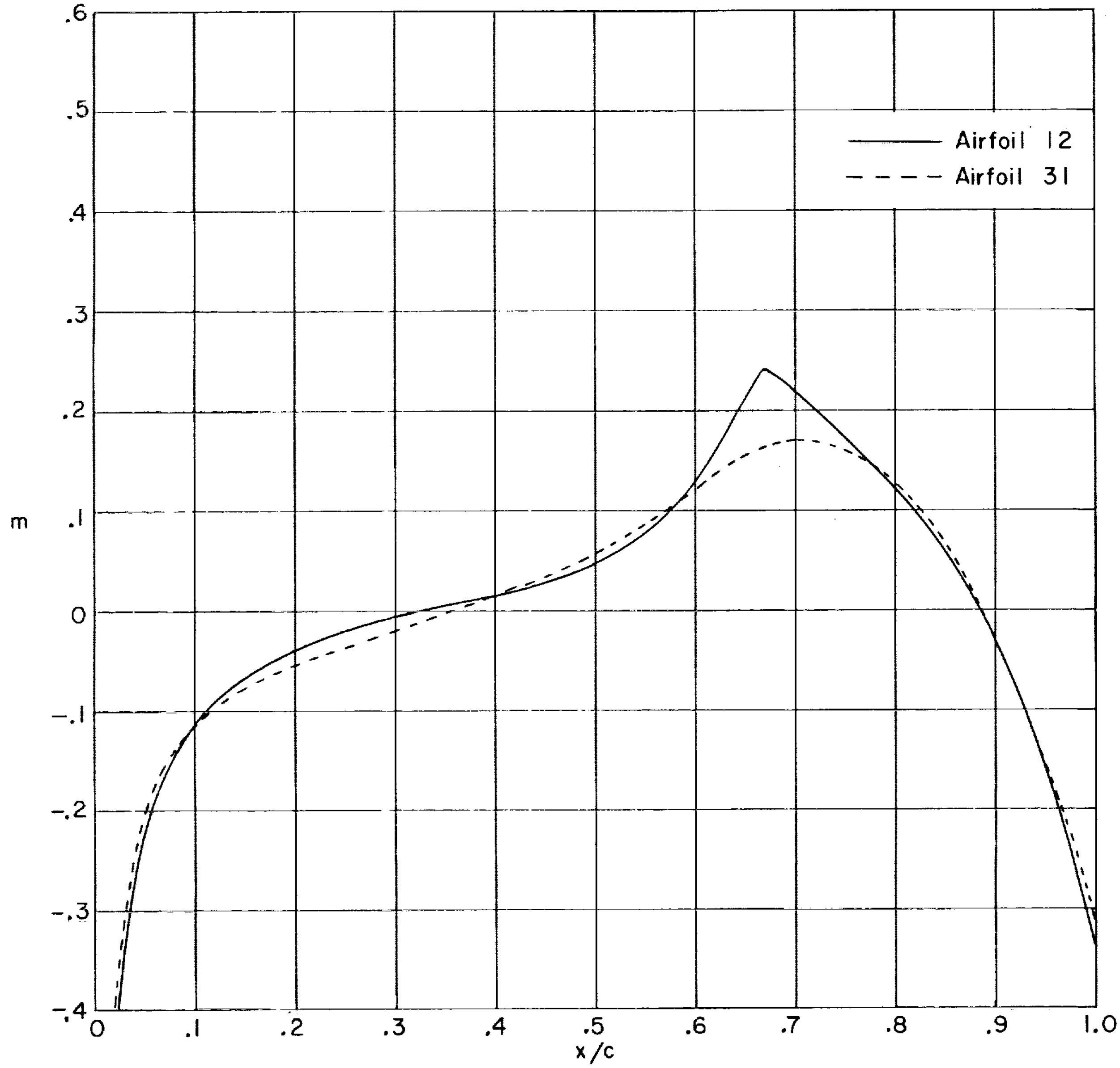

(b) Lower surface.

Figure 2.- Concluded.

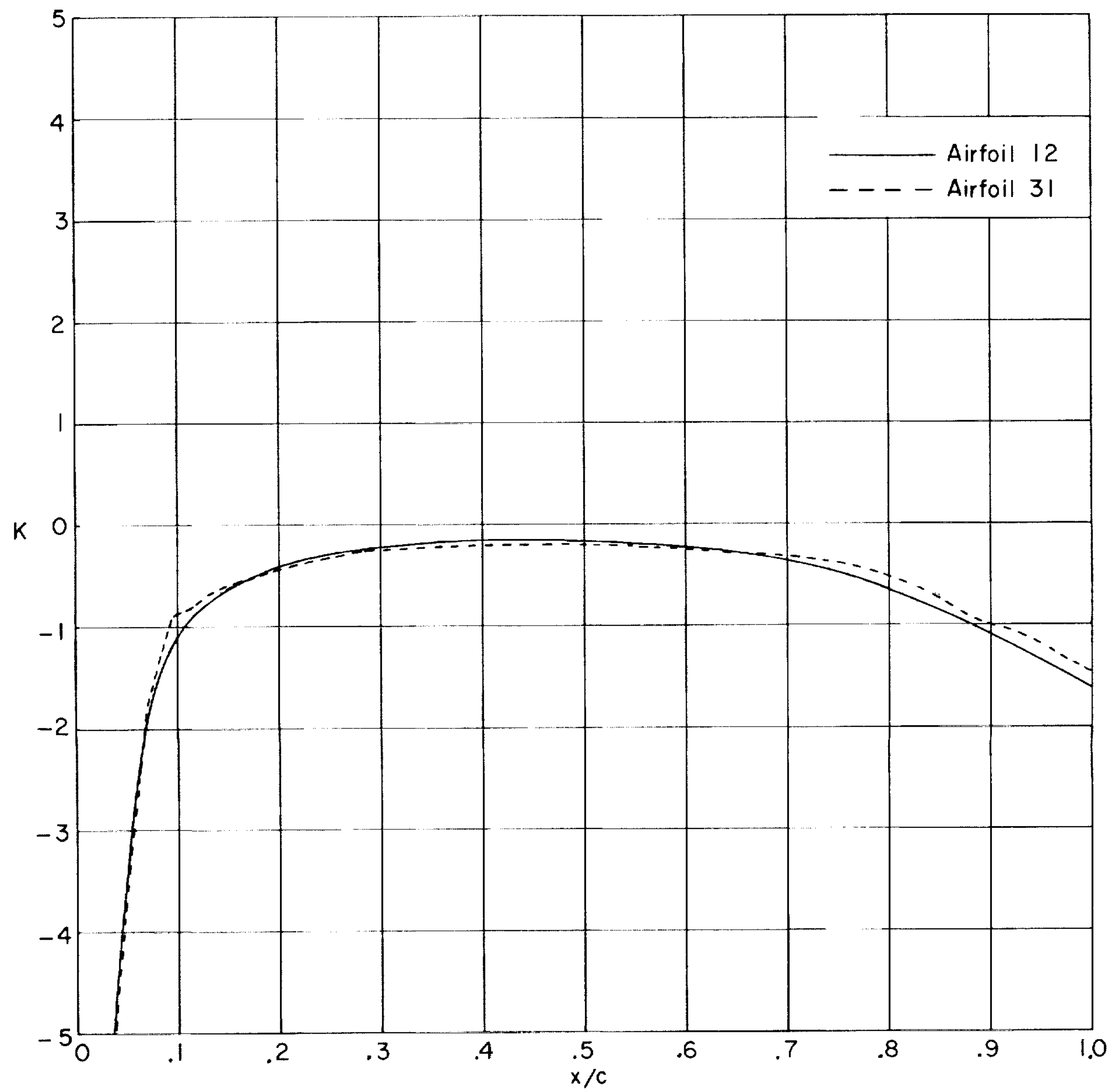

(a) Upper surface.

Figure 3.- Chordwise distribution of airfoil surface curvatures.

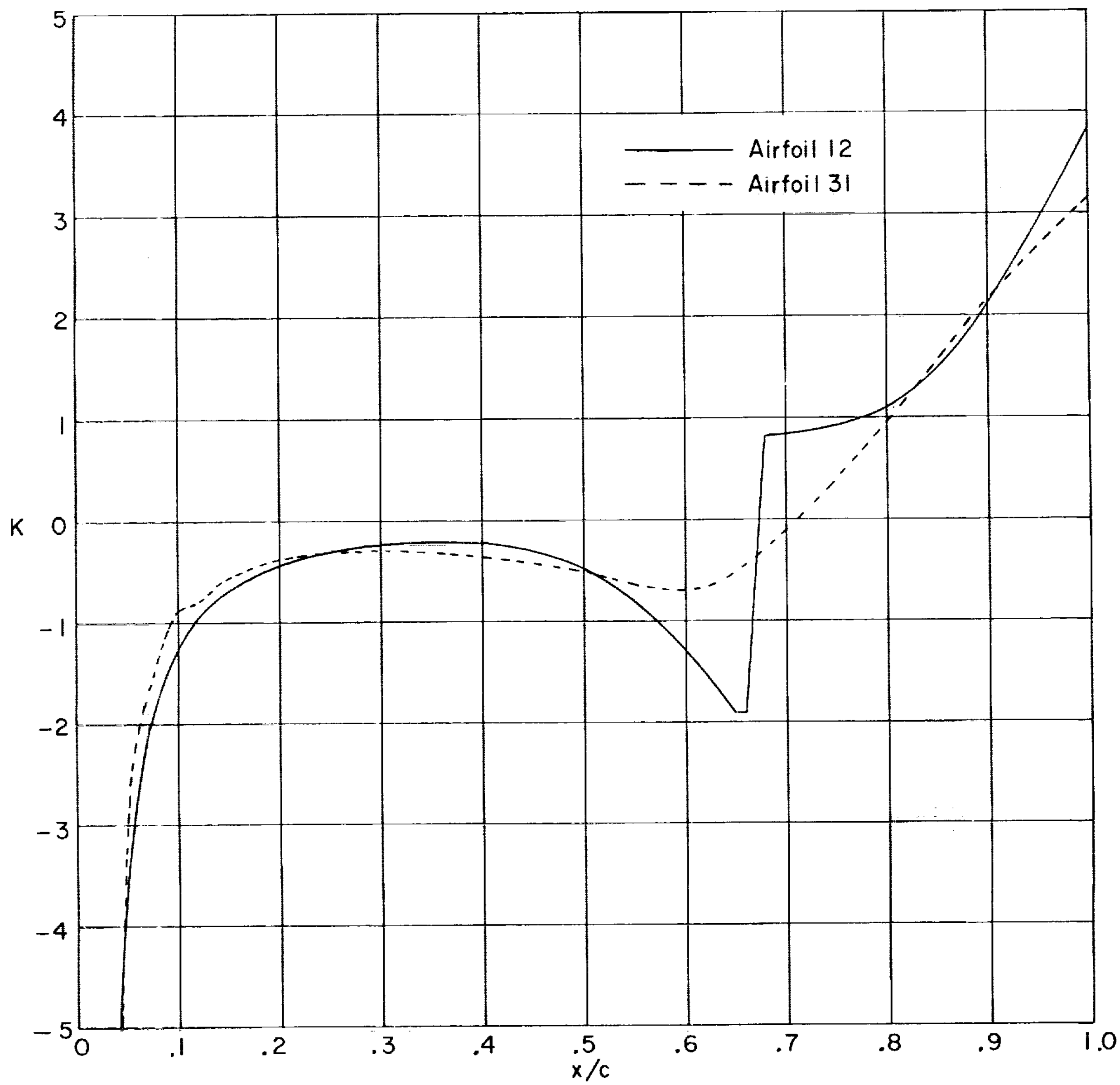

(b) Lower surface.

Figure 3.- Concluded.

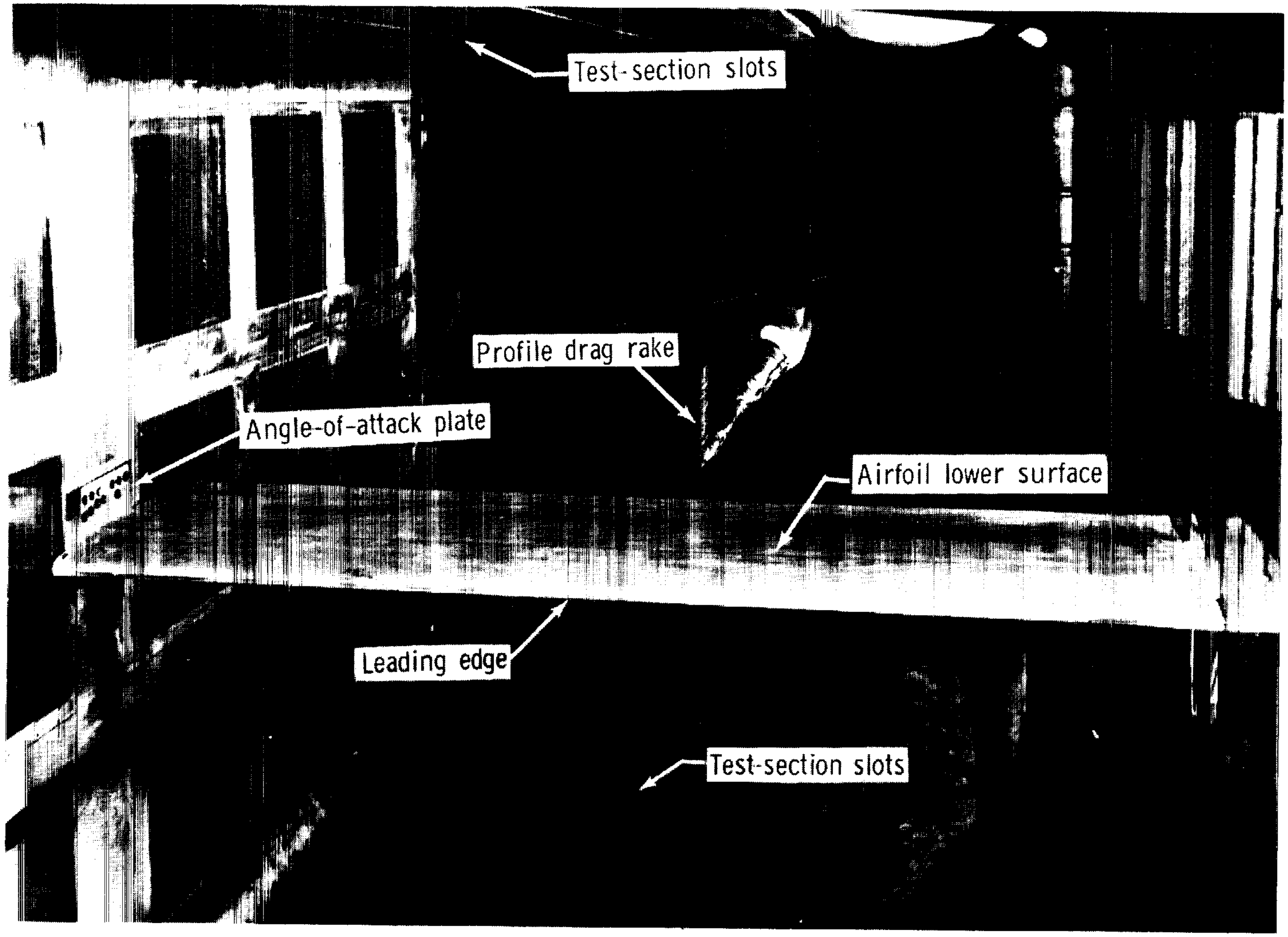

L-73-1225.2

(a) Supercritical airfoil and profile drag rake mounted in tunnel.

Figure 4.- Photographs of model in tunnel.

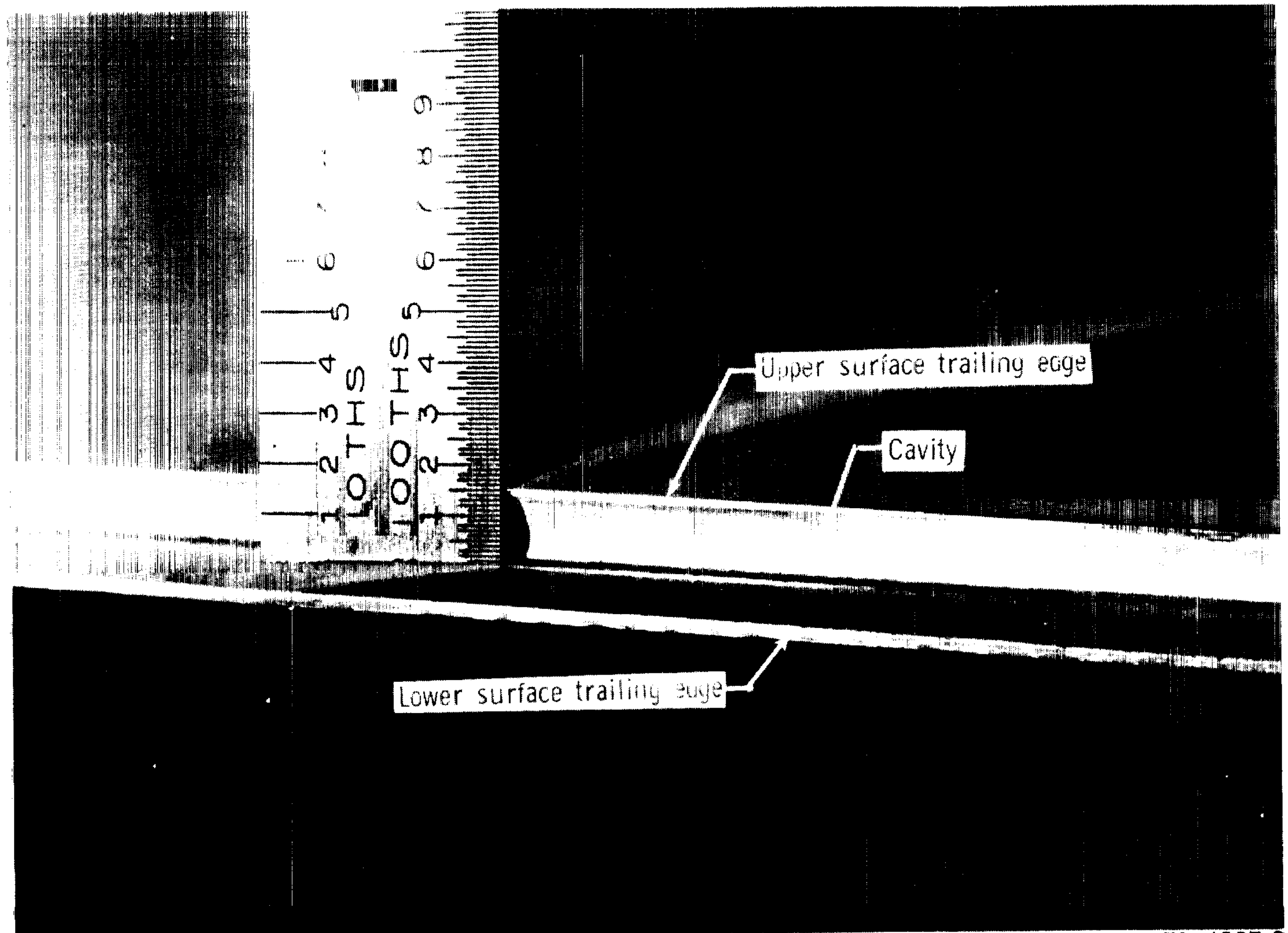

L-73-1227.2

(b) Trailing-edge cavity.

Figure 4.- Concluded.

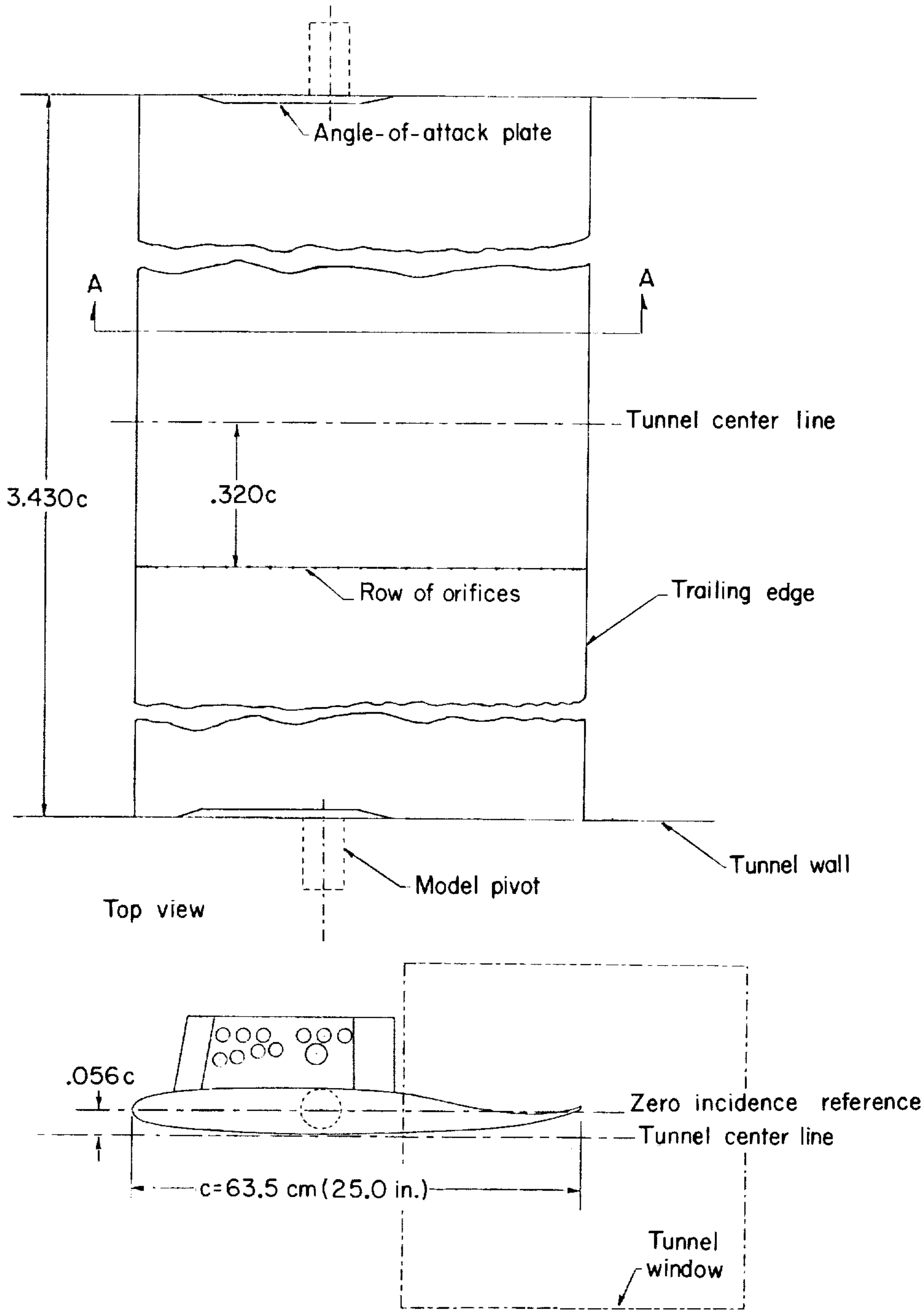

(a) Airfoil mounted in tunnel.

Figure 5.- Apparatus dimensions in terms of chord (c = 63.5 cm (25.0 in.)).

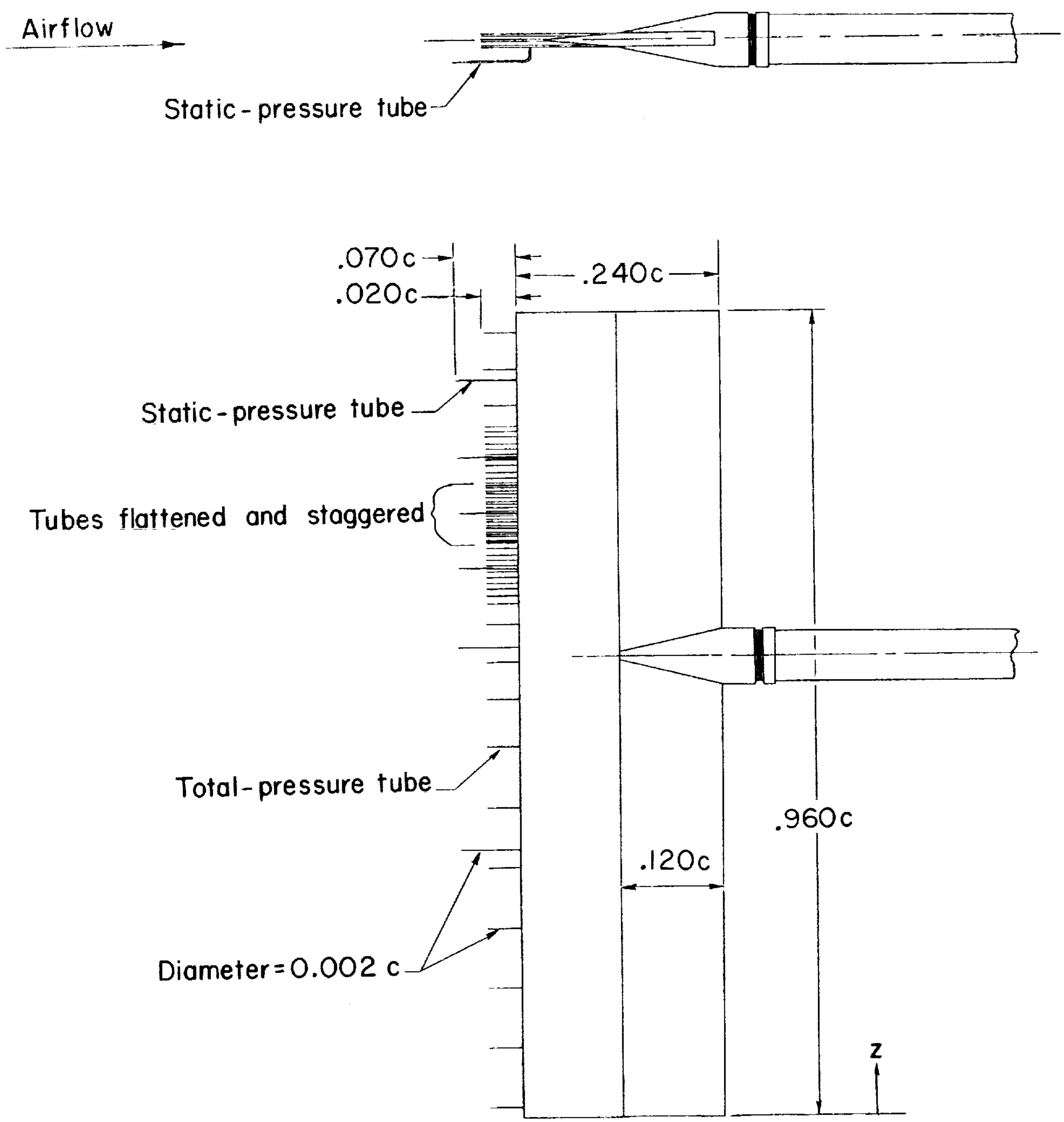

(b) Profile drag rake.

Figure 5.- Concluded.

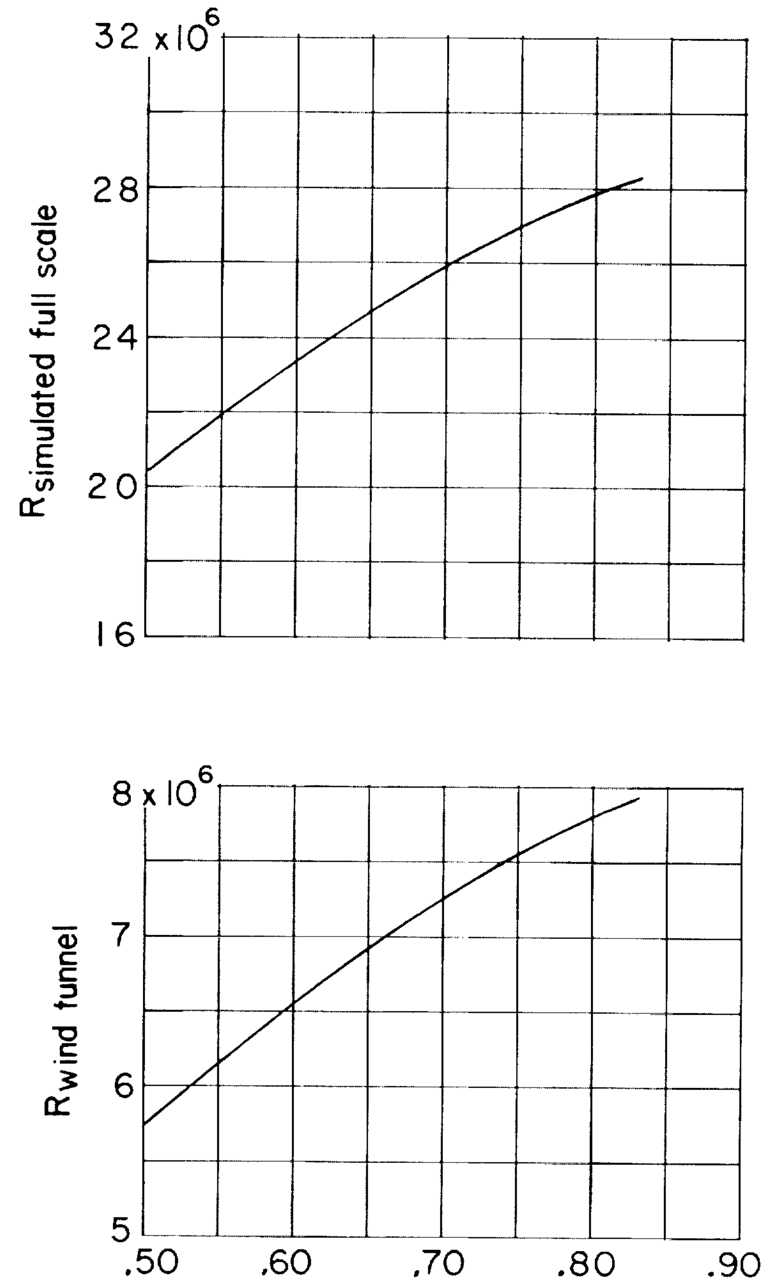

Figure 6.- Variation of Reynolds number with Mach number.

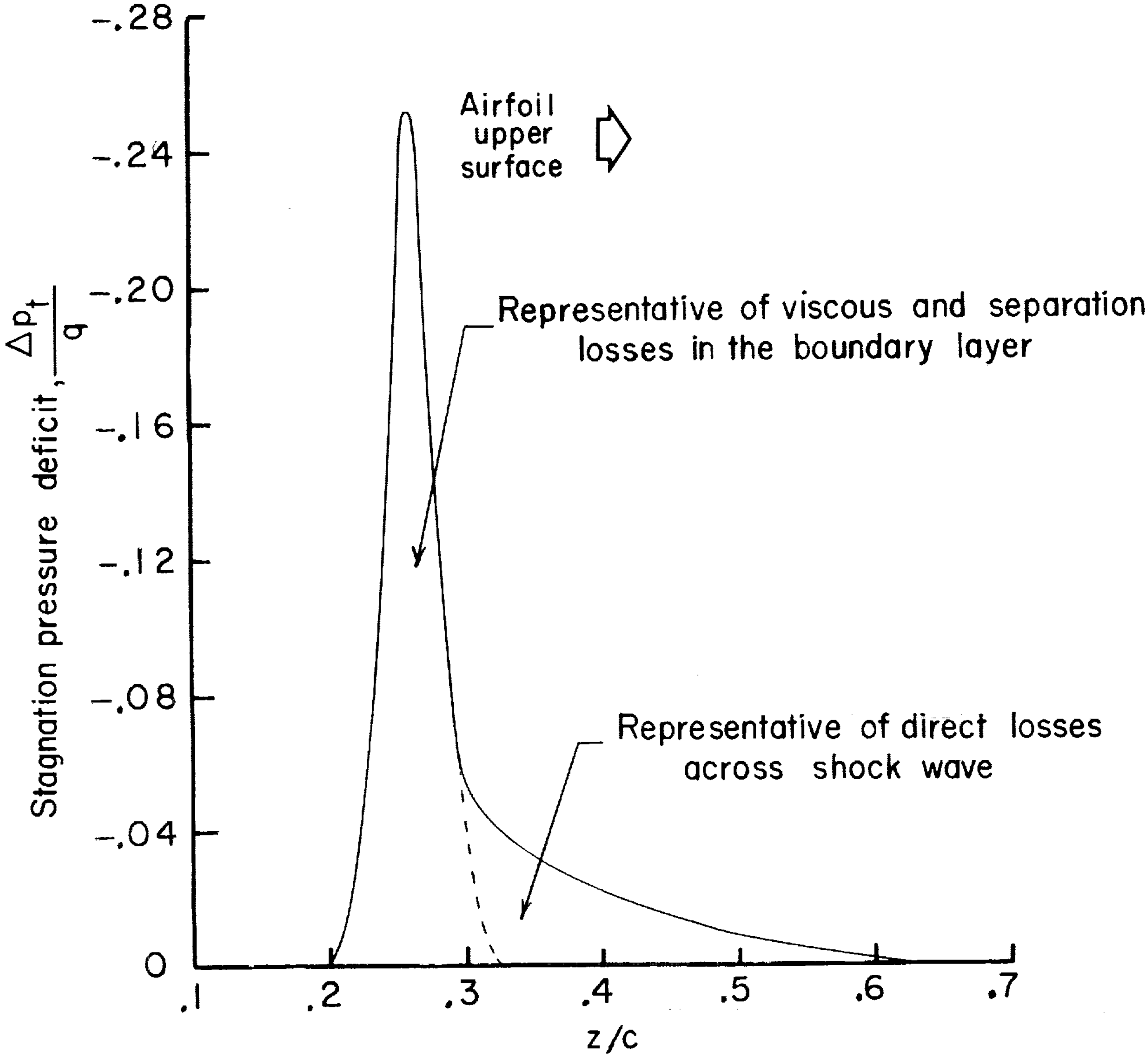

Figure 7.- Schematic of wake profiles.

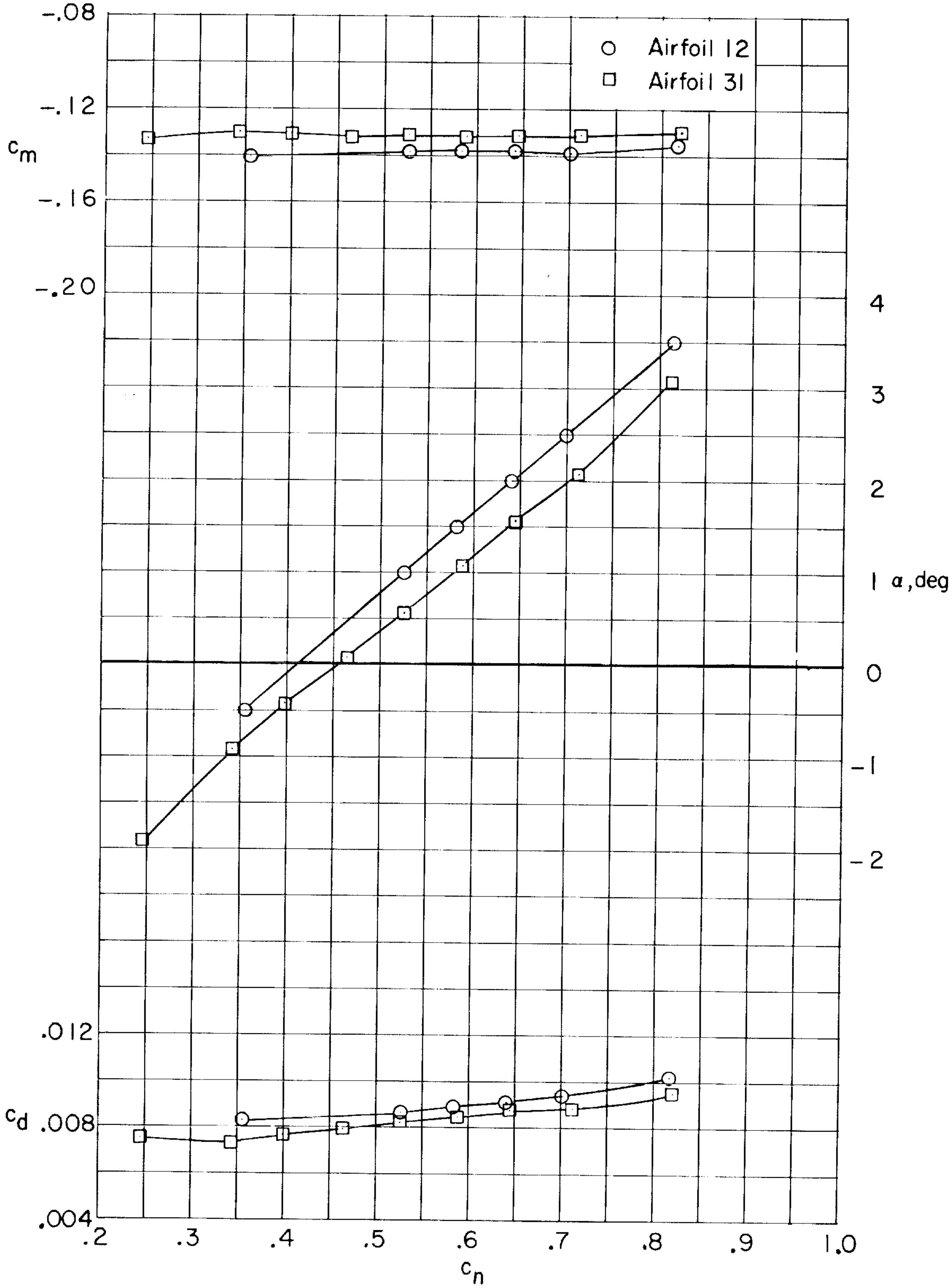

(a) M = 0.50.

Figure 8.- Comparison of force and moment characteristics of supercritical airfoils 12 and 31.

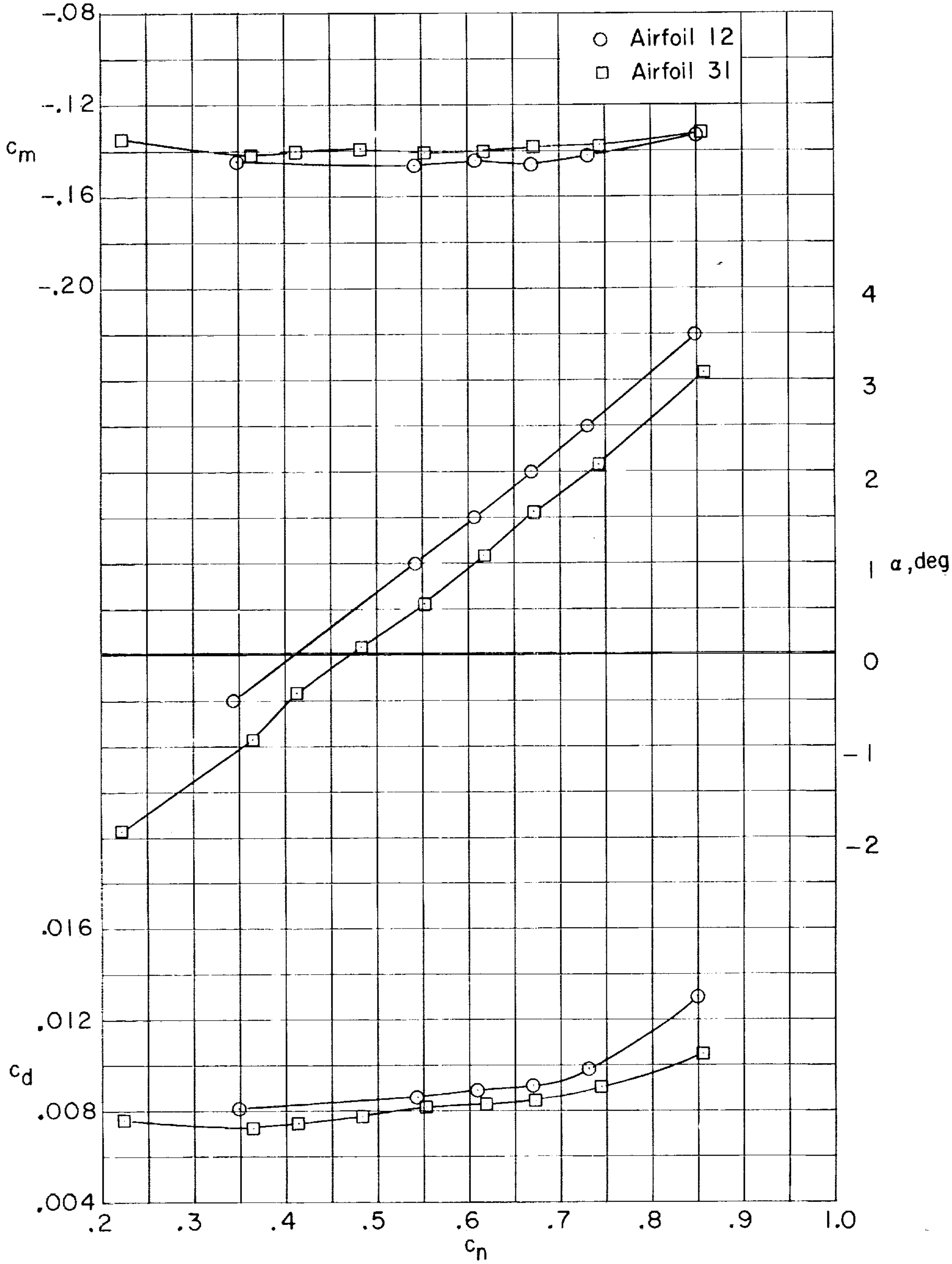

(b) M = 0.60.

Figure 8.- Continued.

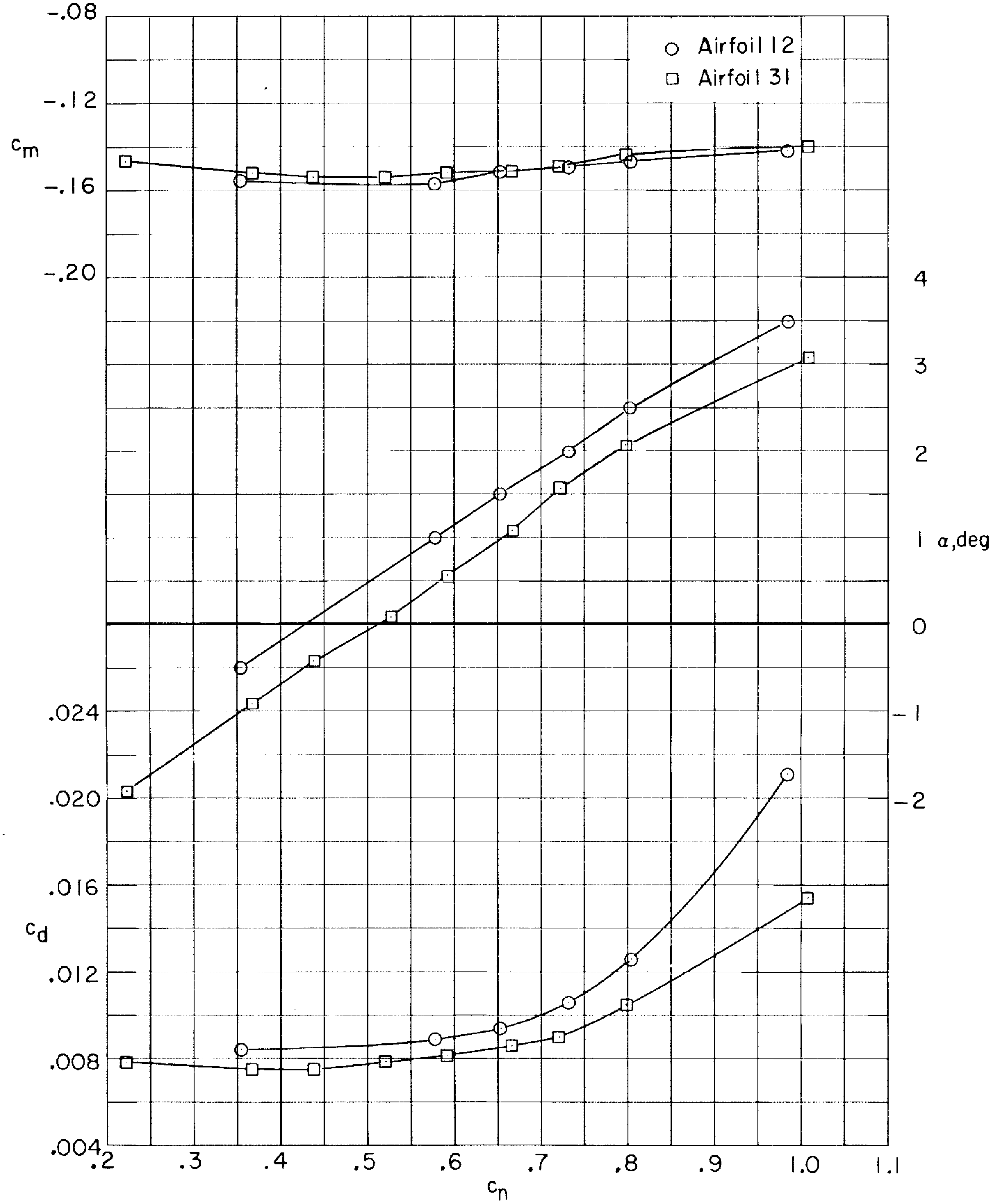

(c) M = 0.70.

Figure 8.- Continued.

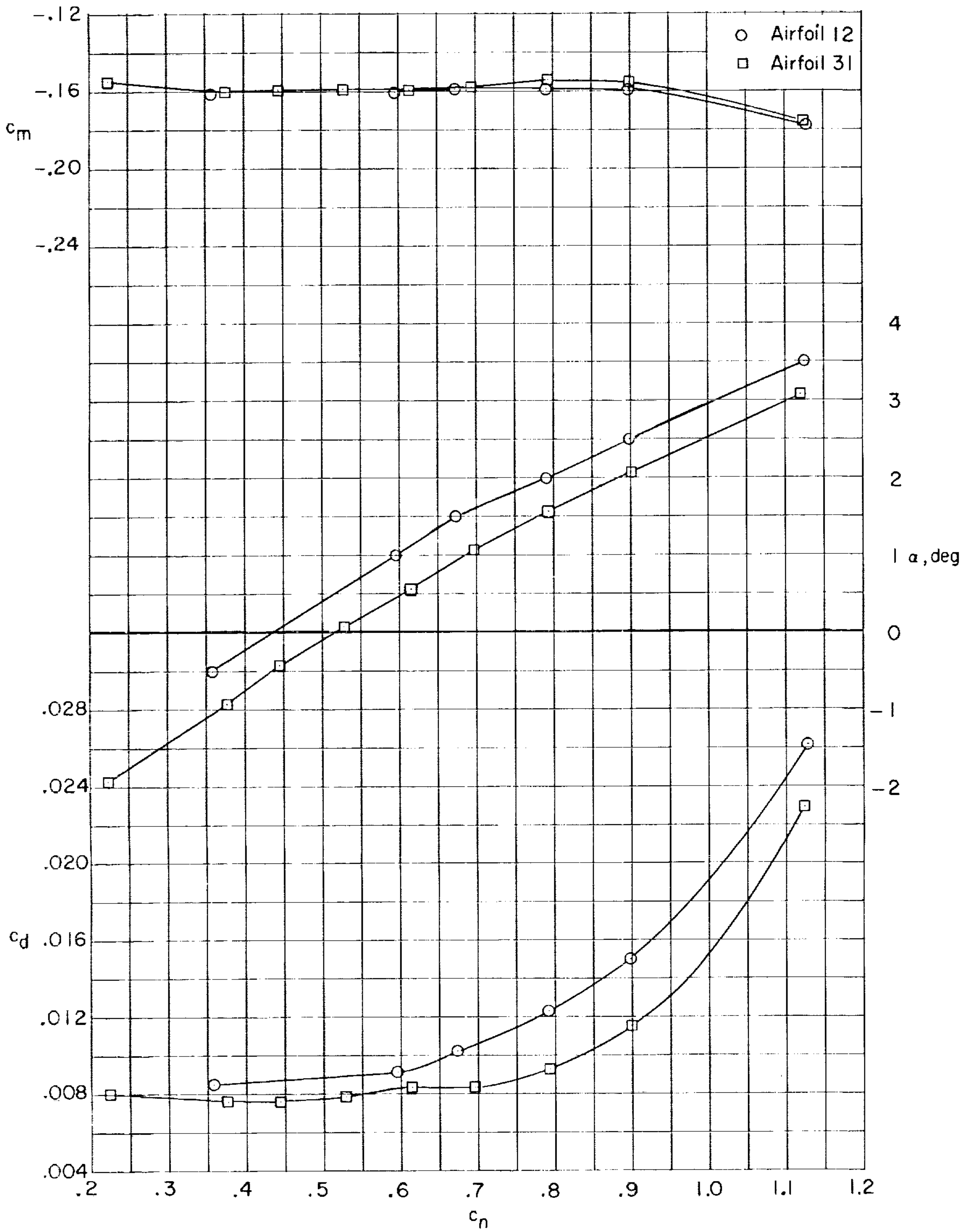

(d) M = 0.74.

Figure 8.- Continued.

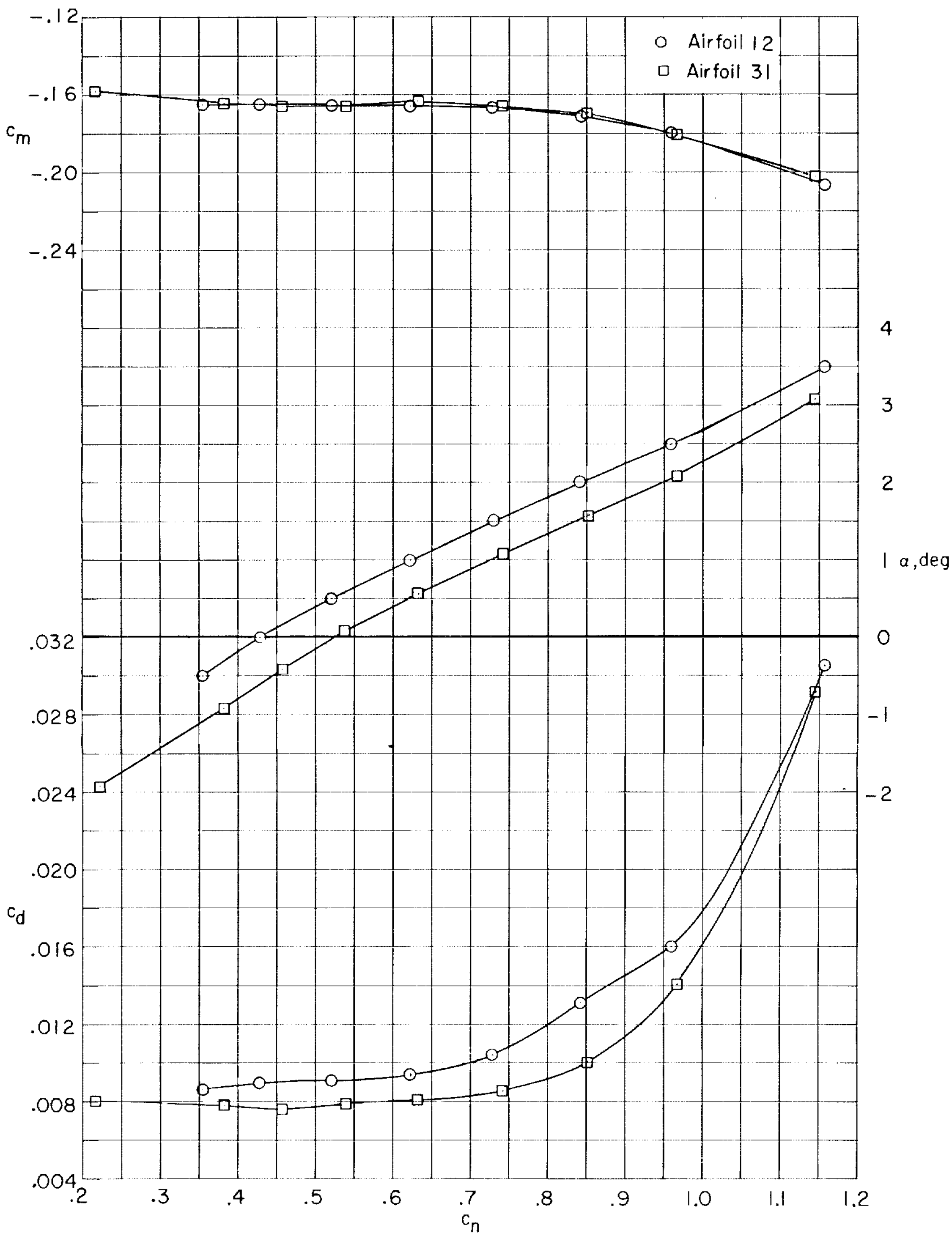

(e) M = 0.76.

Figure 8.- Continued.

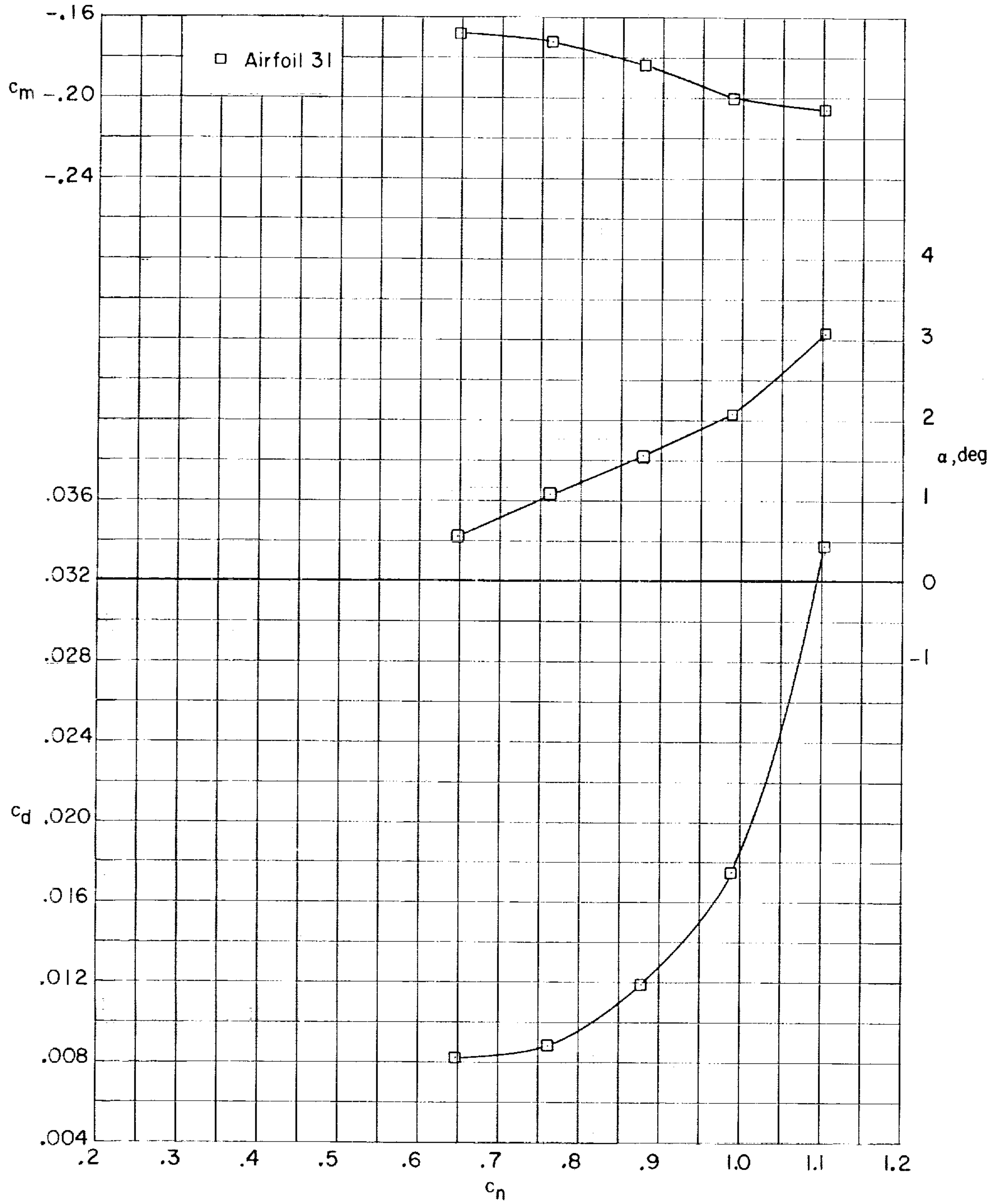

(f) M = 0.77.

Figure 8.- Continued.

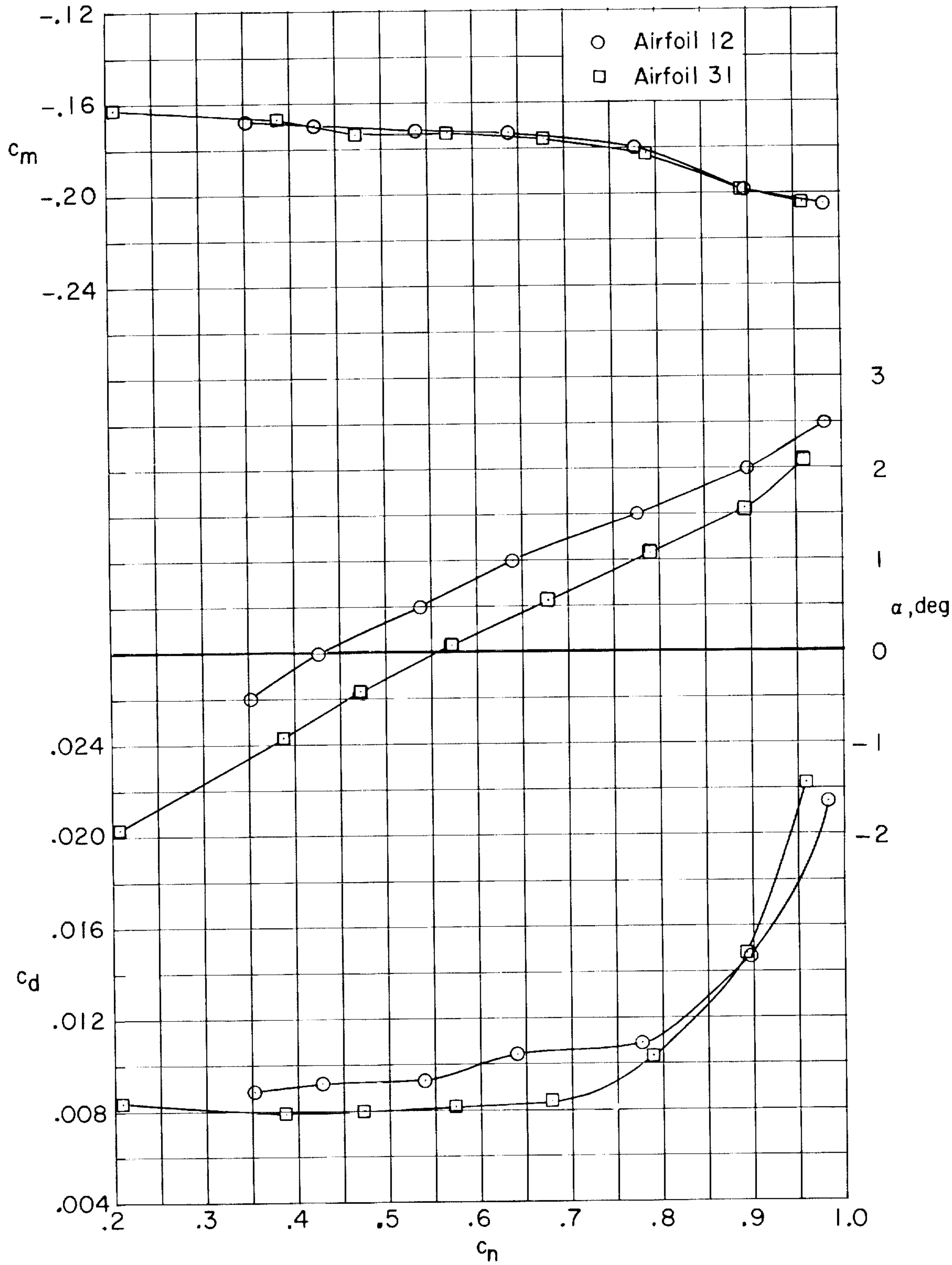

(g) M = 0.78.

Figure 8.- Continued.

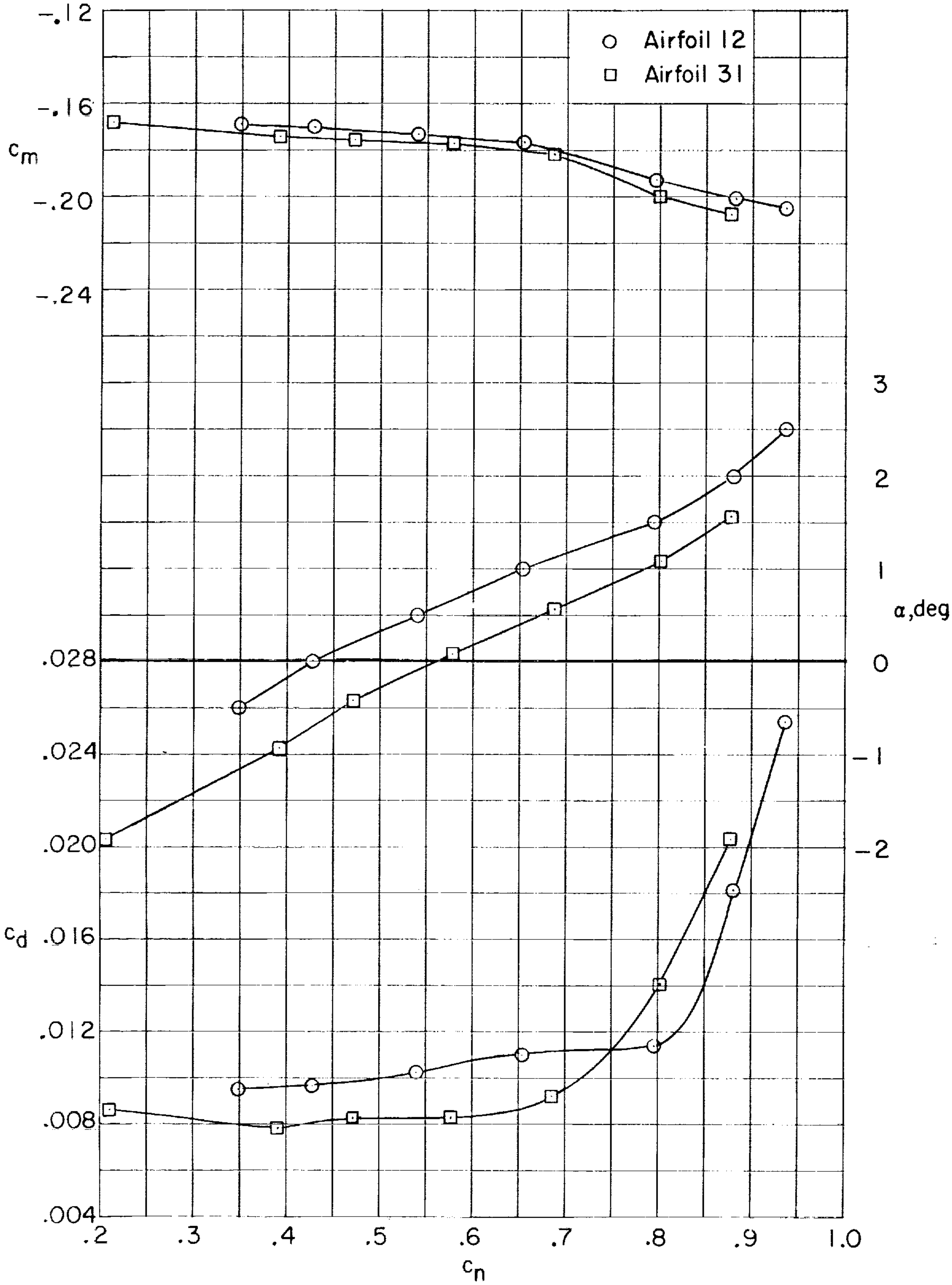

(h) M = 0.79.

Figure 8.- Continued.

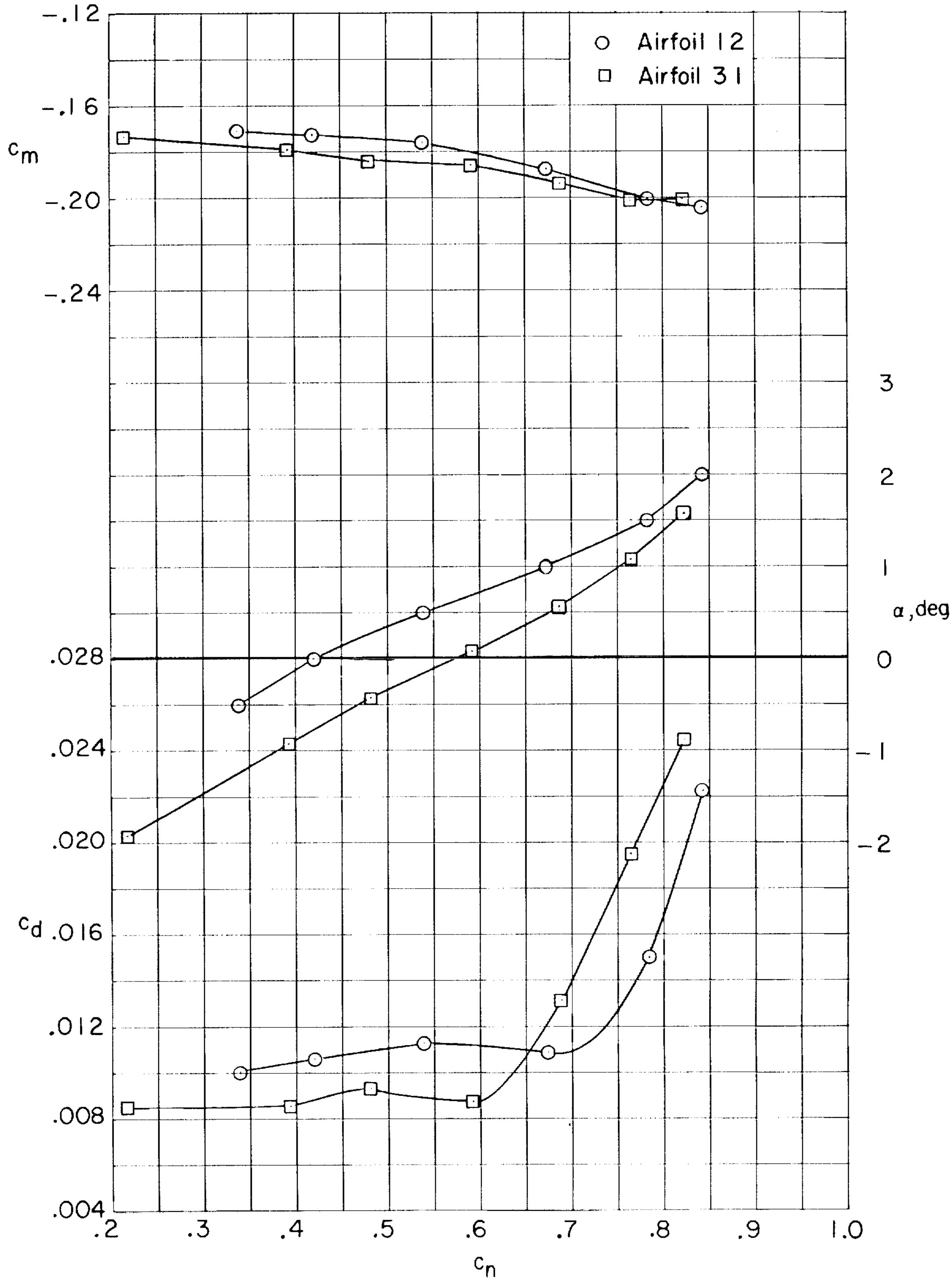

(i) M = 0.80.

Figure 8.- Continued.

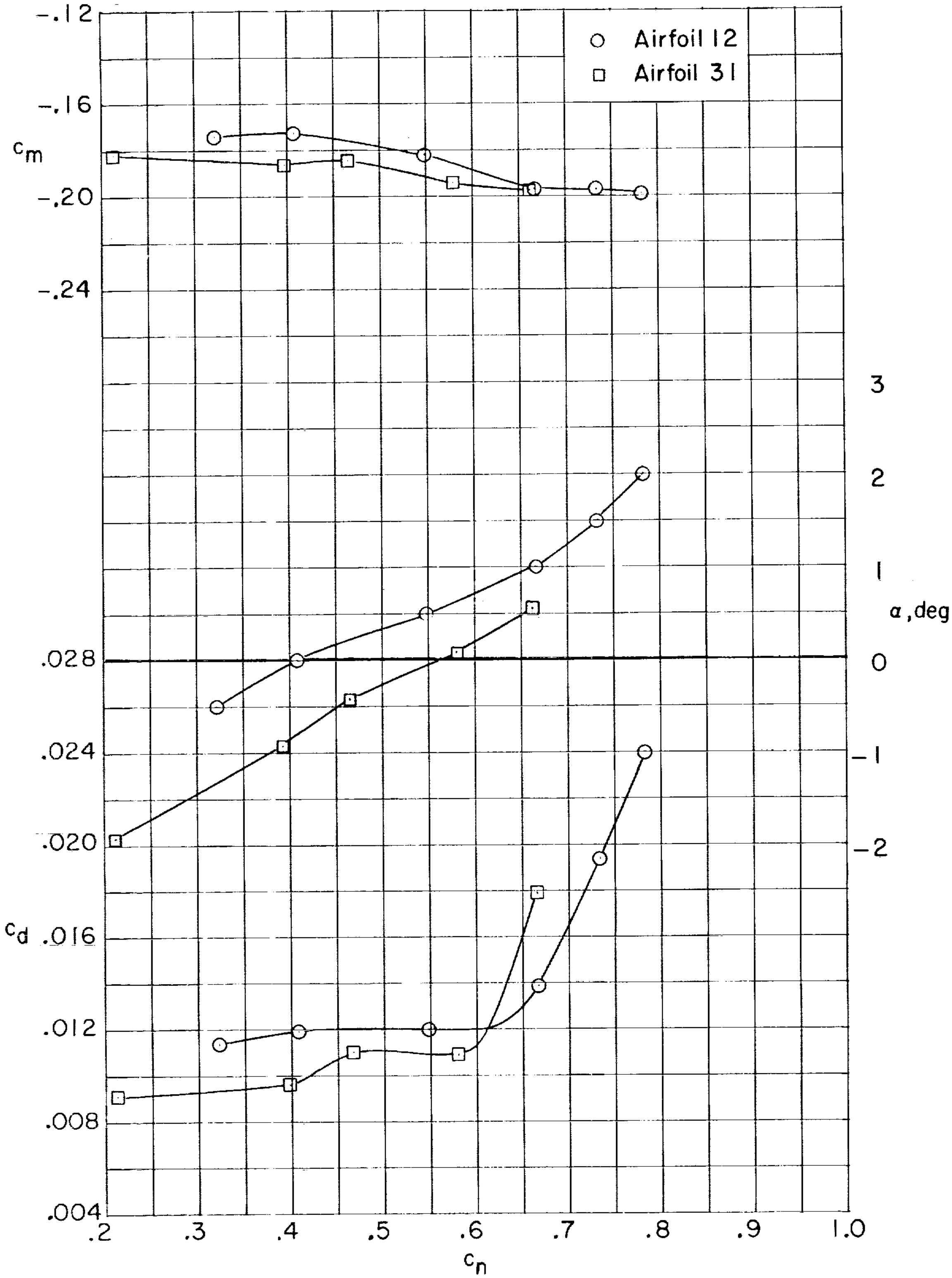

(j) M = 0.81.

Figure 8.- Continued.

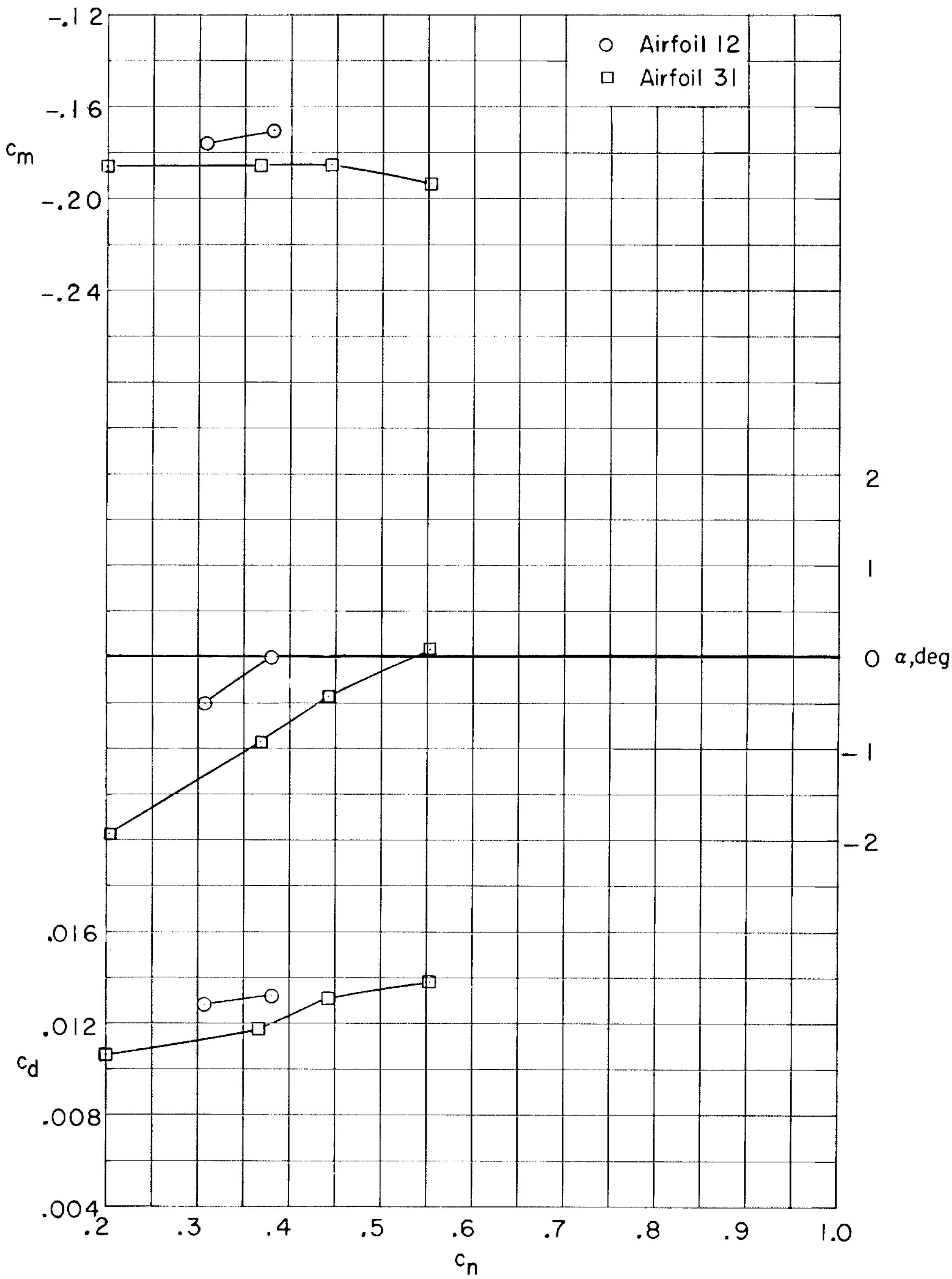

(k) M = 0.82.

Figure 8.- Concluded.

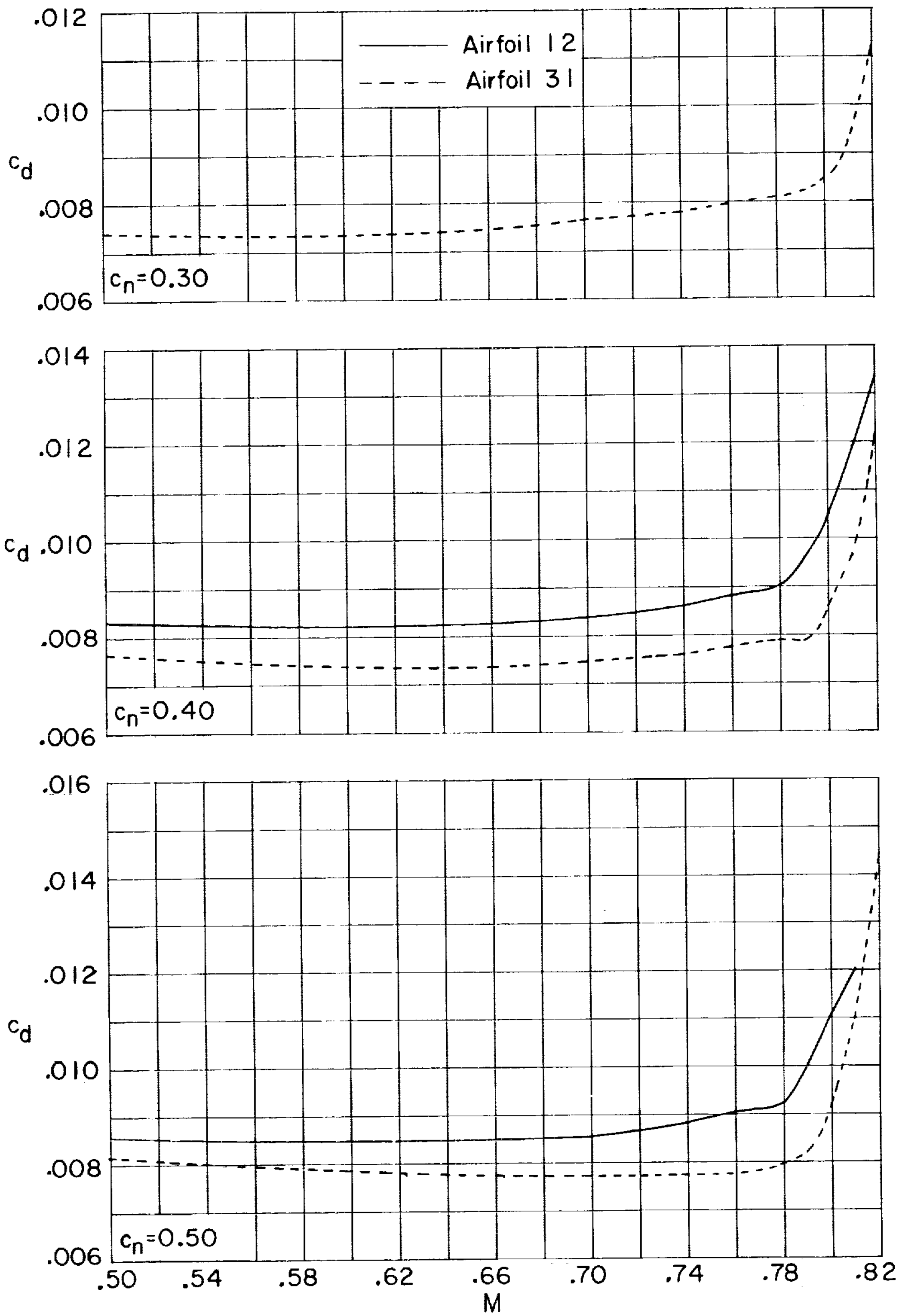

Figure 9.- Variation of section drag coefficient with Mach number of supercritical airfoils 12 and 31 at various normal-force coefficients.

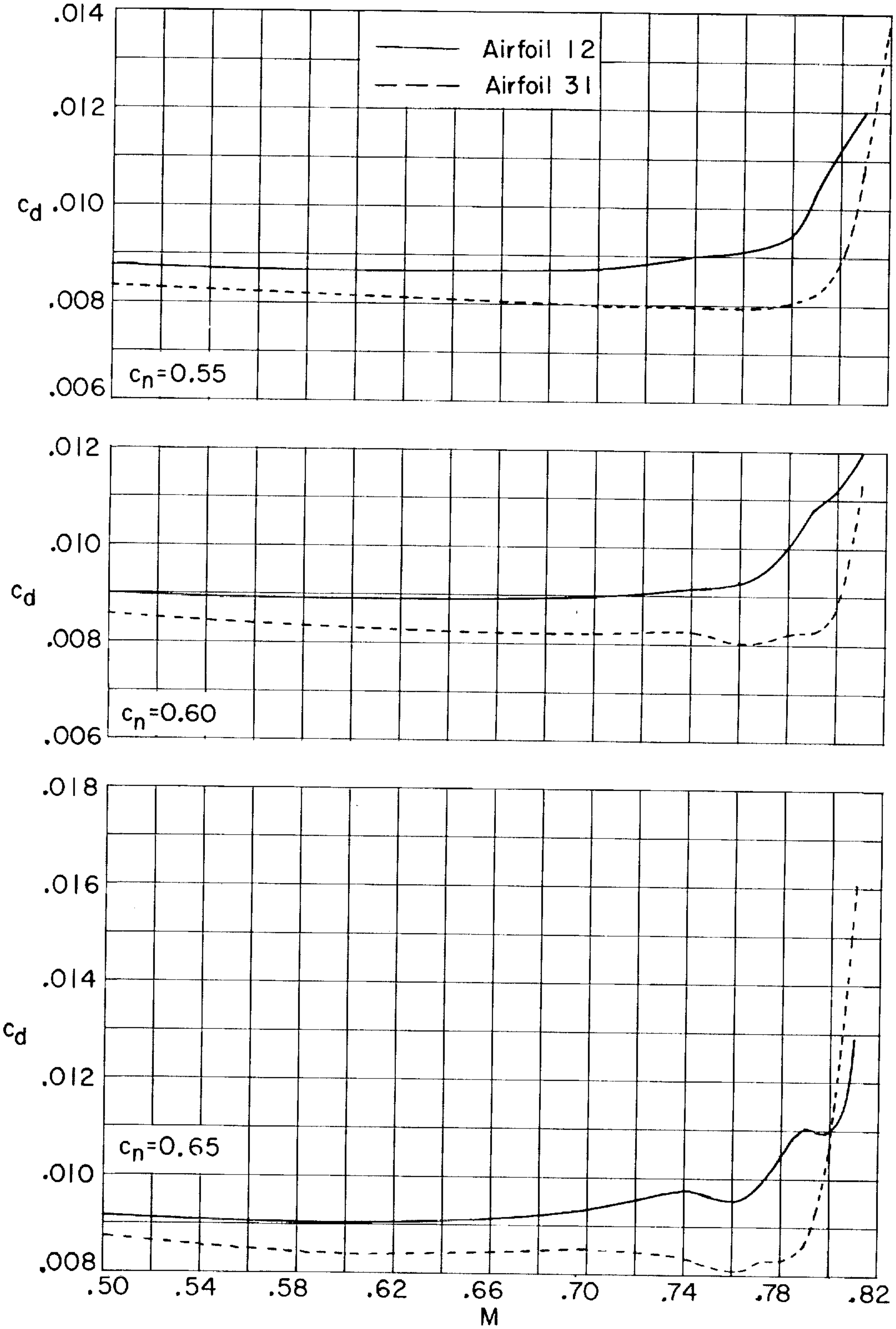

Figure 9.- Continued.

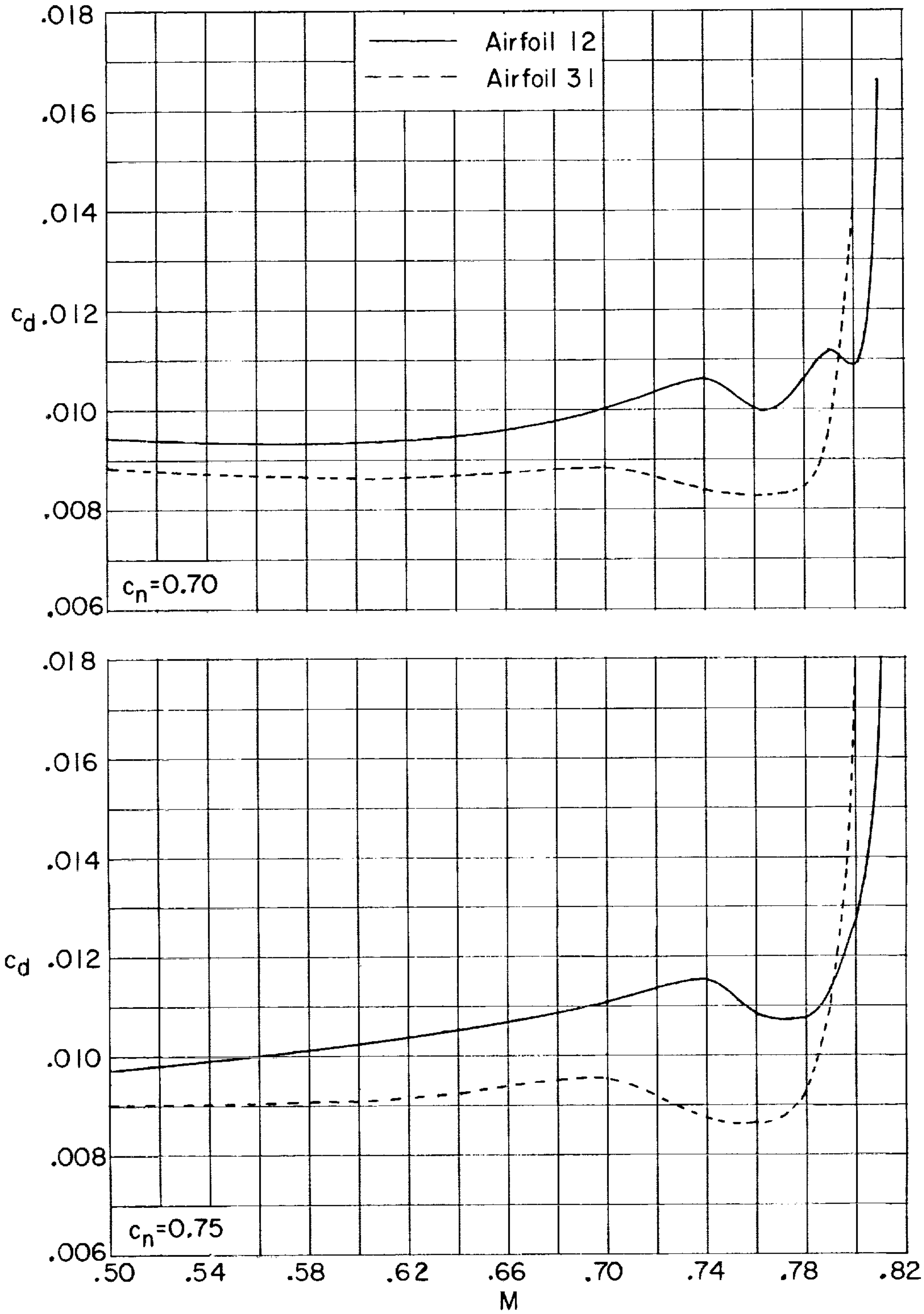

Figure 9.- Continued.

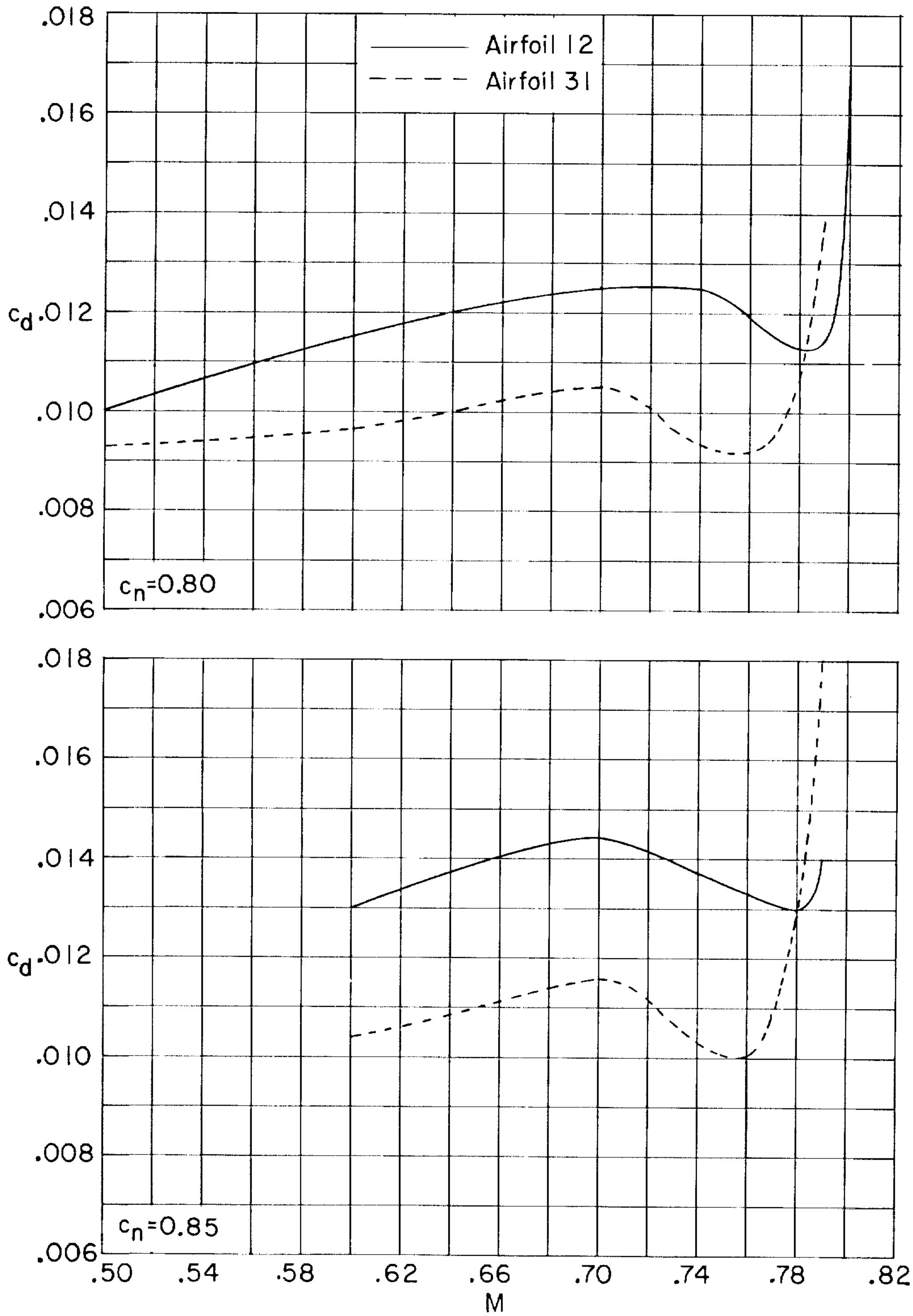

Figure 9. - Continued.

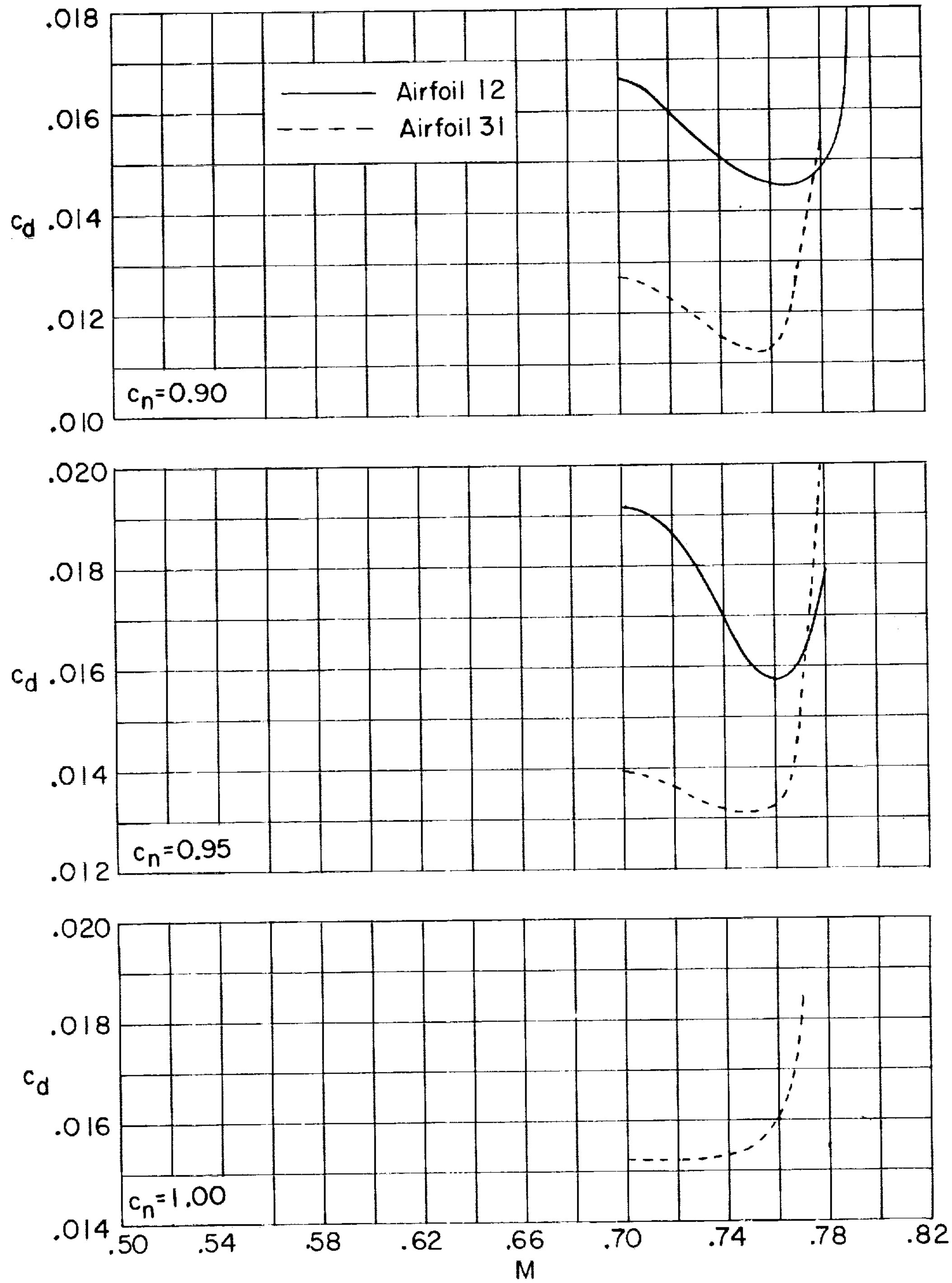

Figure 9.- Concluded.

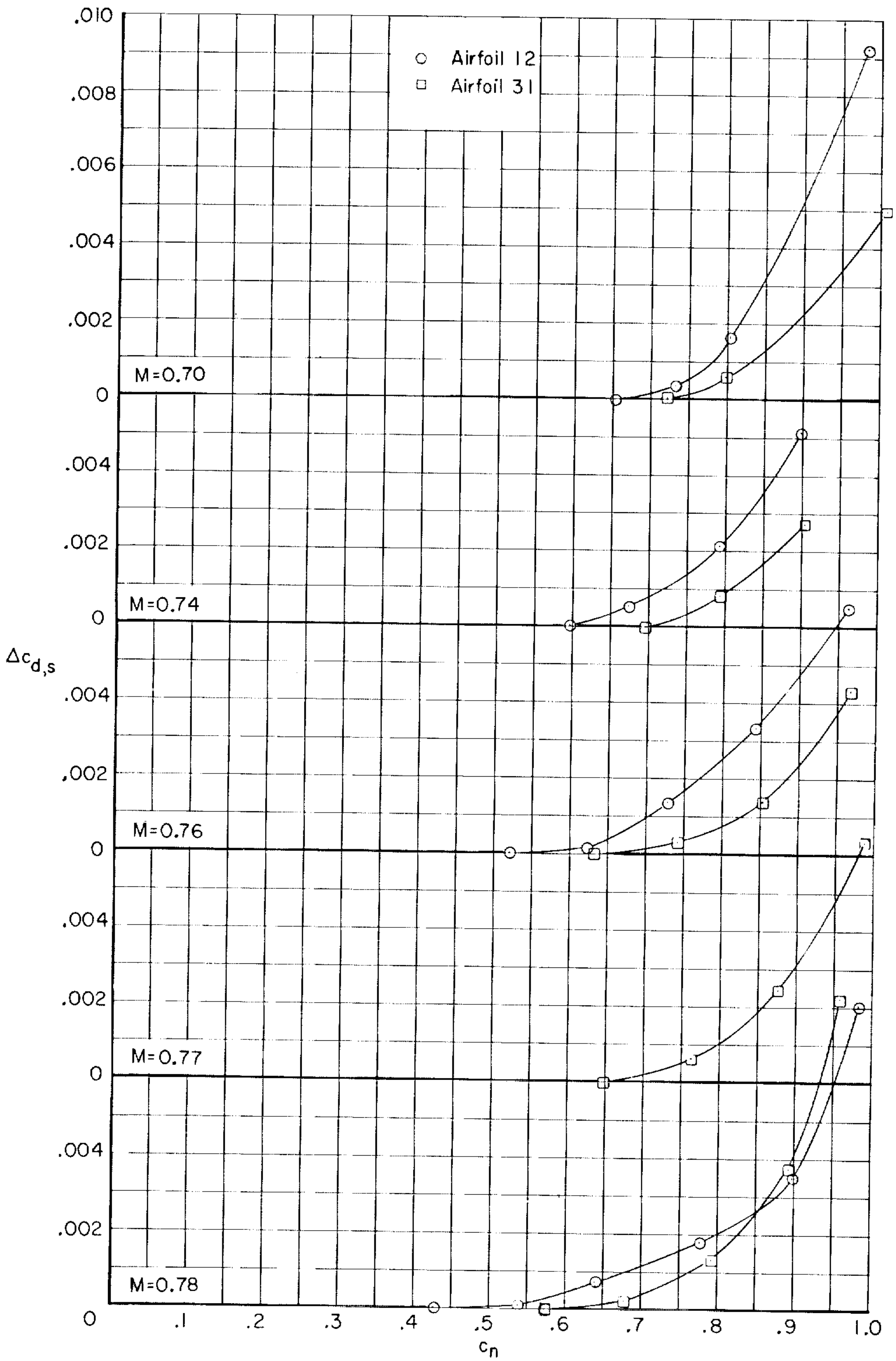

Figure 10.- Drag increment due to shock-wave losses.

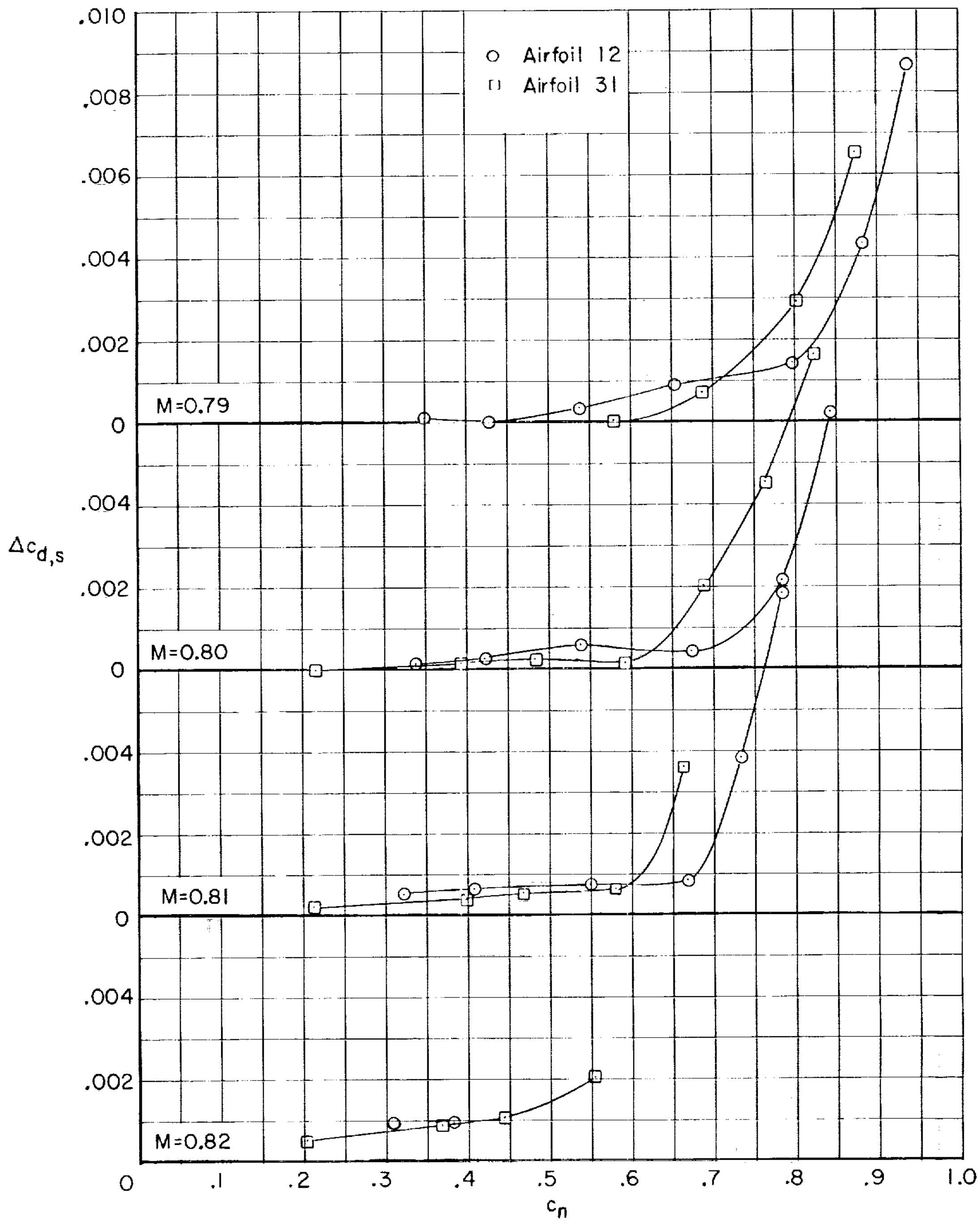

Figure 10.- Concluded.

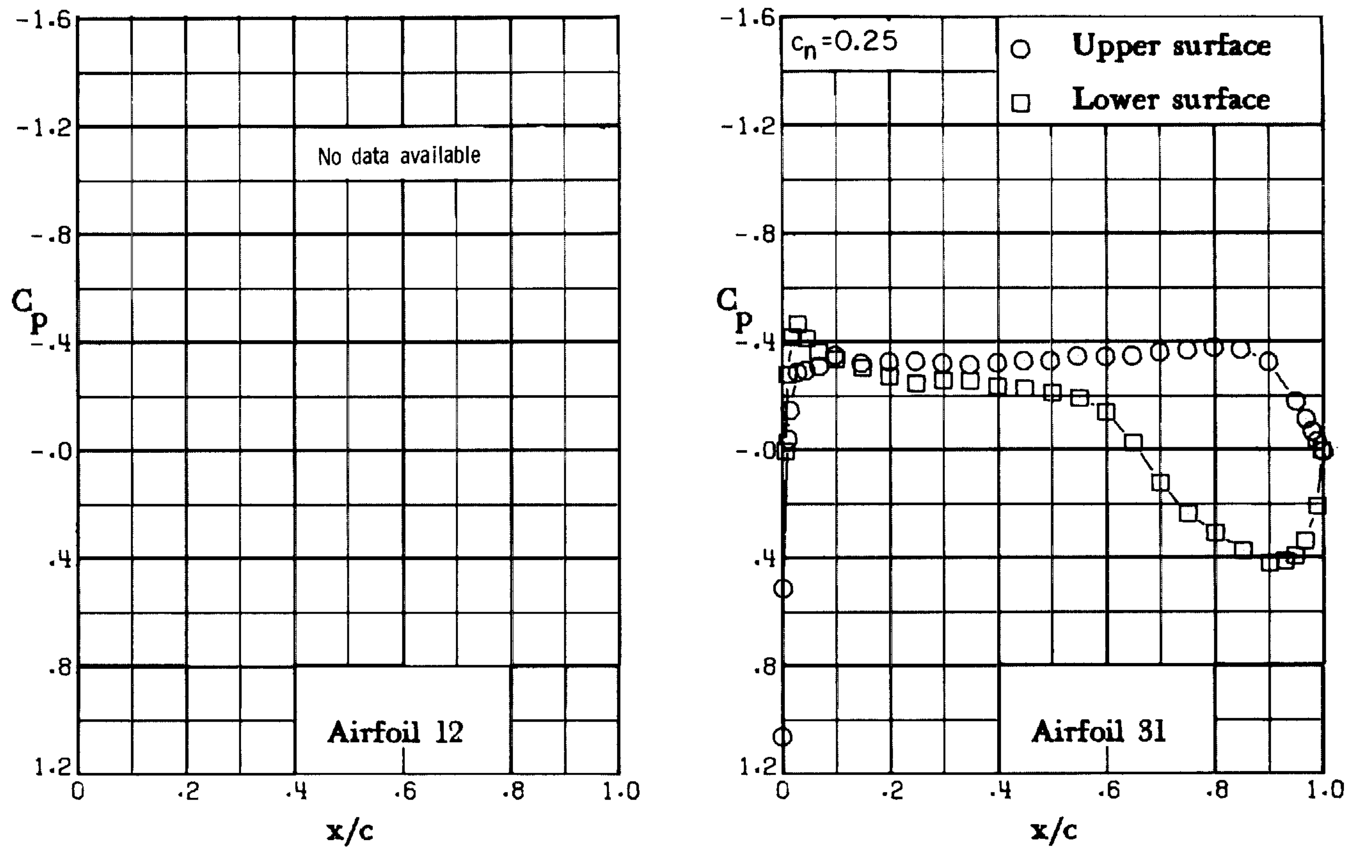

(a) M = 0.50; c_n = 0.25.

Figure 11.- Chordwise pressure distribution. M = 0.50.

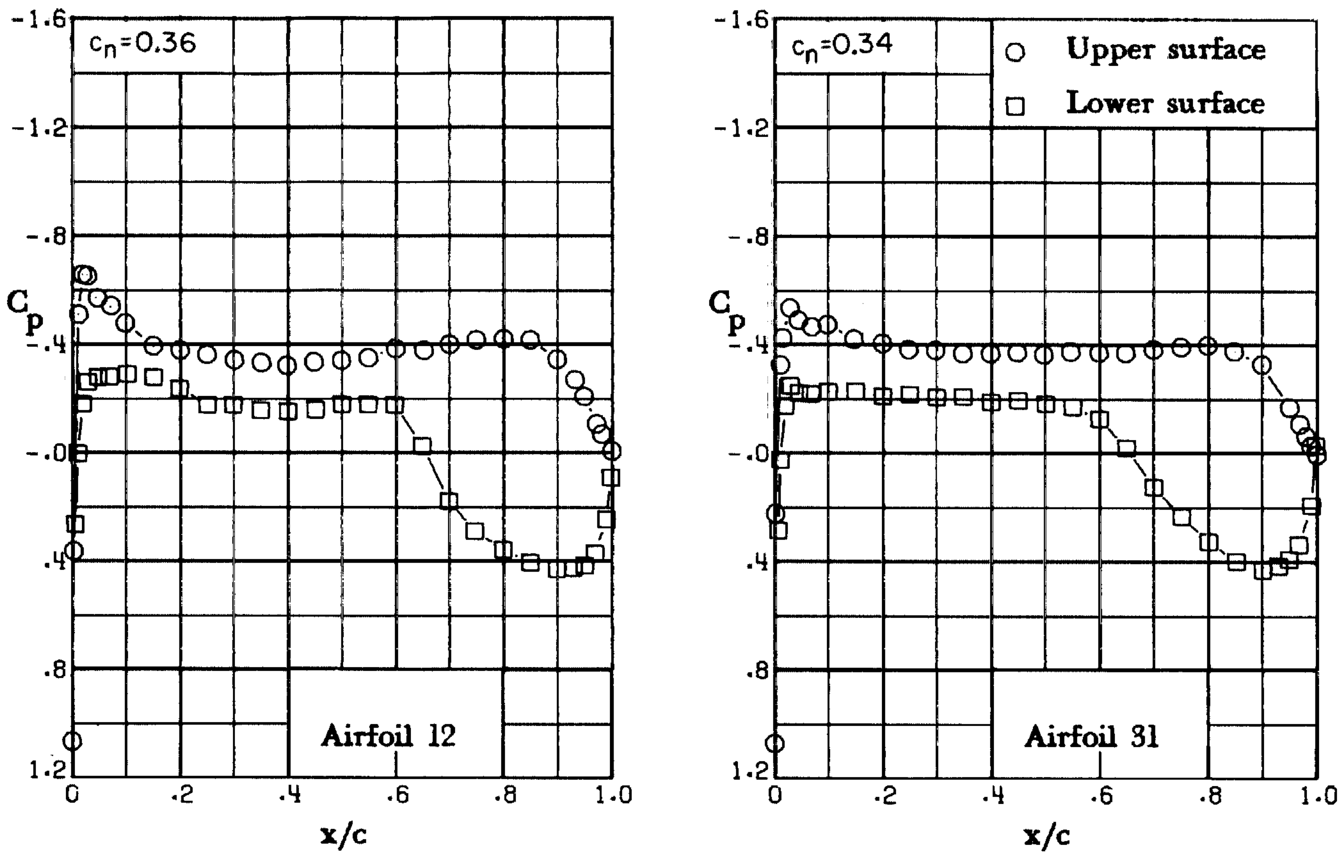

(b) $M = 0.50$; $c_n \approx 0.34$.

Figure 11.- Continued.

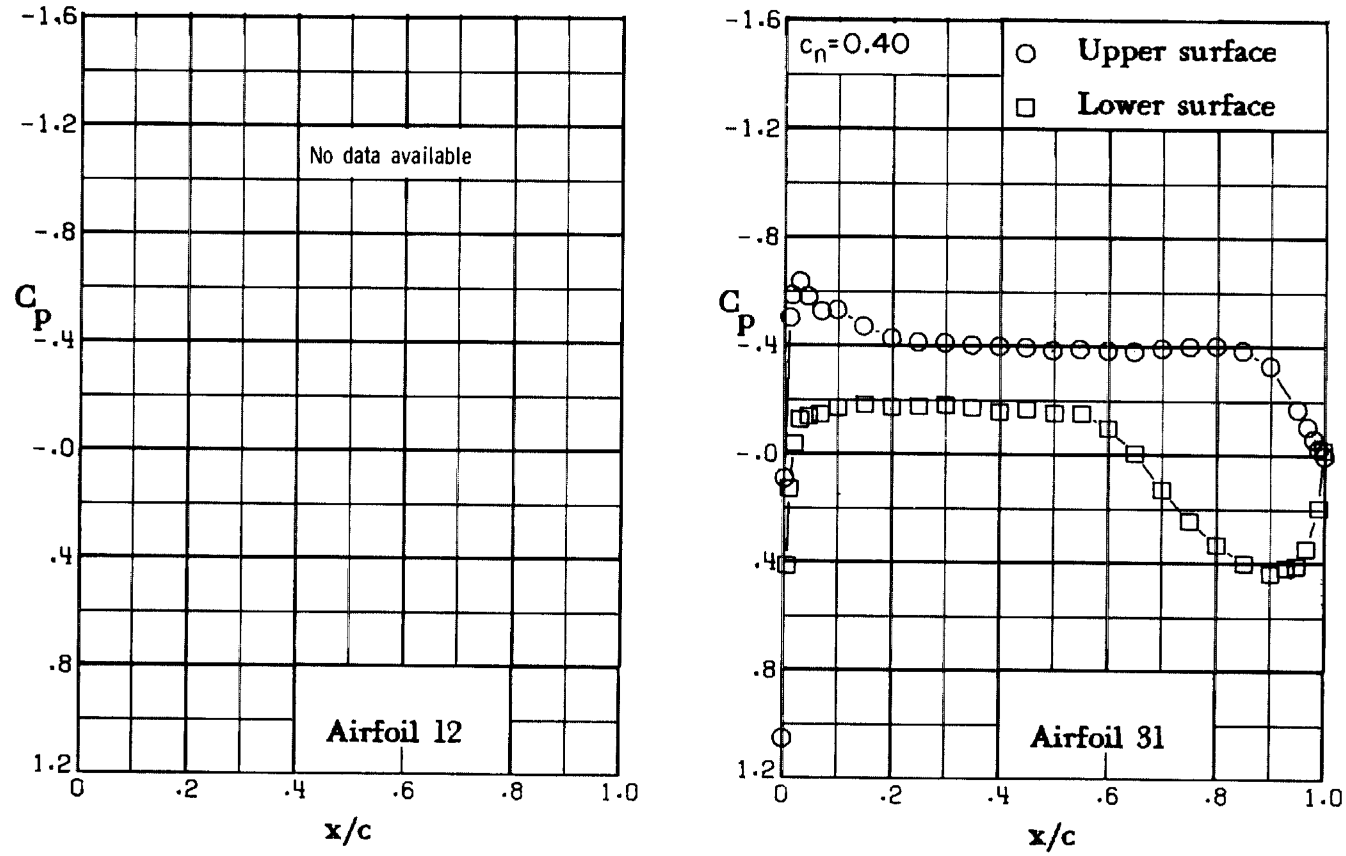

(c) $M = 0.50$; $c_n = 0.40$.

Figure 11. - Continued.

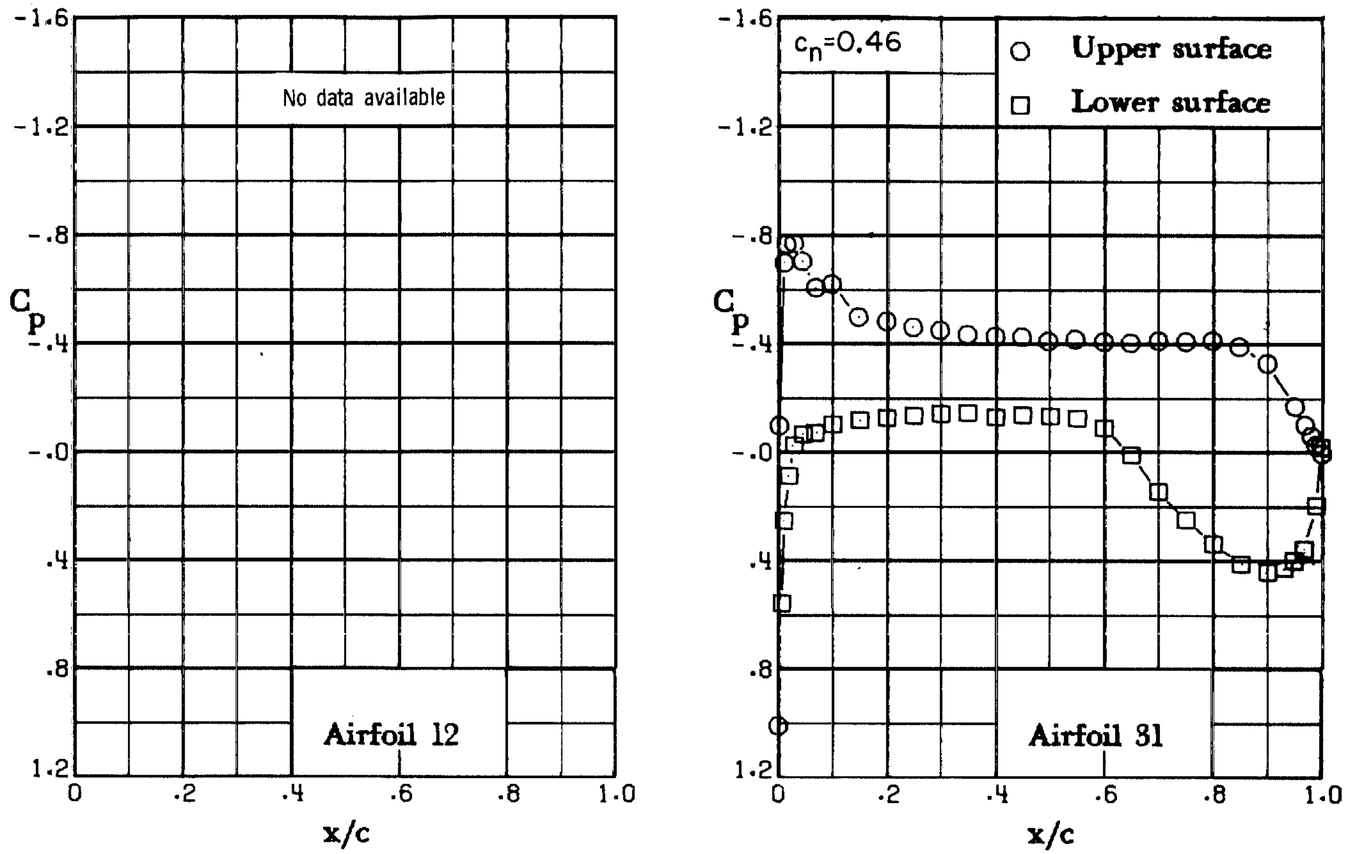

(d) $M = 0.50$; $c_n = 0.46$.

Figure 11.- Continued.

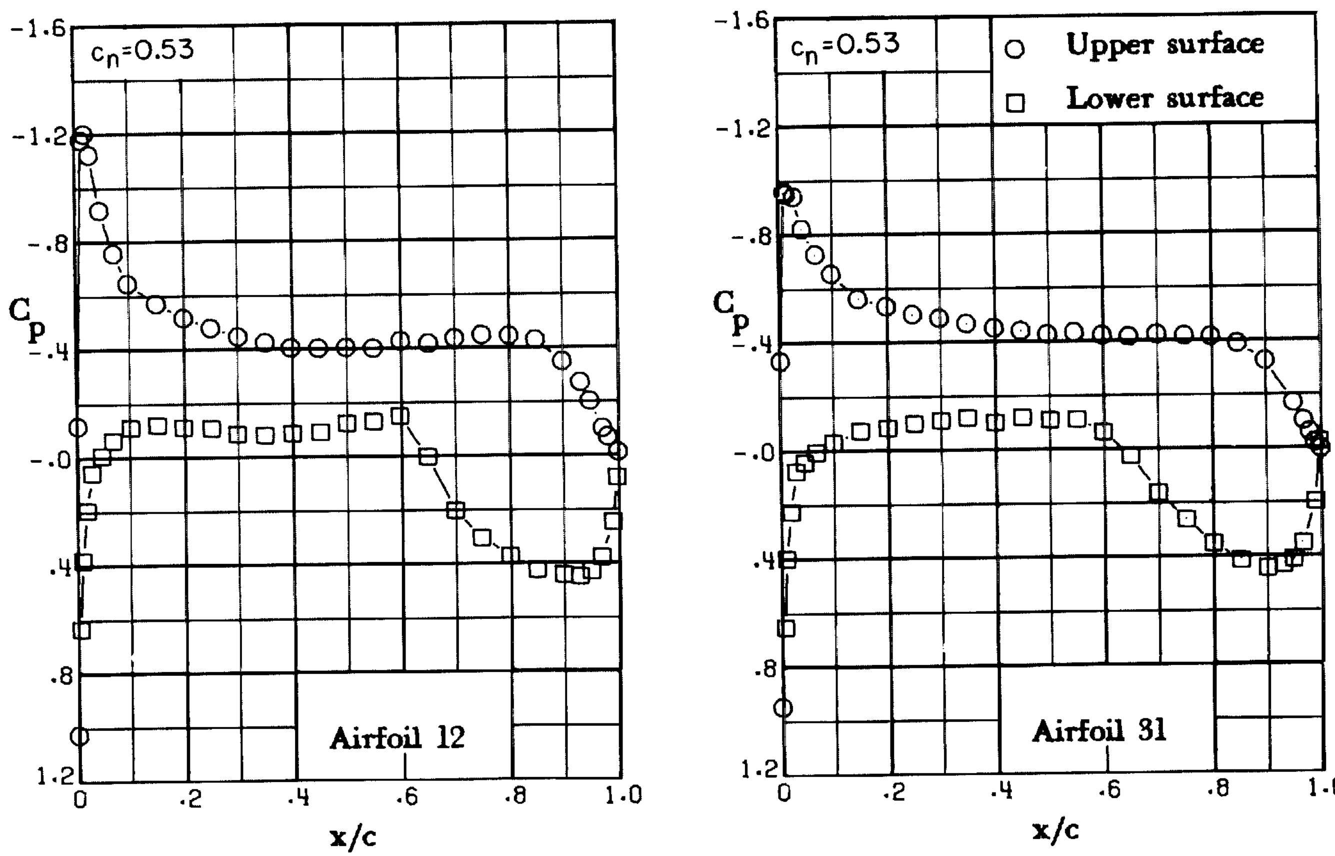

(e) $M = 0.50$; $c_n = 0.53$.

Figure 11.- Continued.

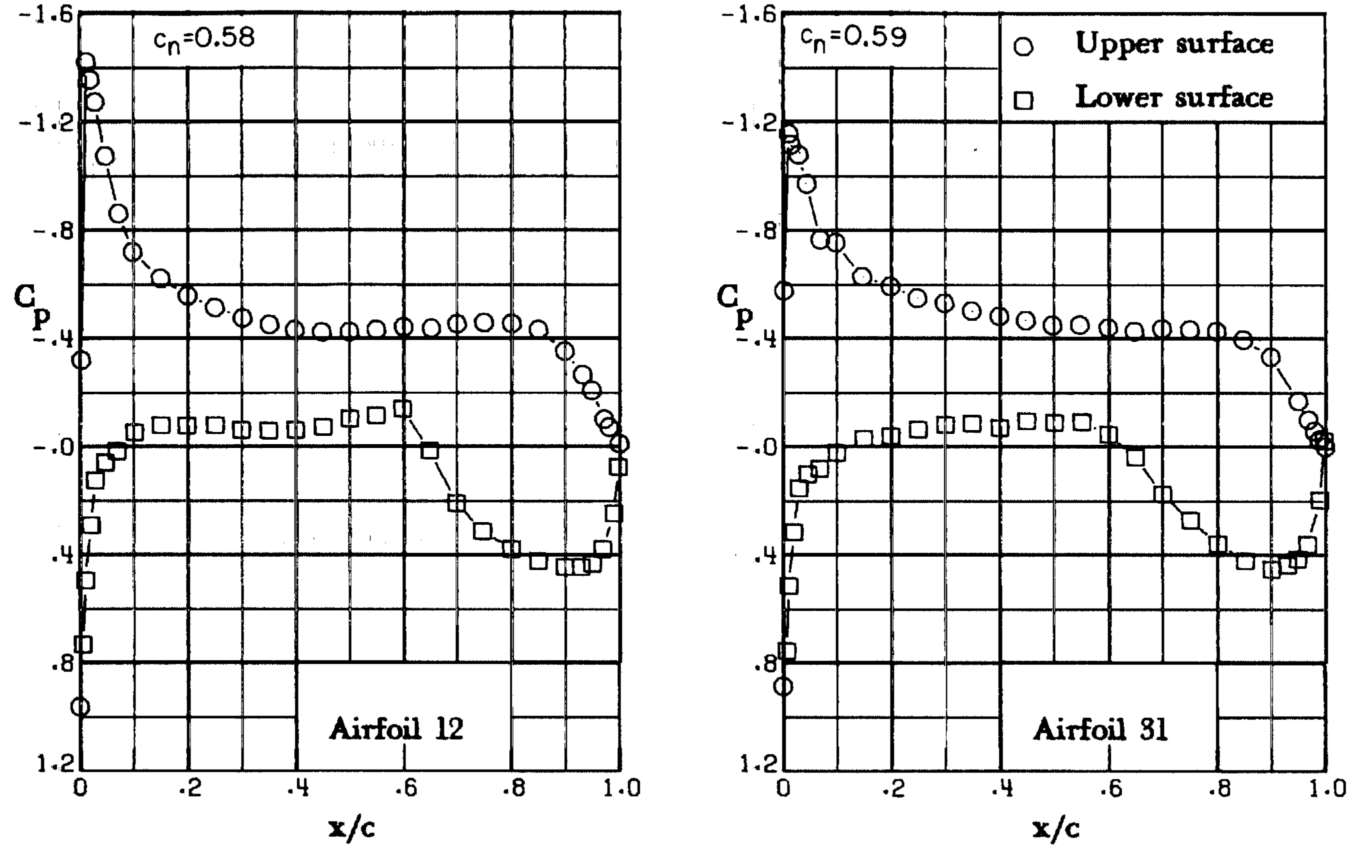

(f) $M = 0.50$; $c_n \approx 0.59$.

Figure 11.- Continued.

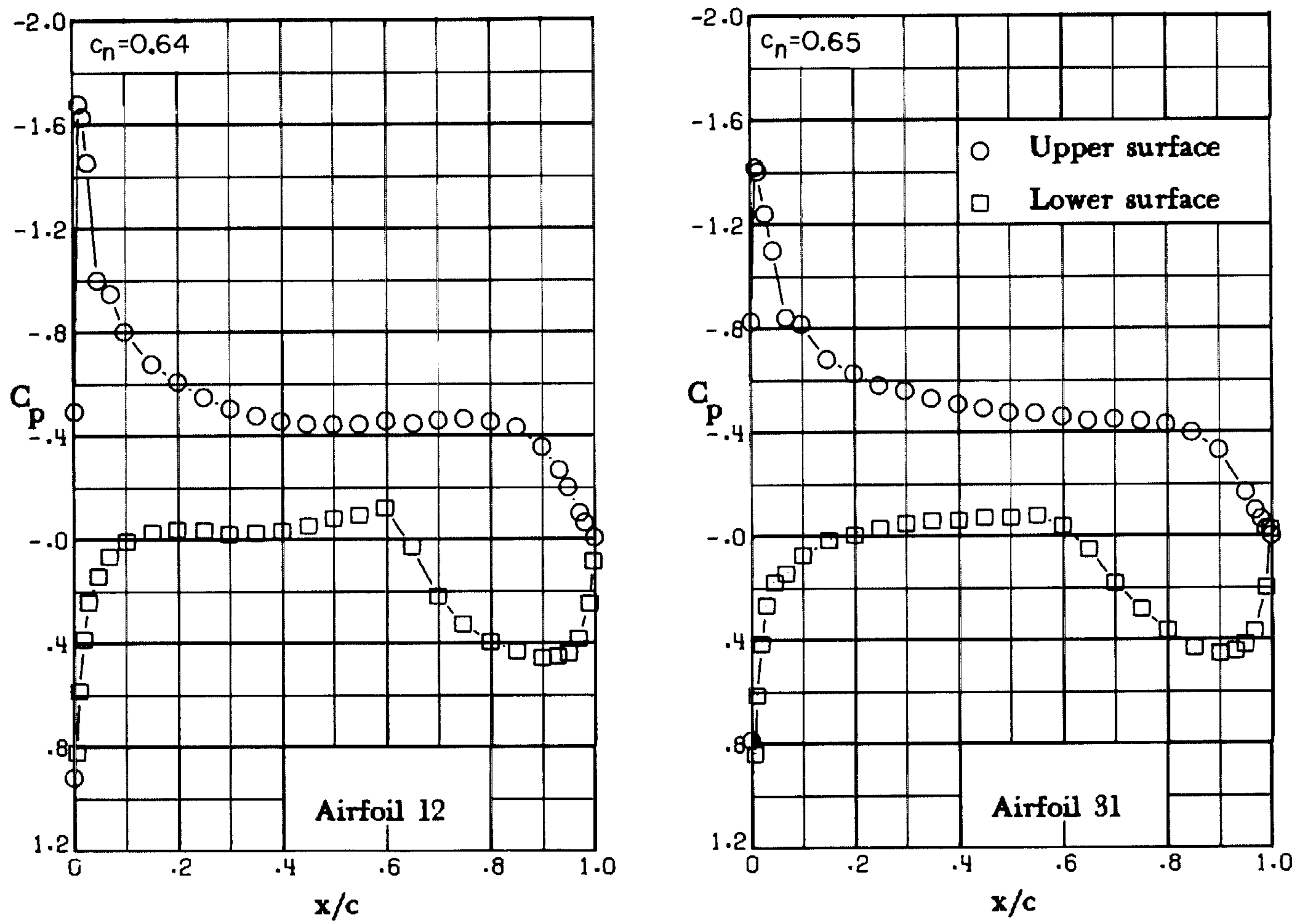

(g) $M = 0.50$; $c_n \approx 0.65$.

Figure 11.- Continued.

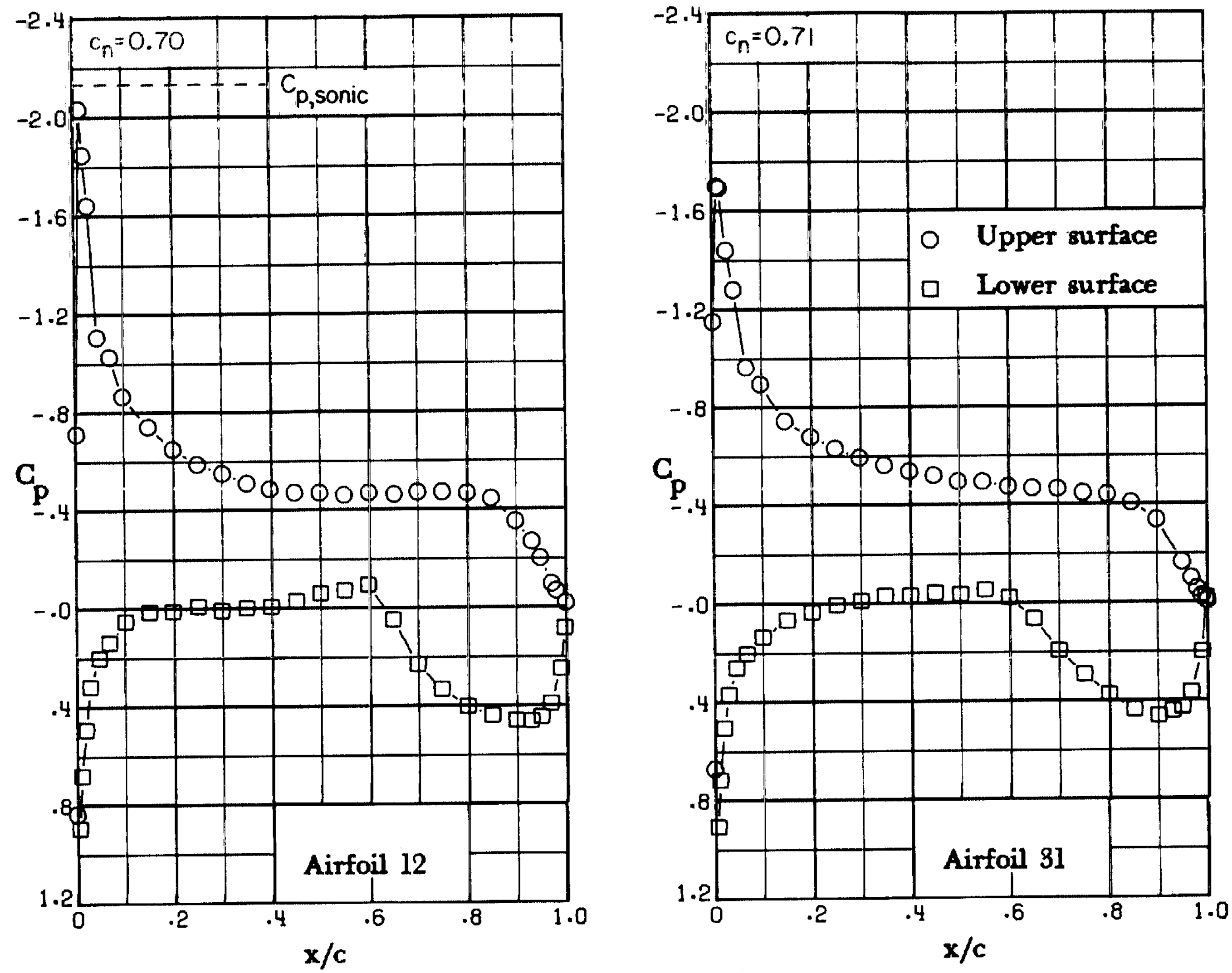

(h) M = 0.50; $c_n \approx 0.71$.

Figure 11.- Continued.

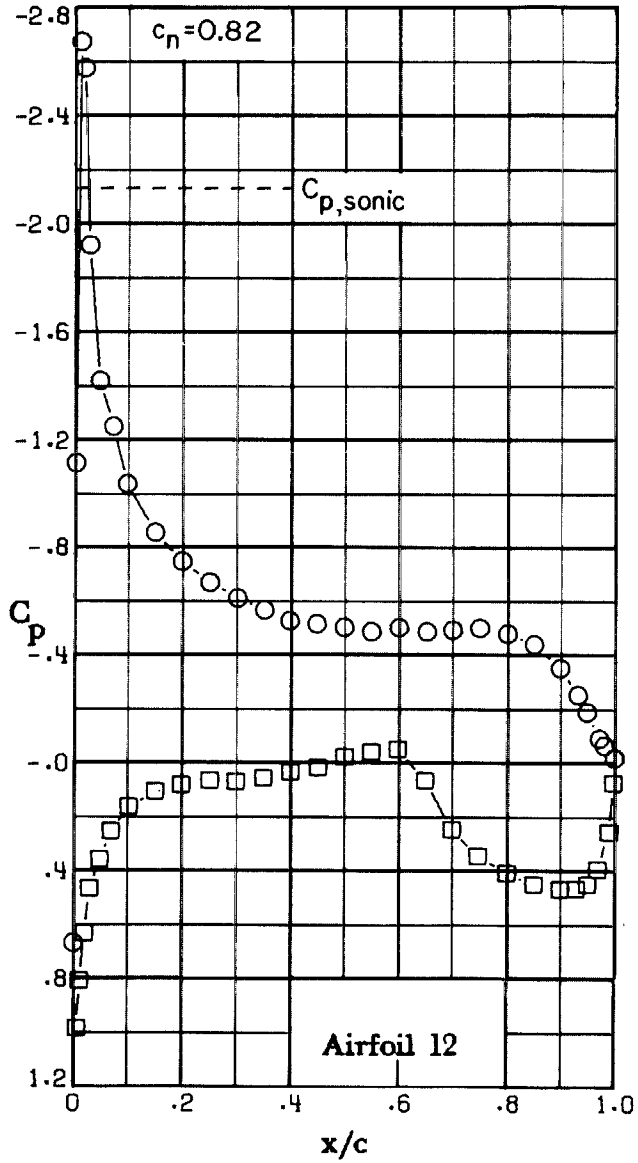

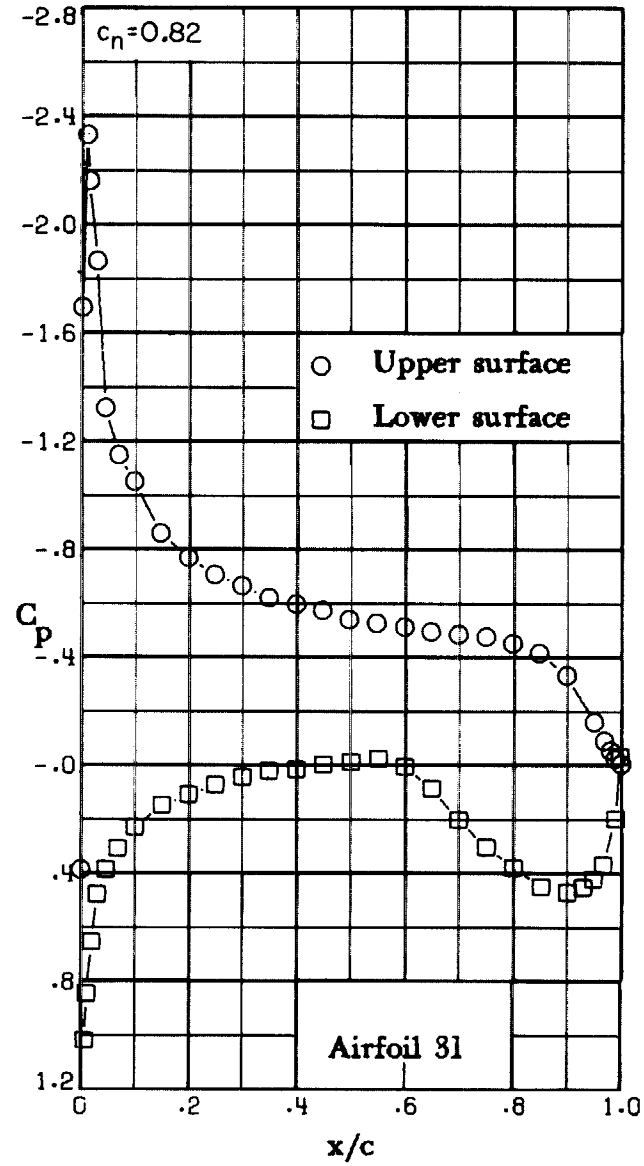

(i) $M = 0.50$; $c_n = 0.82$.

Figure 11.- Concluded.

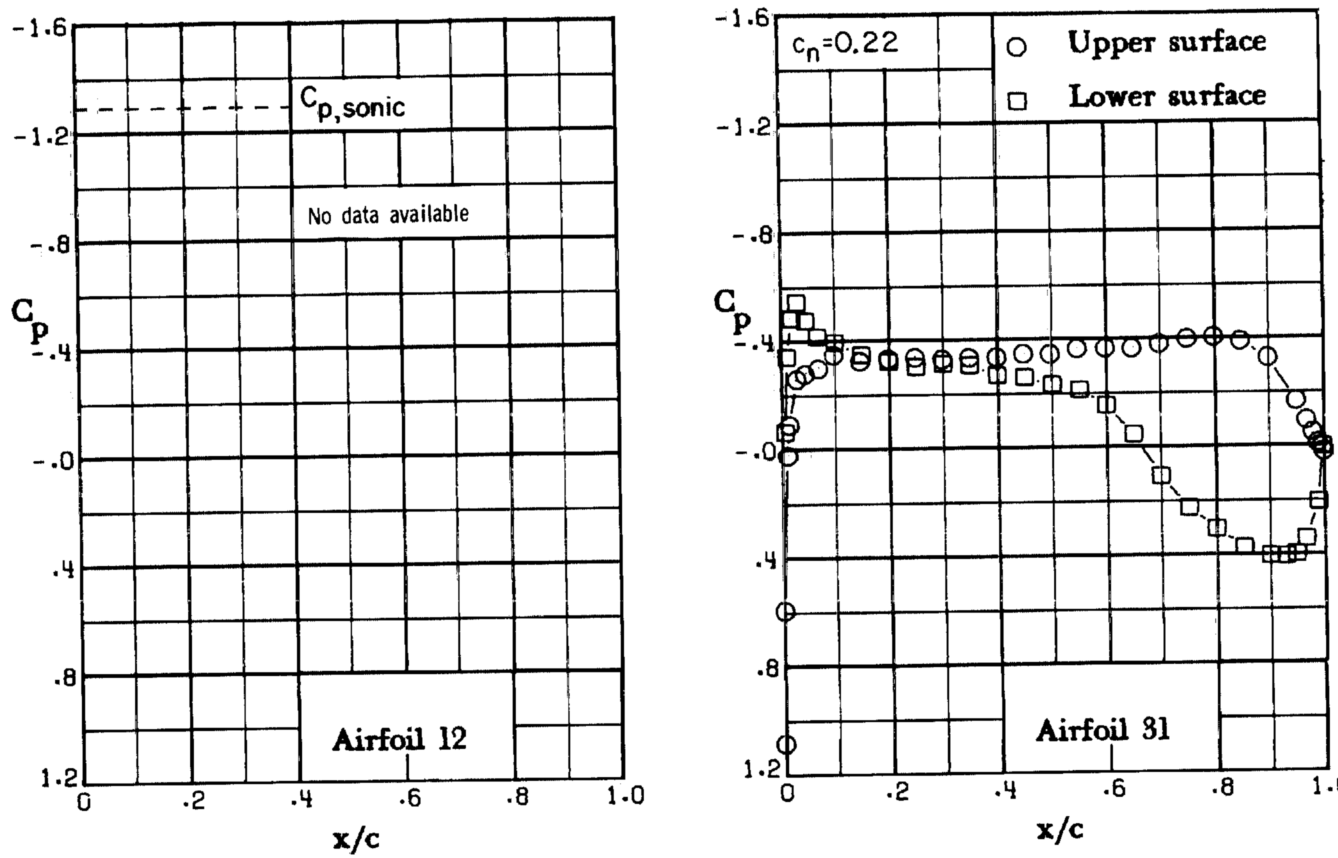

(a) M = 0.60; c_n = 0.22.

Figure 12.- Chordwise pressure distribution. M = 0.60.

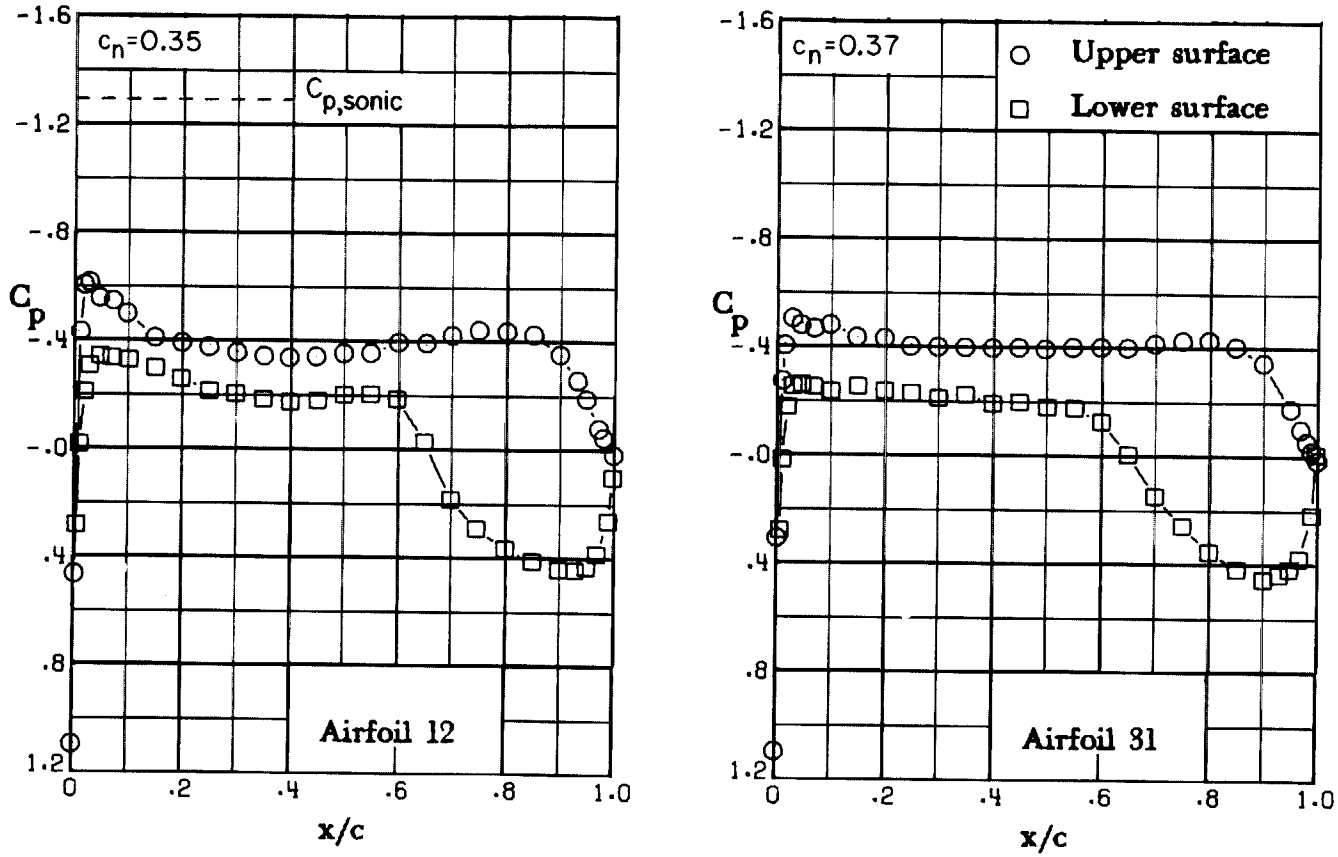

(b) M = 0.60; $c_n \approx 0.37$.

Figure 12.- Continued.

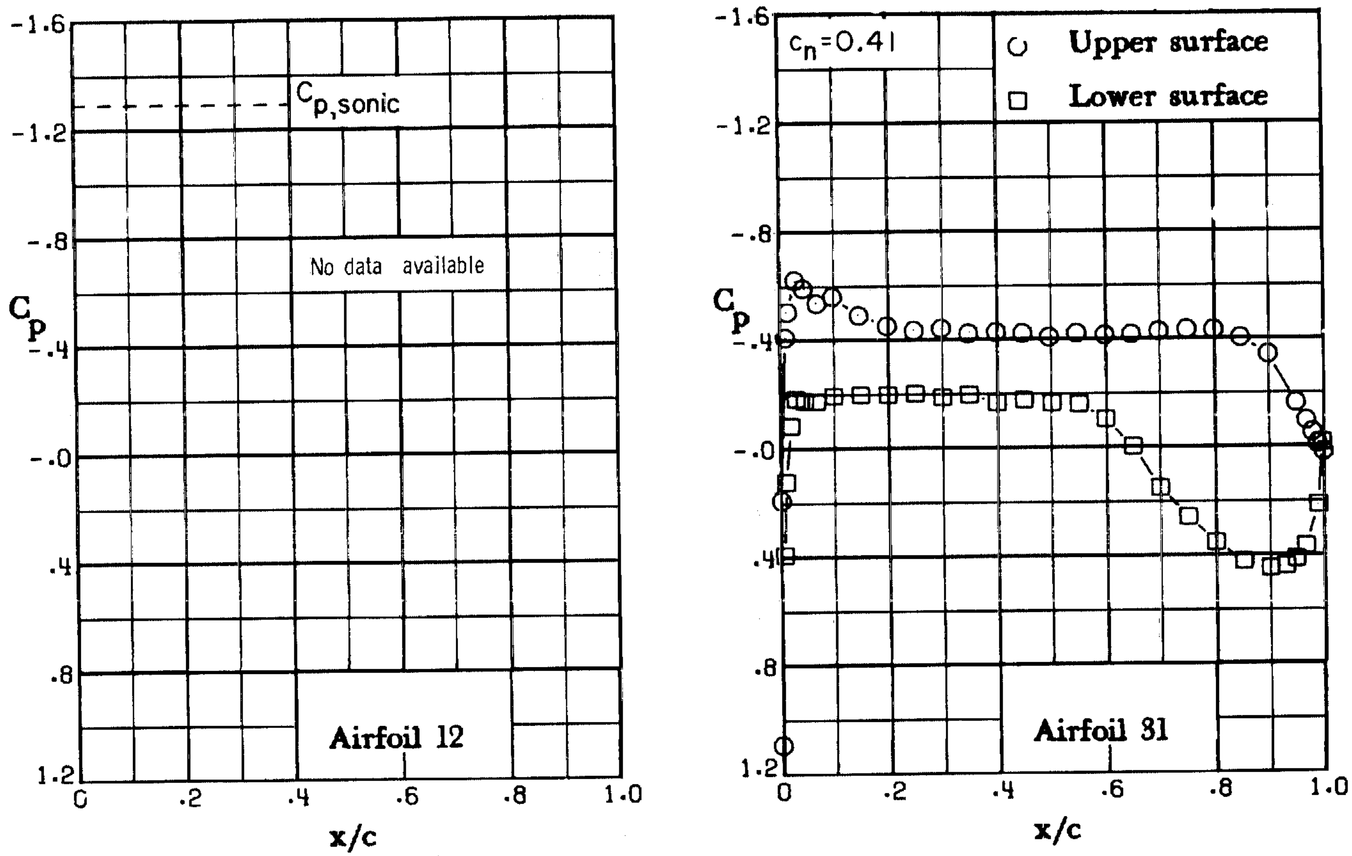

(c) $M = 0.60$; $c_n = 0.41$.

Figure 12.- Continued.

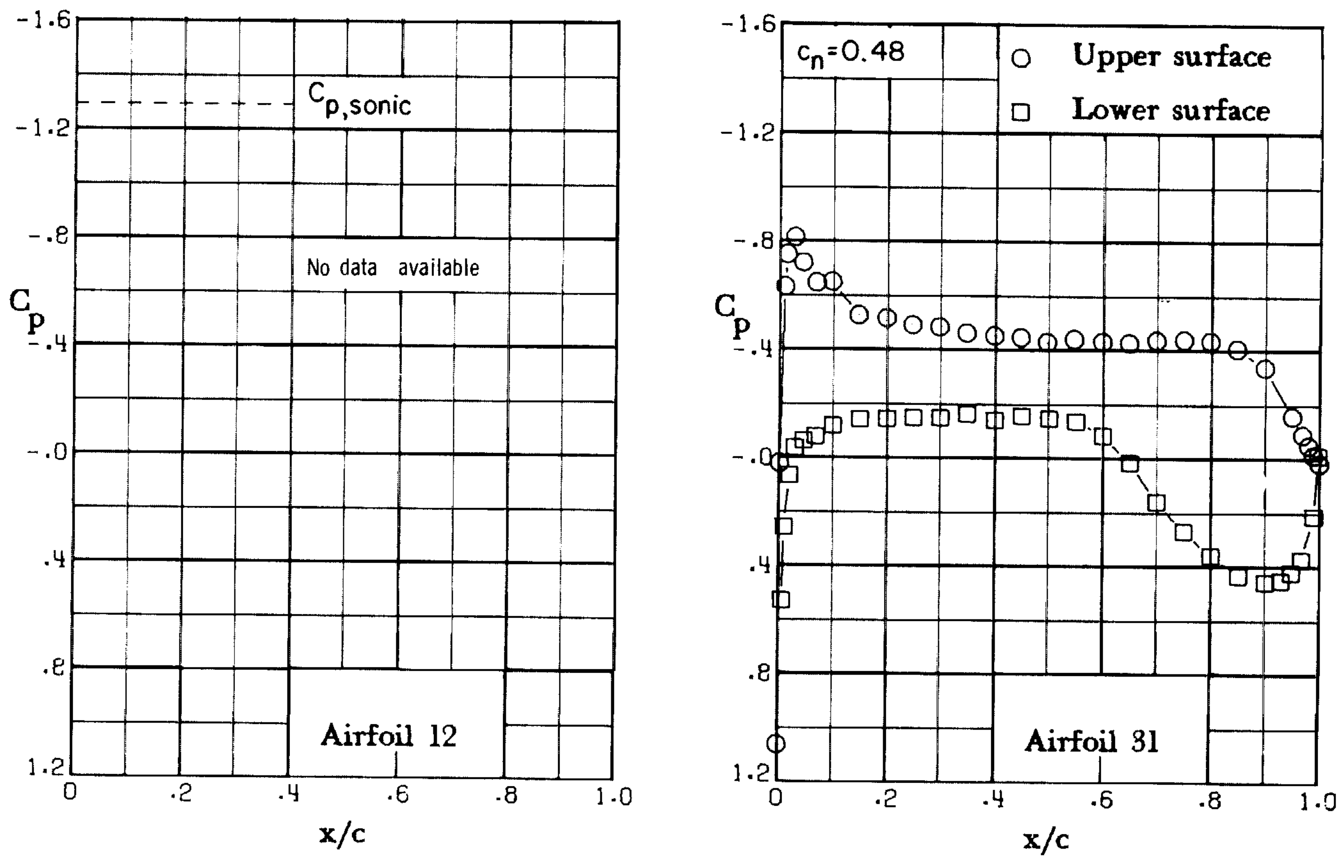

(d) $M = 0.60$; $c_n = 0.48$.

Figure 12.- Continued.

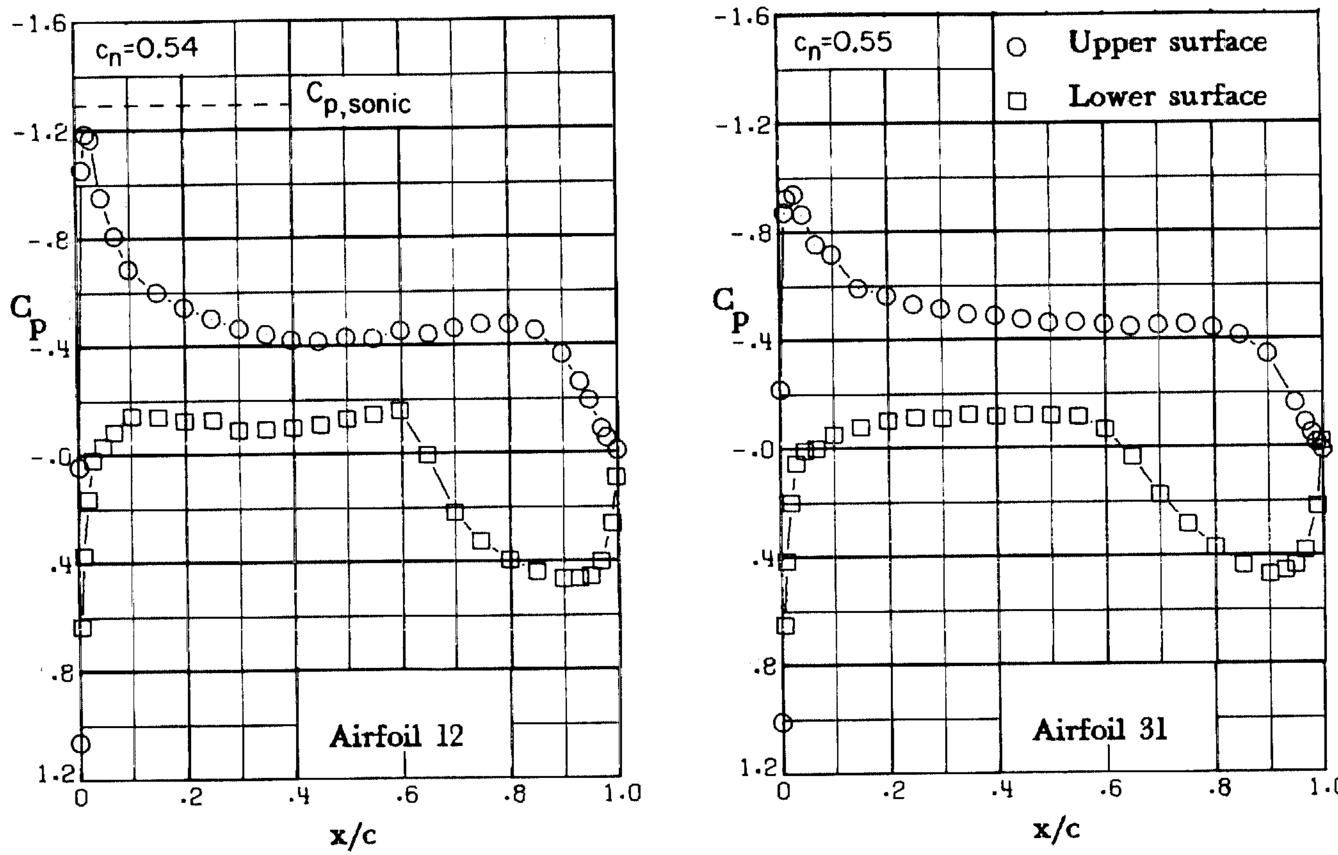

(e) $M = 0.60$; $c_n \approx 0.55$.

Figure 12. - Continued.

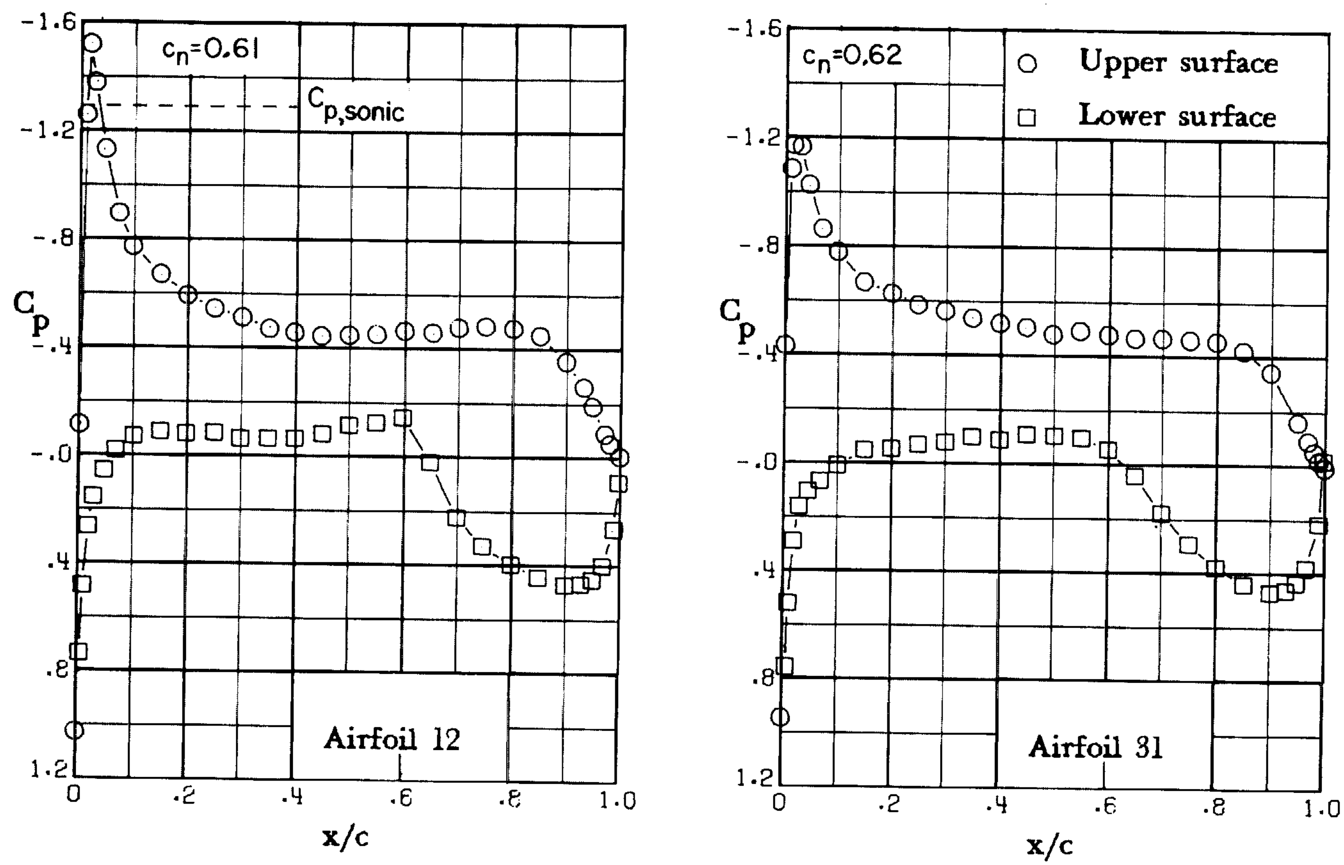

(f) M = 0.60; $c_n \approx 0.62$.

Figure 12.- Continued.

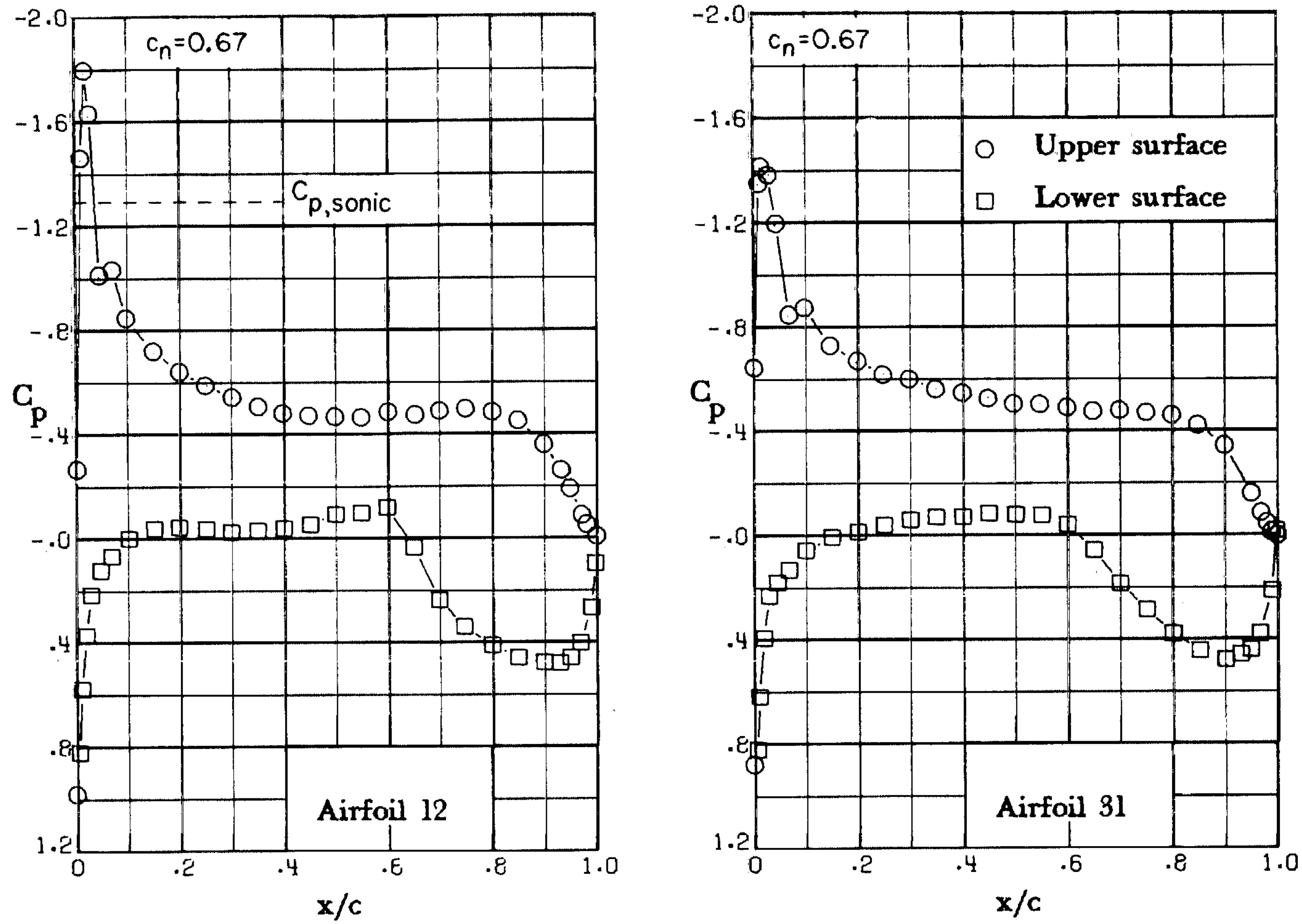

(g) M = 0.60; c_n = 0.67.

Figure 12. - Continued.

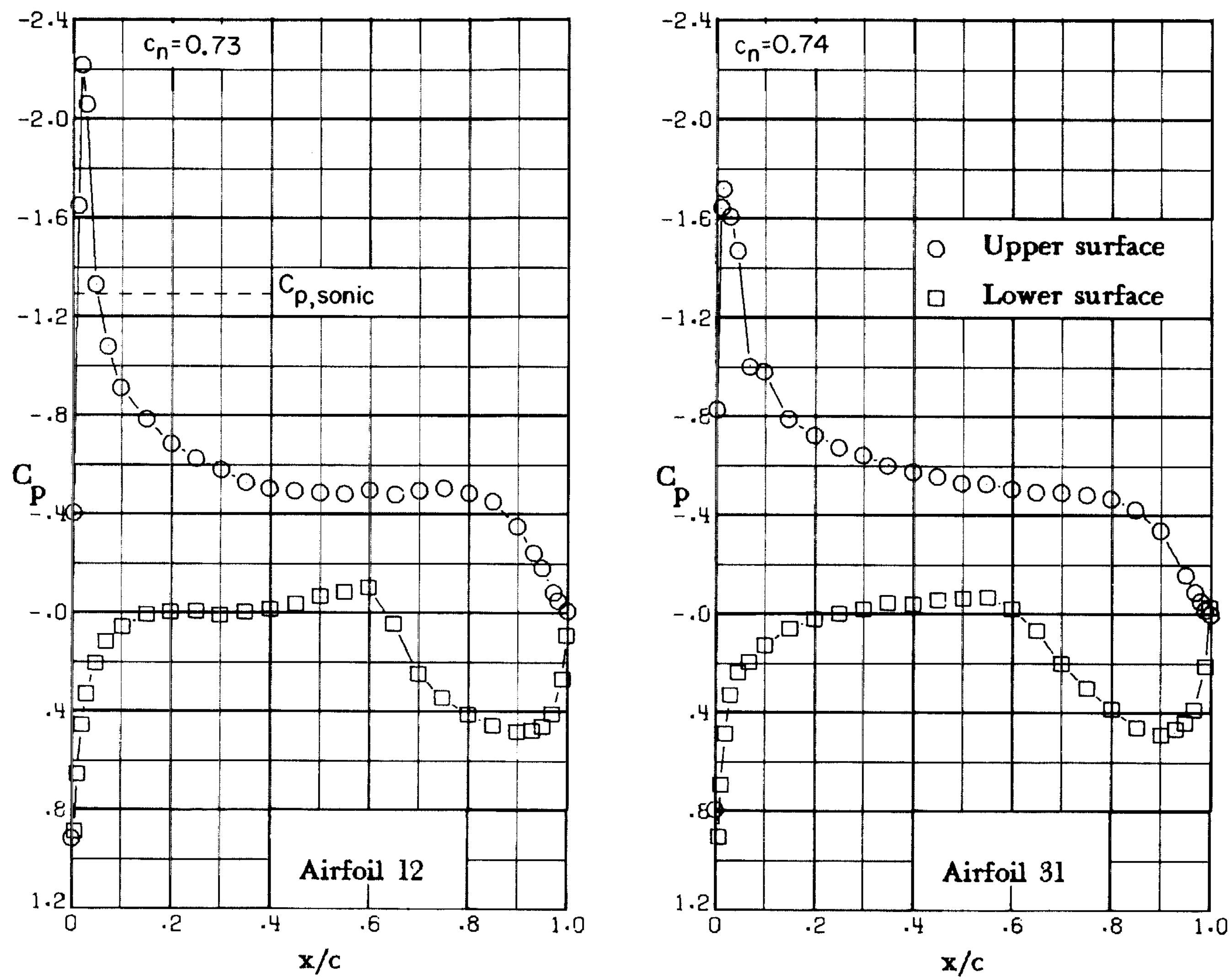

(h) $M = 0.60$; $c_n \approx 0.74$.

Figure 12.- Continued.

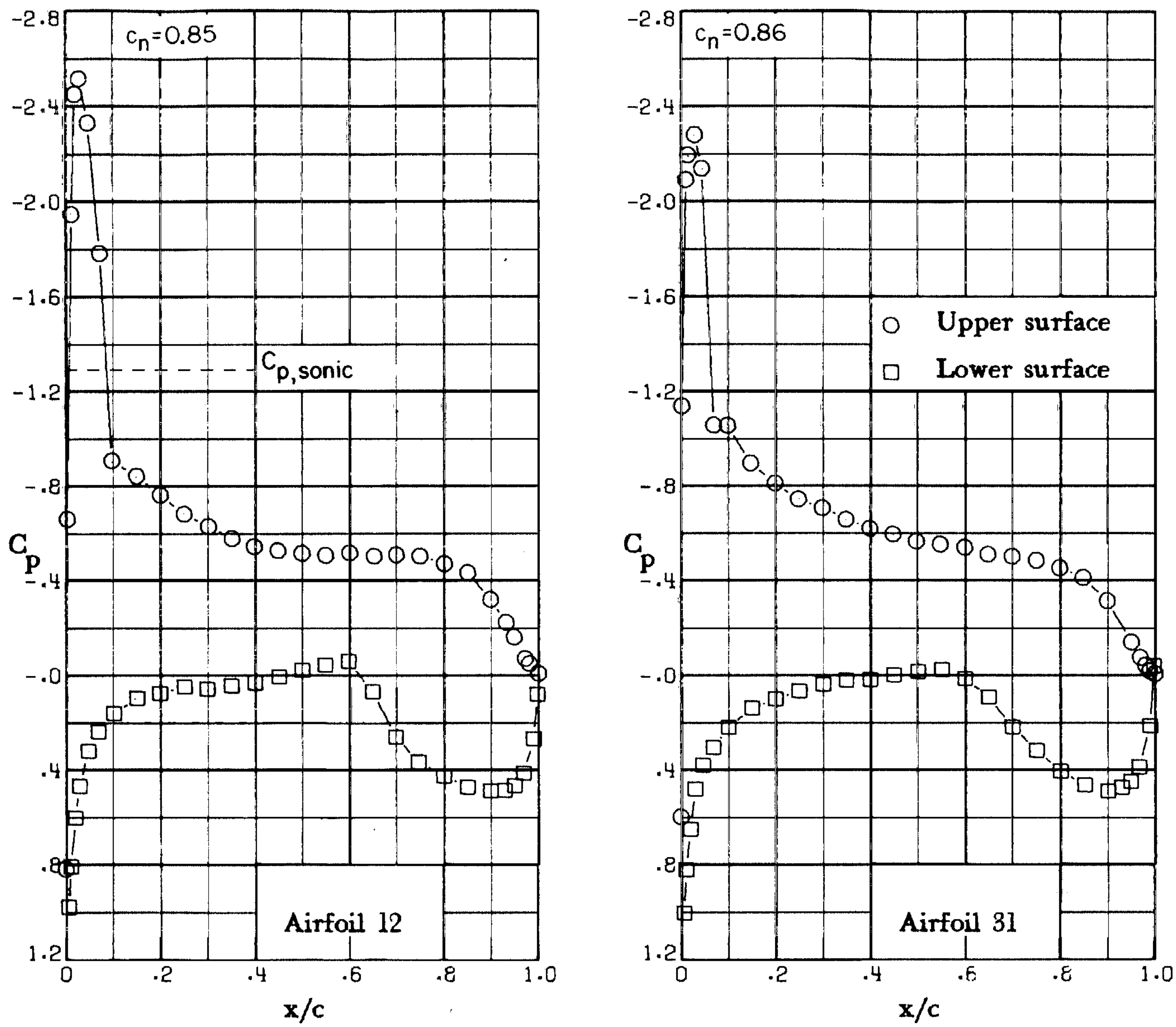

(i) $M = 0.60$; $c_n \approx 0.86$.

Figure 12.- Concluded.

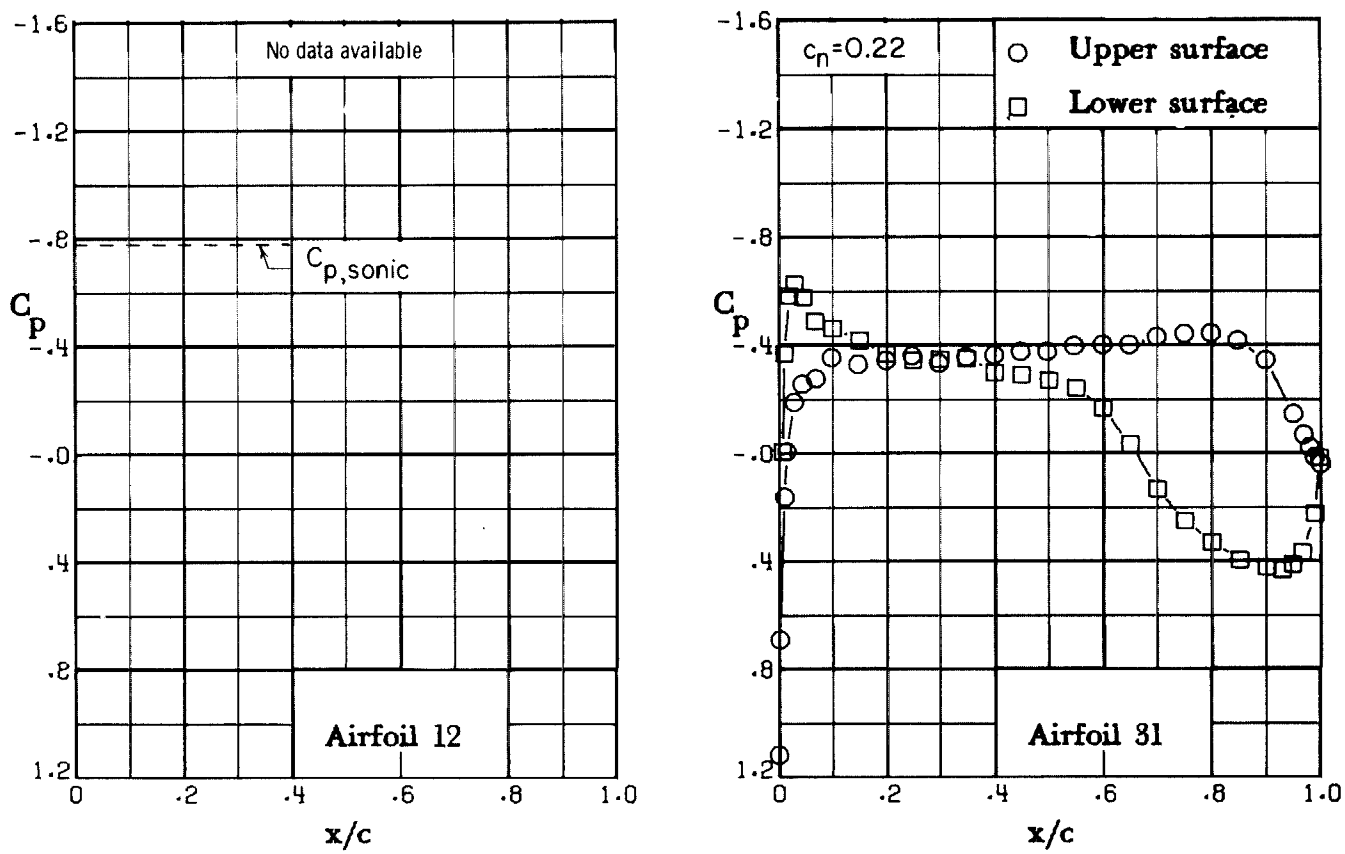

(a) M = 0.70; c_n = 0.22.

Figure 13.- Chordwise pressure distribution. M = 0.70.

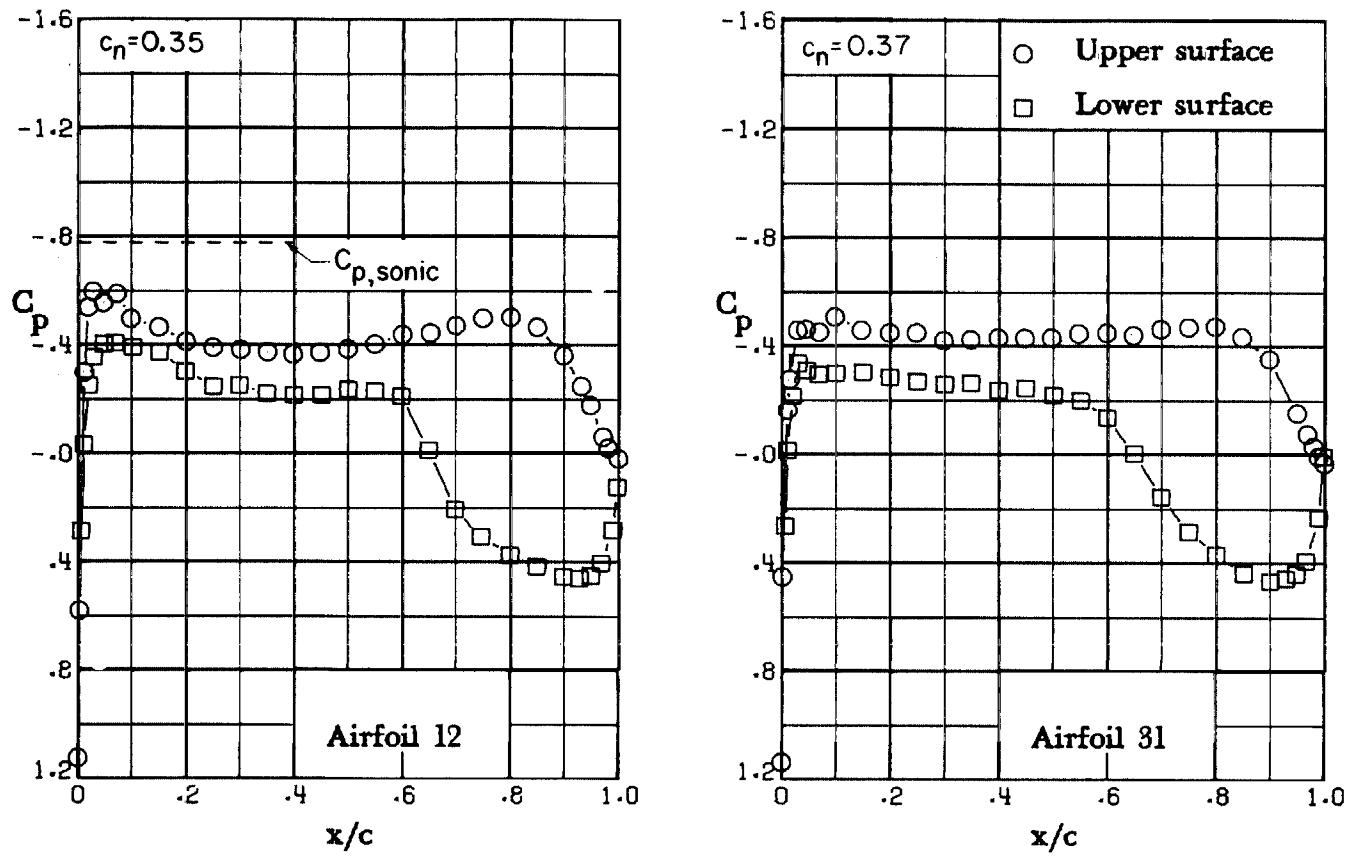

(b) M = 0.70; $c_n \approx 0.37$.

Figure 13.- Continued.

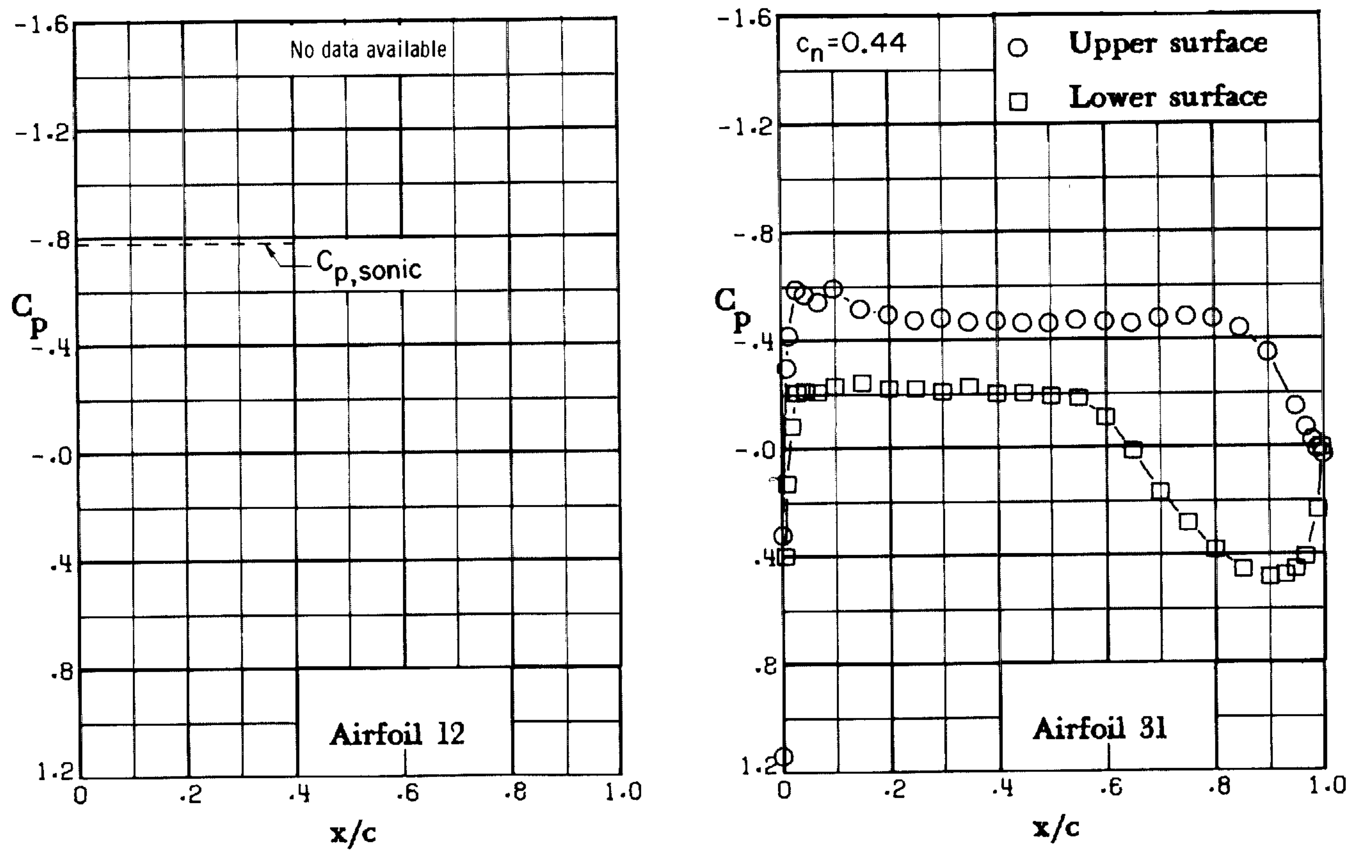

(c) $M = 0.70$; $c_n = 0.44$.

Figure 13. - Continued.

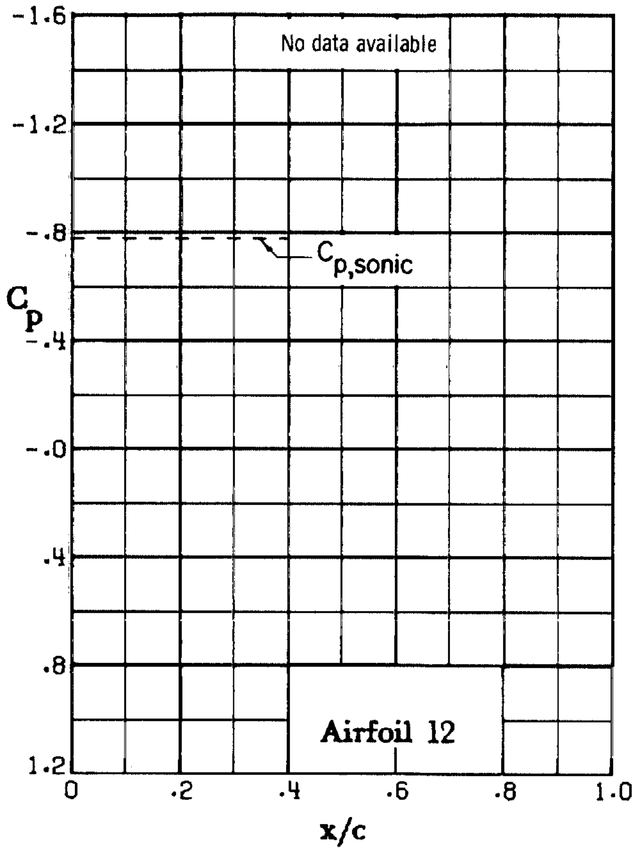

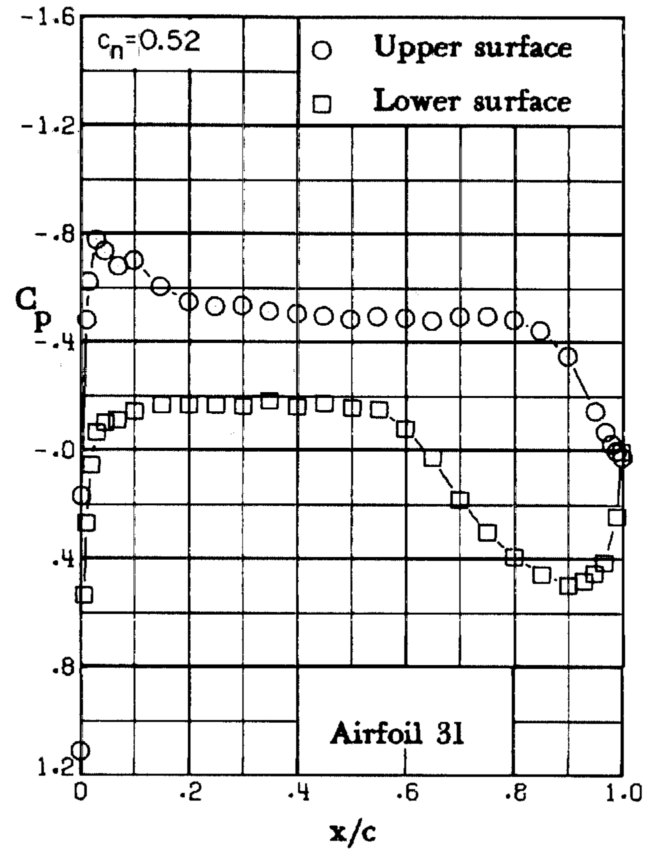

(d) M = 0.70; c_n = 0.52.

Figure 13.- Continued.

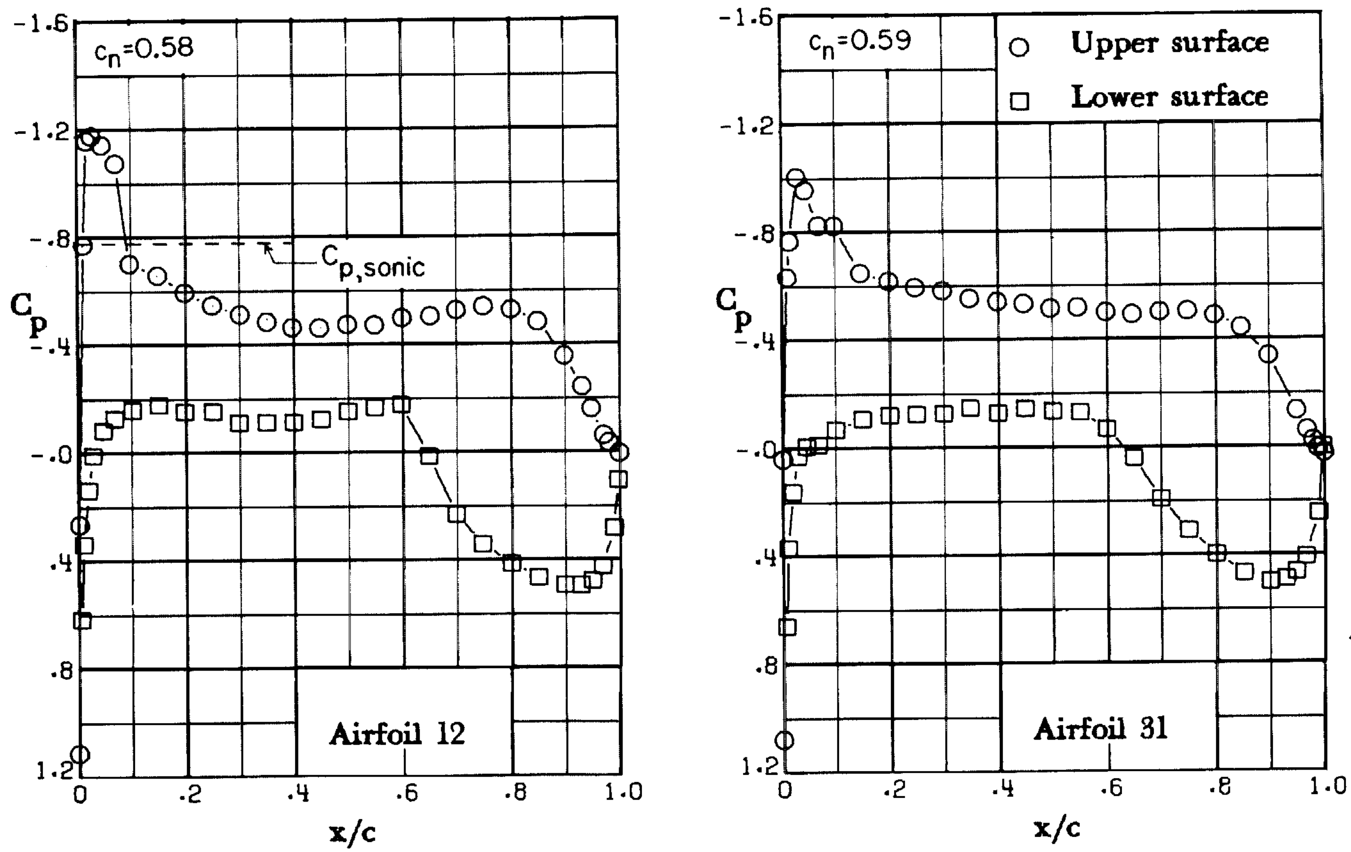

(e) $M = 0.70$; $c_n \approx 0.59$.

Figure 13. - Continued.

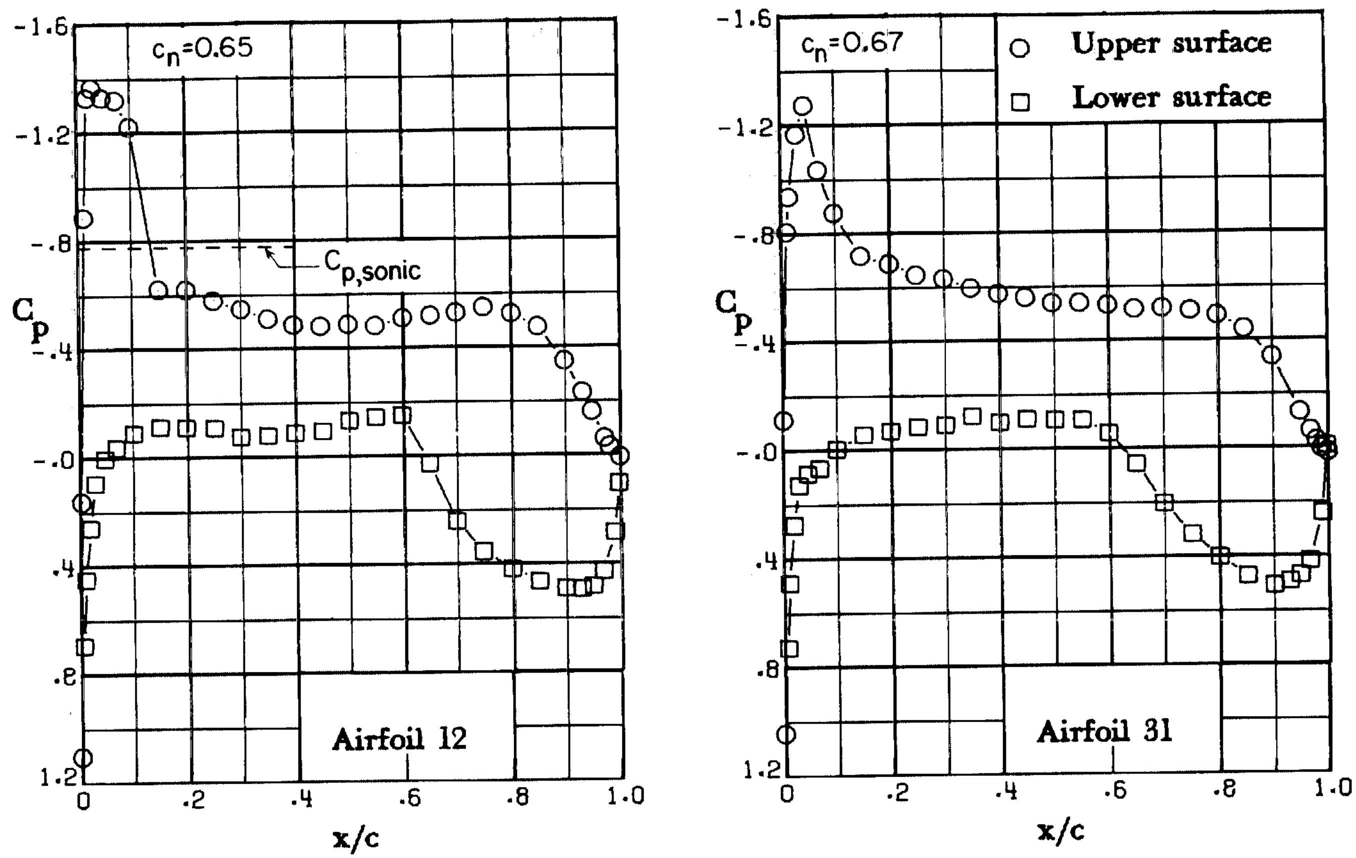

(f) $M = 0.70$; $c_n \approx 0.67$.

Figure 13.- Continued.

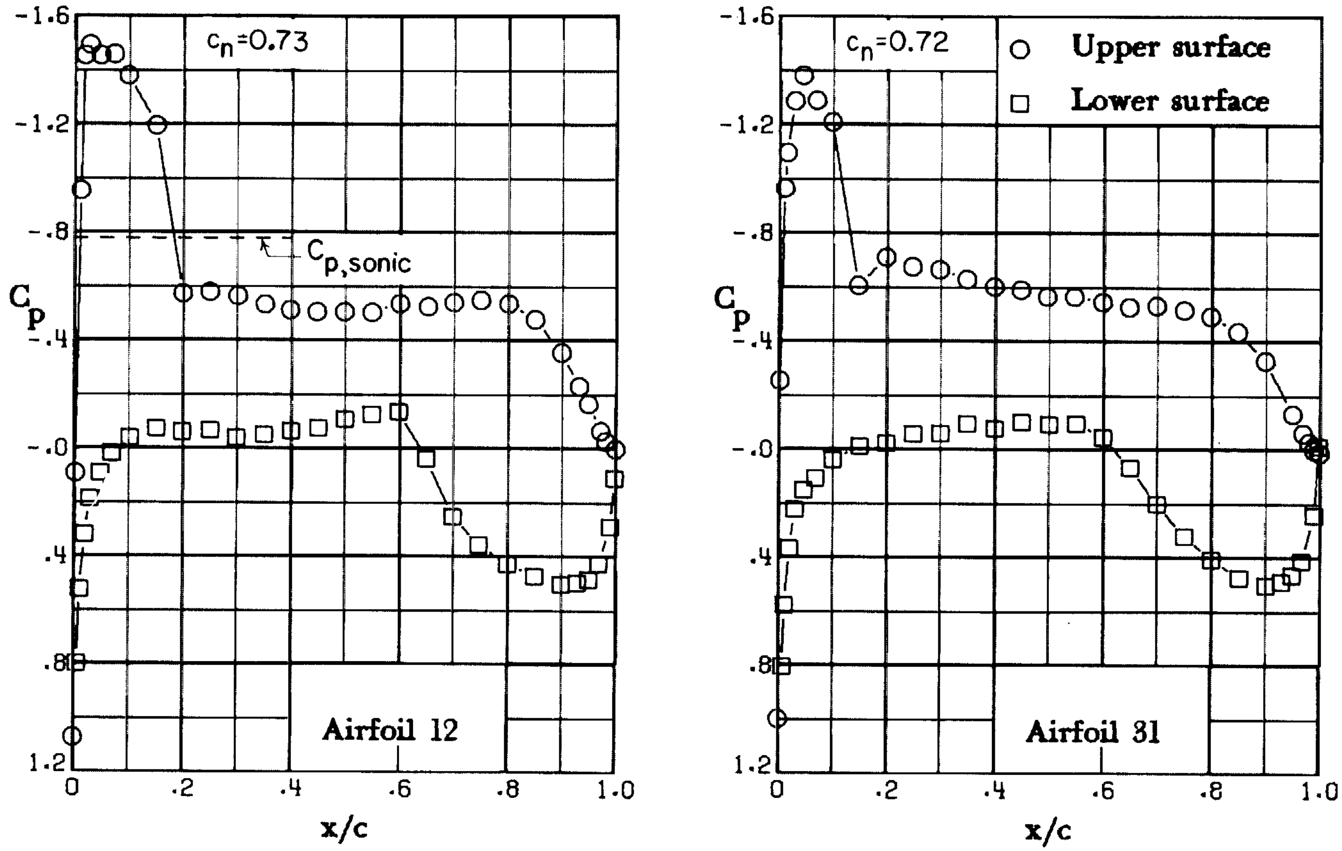

(g) M = 0.70; $c_n \approx 0.72$.

Figure 13. - Continued.

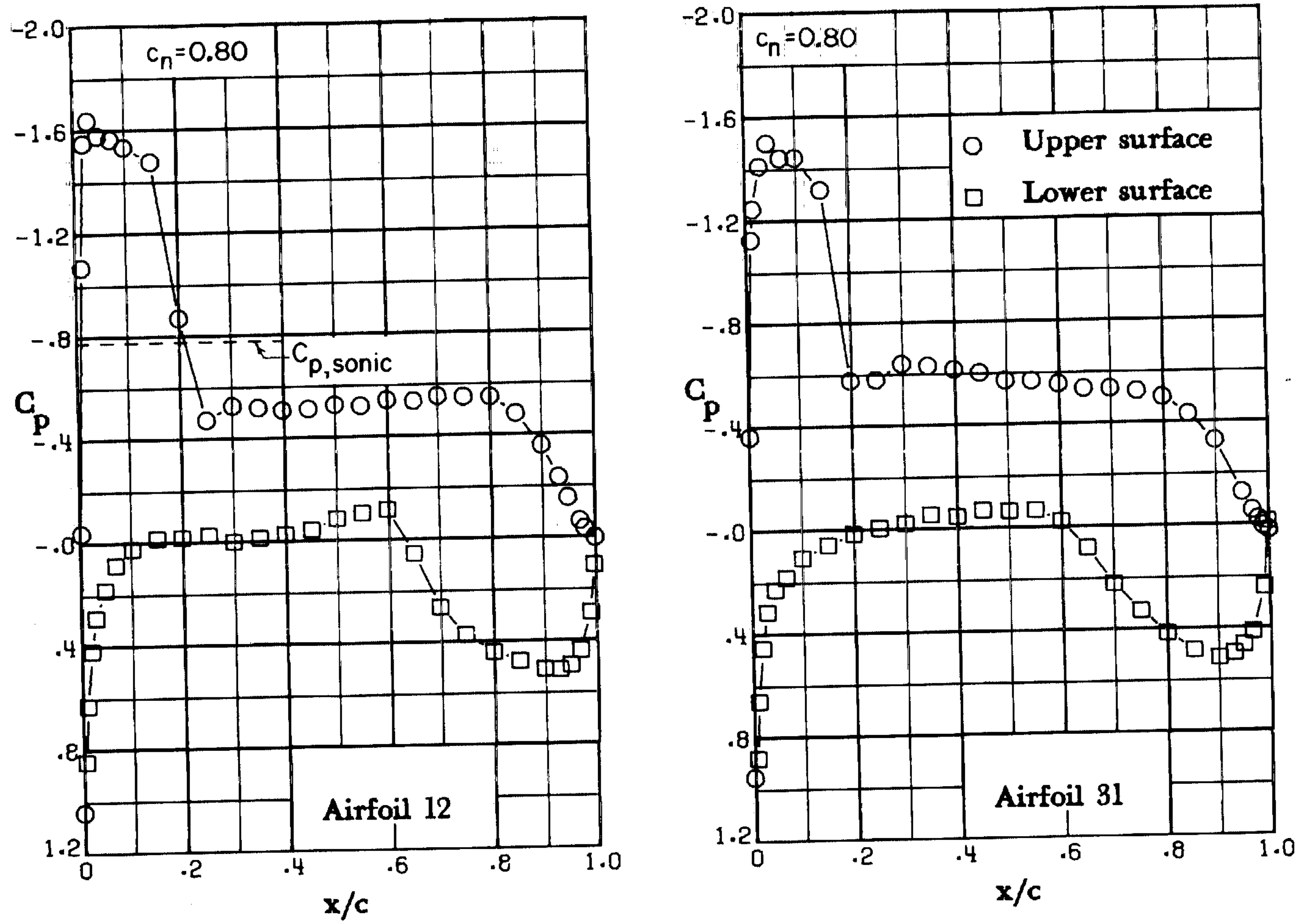

(h) M = 0.70; c_n = 0.80.

Figure 13.- Continued.

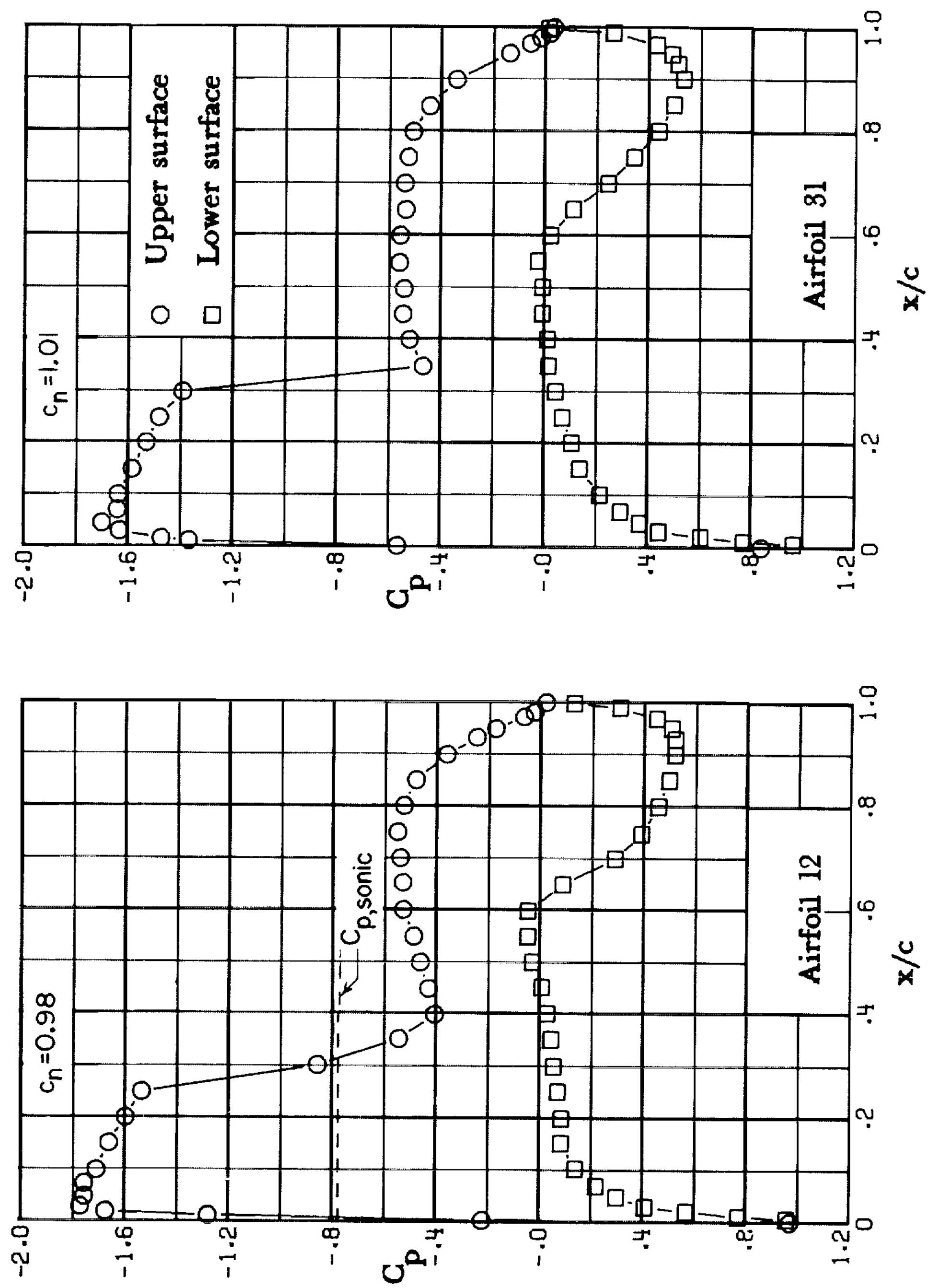

(i) M = 0.70; $c_n \approx 1.01$.

Figure 13.- Concluded.

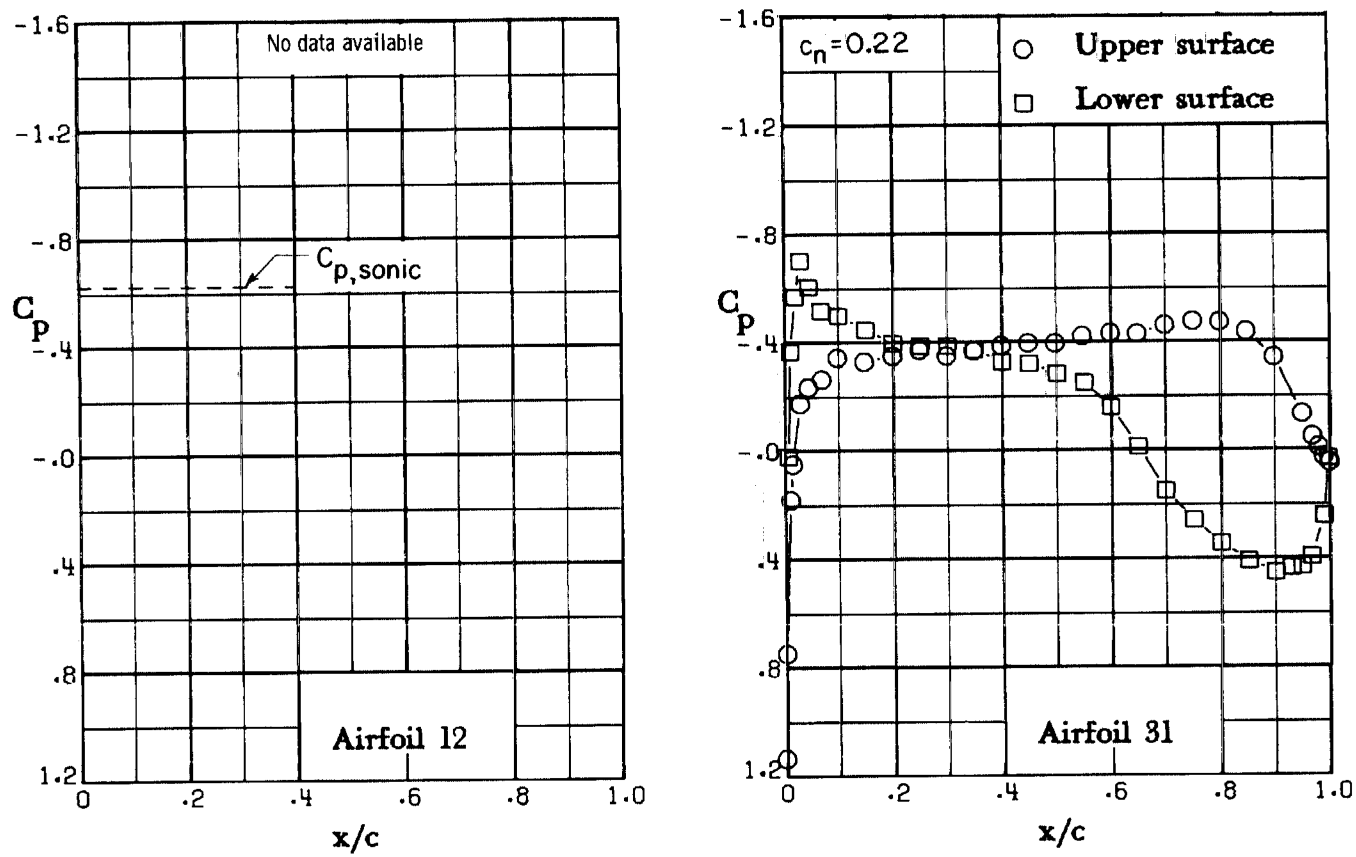

(a) M = 0.74; c_n = 0.22.

Figure 14.- Chordwise pressure distribution. M = 0.74.

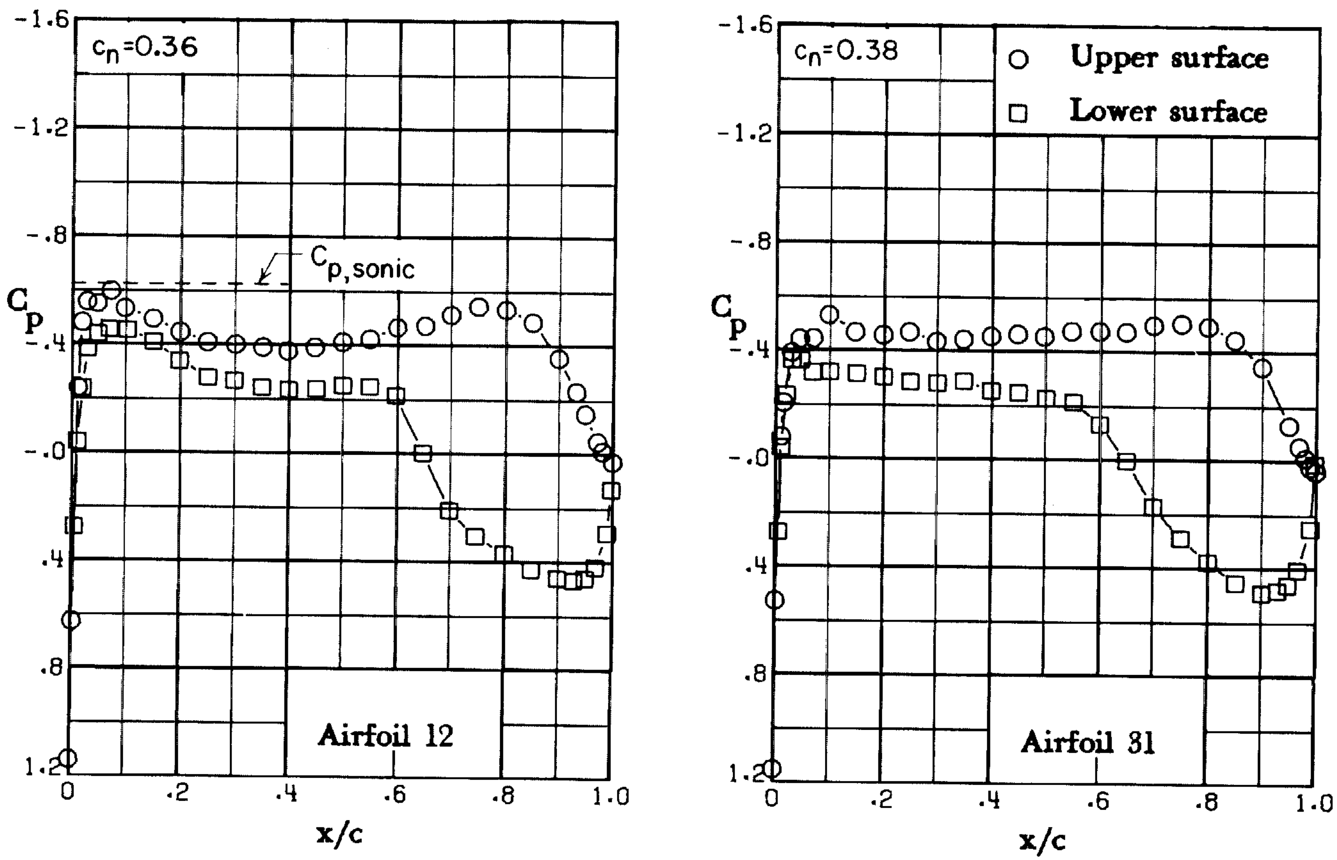

(b) $M = 0.74$; $c_n \approx 0.38$.

Figure 14.- Continued.

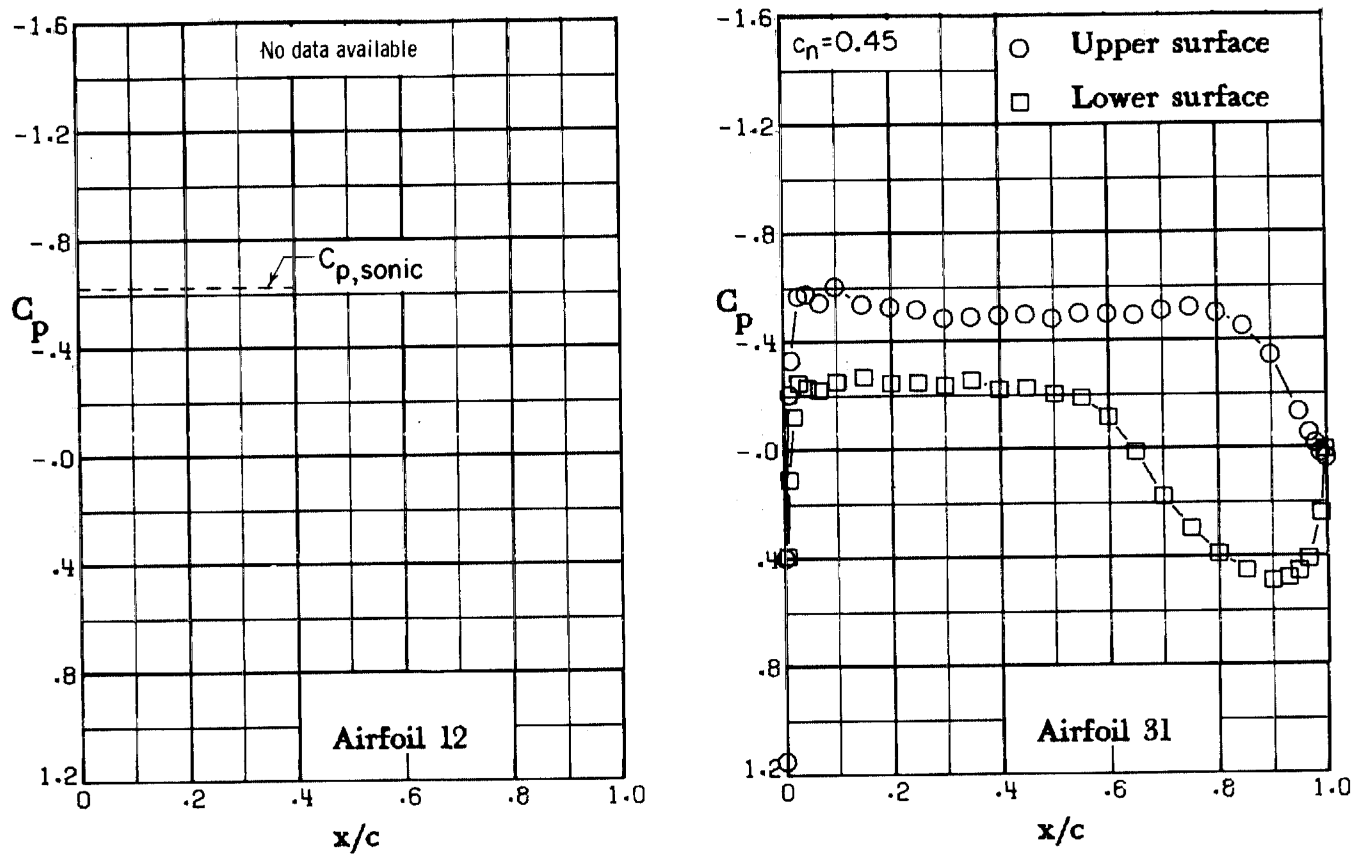

(c) $M = 0.74$; $c_n = 0.45$.

Figure 14.- Continued.

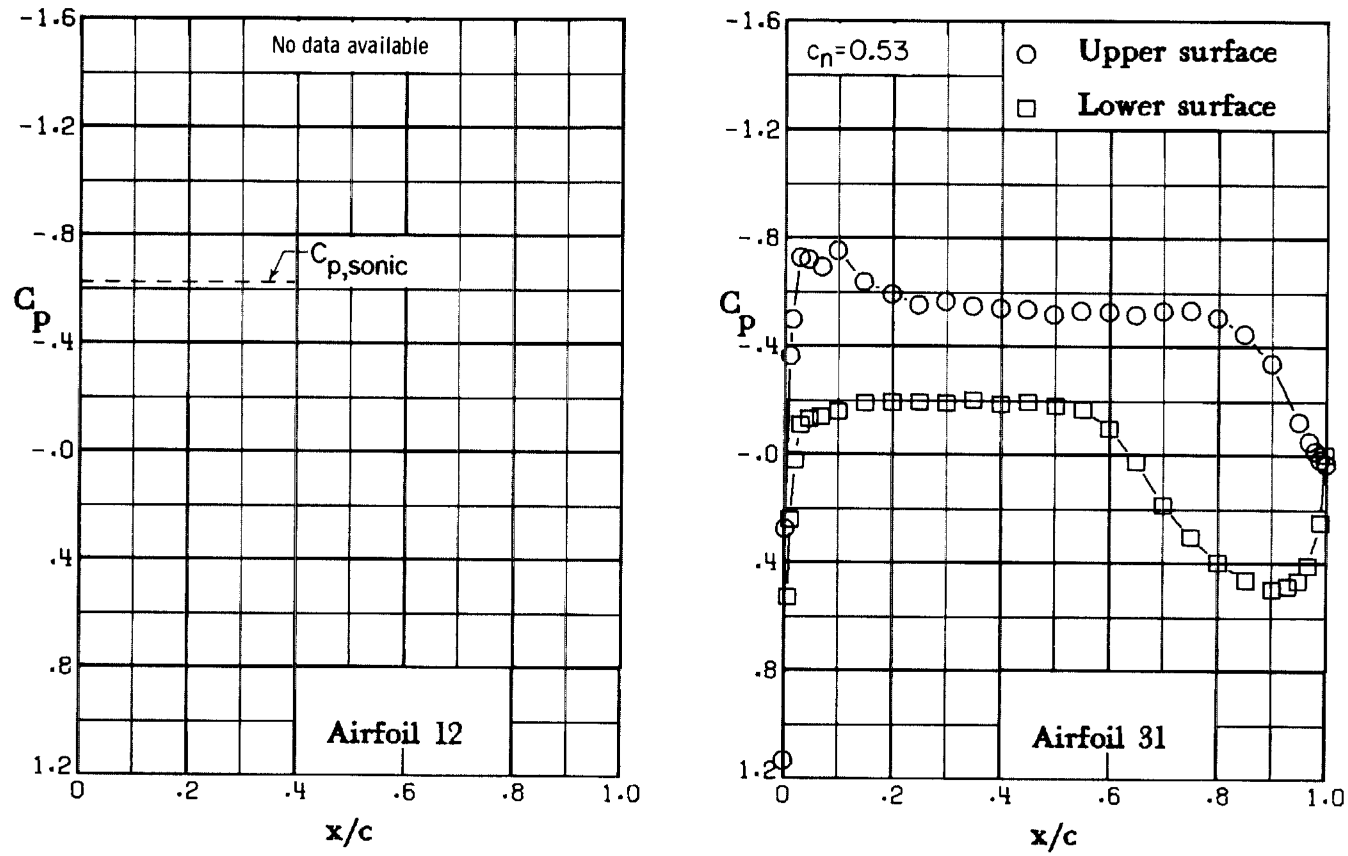

(d) $M = 0.74$; $c_n = 0.53$.

Figure 14.- Continued.

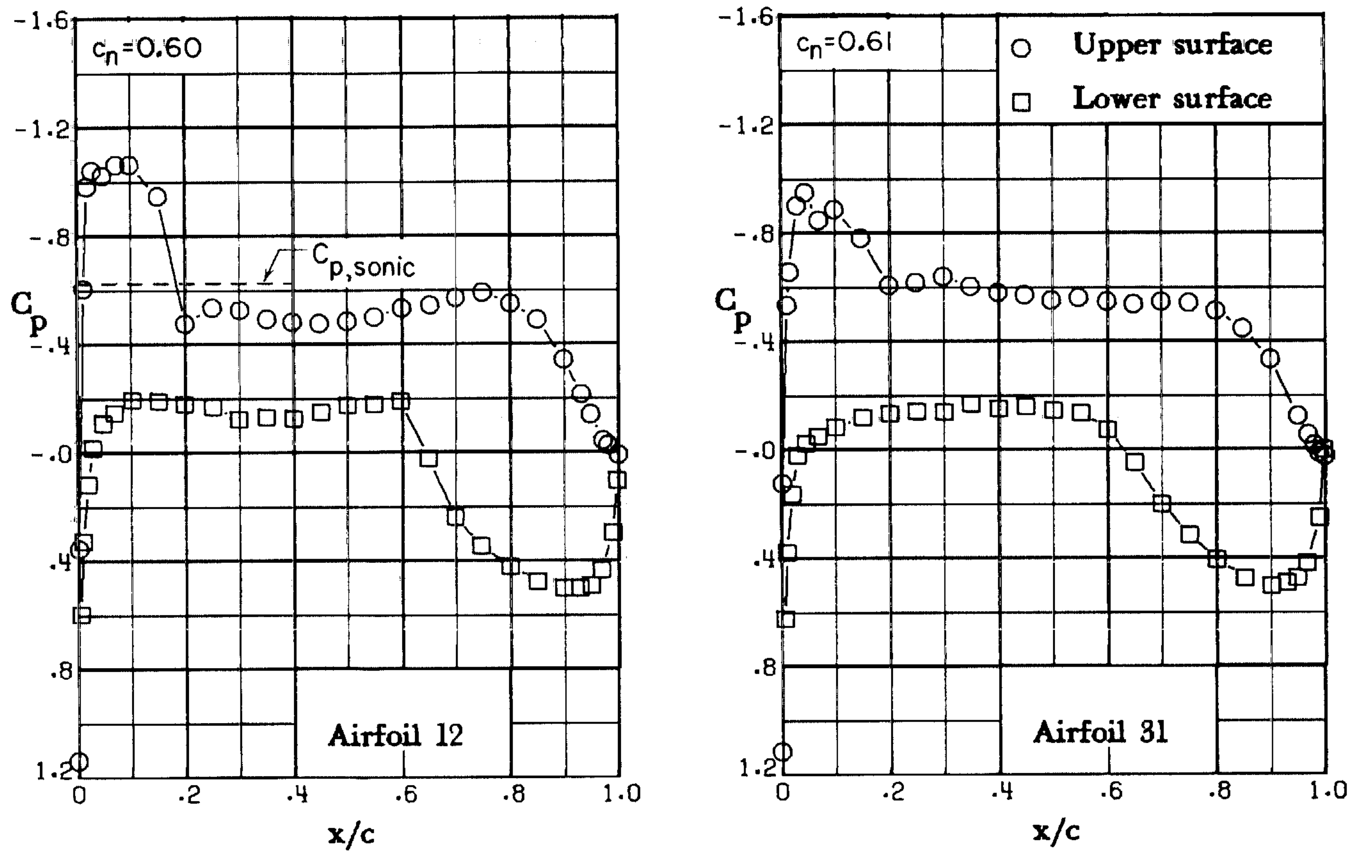

(e) $M = 0.74$; $c_n \approx 0.61$.

Figure 14.- Continued.

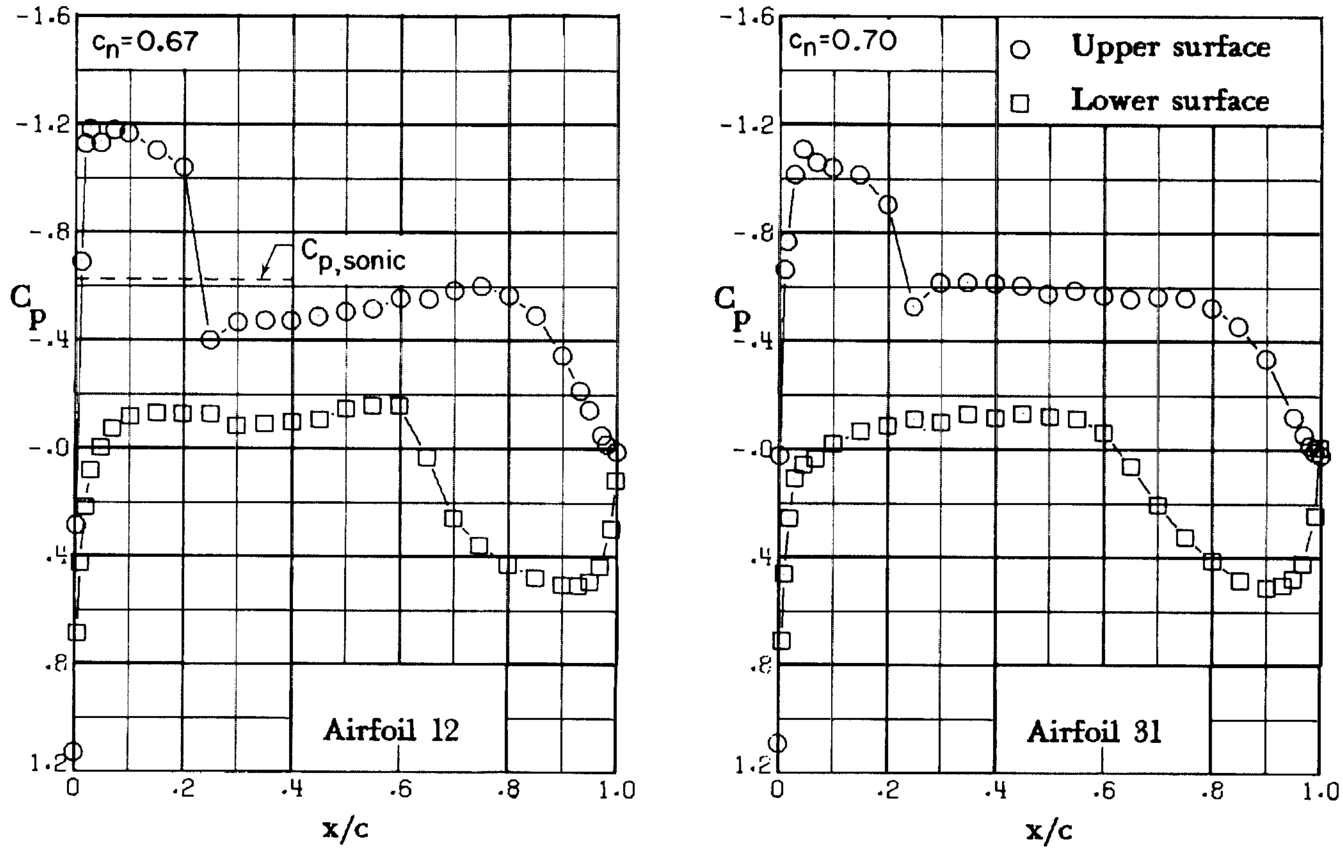

(f) $M = 0.74$; $c_n \approx 0.70$.

Figure 14.- Continued.

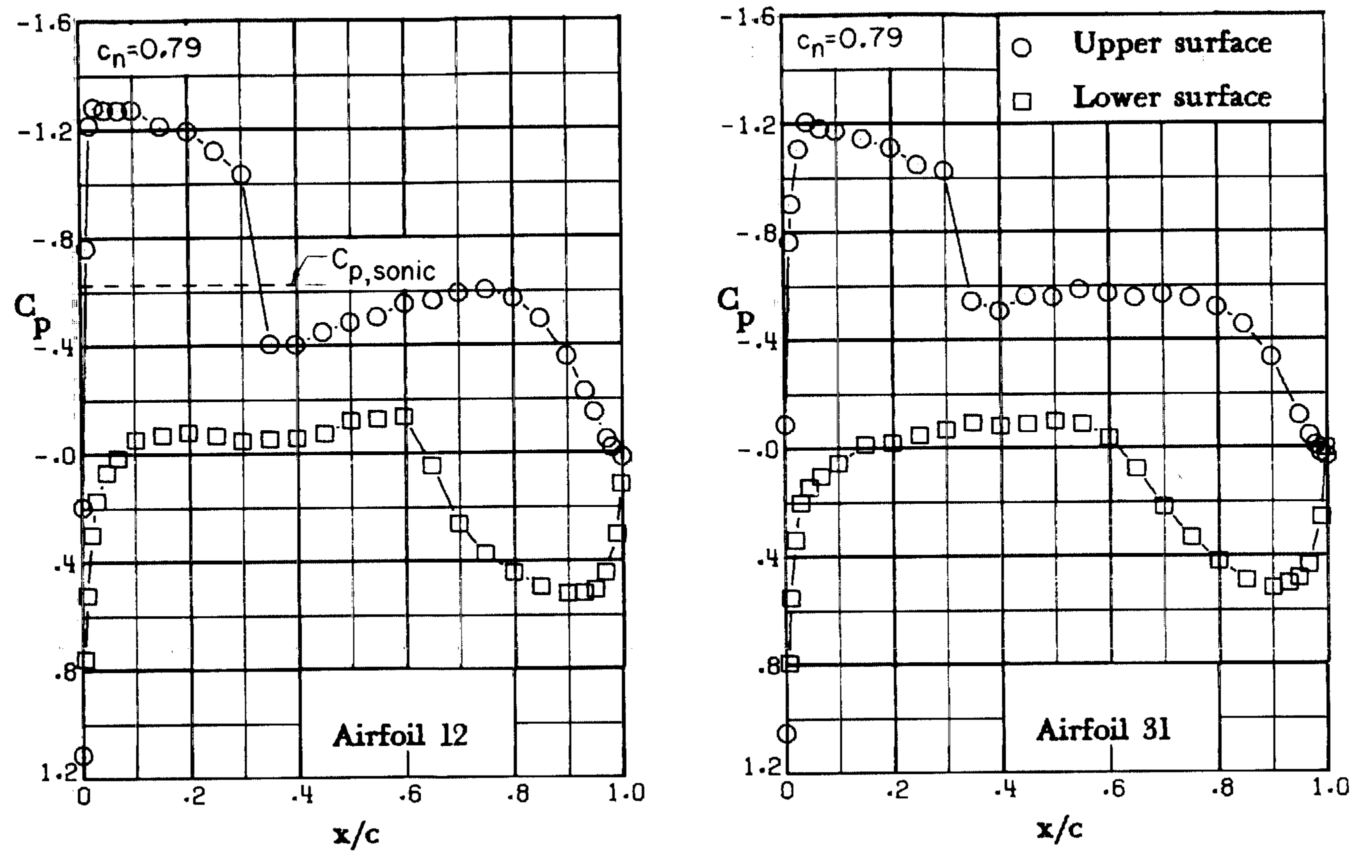

(g) $M = 0.74$; $c_n = 0.79$.

Figure 14. - Continued.

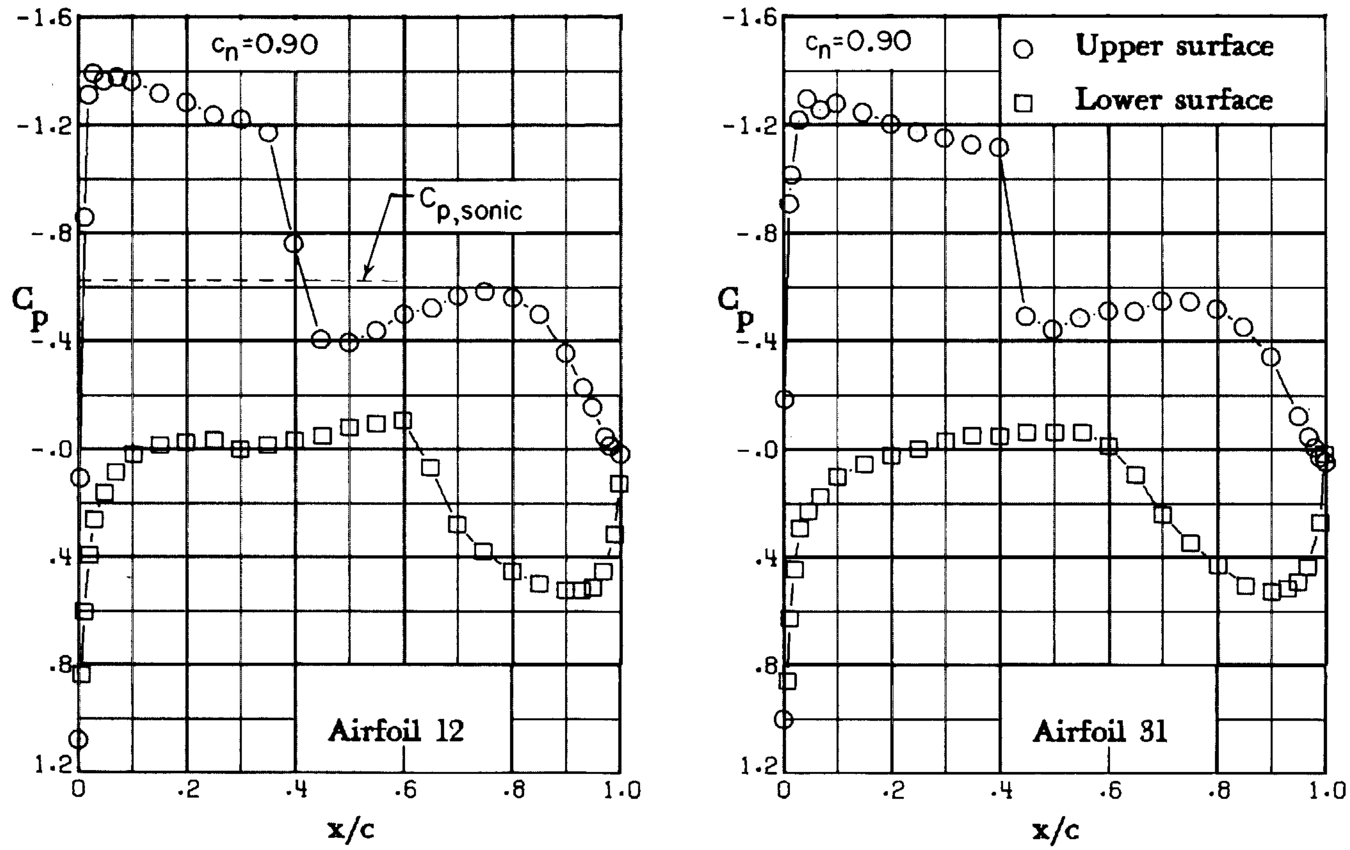

(h) M = 0.74; c_n = 0.90.

Figure 14. - Continued.

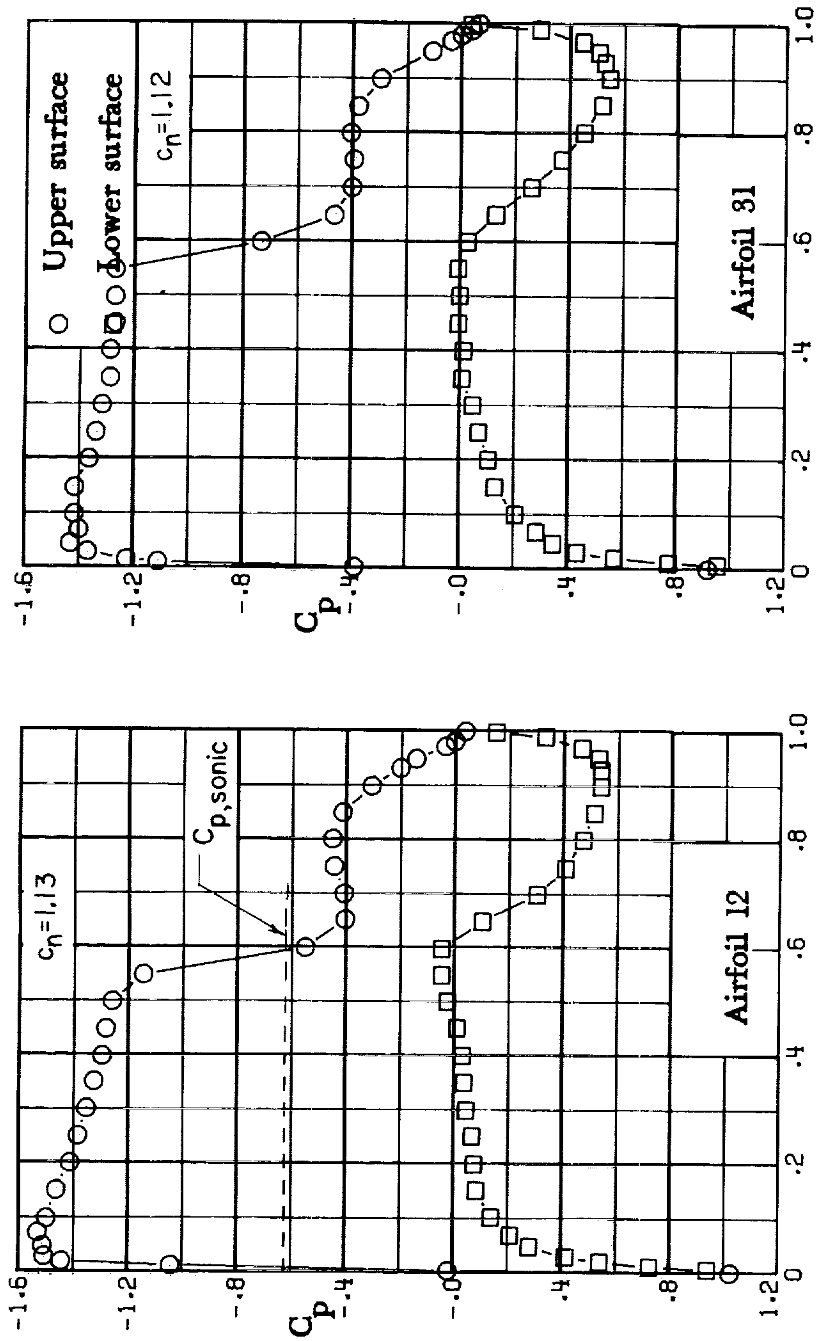

(i) M = 0.74; $c_n \approx 1.12$.

Figure 14.- Concluded.

[redacted]

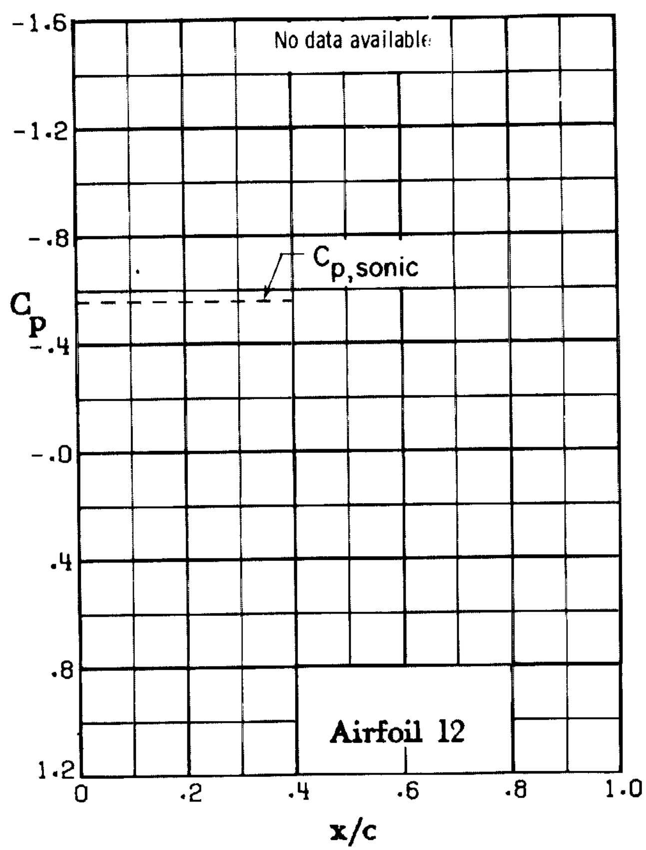

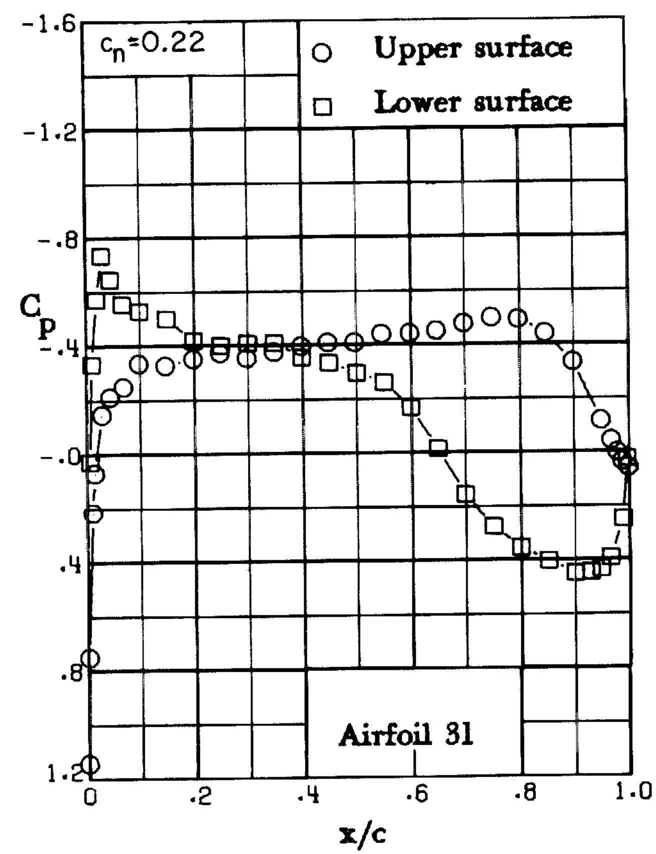

(a) $M = 0.76$; $c_n = 0.22$.

Figure 15.- Chordwise pressure distribution. $M = 0.76$.

[redacted]

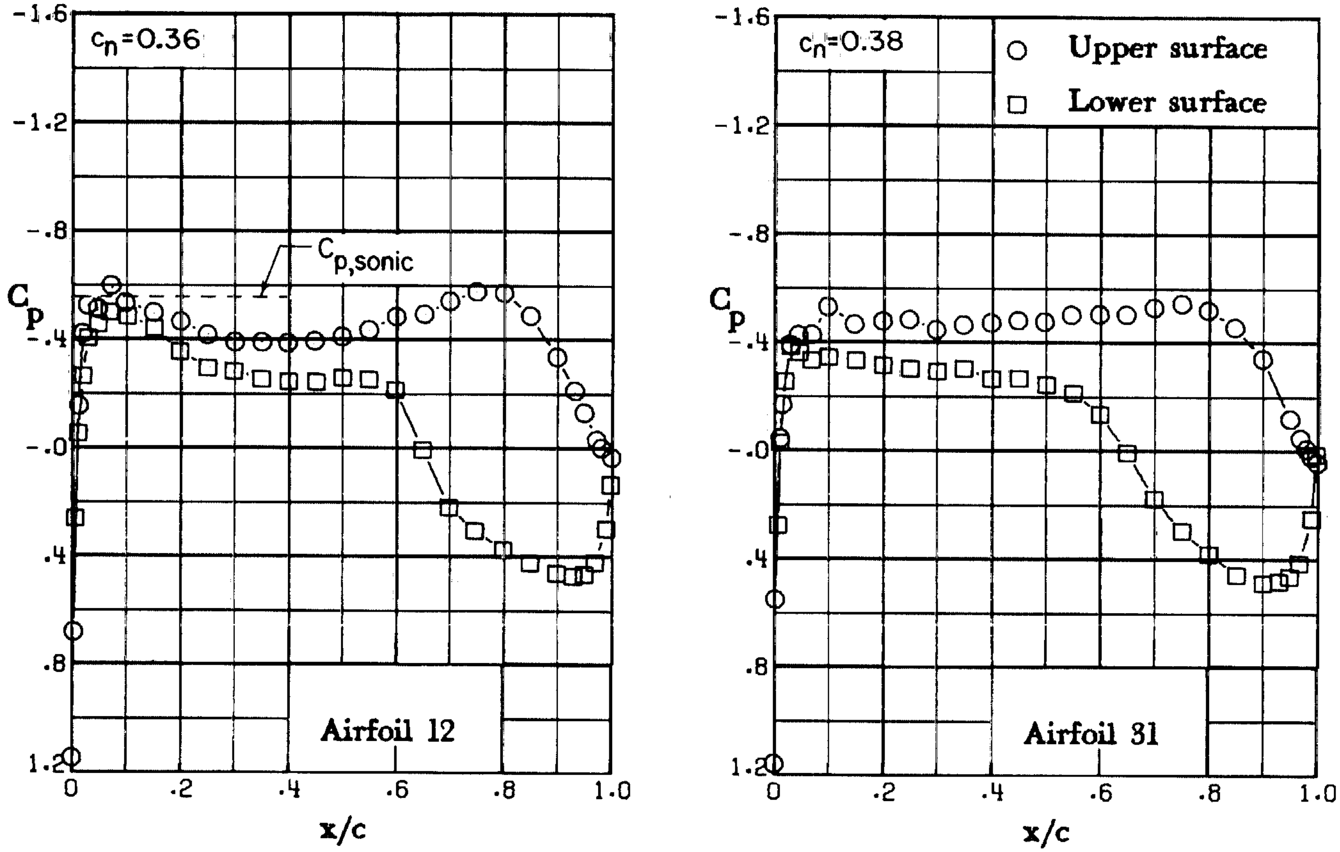

(b) M = 0.76; $c_n \approx 0.38$.

Figure 15. - Continued.

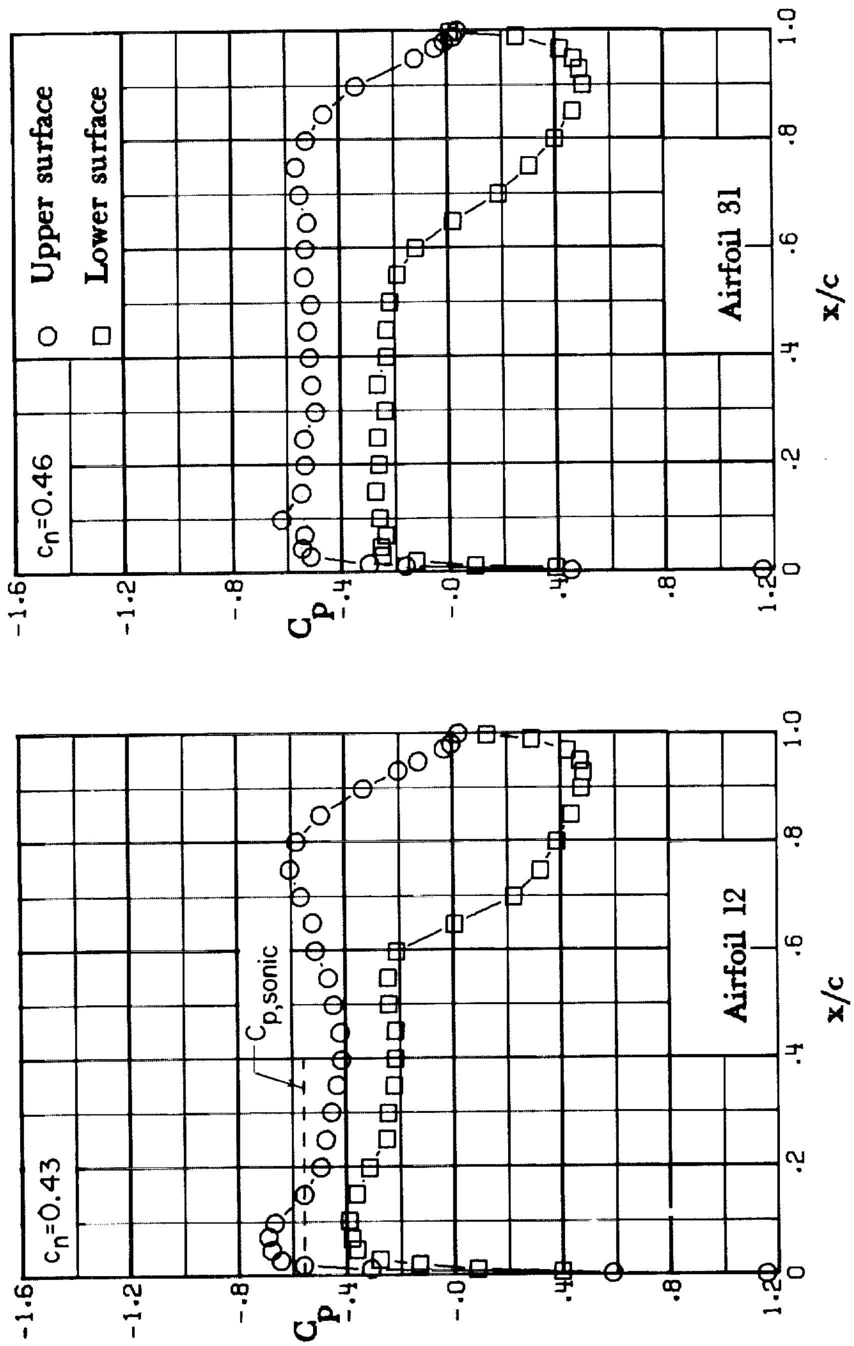

(c) M = 0.76; $c_n \approx 0.46$.

Figure 15.- Continued.

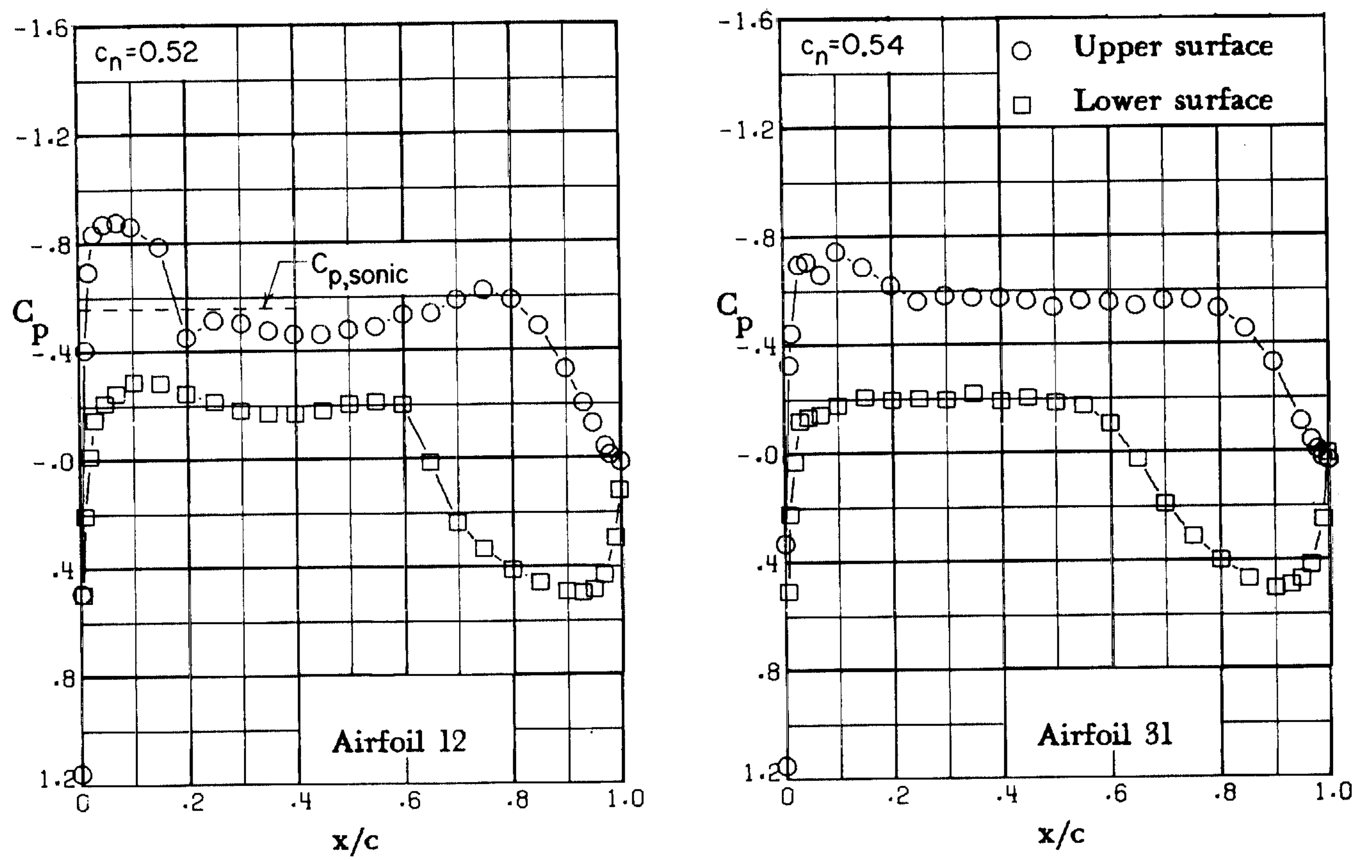

(d) M = 0.76; $c_n \approx 0.54$.

Figure 15. - Continued.

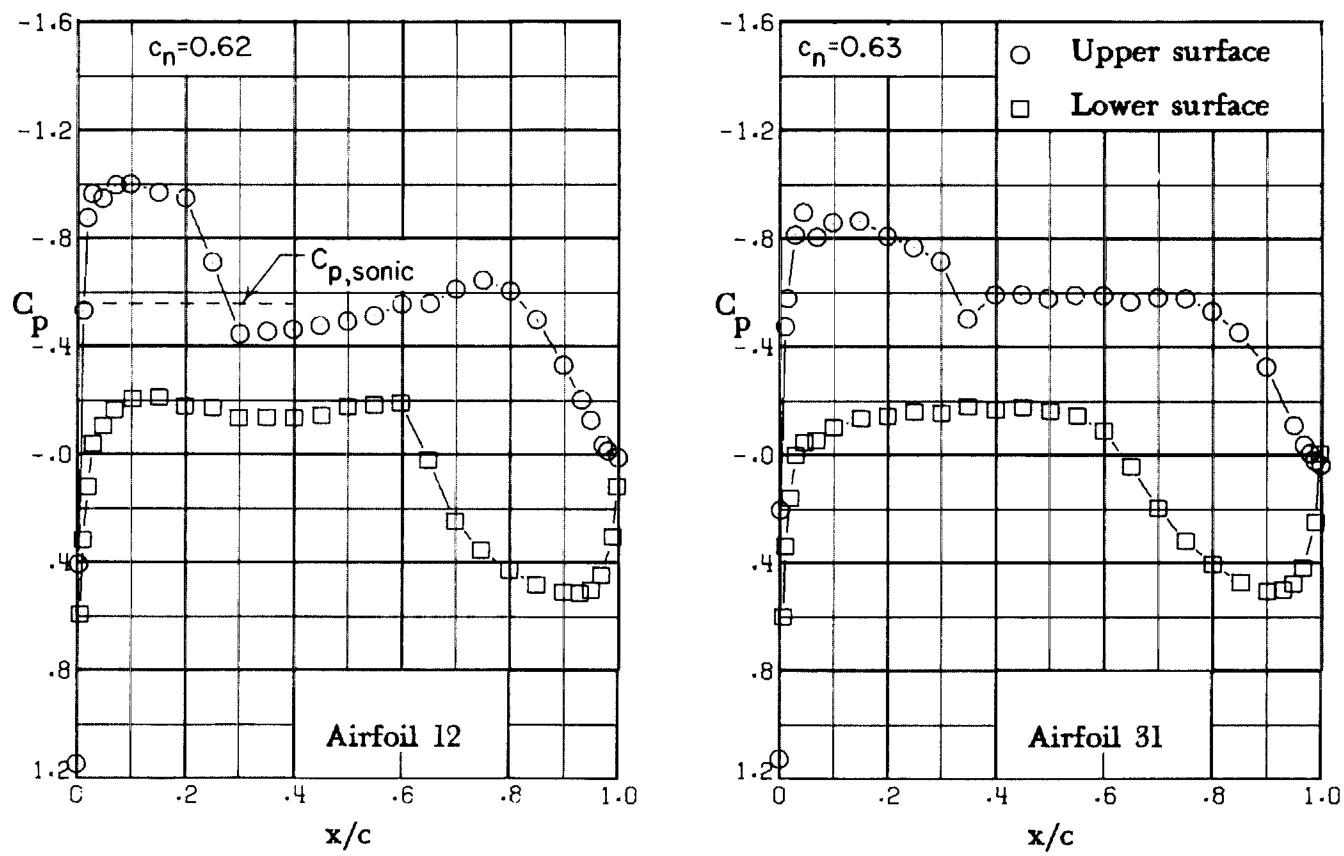

(e) $M = 0.76$; $c_n \approx 0.63$.

Figure 15. - Continued.

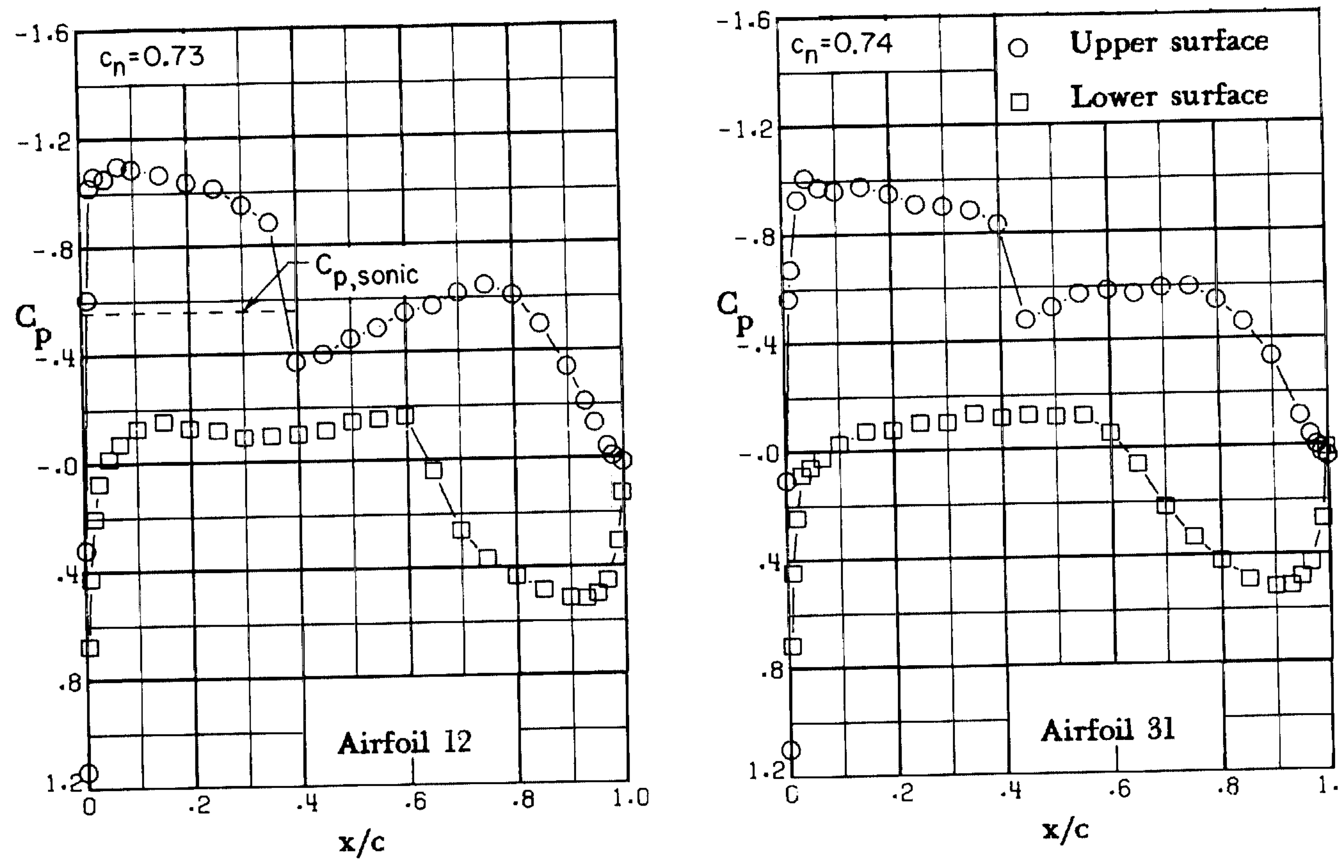

(f) M = 0.76; $c_n \approx 0.74$.

Figure 15. - Continued.

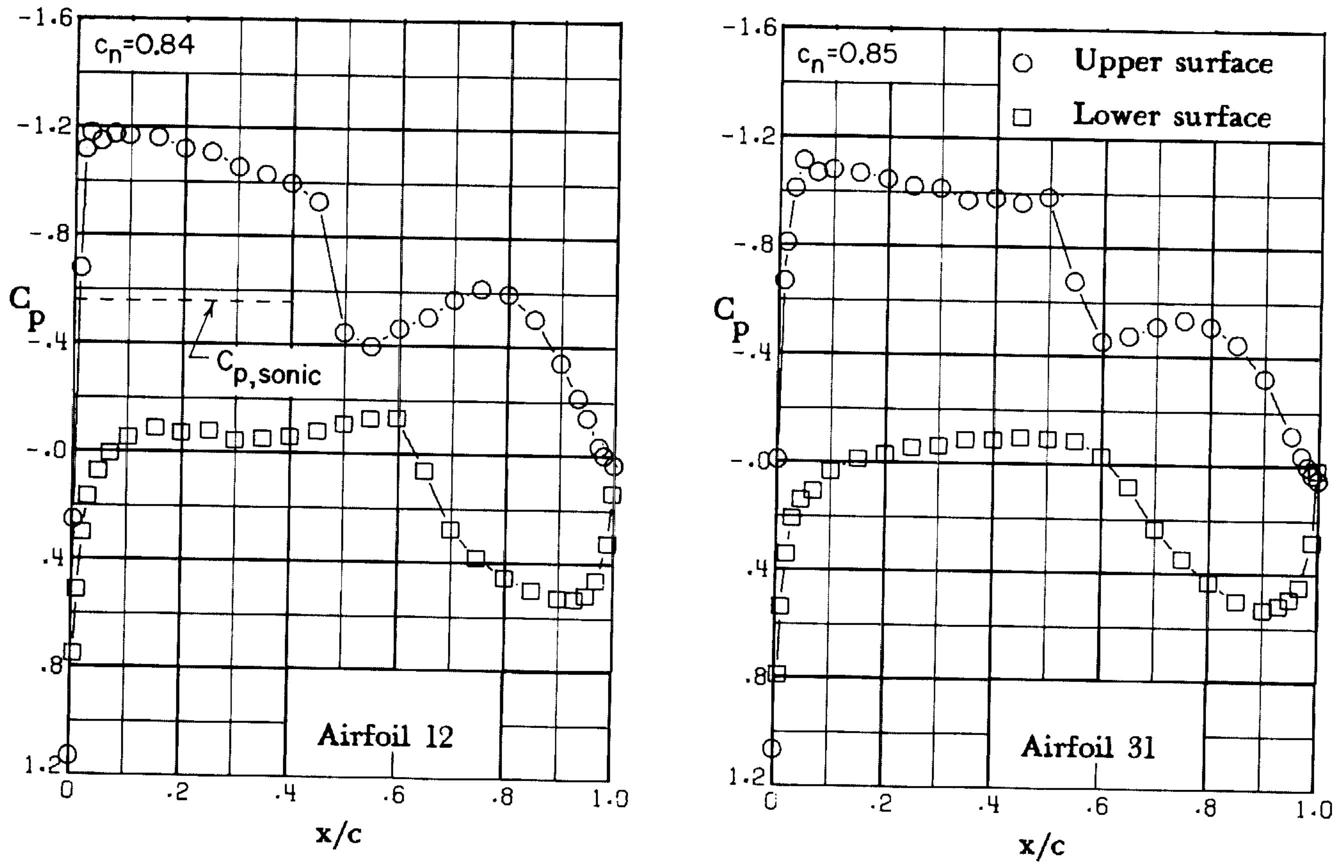

(g) $M = 0.76$; $c_n \approx 0.85$.

Figure 15.- Continued.

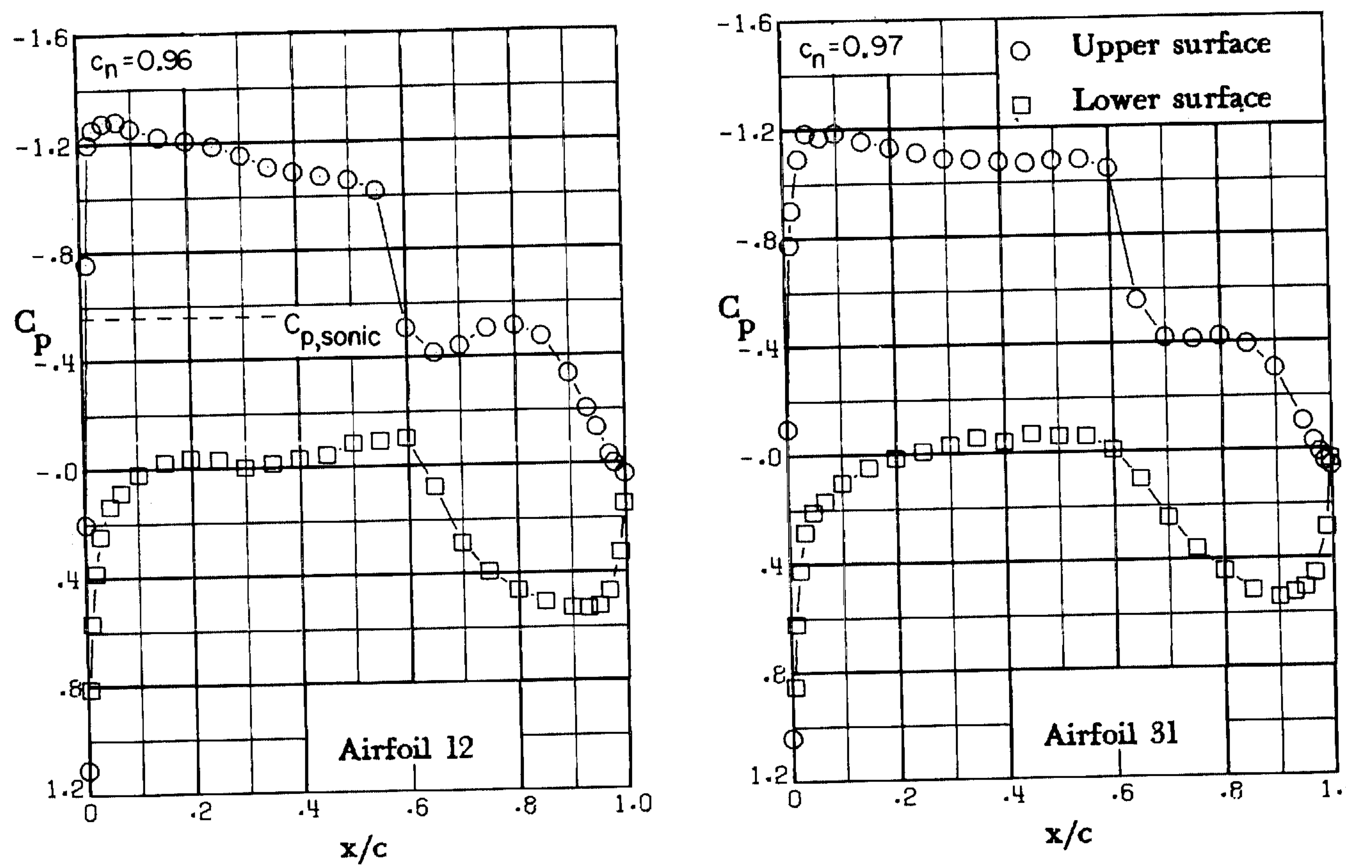

(h) M = 0.76; $c_n \approx 0.97$.

Figure 15.- Continued.

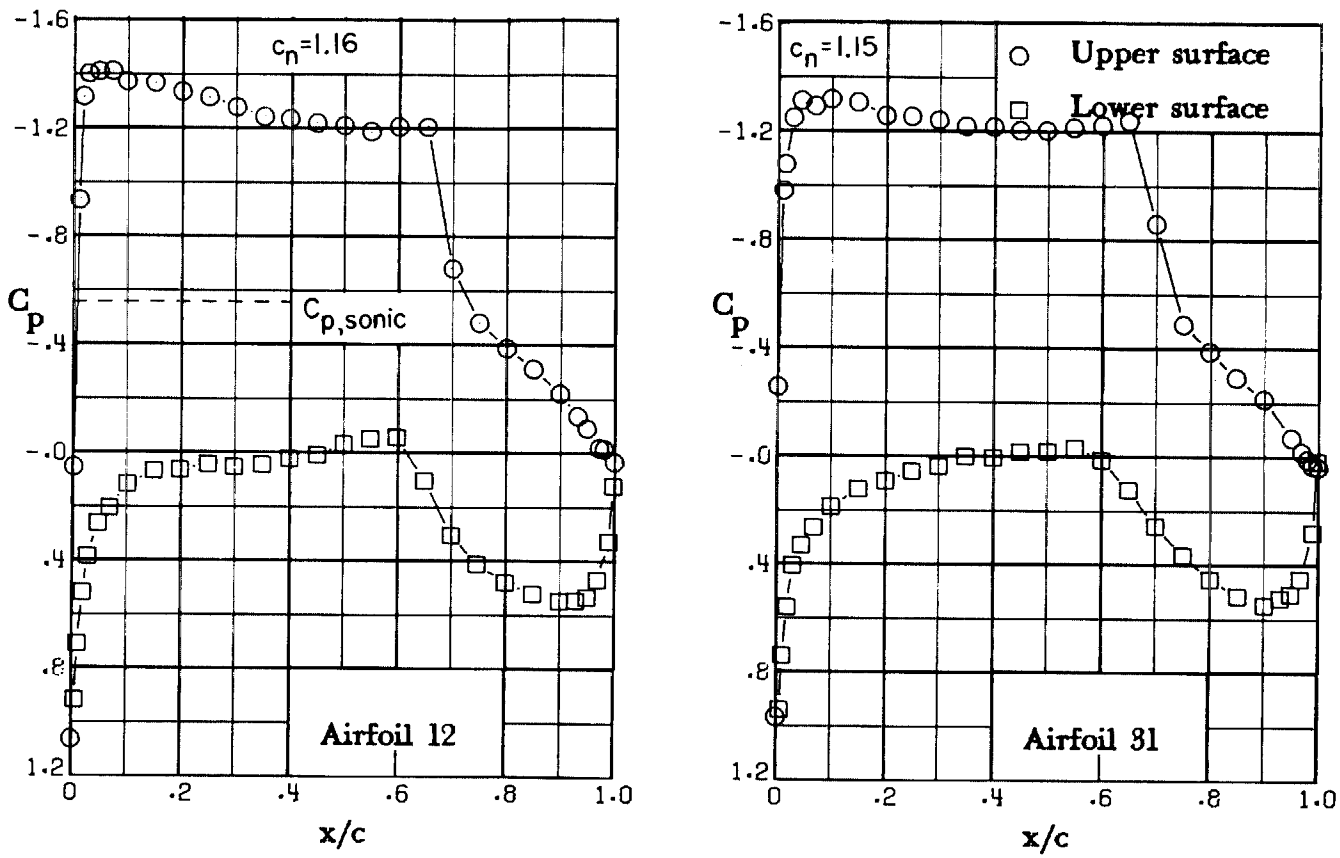

(i) M = 0.76; $c_n \approx 1.15$.

Figure 15. - Concluded.

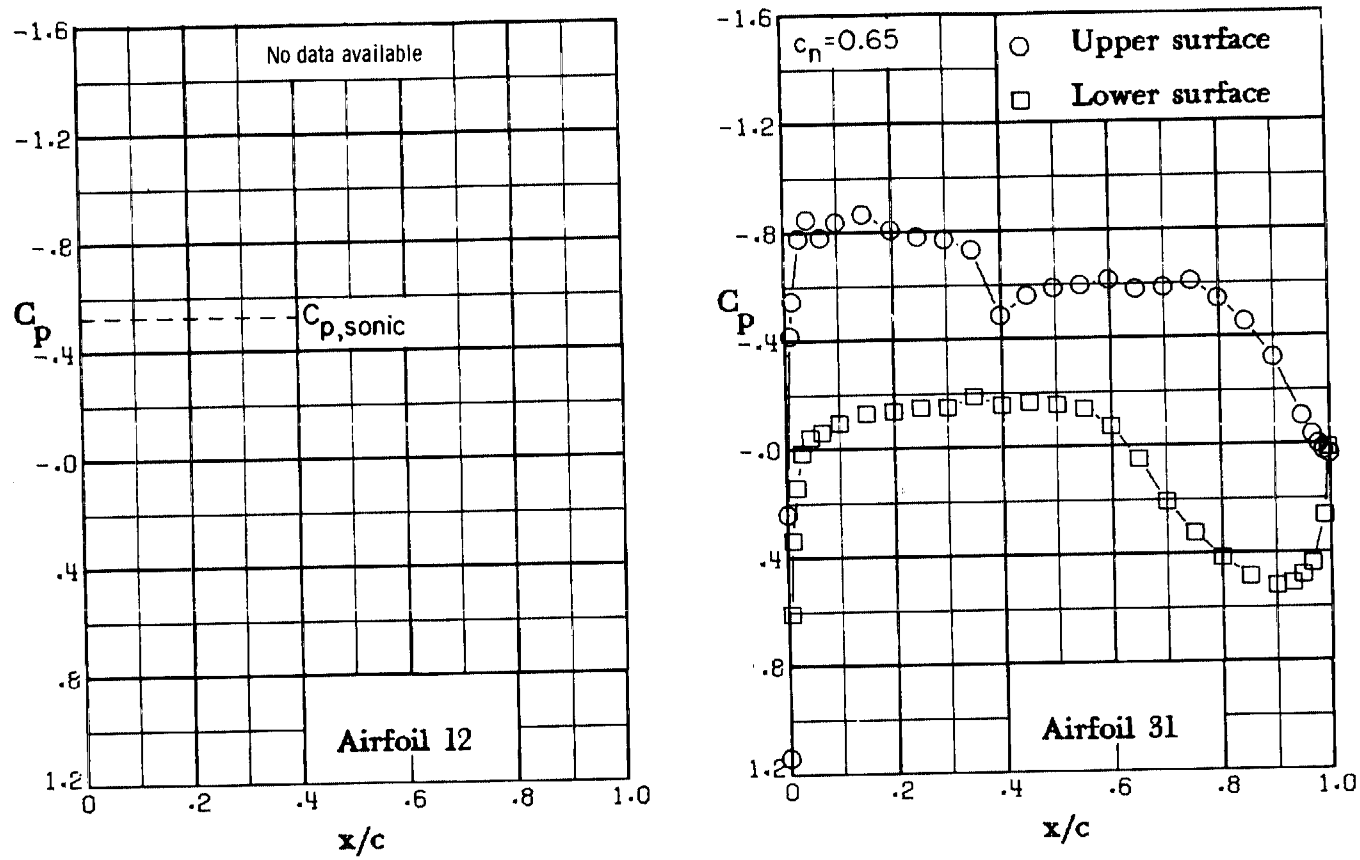

(a) M = 0.77; c_n = 0.65.

Figure 16.- Chordwise pressure distribution. M = 0.77.

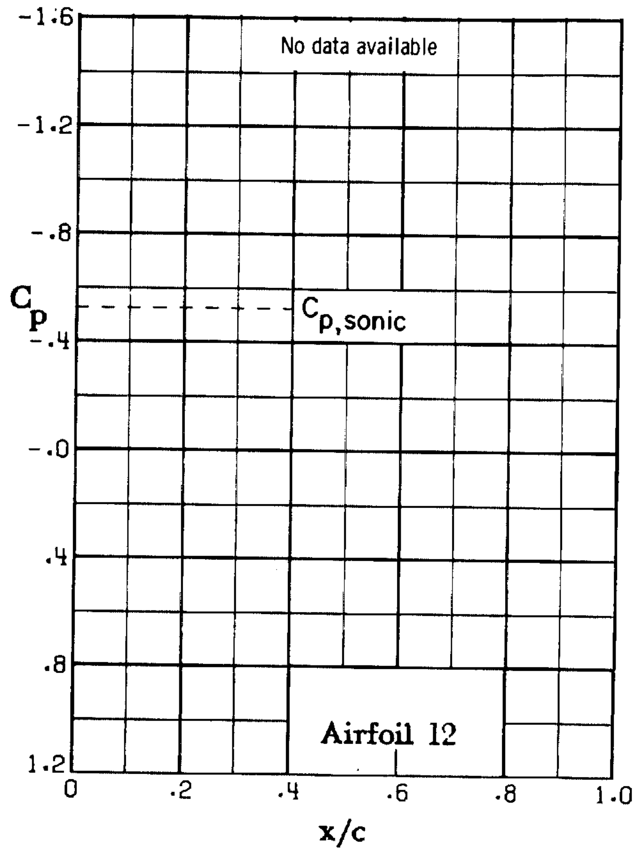

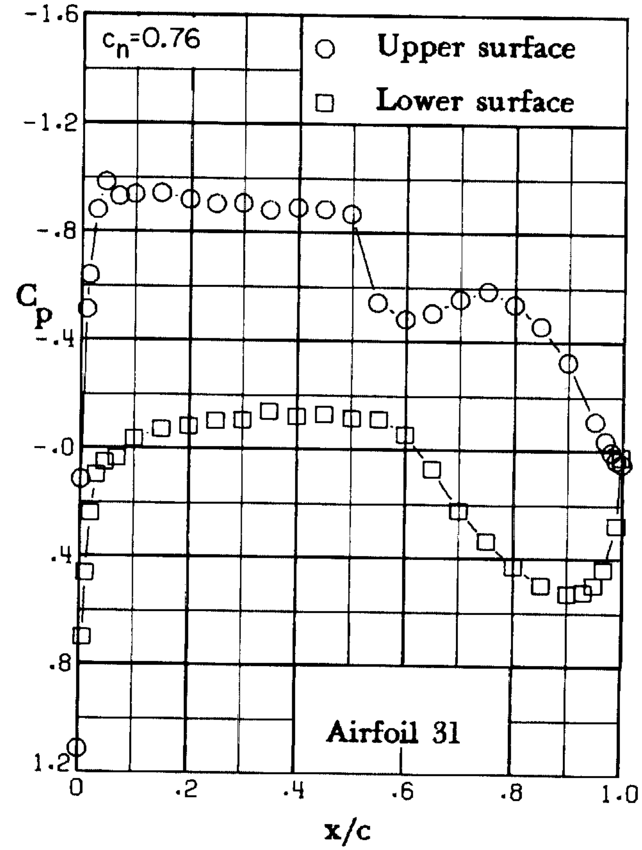

(b) $M = 0.77$; $c_n = 0.76$.

Figure 16. - Continued.

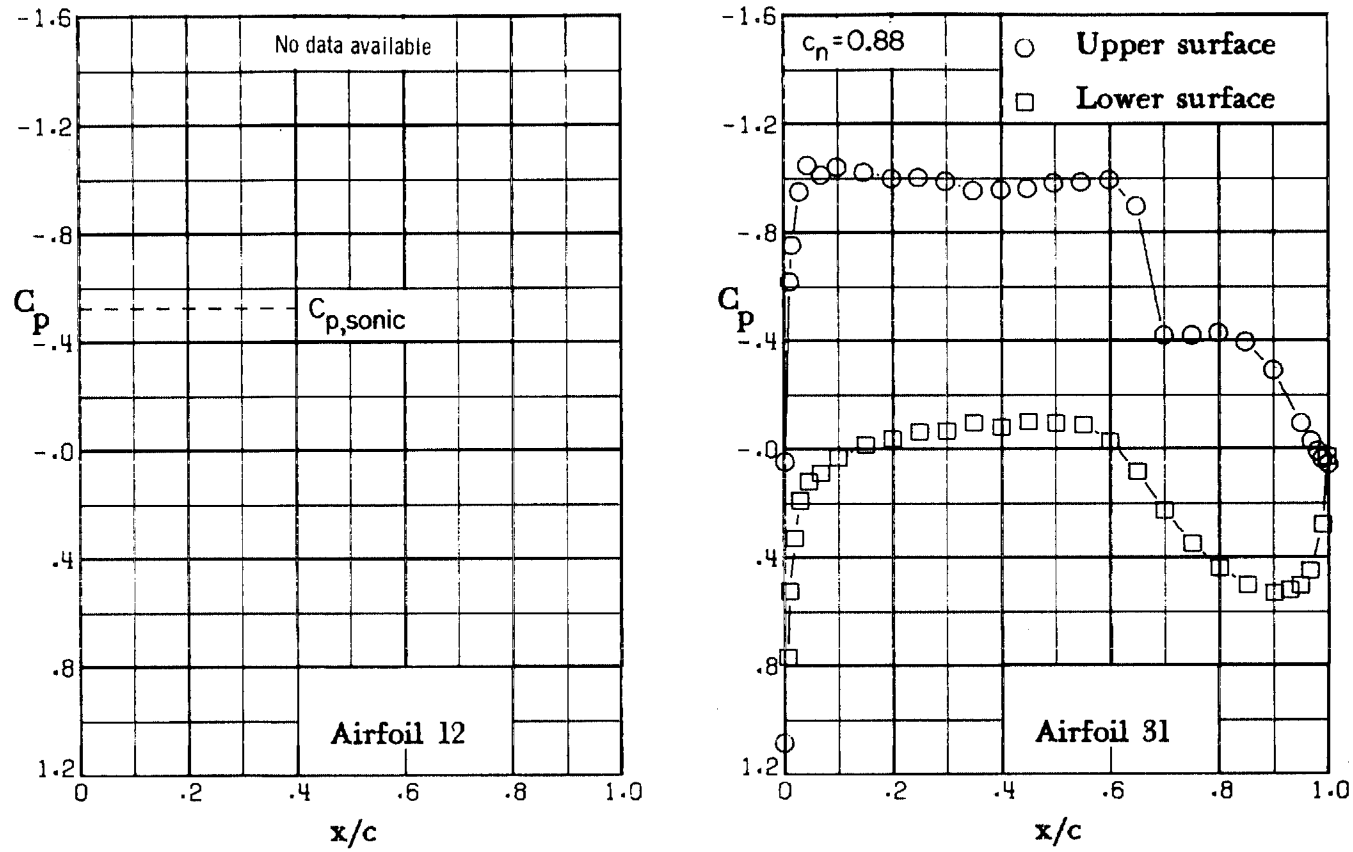

(c) $M = 0.77$; $c_n = 0.88$.

Figure 16.- Continued.

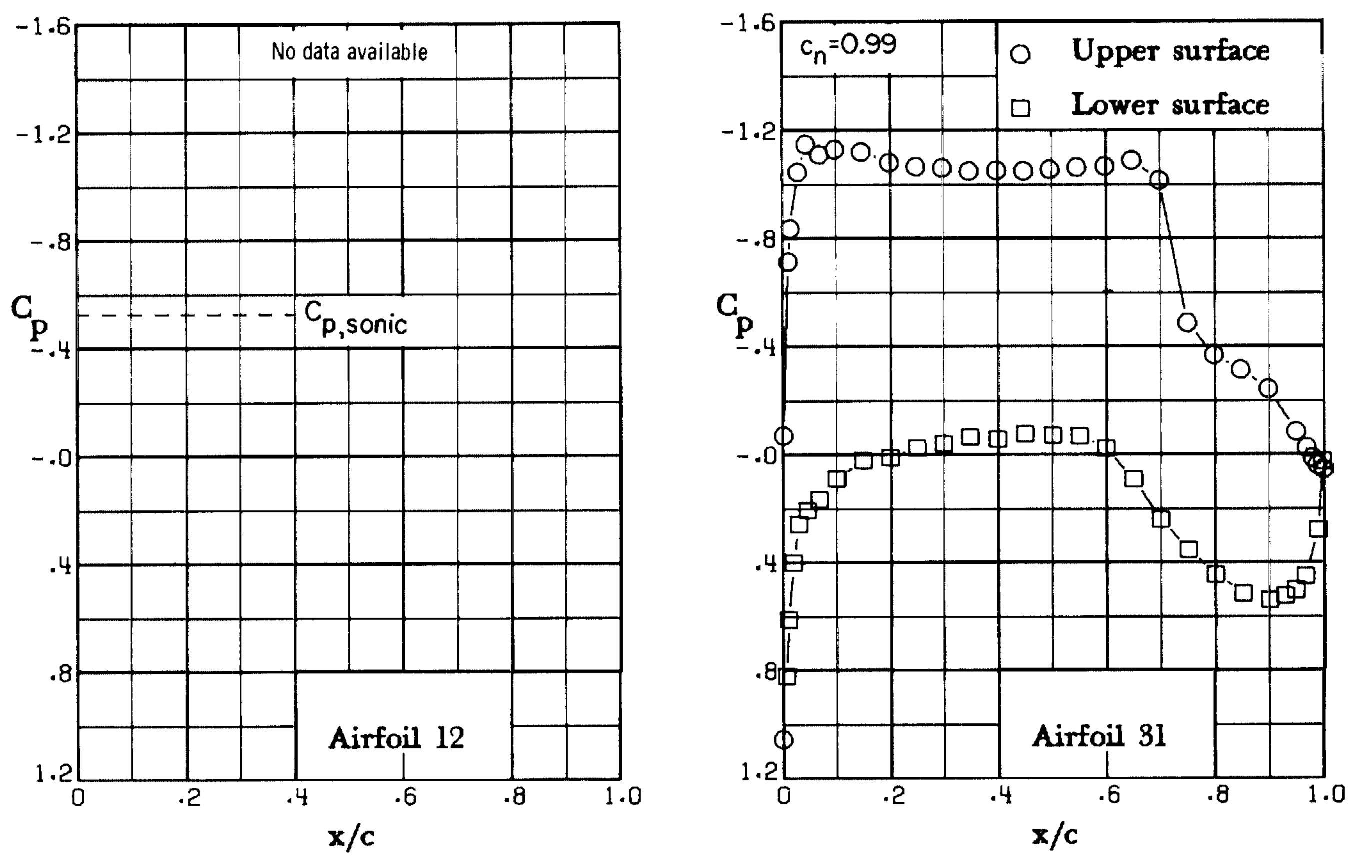

(d) $M = 0.77$; $c_n = 0.99$.

Figure 16.- Continued.

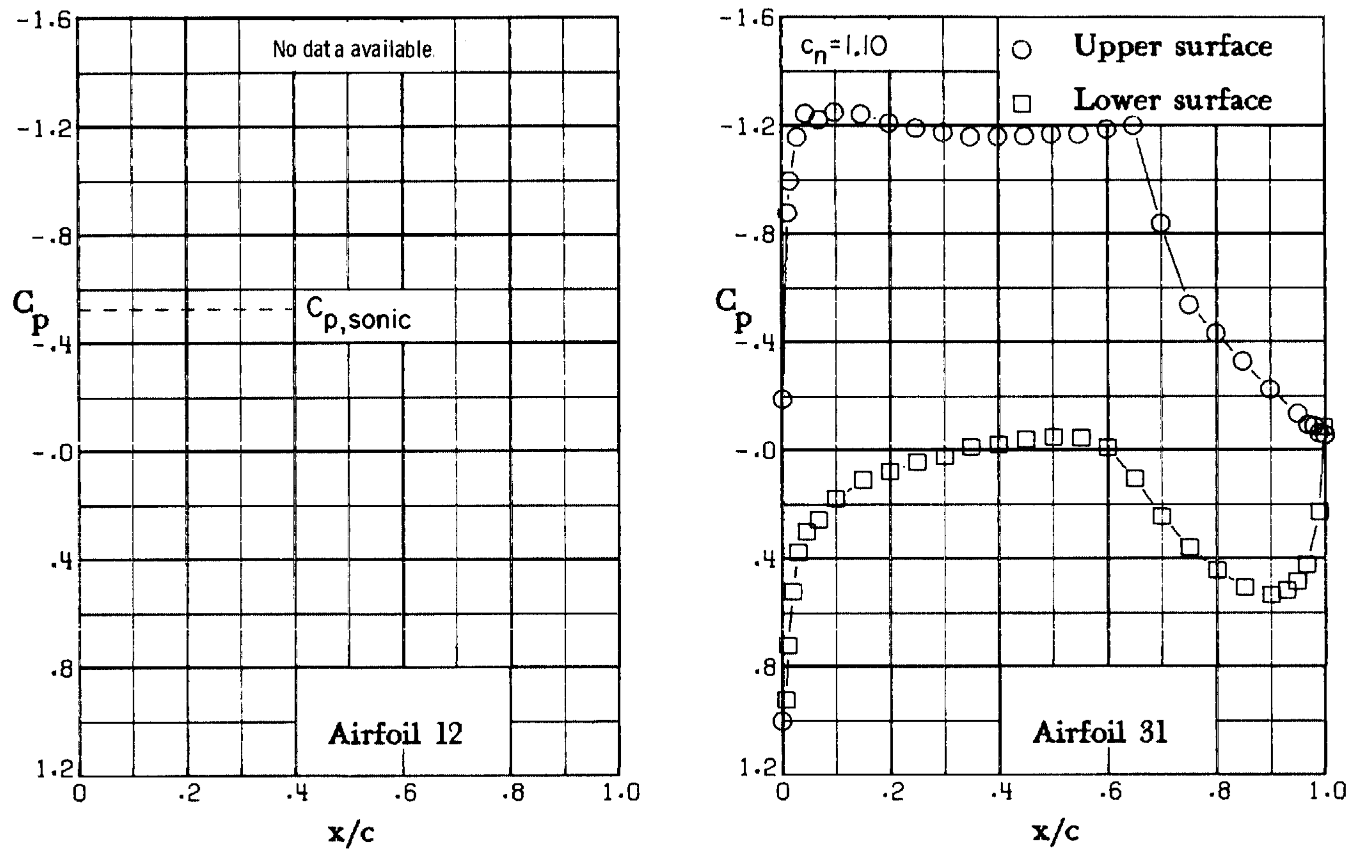

(e) $M = 0.77$; $c_n = 1.10$.

Figure 16.- Concluded.

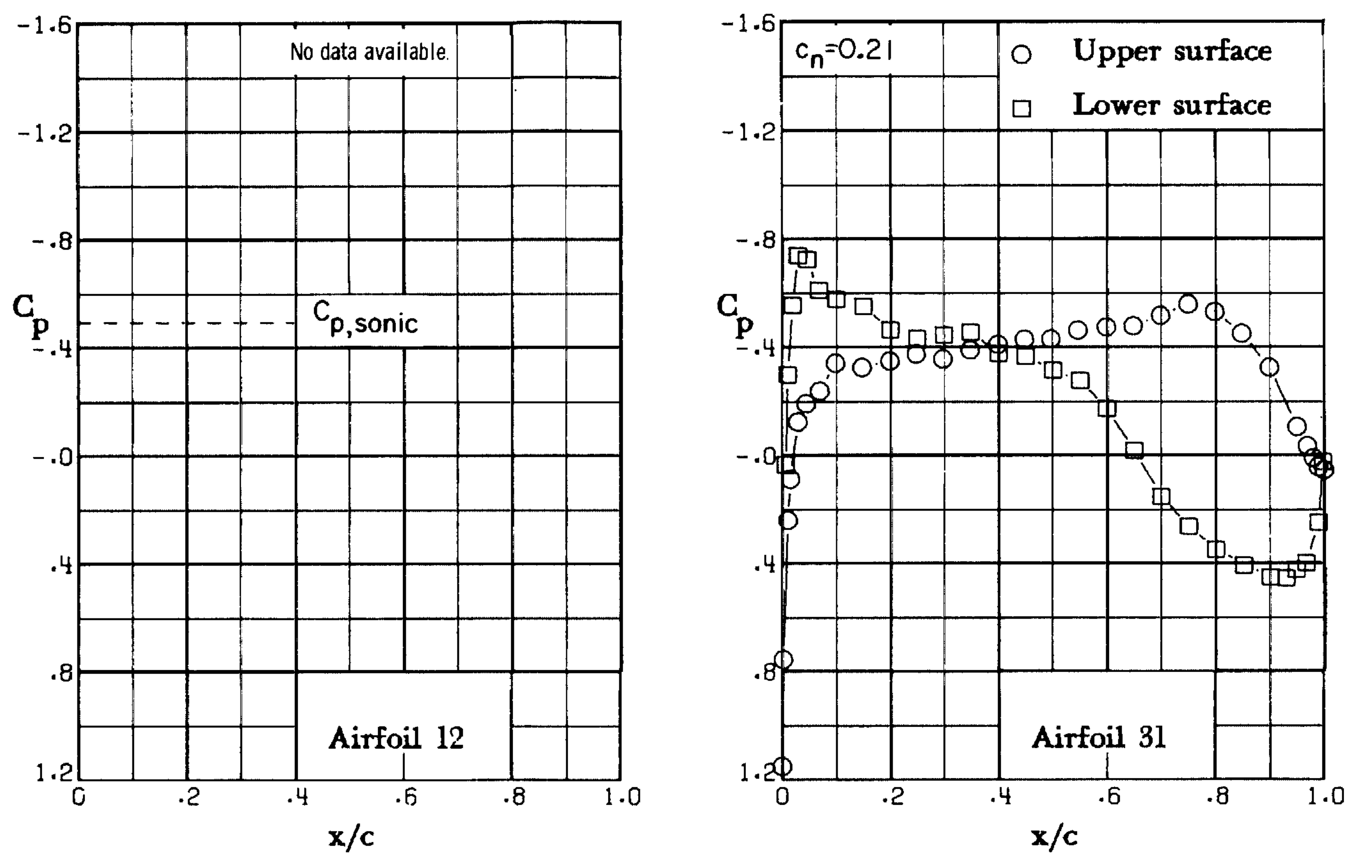

(a) M = 0.78; c_n = 0.21.

Figure 17.- Chordwise pressure distribution. M = 0.78.

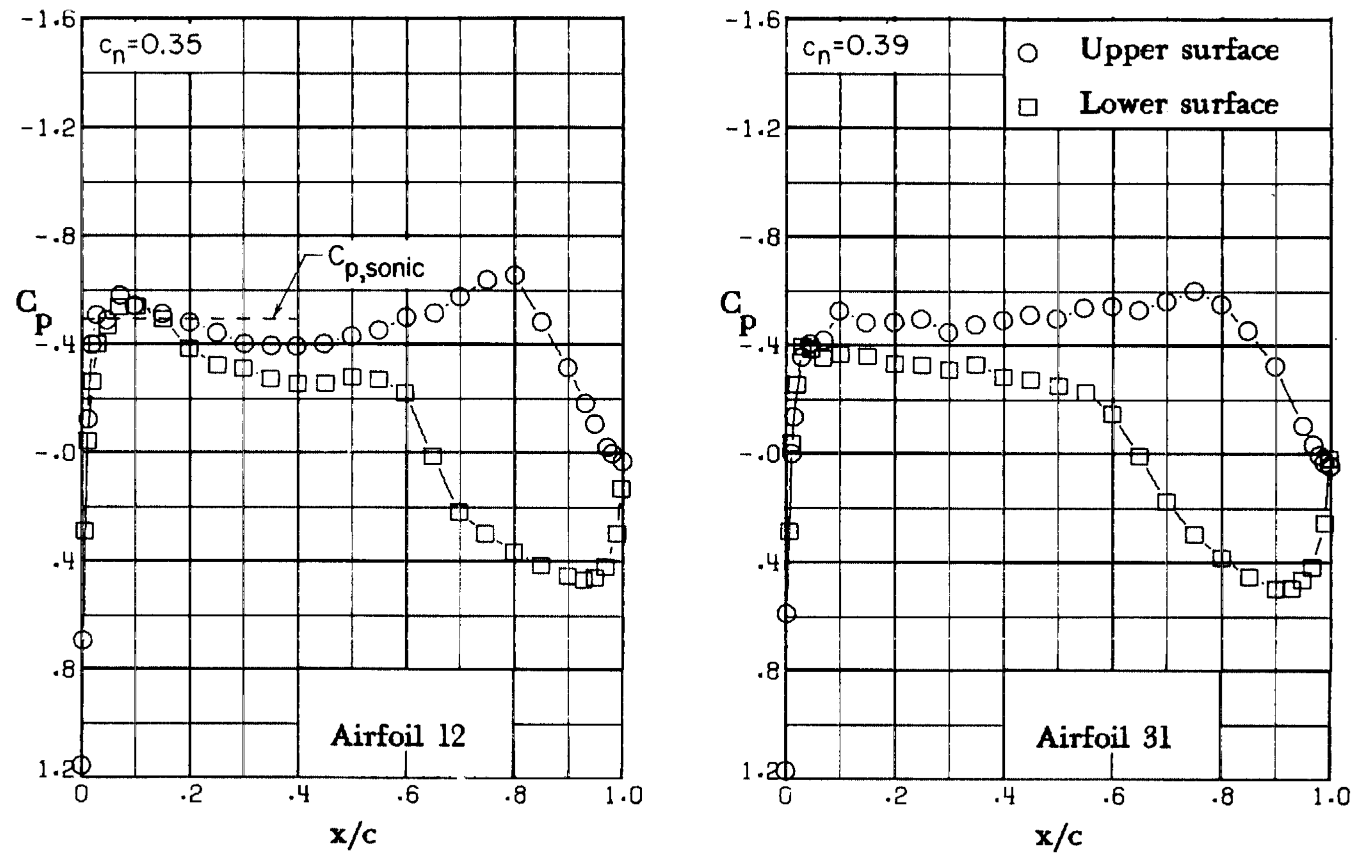

(b) M = 0.78; $c_n \approx 0.39$.

Figure 17. - Continued.

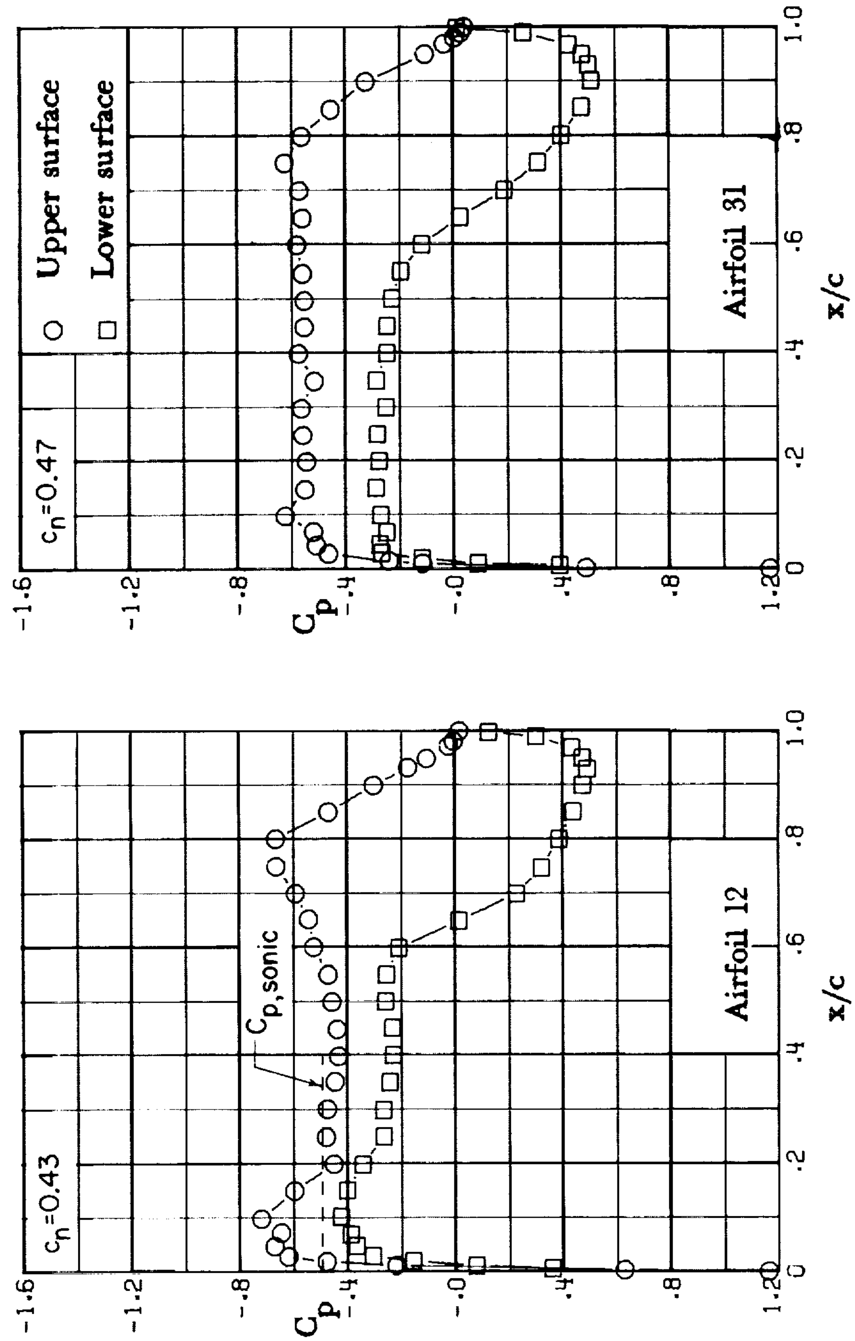

(c) M = 0.78; $c_n \approx 0.47$.

Figure 17. - Continued.

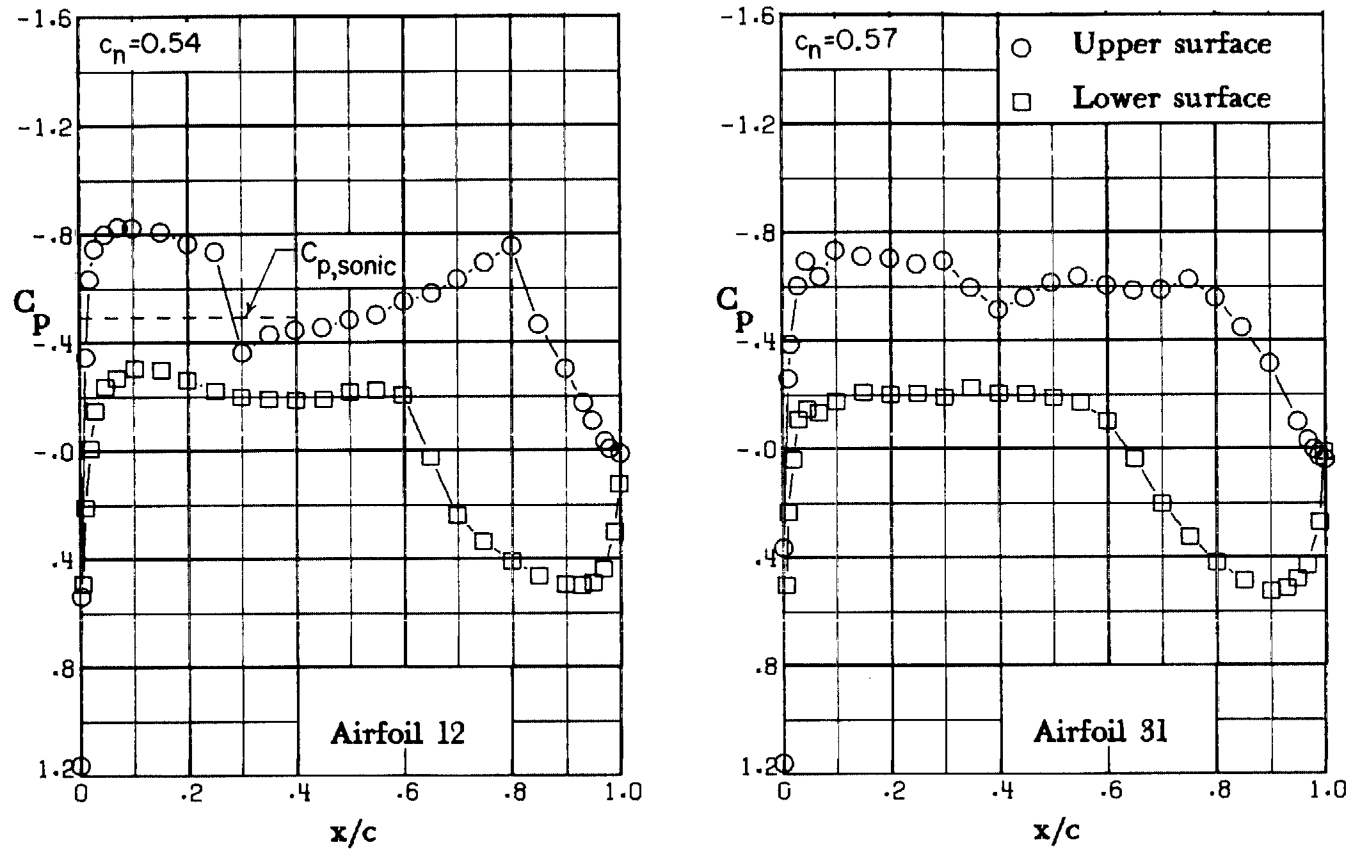

(d) M = 0.78; $c_n \approx 0.57$.

Figure 17. - Continued.

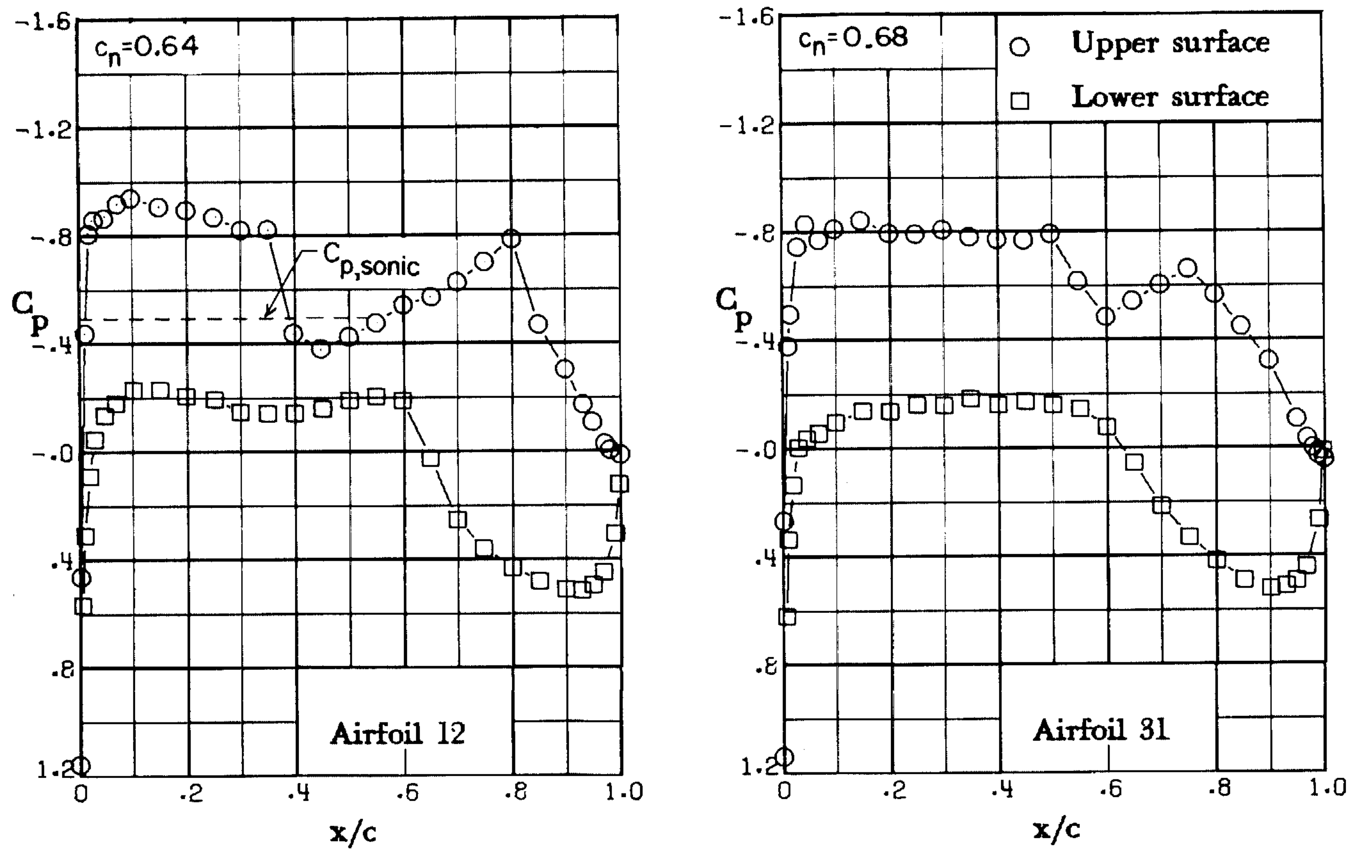

(e) M = 0.78; $c_n \approx 0.68$.

Figure 17. - Continued.

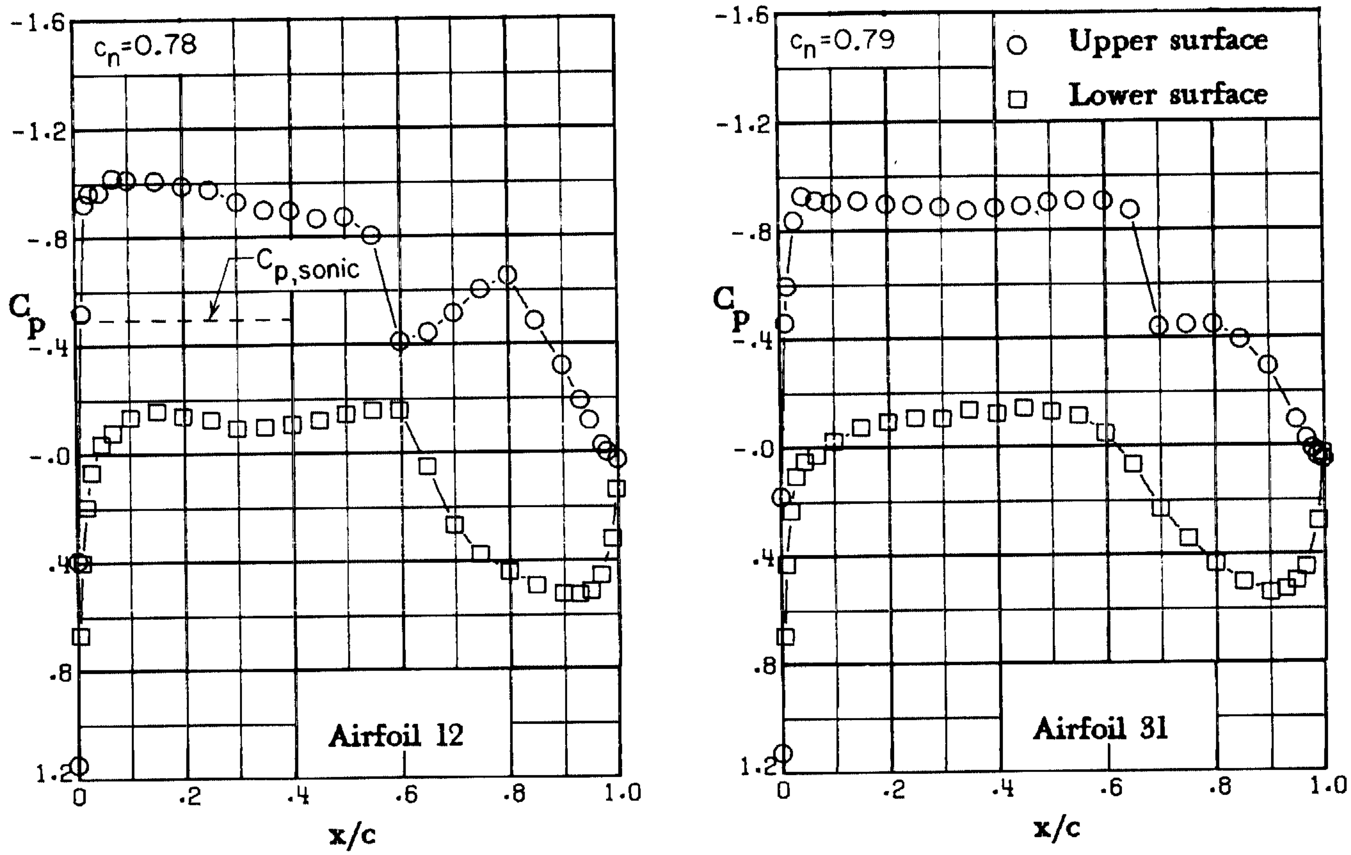

(f) M = 0.78; $c_n \approx 0.79$.

Figure 17.- Continued.

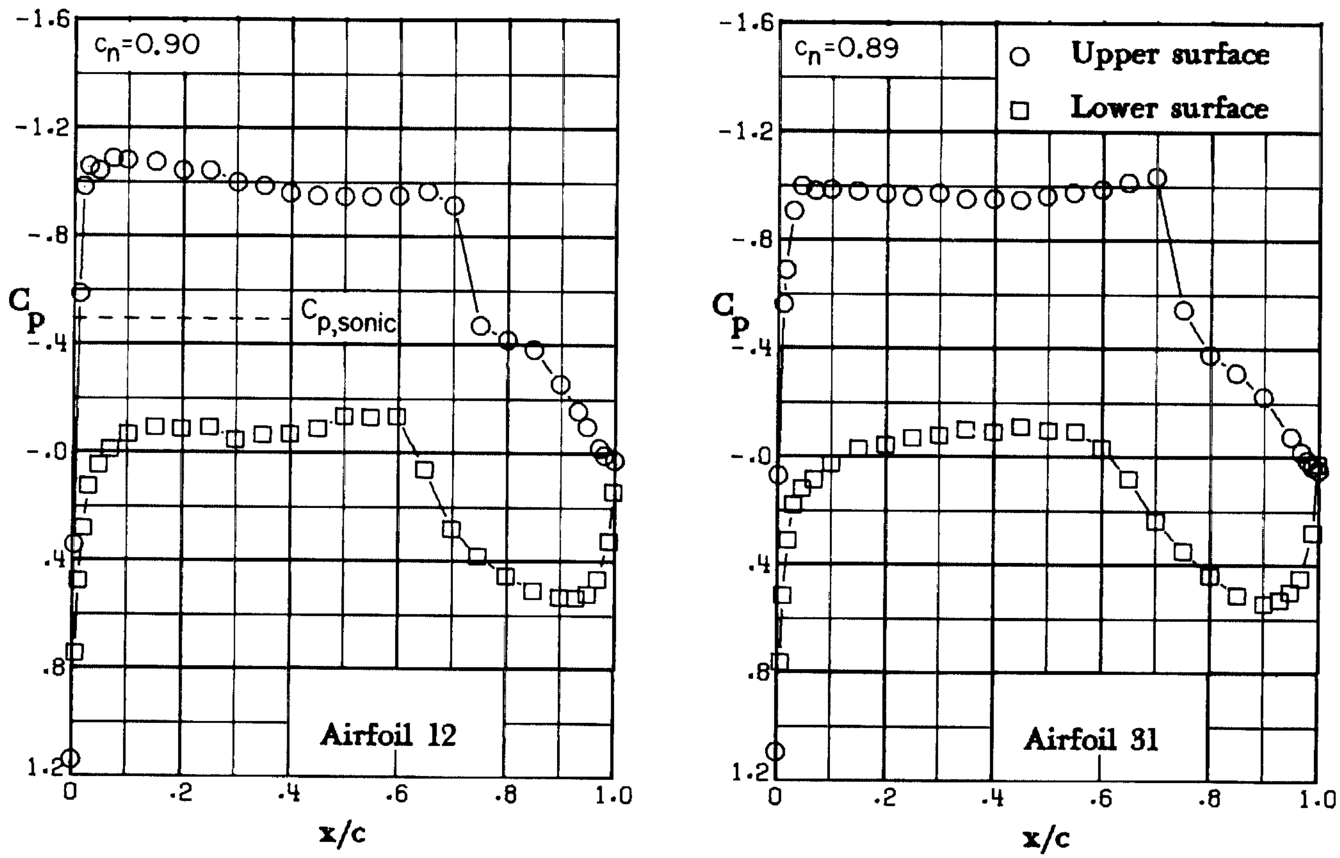

(g) M = 0.78; $c_n \approx 0.89$.

Figure 17.- Continued.

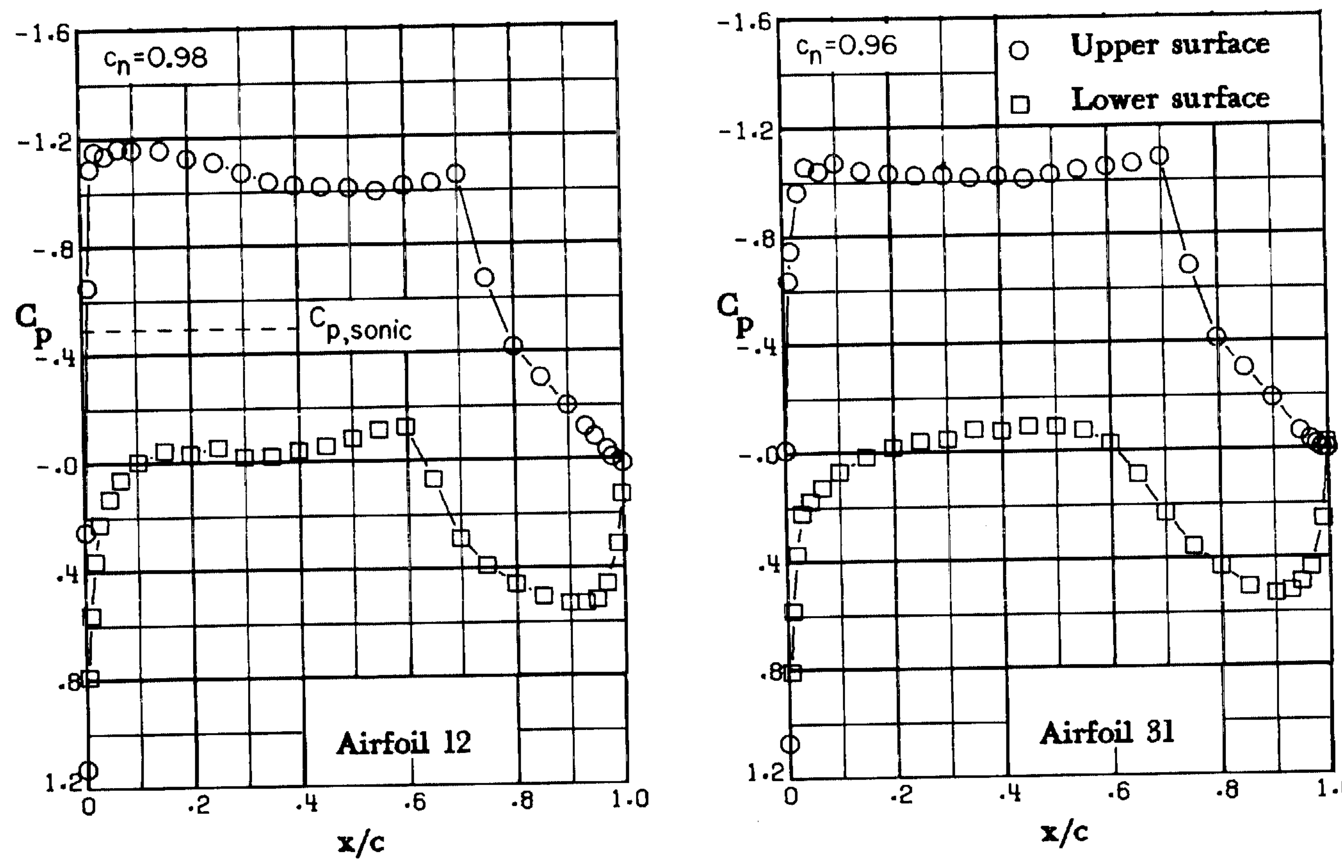

(h) $M = 0.78$; $c_n \approx 0.96$.

Figure 17.- Concluded.

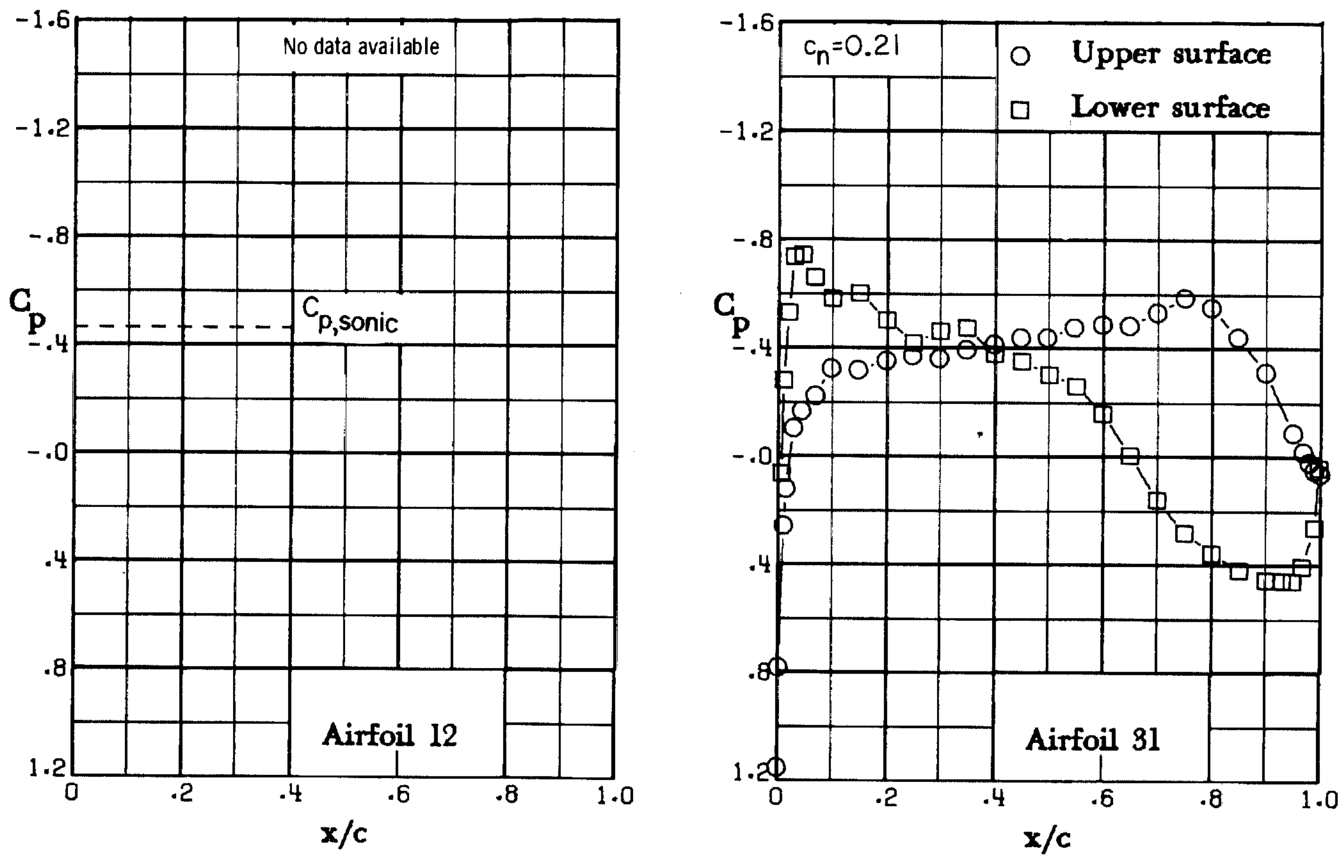

(a) $M = 0.79$; $c_n = 0.21$.

Figure 18.- Chordwise pressure distribution. $M = 0.79$.

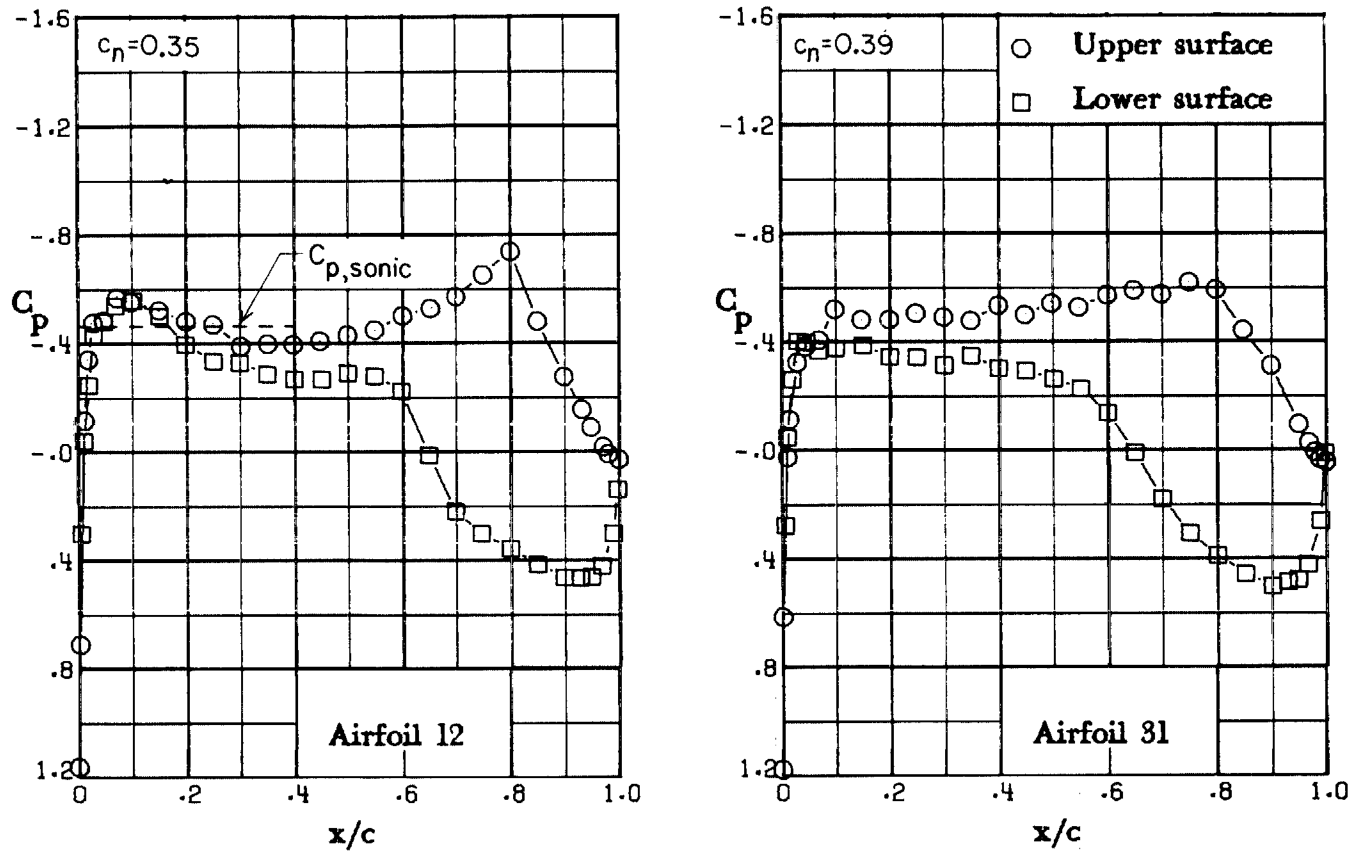

(b) M = 0.79; $c_n \approx 0.39$.

Figure 18. - Continued.

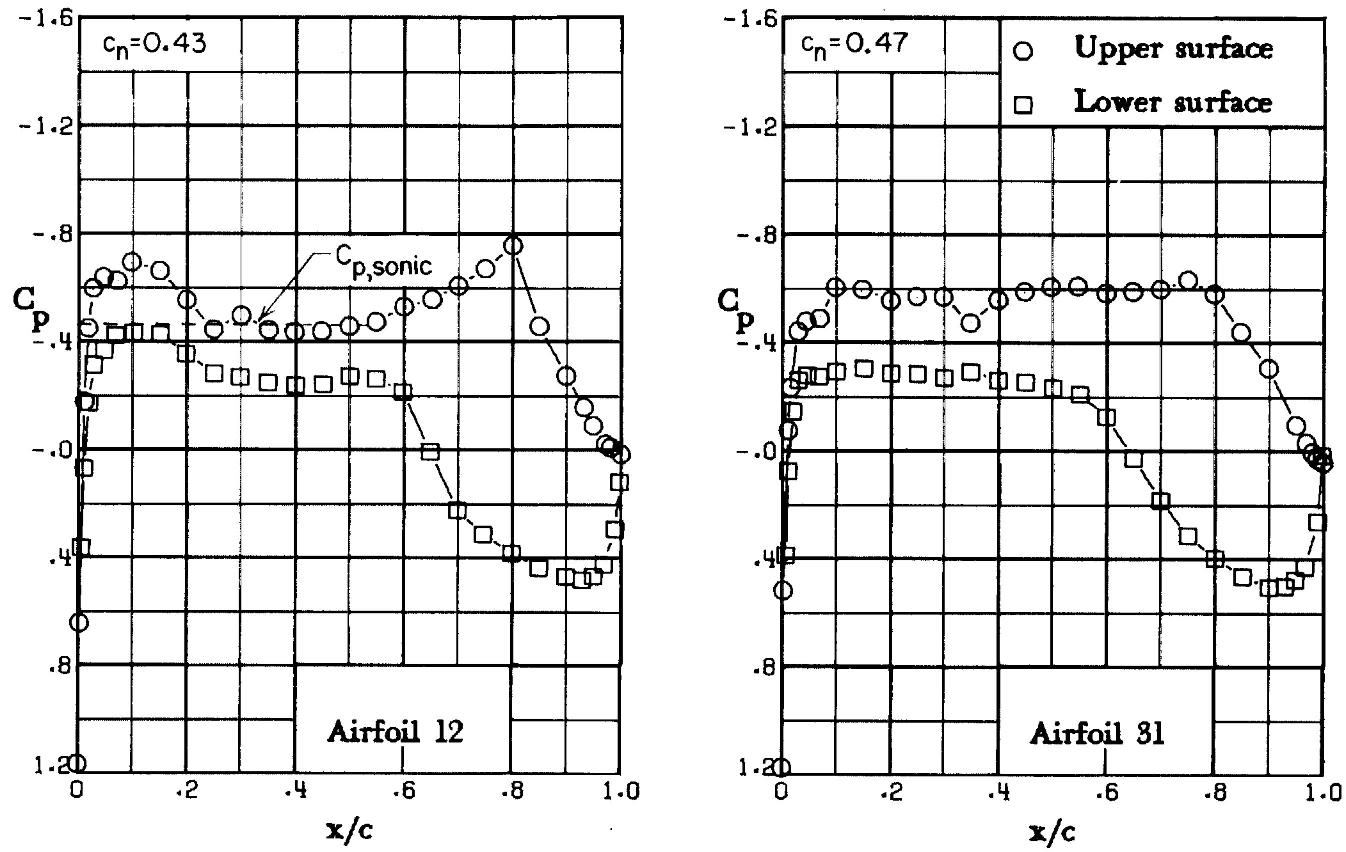

(c) $M = 0.79$; $c_n \approx 0.47$.

Figure 18.- Continued.

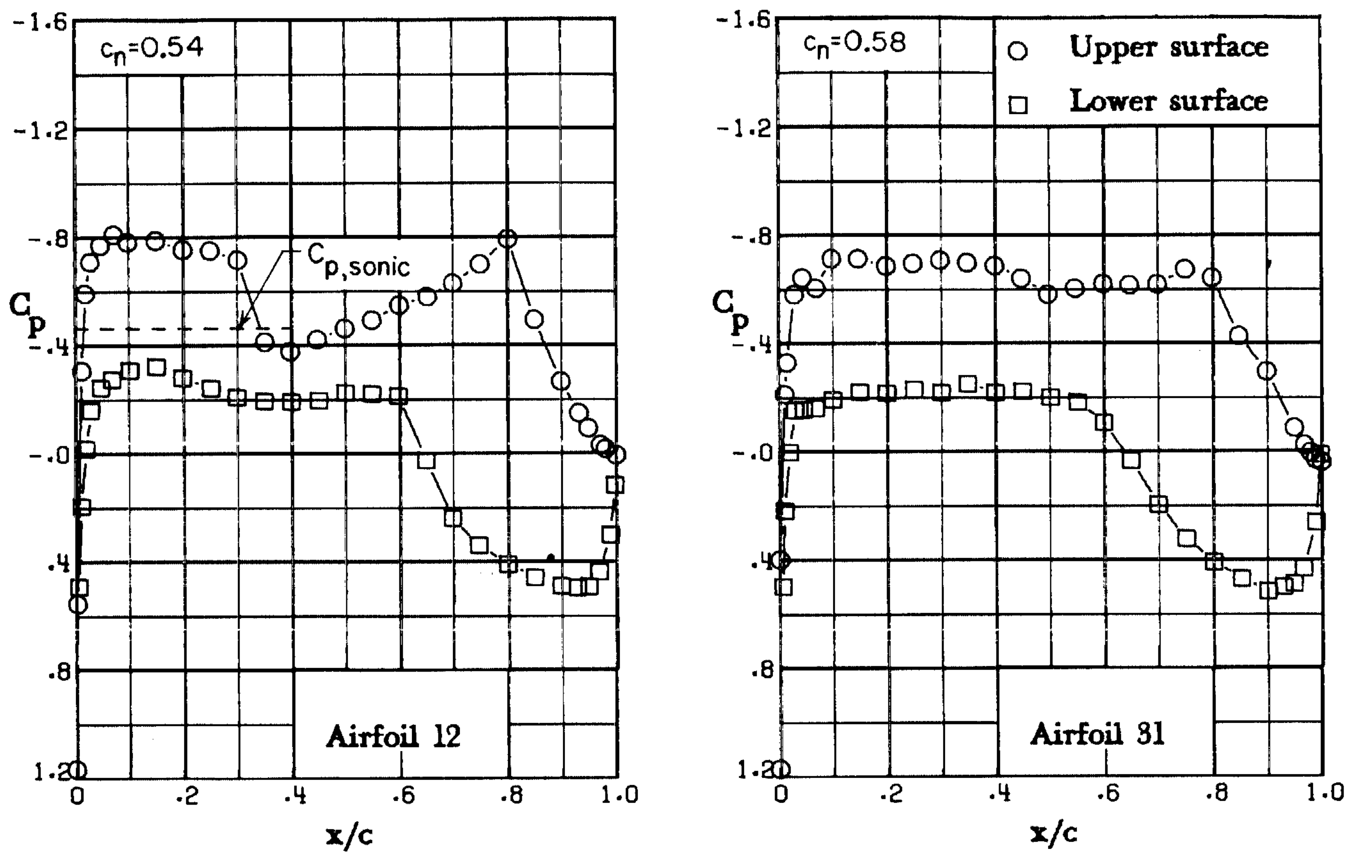

(d) M = 0.79; $c_n \approx 0.58$.

Figure 18.- Continued.

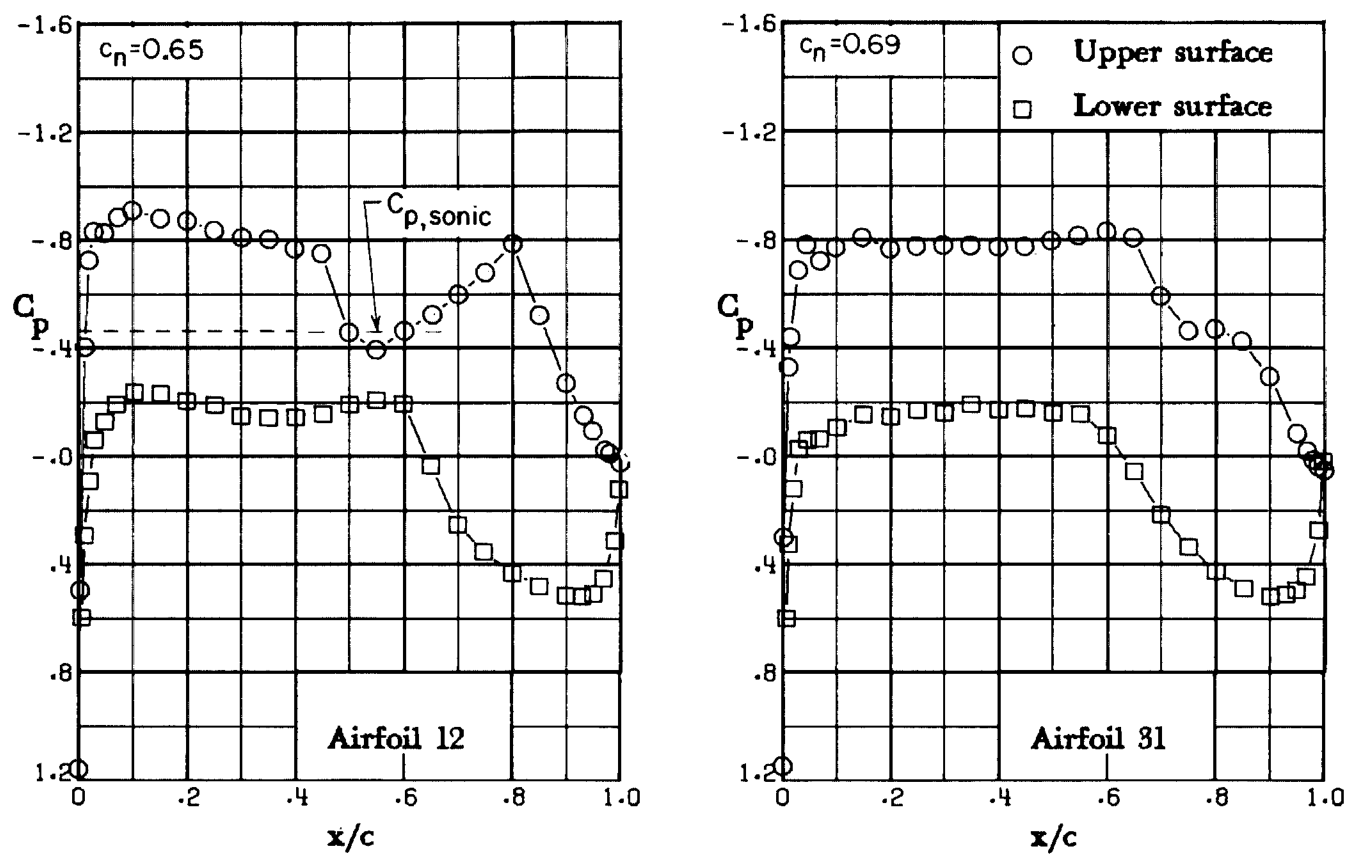

(e) M = 0.79; $c_n \approx 0.69$.

Figure 18. - Continued.

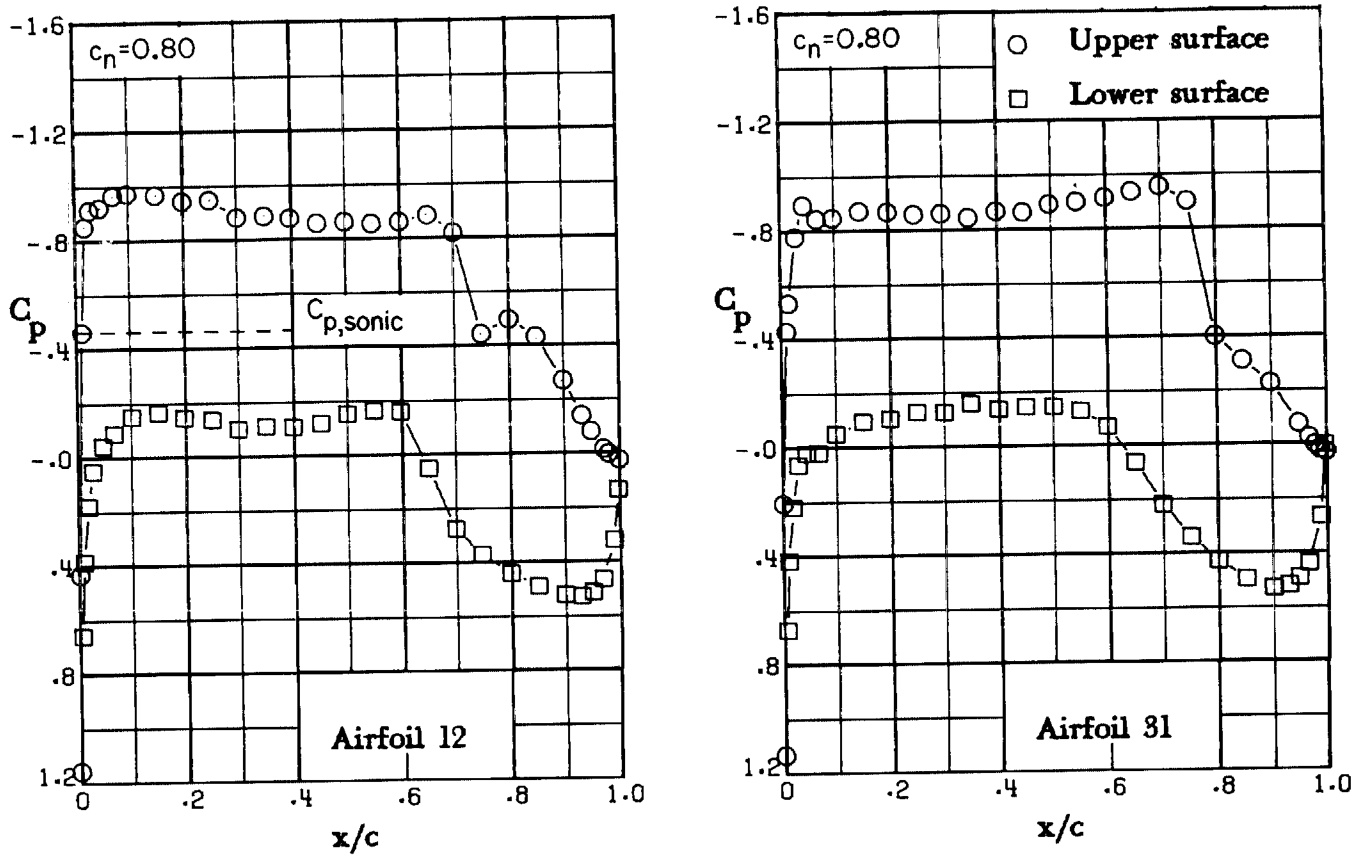

(f) $M = 0.79$; $c_n = 0.80$.

Figure 18.- Continued.

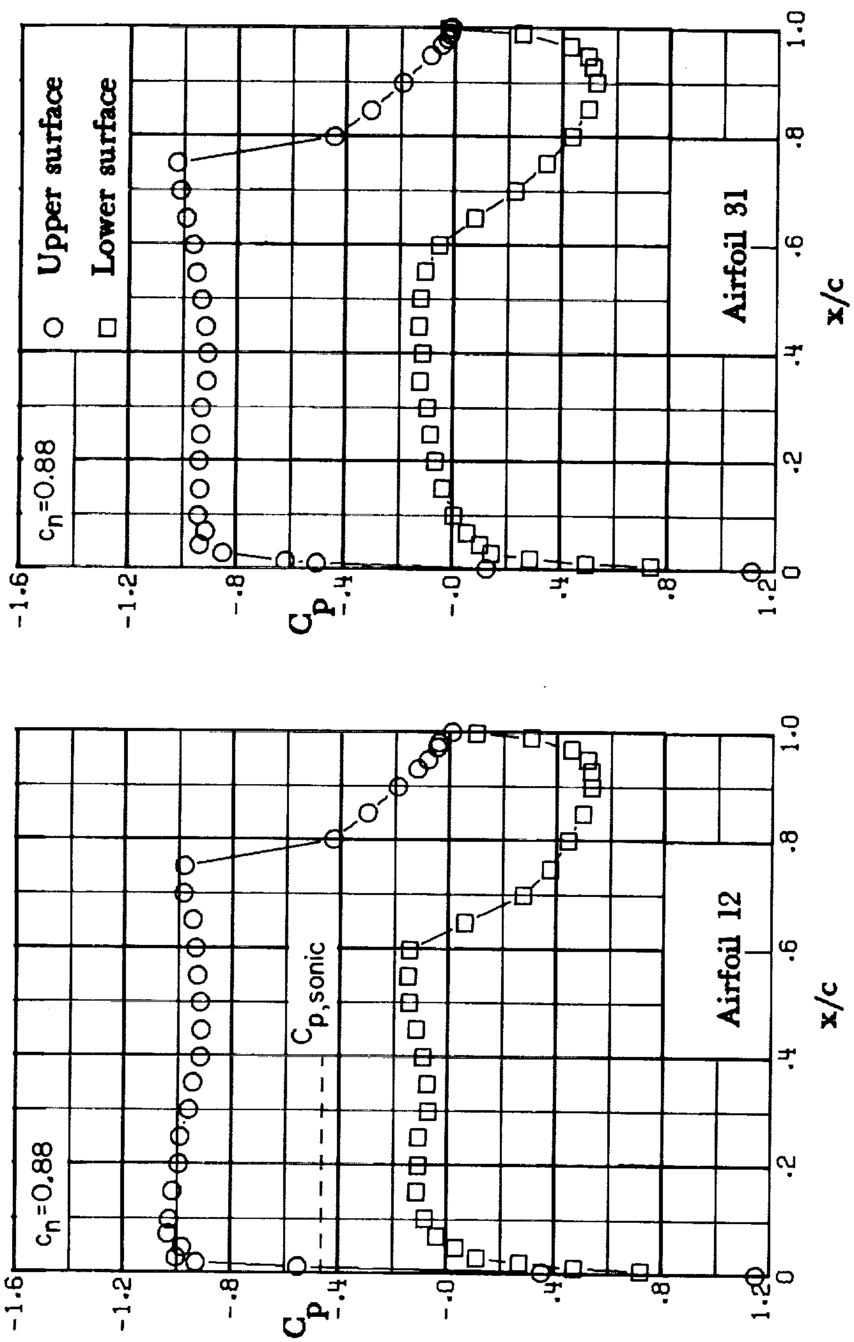

(g) M = 0.79; c_n = 0.88.

Figure 18.- Concluded.

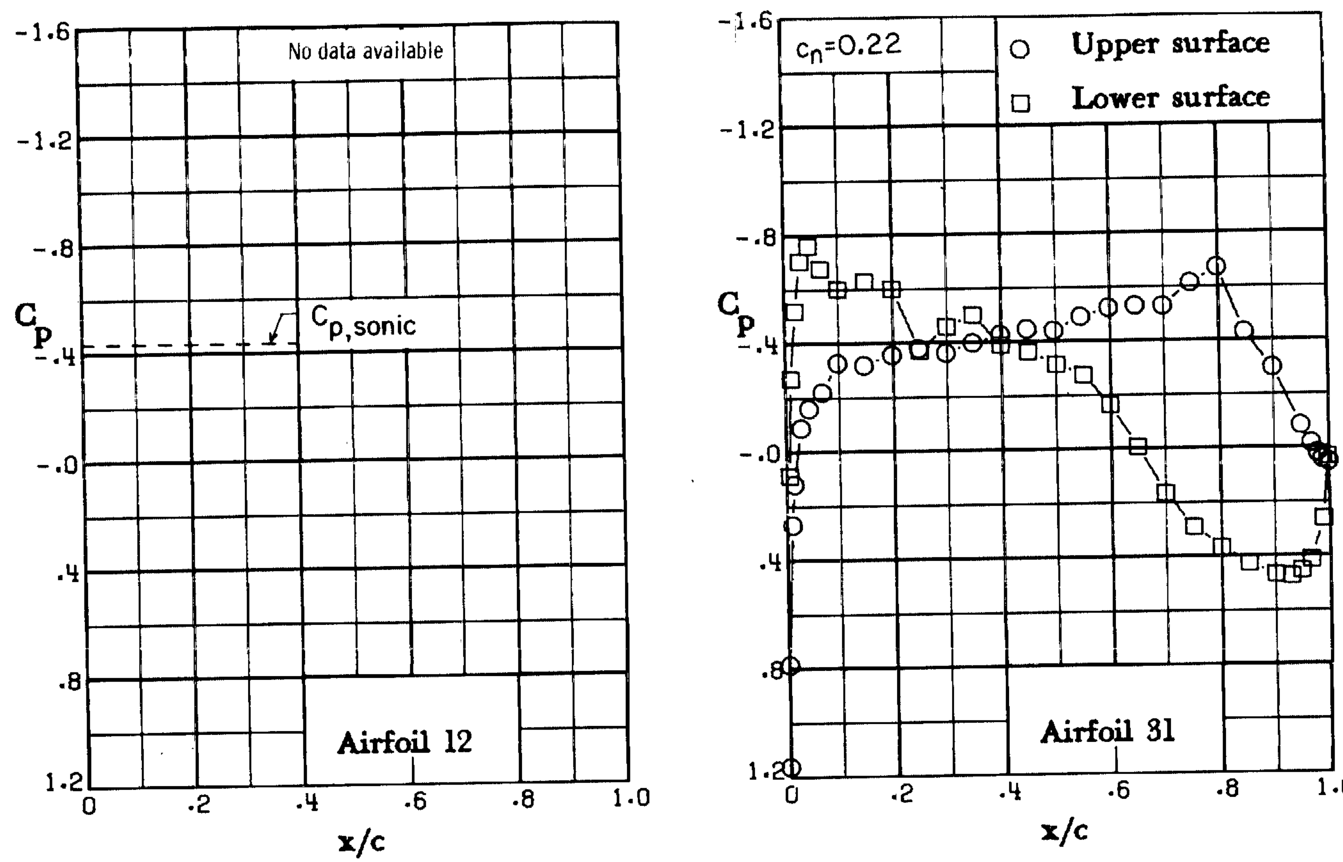

(a) M = 0.80; c_n = 0.22.

Figure 19.- Chordwise pressure distribution. M = 0.80.

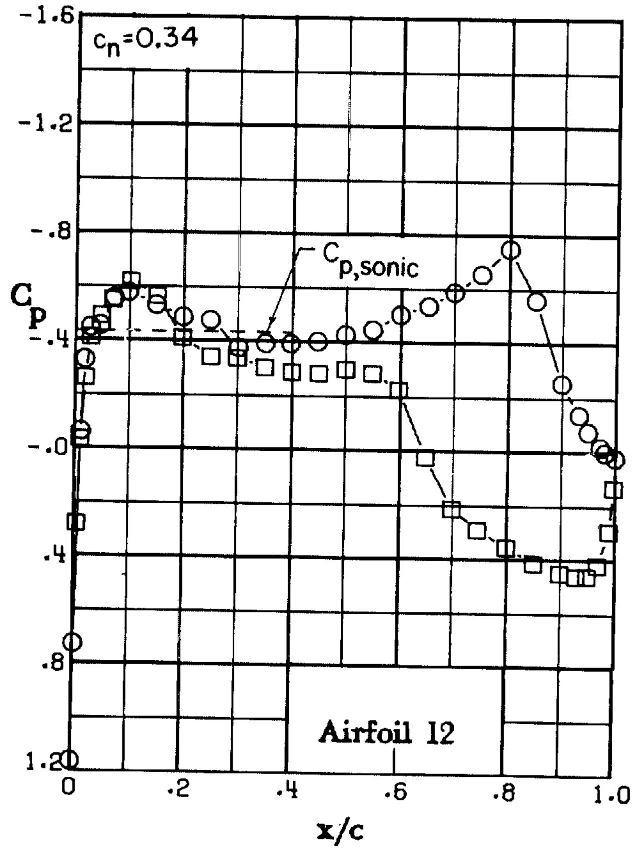

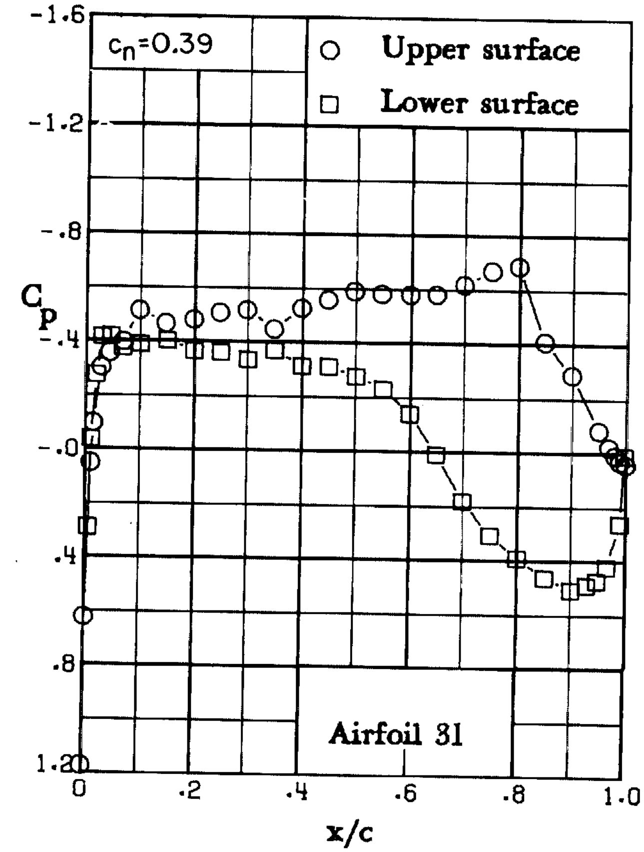

(b) $M = 0.80$; $c_n \approx 0.39$.

Figure 19.- Continued.

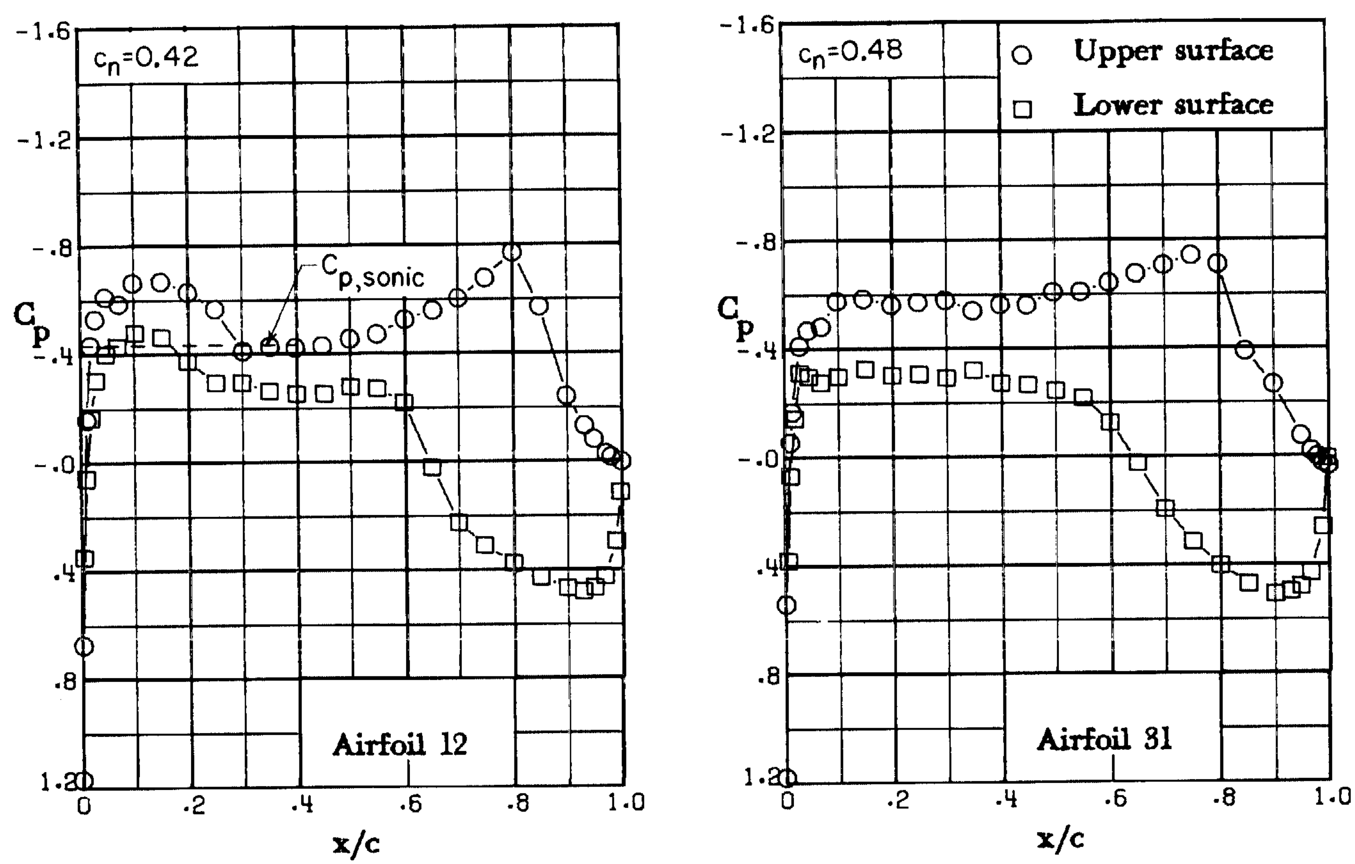

(c) M = 0.80; $c_n \approx 0.48$.

Figure 19.- Continued.

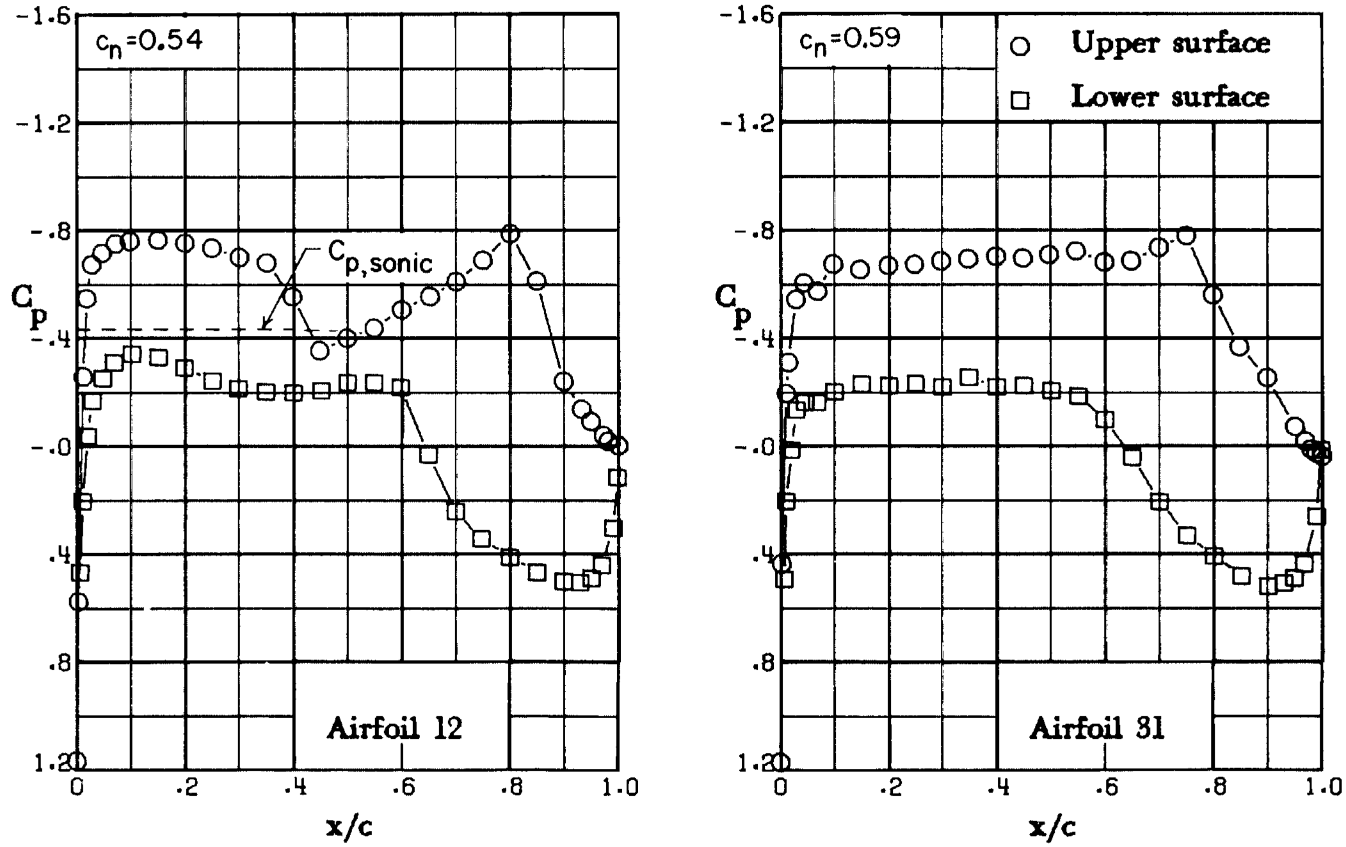

(d) M = 0.80; $c_n \approx 0.59$.

Figure 19. - Continued.

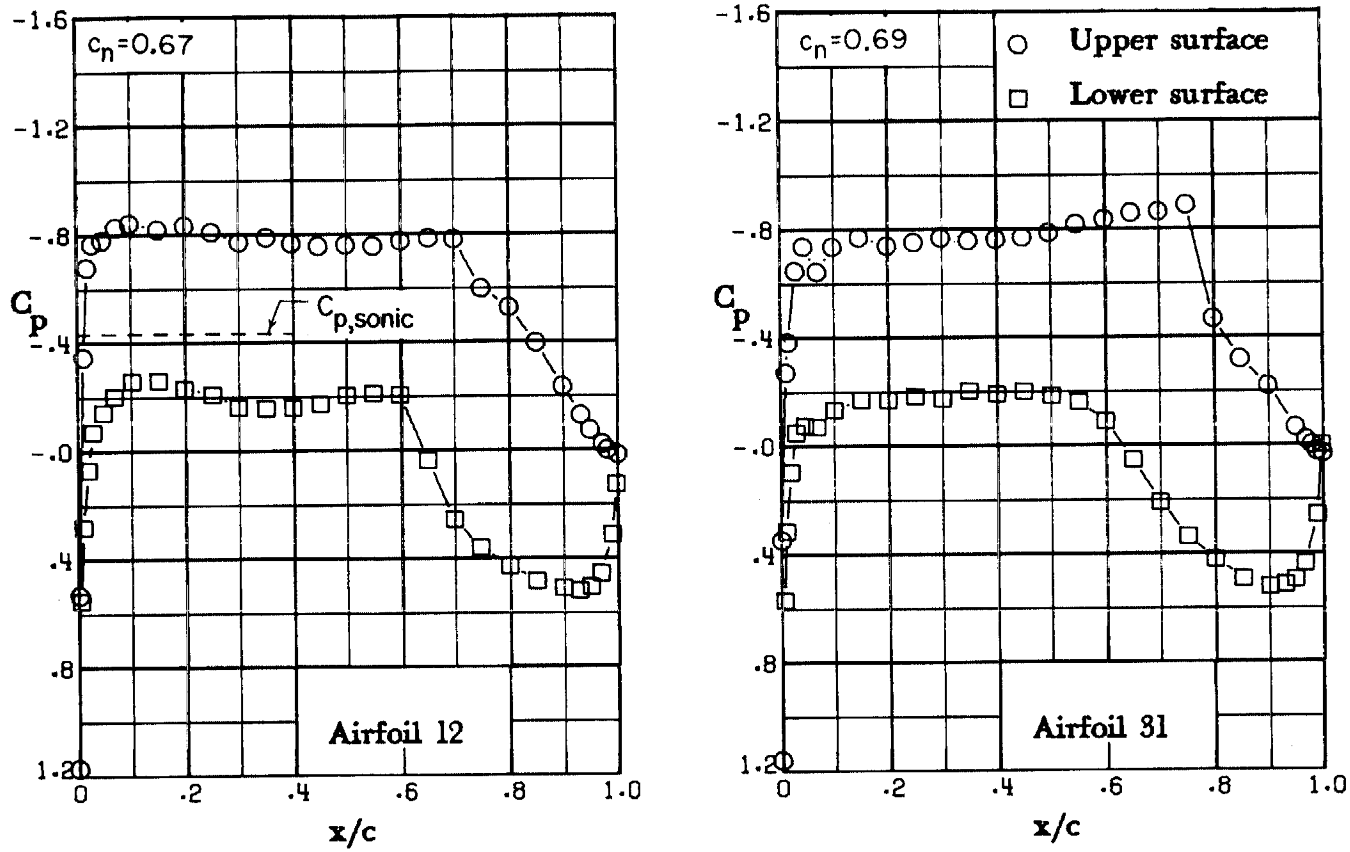

(e) M = 0.80; $c_n \approx 0.69$.

Figure 19. - Continued.

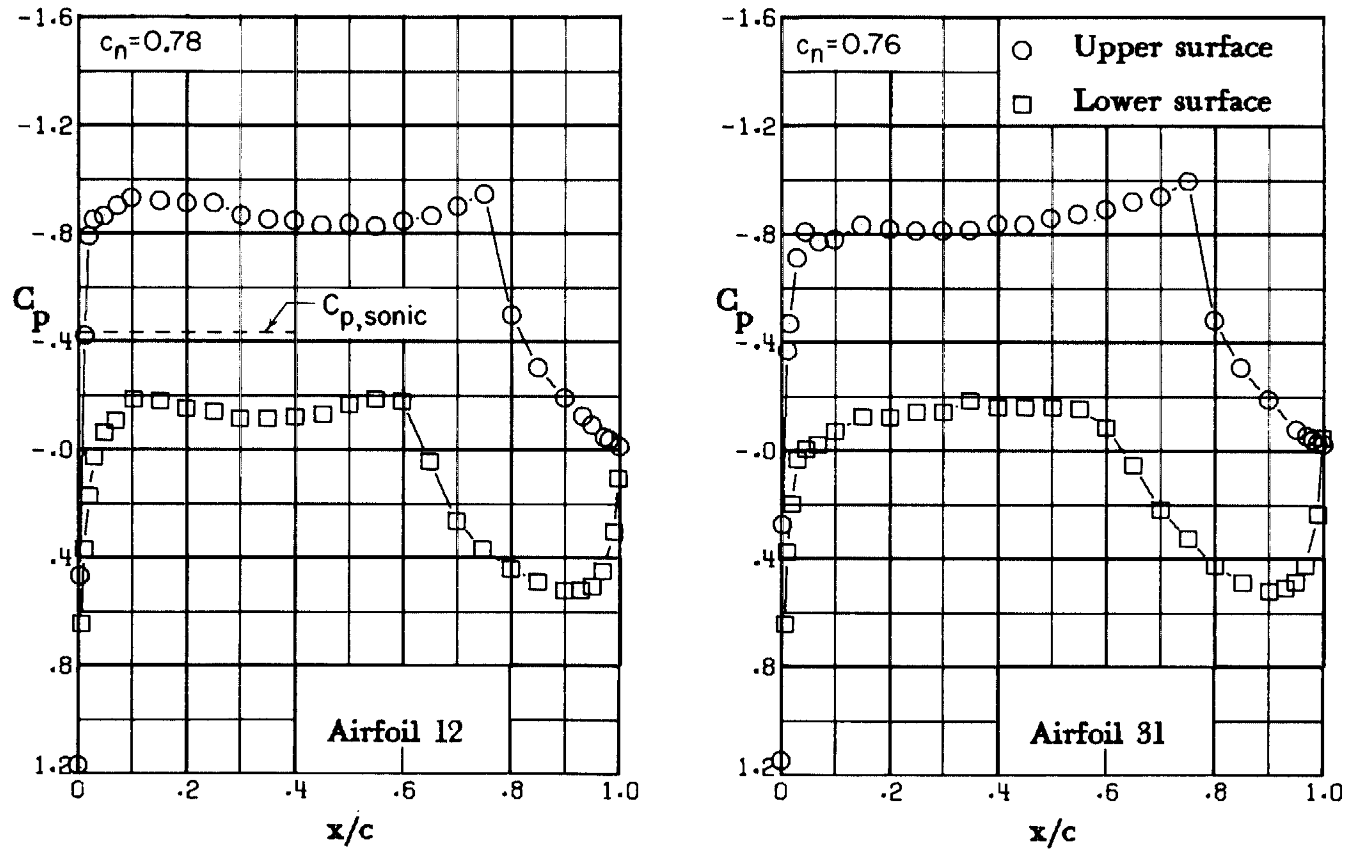

(f) M = 0.80; $c_n \approx 0.76$.

Figure 19. - Continued.

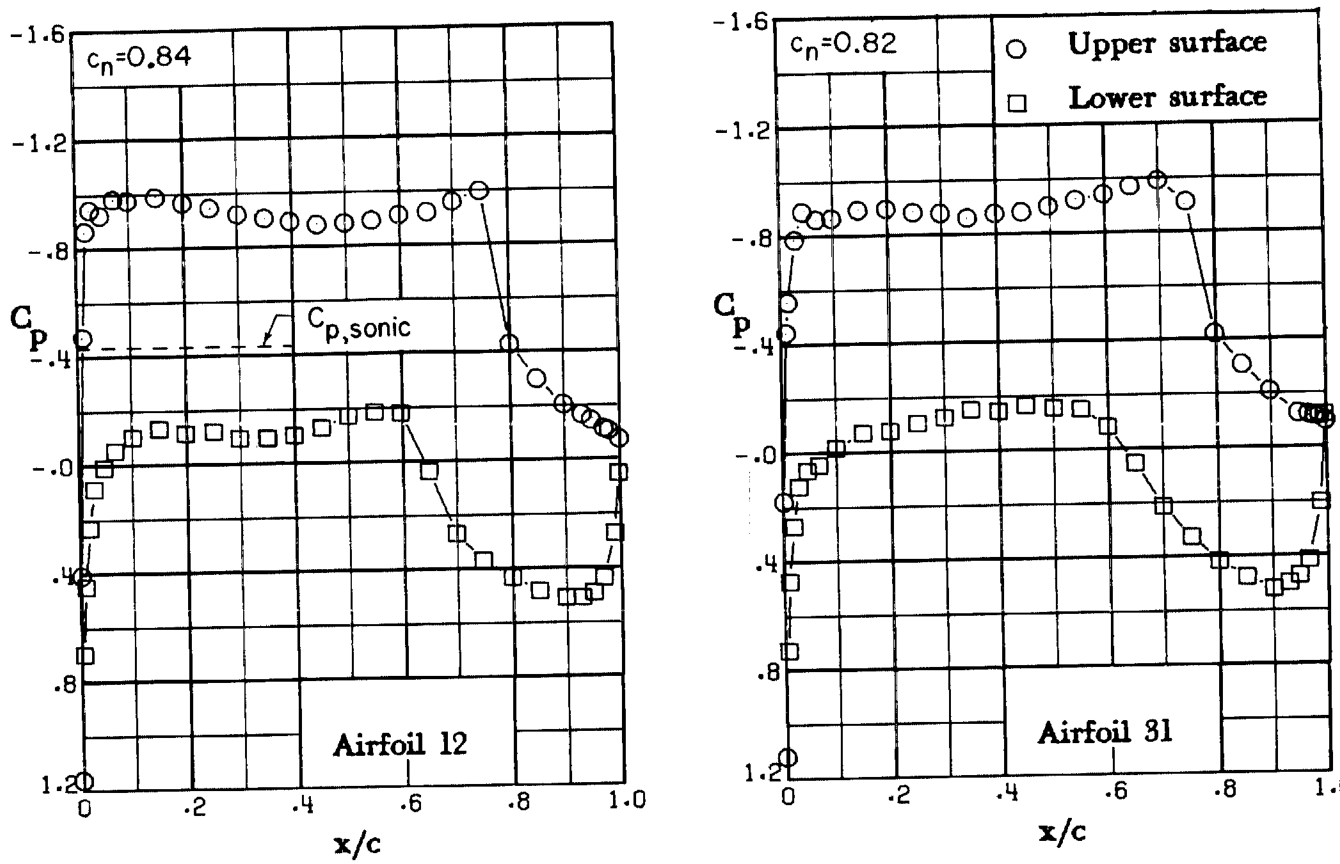

(g) M = 0.80; $c_n \approx 0.82$.

Figure 19.- Concluded.

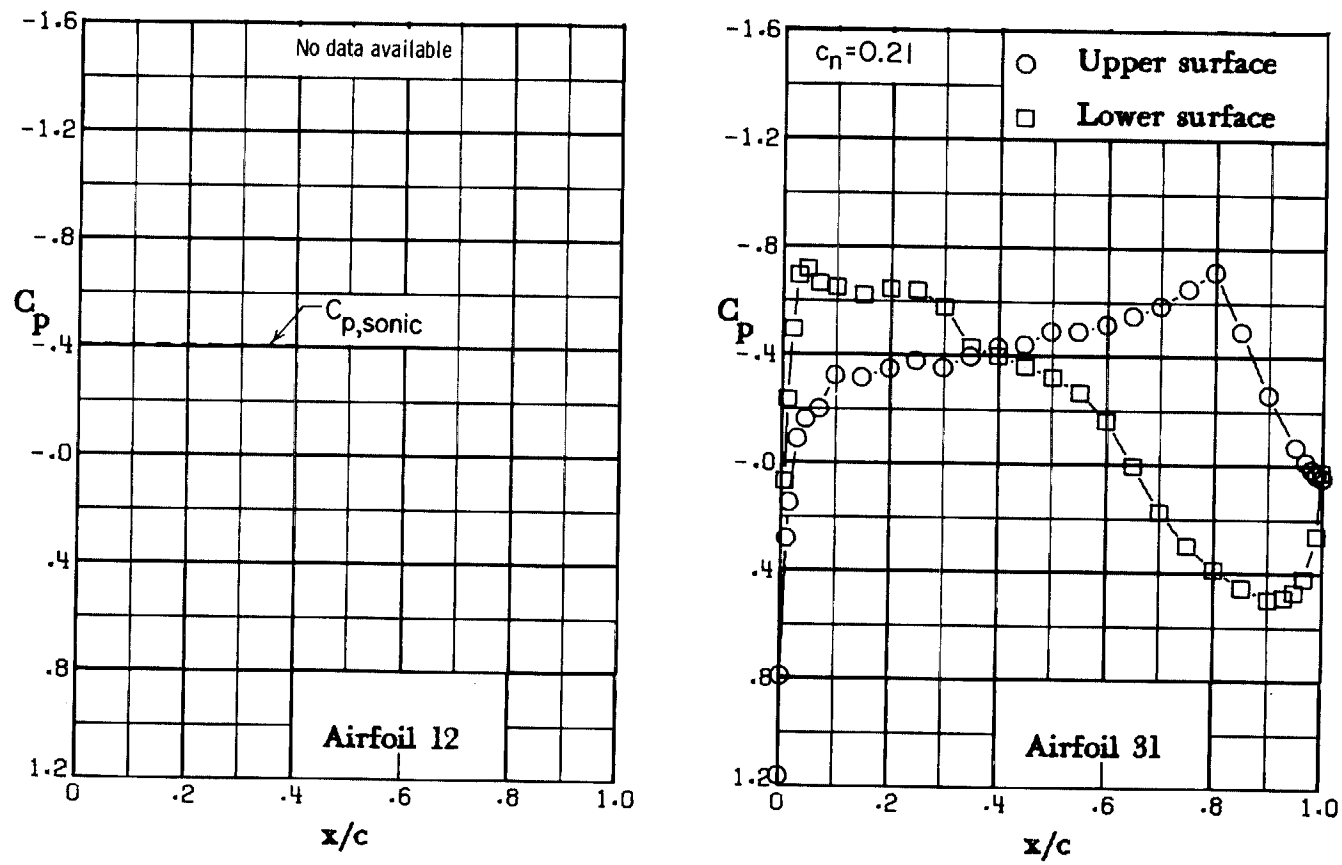

(a) M = 0.81; c_n = 0.21.

Figure 20. - Chordwise pressure distribution. M = 0.81.

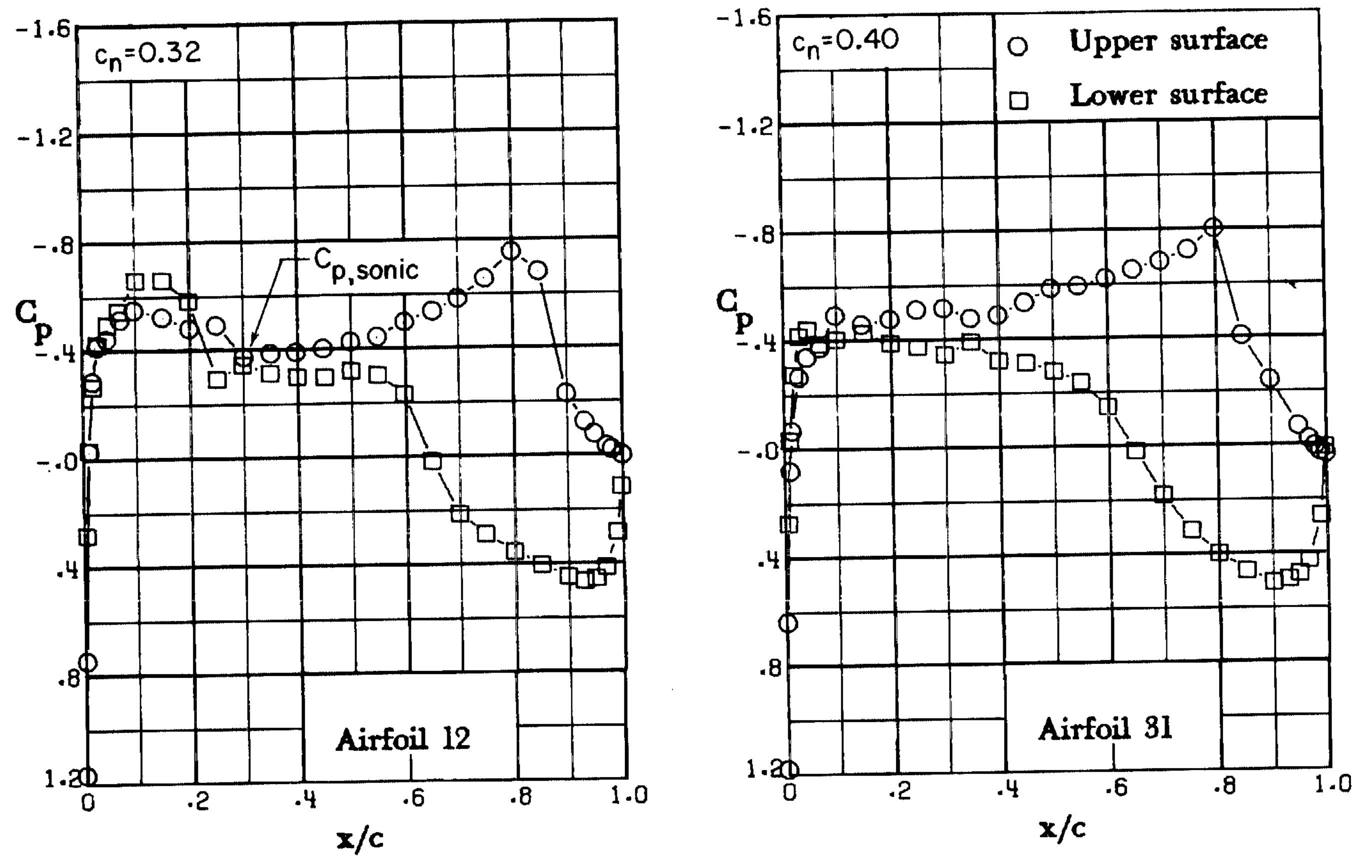

(b) M = 0.81; $c_n \approx 0.40$.

Figure 20. - Continued.

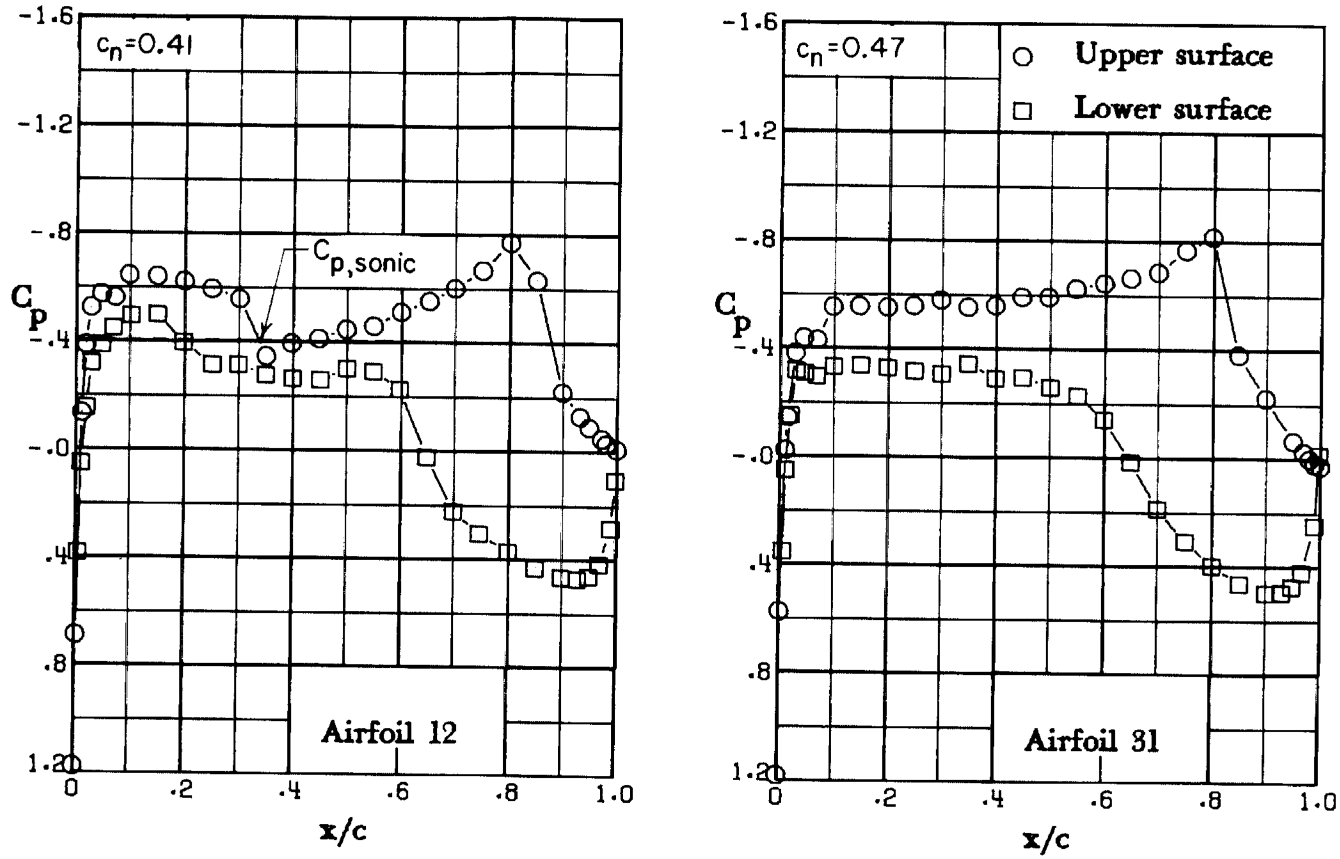

(c) $M = 0.81$; $c_n \approx 0.47$.

Figure 20.- Continued.

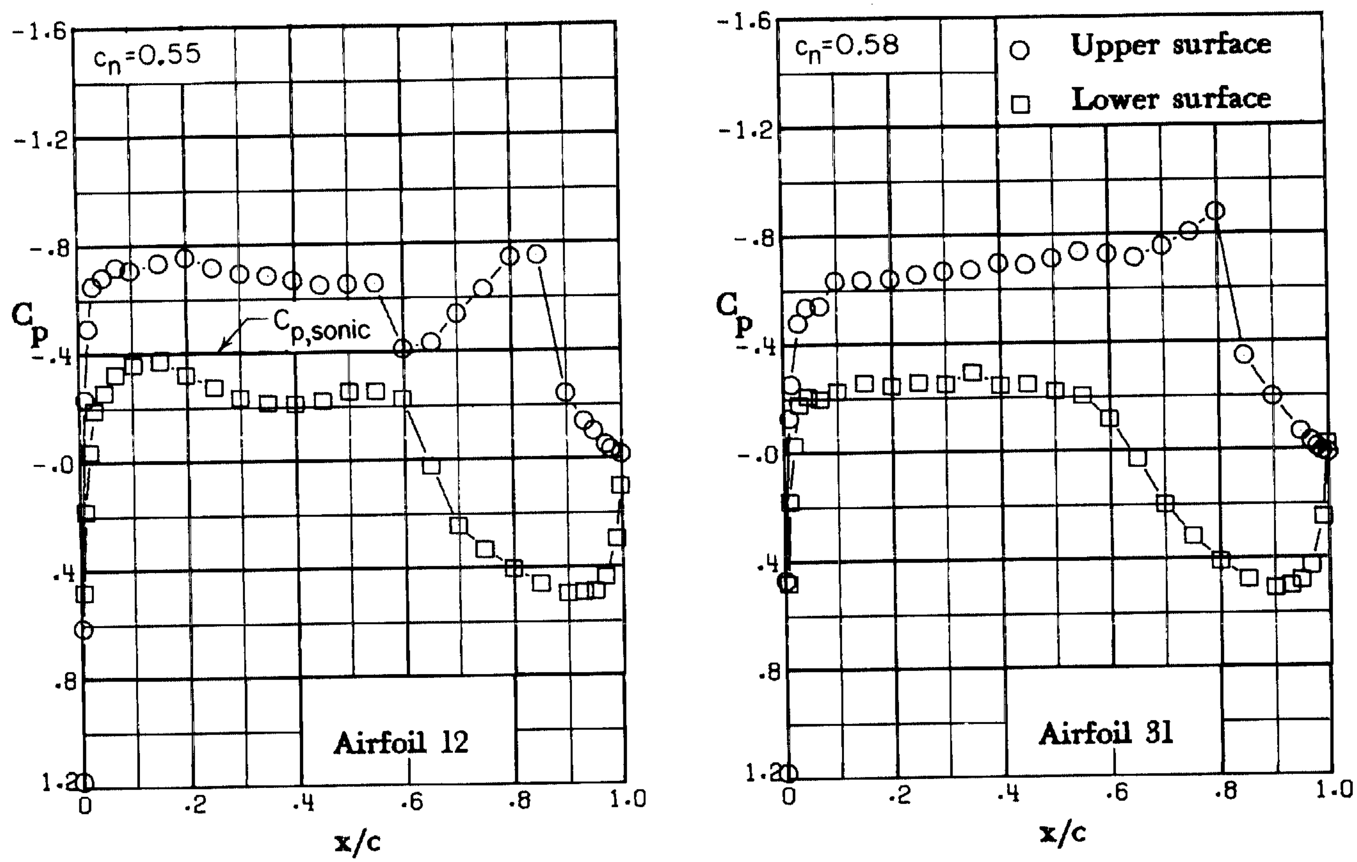

(d) $M = 0.81$; $c_n \approx 0.58$.

Figure 20.- Continued.

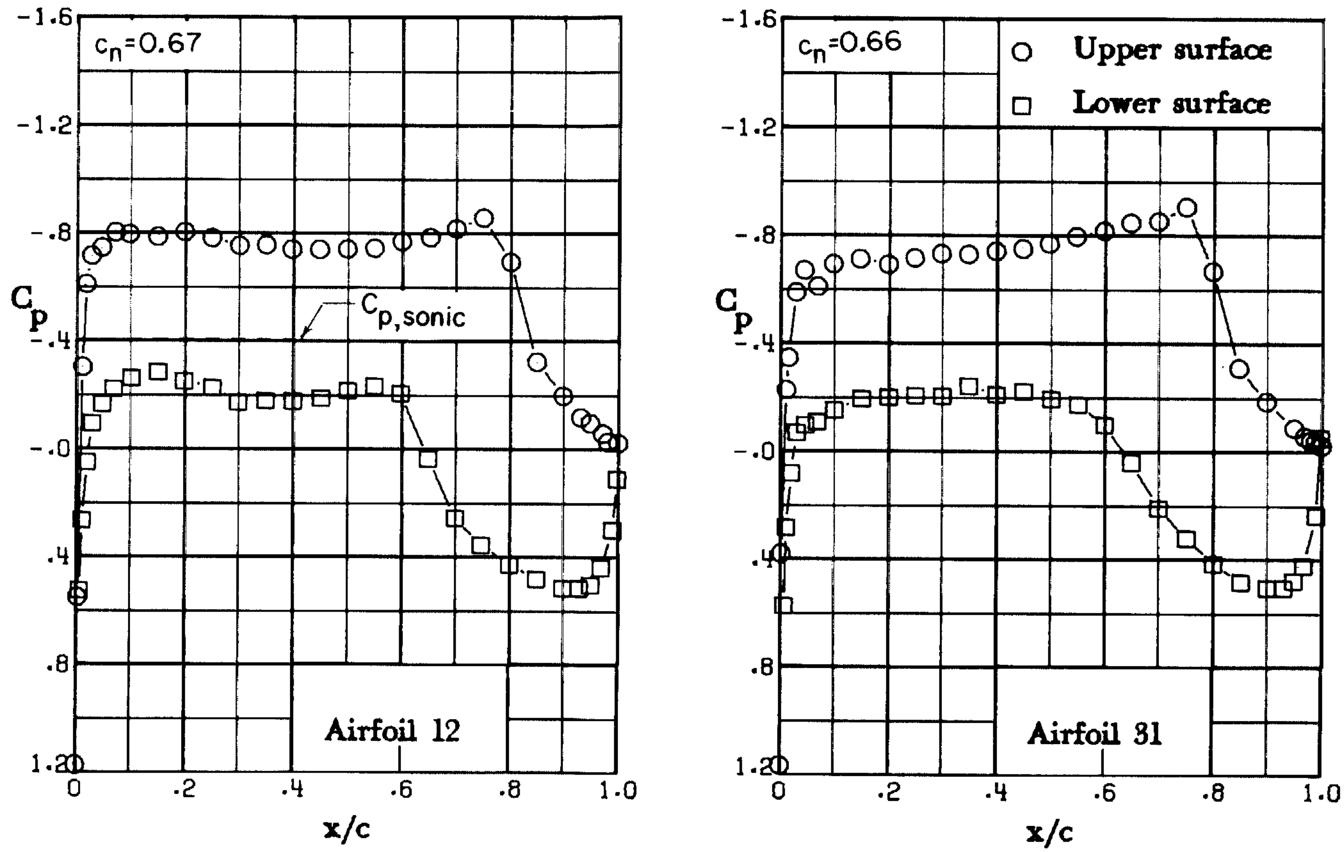

(e) $M = 0.81$; $c_n \approx 0.66$.

Figure 20.- Concluded.

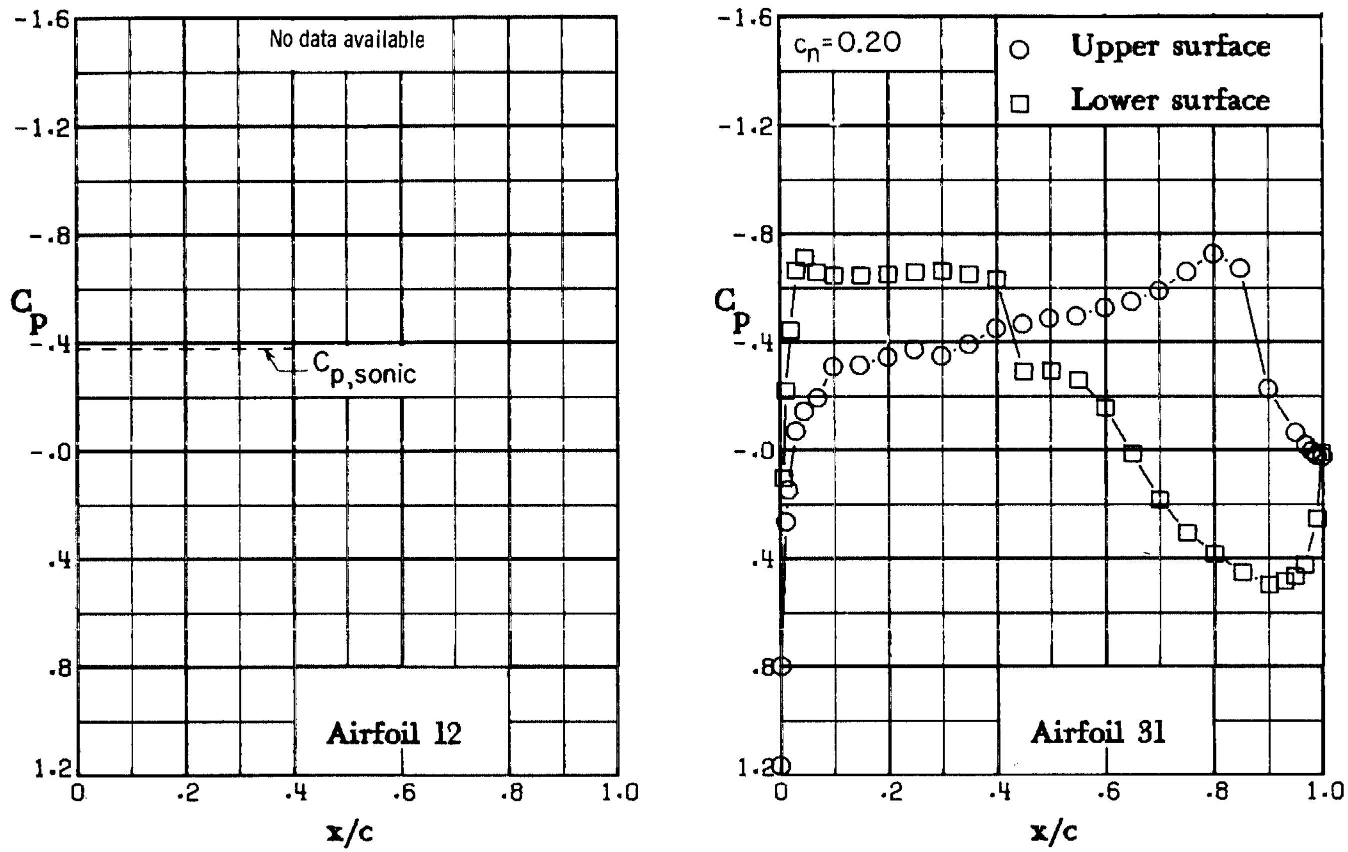

(a) $M = 0.82$; $c_n = 0.20$.

Figure 21.- Chordwise pressure distribution. $M = 0.82$.

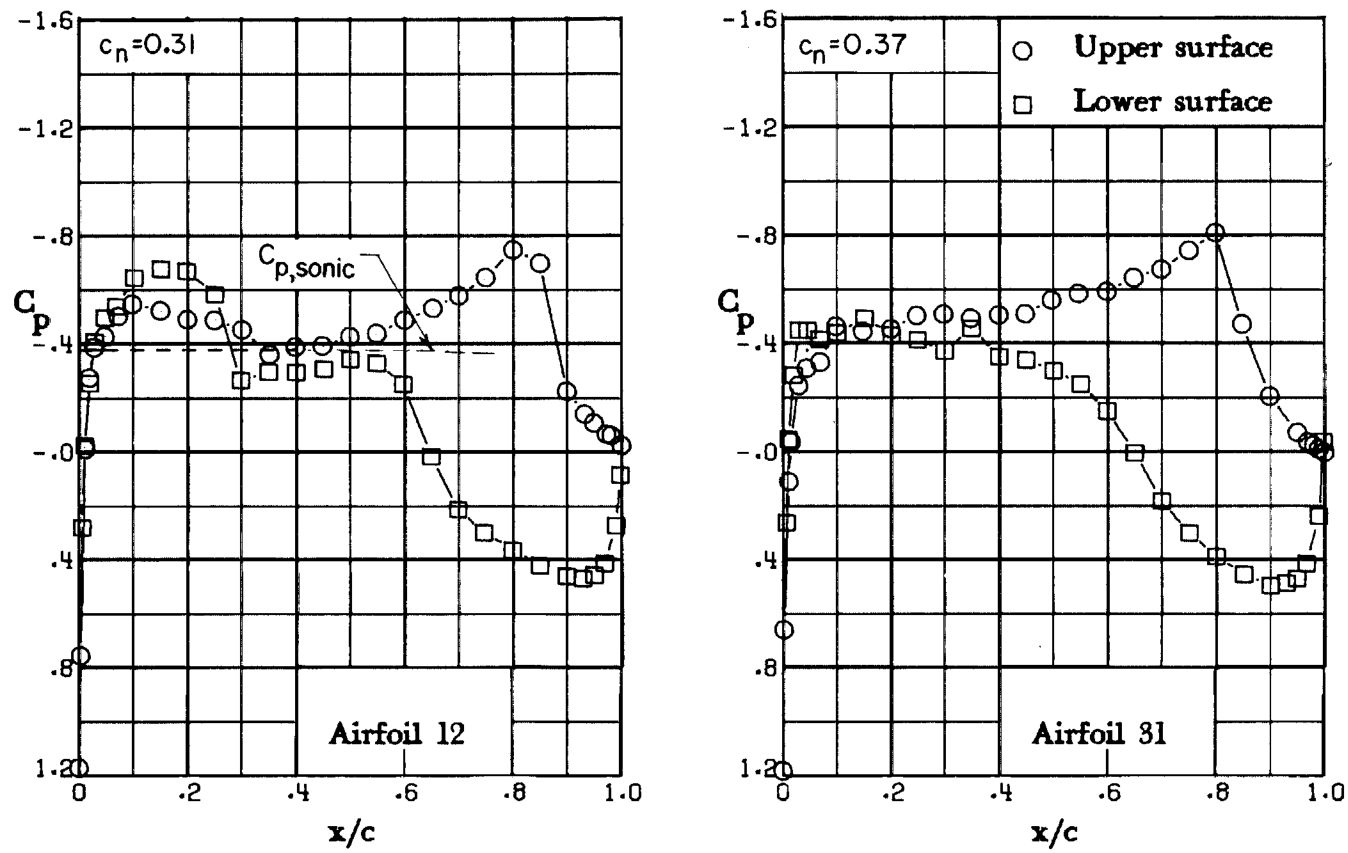

(b) M = 0.82; $c_n \approx 0.37$.

Figure 21.- Continued.

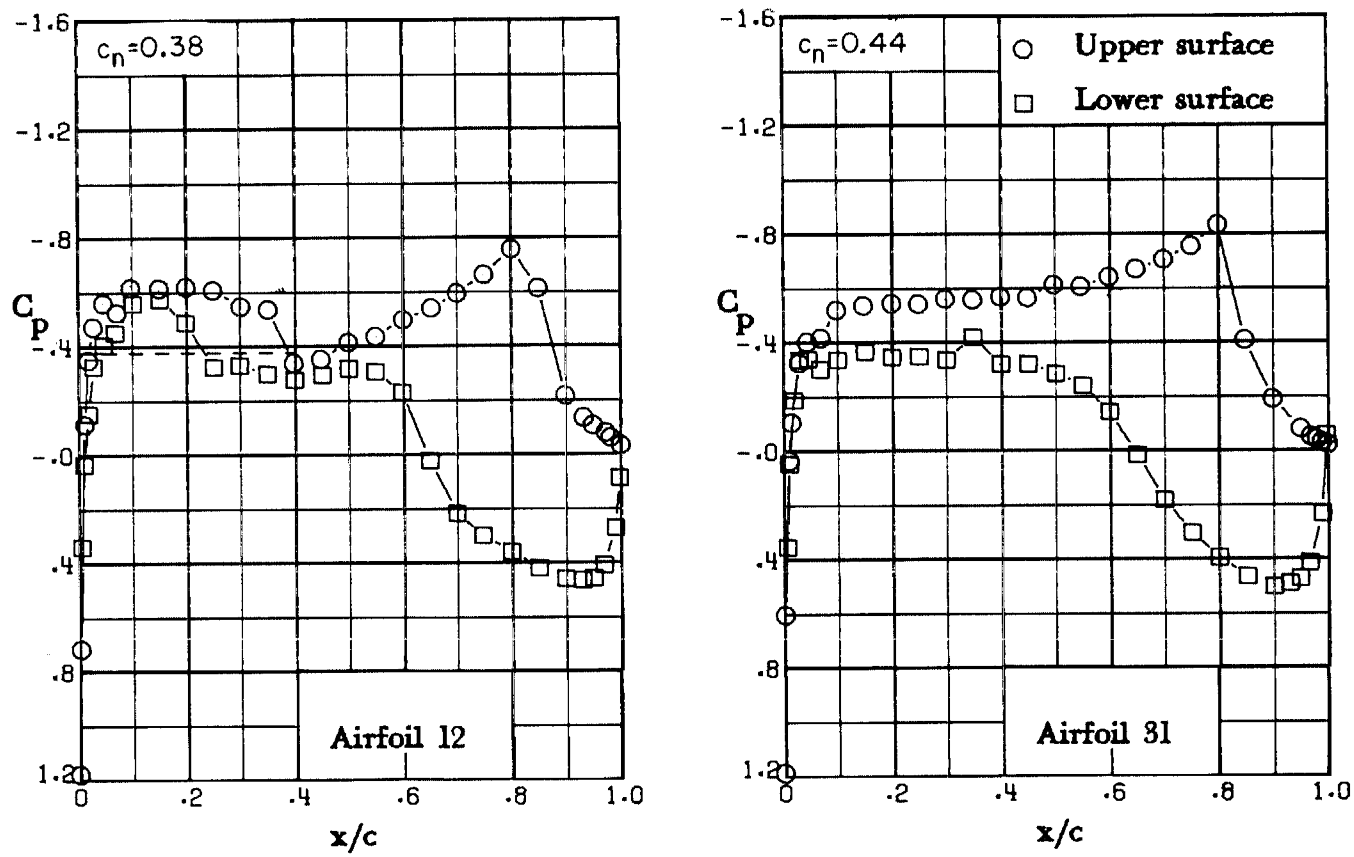

(c) $M = 0.82$; $c_n \approx 0.44$.

Figure 21. - Continued.

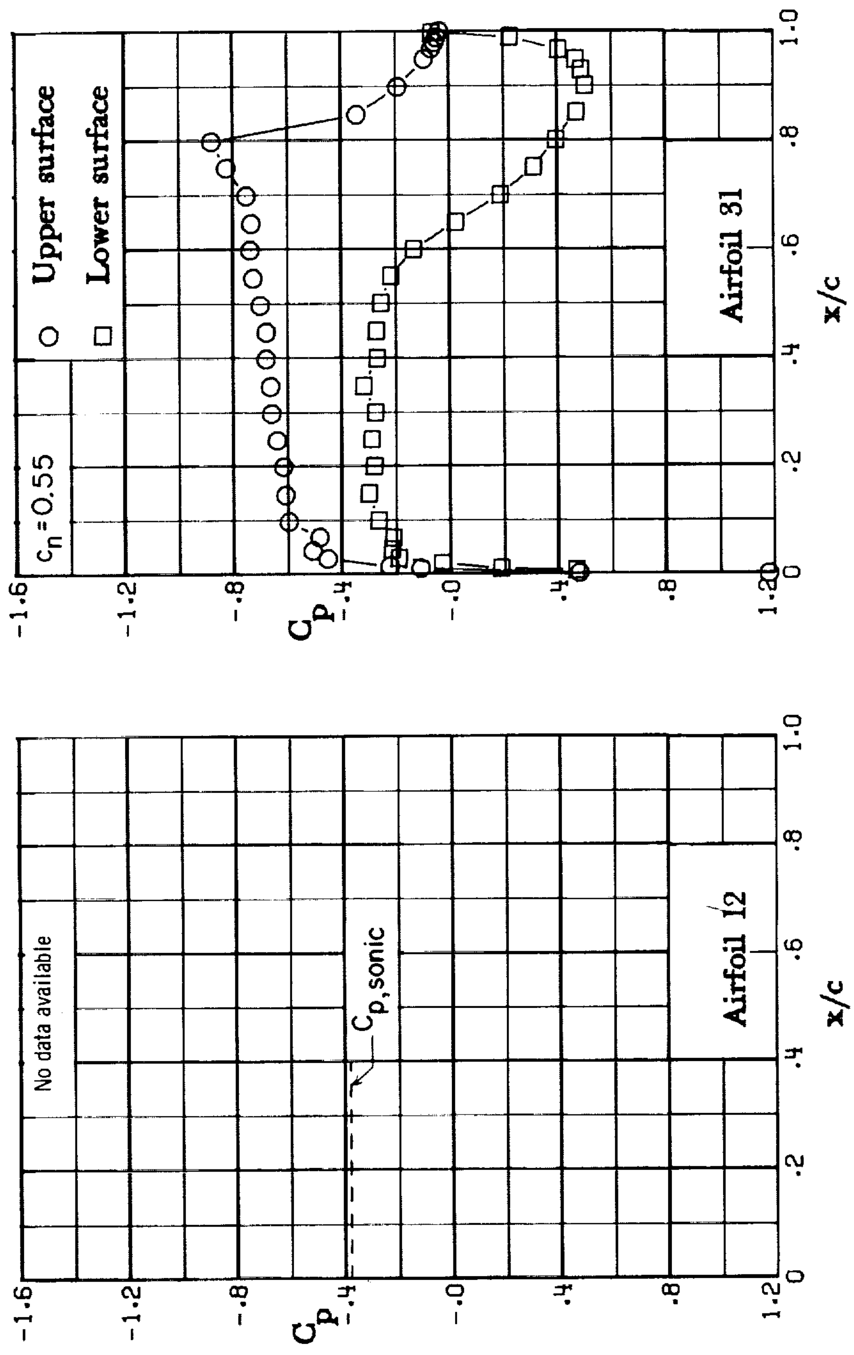

(d) $M = 0.82$; $c_n = 0.55$.

Figure 21.- Concluded.

NASA-Langley, 1975 L-9841